Effect of Cold Plasma Permittivity on Scattering of Waves in a Waveguide

By

Tufail Ahmad Khan

Department of Mathematics
Quaid-i-Azam University
Islamabad, Pakistan
2016

Effect of Cold Plasma Permittivity on Scattering of Waves in a Waveguide

By

Tufail Ahmad Khan

Supervised By

Prof. Dr. Muhammad Ayub

Department of Mathematics
Quaid-i-Azam University
Islamabad, Pakistan
2016

Effect of Cold Plasma Permittivity on Scattering of Waves in a Waveguide

By

Tufail Ahmad Khan

A THESIS SUBMITTED IN THE PARTIAL FULFILLMENT OF THE REQUIREMENTS FOR THE DEGREE OF

DOCTOR OF PHILOSOPHY

IN

MATHEMATICS

Supervised By

Prof. Dr. Muhammad Ayub

Department of Mathematics
Quaid-i-Azam University
Islamabad, Pakistan
2016

Effect of Cold Plasma Permittivity on Scattering of Waves in a Waveguide

By

Tufail Ahmad Khan

CERTIFICATE

A THESIS SUBMITTED IN THE PARTIAL FULFILLMENT OF THE REQUIREMENTS FOR THE DEGREE OF THE DOCTOR OF PHILOSOPHY

We accept this dissertation as conforming to the required standard

1. _____
Prof. Dr. Muhammad Ayub
(Supervisor)

2. _____
Prof. Dr. Tasawar Hayat
(Chairman)

3. _____
Dr. Rahmat Ellahi
(External Examiner)

4. _____
Dr. Muhammad Mushtaq
(External Examiner)

Department of Mathematics
Quaid-i-Azam University
Islamabad, Pakistan
2016

ABSTRACT

A number of diffraction problems having a practical application in science and engineering can be solved through Wiener-Hopf and Mode Matching techniques. Whilst using these techniques, this dissertation addresses a class of boundary-value problems related to the effect of cold plasma and wave scattering. These problems find applications in a broad area of physics and engineering. The envisaged mathematical model is governed by the Helmholtz equation in cold plasma along with soft, hard and impedance boundary conditions. The diffracted, scattered, transmitted and radiated fields are obtained for waveguide structures located in cold plasma. The numerical analysis is made in its factual perspective by using different material properties of the waveguide. It is revealed that the amplitude of obtained field is affected drastically in the presence of an ionosphere plasma medium. Likewise it is observed that the field showed impedance dependent variations that are actually related to the magnetic and electric susceptibilities of the waveguide surfaces. We conclude that such types of results can be used to improve the radiated signal quality transmitted by an artificial satellite in the ionosphere.

CONTENTS

ABSTRACT i

CONTENTS ii

LIST OF FIGURES v

1 INTRODUCTION 1

1.1 Motivation 1

1.2 State of the art 3

1.3 Avant garde 7

1.4 Dissertation catalog 9

2 PRELIMINARIES 11

2.1 Analytical properties of the Fourier transform 11

2.2 Wiener-Hopf technique 14

2.2.1 General scheme of Wiener-Hopf technique 15

2.3 Additive decomposition theorem 17

2.4 Multiplicative decomposition theorem 18

2.5 Maliuzhinetz's function 19

2.6 Helmholtz equation in cold plasma 20

2.7 Canonical problem in cold plasma 22
2.7.1 Mathematical model of the problem 22
2.7.2 Formulation of Wiener-Hopf equation 24
2.7.3 Solution of Wiener-Hopf equation 29
2.7.4 The diffracted field 32
2.7.5 Computational results and discussion 32

3 EFFECT OF COLD PLASMA PERMITTIVITY ON SCATTERING OF E-POLARIZED PLANE WAVE BY AN IMPEDANCE LOADED STEP 37

3.1 Mathematical model of the problem in cold plasma 38
3.2 Formulation of Wiener-Hopf equation 39
3.3 Solution of Wiener-Hopf equation 44
3.4 The diffracted field 47
3.5 Computational results and discussion 48

4 E-POLARIZED PLANE WAVE DIFFRACTION BY AN IMPEDANCE LOADED PARALLEL-PLATE WAVEGUIDE LOCATED IN COLD PLASMA 53

4.1 Mathematical model of the problem in cold plasma 54
4.2 Formulation of Wiener-Hopf equation 56
4.3 Solution of Wiener-Hopf equation 61
4.4 Determination of the unknown coefficients 63
4.5 The diffracted field 64
4.6 Computational results and discussion 66

5 EFFECT OF COLD PLASMA PERMITTIVITY ON THE RADIATION OF THE DOMINANT TEM-WAVE BY AN IMPEDANCE LOADED PARALLEL-PLATE WAVEGUIDE RADIATOR 71

5.1 Mathematical model of the problem 72
5.2 Formulation of Wiener-Hopf equation 73
5.3 Solution of Wiener-Hopf equation 78

5.4 Determination of the unknown coefficients 80
5.5 Radiated field 82
5.6 Computational results and discussion 82

6 DIFFRACTED AND TRANSMITTED FIELDS BY AN IMPEDANCE LOADED WAVEGUIDE LOCATED IN COLD PLASMA 89

6.1 Mathematical model of the problem in cold plasma 90
6.2 Formulation of Wiener-Hopf equation 92
6.3 Solution of Wiener-Hopf equation 102
6.4 Determination of the unknown coefficients 105
6.5 The diffracted and transmitted fields 107
6.6 Computational results and discussion 109

7 CONCLUSION AND PERSPECTIVES 115

7.1 Future directions and open questions 118

BIBLIOGRAPHY 121

LIST OF FIGURES

2.1 Strip of analyticity 14

2.2 Contour of integration 17

2.3 The physical configuration of the waveguide structure in cold plasma 23

2.4 The depiction of Branch cuts 25

2.5 Variation in the diffracted field amplitude versus "N" at $k = 5$, $\theta_0 = 90^o$, $\theta = 60^o$, $\eta = 0.3\iota$, $\epsilon_1 = 0.8$, $\epsilon_2 = 0.1$ and $b = 0.2\lambda$. 33

2.6 Variation in the diffracted field amplitude versus "b" at $k = 5$, $\theta_0 = 90^o$, $\eta = 0.7\iota$, $\epsilon_1 = 0.8$ and $\epsilon_2 = 0.1$. 34

2.7 Variation in the diffracted field amplitude versus "θ_0" at $k = 5$, $\eta = 0.7\iota$, $\epsilon_1 = 0.8$, $\epsilon_2 = 0.1$ and $b = 0.2\lambda$. 34

2.8 Variation in the diffracted field amplitude versus "η" at $\theta_0 = 90^0$, $k = 5$, $\epsilon_1 = 0.8$, $\epsilon_2 = 0.1$ and $b = 0.2\lambda$. 35

2.9 Variation in the diffracted field amplitude versus "ϵ_1" at $k = 5$, $\theta_0 = 90^o$, $\eta = 0.7\iota$, $\epsilon_2 = 0.1$ and $b = 0.2\lambda$. 35

2.10 Variation in the diffracted field amplitude versus "ϵ_2" at $k = 5$, $\theta_0 = 90^o$, $\eta = 0.7\iota$, $\epsilon_1 = 0.8$ and $b = 0.2\lambda$. 36

3.1 Geometrical configuration of the waveguide structure in cold plasma 38

3.2 Variation in the diffracted field amplitude versus "N" at $k = 5$, $\theta_0 = 90^o$, $\theta = 60^o$, $\eta_1 = 0.3\iota$, $\eta_2 = 0.5\iota$, $\epsilon_1 = 0.8$, $\epsilon_2 = 0.1$ and $b = 0.2\lambda$. 49

3.3 Variation in the diffracted field amplitude versus "b" at $k = 5$, $\theta_0 = 90^o$, $\eta_1 = 0.7\iota$, $\eta_2 = 0.5\iota$, $\epsilon_1 = 0.8$ and $\epsilon_2 = 0.1$. 49

3.4 Variation in the diffracted field amplitude versus "θ_0" at $k = 5$, $\eta_1 = 0.7\iota$, $\eta_2 = 0.5\iota$, $\epsilon_1 = 0.8$, $\epsilon_2 = 0.1$ and $b = 0.2\lambda$. 50

3.5 Variation in the diffracted field amplitude versus "η_1" at $\theta_0 = 90^0$, $k = 5$, $\eta_2 = 0.5\iota$, $\epsilon_1 = 0.8$, $\epsilon_2 = 0.1$ and $b = 0.2\lambda$. 50

3.6 Variation in the diffracted field amplitude versus "η_2" at $k = 5$, $\theta_0 = 90^0$, $\eta_1 = 0.3\iota$, $\epsilon_1 = 0.8$, $\epsilon_2 = 0.1$ and $b = 0.2\lambda$. 51

3.7 Variation in the diffracted field amplitude versus "ϵ_1" at $k = 5$, $\theta_0 = 90^o$, $\eta_1 = 0.7\iota$, $\eta_2 = 0.5\iota$ $\epsilon_2 = 0.1$ and $b = 0.2\lambda$. 51

3.8 Variation in the diffracted field amplitude versus "ϵ_2" at $k = 5$, $\theta_0 = 90^o$, $\eta_1 = 0.7\iota$, $\eta_2 = 0.5\iota$ $\epsilon_1 = 0.8$ and $b = 0.2\lambda$. 52

4.1 Geometrical configuration of a waveguide structure in cold plasma . 54

4.2 Variation in the diffracted field amplitude versus truncation number "N" at$\theta_0 = 90^o$, $\theta = 45^o$, $k = 5$, $\eta_1 = 0.3\iota$, $\eta_2 = 0.9\iota$, $\eta_3 = 0.6\iota$, $\eta_4 = 0.4\iota$, $\epsilon_1 = 0.8$, $\epsilon_2 = 0.0$ and $b = 0.2\lambda$. 67

4.3 Variation in the diffracted field amplitude versus "b" at $\theta_0 = 90^o$, $k = 5$, $\eta_1 = 0.6\iota$, $\eta_2 = 0.4\iota$, $\eta_3 = 0.7\iota$, $\eta_4 = 0.5\iota$, $\epsilon_1 = 0.8$ and $\epsilon_2 = 0$. 67

4.4 Variation in the diffracted field amplitude versus "η_1" at $\phi_0 = 90^o$, $k = 5$, $\eta_2 = 0.4t\iota$, $\eta_3 = 0.7\iota$, $\eta_4 = 0.5\iota$, $t\epsilon_1 = 0.8$, $\epsilon_2 = 0$ and $b = 0.2\lambda$. 68

4.5 Variation in the diffracted field amplitude versus "η_2" at $\theta_0 = 90^o$, $k = 5$, $\eta_1 = 0.4\iota$, $\eta_3 = 0.7\iota$, $\eta_4 = 0.5\iota$, $\epsilon_1 = 0.8$, $\epsilon_2 = 0$ and $b = 0.2\lambda$. 68

4.6 Variation in the diffracted field amplitude versus "η_3" at $\theta_0 = 90^o$, $k = 5$, $\eta_1 = 0.4\iota$, $\eta_2 = 0.3\iota$, $\eta_4 = 0.5\iota$, $\epsilon_1 = 0.8$, $\epsilon_2 = 0$ and $b = 0.2\lambda$. 69

4.7 Variation in the diffracted field amplitude versus "η_4" at $\theta_0 = 90^o$,$k = 5$, $\eta_1 = 0.4\iota$, $\eta_2 = 0.3\iota$, $\eta_3 = 0.5\iota$, $\epsilon_1 = 0.8$, $\epsilon_2 = 0$ and $b = 0.2\lambda$. 69

4.8 Variation in the diffracted field amplitude versus "ϵ_1" at $\theta_0 = 90^o$, $k = 5$, $\eta_1 = 0.4\iota$, $\eta_2 = 0.3\iota$, $\eta_3 = 0.5\iota$, $\eta_4 = 0.7$, $\epsilon_2 = 0$ and $b = 0.2\lambda$. 70

4.9 Variation in the diffracted field amplitude versus "ϵ_2" at $\theta_0 = 90^o$, $k = 5$, $\eta_1 = 0.4\iota$, $\eta_2 = 0.3\iota$, $\eta_3 = 0.5\iota$, $\eta_4 = 0.7$, $\epsilon_1 = 0.9$ and $b = 0.2\lambda$. 70

5.1 Geometry of the impedance loaded parallel-plate waveguide radiator located in cold plasma 72

5.2 Variation in the radiated field amplitude versus truncation number "N". The other parameters are $\theta = 45^o$ $\eta_1 = 0.2$, $\eta_2 = 0.5$, $\eta_3 = 0.3$, $\eta_4 = 0.6$, $\epsilon_1 = 0.8$, $\epsilon_2 = 0$, $k = 5$ and $b = 0.2\lambda$. 84

5.3 Variation in the radiated field amplitude versus "b". The other parameters are $k = 5$, $\eta_1 = 0.5$, $\eta_2 = 0.3$, $\eta_3 = 0.6$, $\eta_4 = 0.7$, $\epsilon_1 = 0.8$ and $\epsilon_2 = 0$. . . 85

5.4 Variation in the radiated field amplitude versus "η_1". The other parameters are $k = 5$, $\eta_2 = 0.3$, $\eta_3 = 0.6$, $\eta_4 = 0.5$, $\epsilon_1 = 0.8$, $\epsilon_2 = 0$ and $b = 0.2\lambda$. 85

5.5 Variation in the radiated field amplitude versus "η_2". The other parameters are $k = 5$, $\eta_1 = 0.7$, $\eta_3 = 0.6$, $\eta_4 = 0.4$, $\epsilon_1 = 0.8$, $\epsilon_2 = 0$ and $b = 0.2\lambda$. 86

5.6 Variation in the radiated field amplitude versus "η_3". The other parameters are $k = 5$ $\eta_1 = 0.5$, $\eta_2 = 0.3$, $\eta_4 = 0.4$, $\epsilon_1 = 0.8$, $\epsilon_2 = 0$ and $b = 0.2\lambda$. 86

5.7 Variation in the radiated field amplitude versus "η_4". The other parameters are $k = 5$, $\eta_1 = 0.5$, $\eta_2 = 0.3$, $\eta_3 = 0.6$, $\epsilon_1 = 0.8$, $\epsilon_2 = 0$ and $b = 0.2\lambda$. 87

5.8 Variation in the radiated field amplitude versus "ϵ_1". The other parameters are $k = 5$, $\eta_1 = 0.5$, $\eta_2 = 0.3$, $\eta_3 = 0.6$, $\eta_4 = 0.7$, $\epsilon_2 = 0$ and $b = 0.2\lambda$. 87

5.9 Variation in the radiated field amplitude versus "ϵ_2". The other parameters are $k = 5$, $\eta_1 = 0.5$, $\eta_2 = 0.3$, $\eta_3 = 0.6$, $\eta_4 = 0.7$, $\epsilon_1 = 0.8$ and $b = 0.2\lambda$. 88

6.1 The physical configuration of the waveguide located in cold plasma . 90

6.2 Variation in the diffracted field amplitude versus "N" at $k = 5$, $\theta_0 = 45^o$, $\theta = 90^0$, $\eta_1 = 0.2\iota$, $\epsilon_1 = 0.8$, $\epsilon_2 = 0.1$, $b = 0.2\lambda$. 110

6.3 Variation in the transmitted field amplitude versus "N" at $k = 5$, $\theta_0 = 45^o$, $\theta = 90^0$, $\eta_5 = 0.4\iota$, $\epsilon_1 = 0.5$, $\epsilon_2 = 0.1$, $b = 0.2\lambda$. 110

6.4 Variation in the diffracted field amplitude versus "θ_1" at $\theta_0 = 45^0$, $k = 5$, $\epsilon_1 = 0.8$, $\epsilon_2 = 0.1$ and $b = 0.2\lambda$. 111

6.5 Variation in the diffracted field amplitude versus "ϵ_1" at $k = 5$, $\theta_0 = 45^0$, $\eta_1 = 0.2\iota$, $\epsilon_2 = 0.1$ and $b = 0.2\lambda$. 111

6.6 Variation in the diffracted field amplitude versus "ϵ_2" at $k = 5$, $\theta_0 = 45^0$, $\eta_1 = 0.2\iota$, $\epsilon_1 = 0.8$ and $b = 0.2\lambda$. 112

6.7 Variation in the transmitted field amplitude versus "η_2" at $k = 5$, $\theta_0 = 45^o$, $\epsilon_1 = 0.8$, $\epsilon_2 = 0.1$ and $b = 0.2\lambda$. 112

6.8 Variation in the transmitted field amplitude versus "ϵ_1" at $k = 5$, $\eta_2 = 0.2\iota$, $\epsilon_2 = 0.1$ and $b = 0.2\lambda$. 112

6.9 Variation in the transmitted field amplitude versus "ϵ_2" at $k = 5$, $\eta_2 = 0.2\iota$, $\epsilon_1 = 0.8$ and $b = 0.2\lambda$. 113

CHAPTER 1

INTRODUCTION

1.1 MOTIVATION

The problems involving wave scattering in cold plasma have been of great interest to scientists and engineers. The study of the propagation of electromagnetic (EM) waves through the earth's ionosphere is of deep interest and importance providing with a natural mean of radio communication [1, 2, 3]. Ionosphere consists of ions and electrons formed by solar photo-ionization and soft x-ray radiation [4]. Such ions and electrons, of course, form weak neutral plasma and hence, the physics of ionosphere can be coined in terms of plasma physics. Earth's ionosphere has been divided into four broad regions, namely, D, E, F, and topside regions. For radio communications the region of interest is F-region lying above the height of 150 km. The F-region contains an important reflecting layer for communication signals arriving from an earth station. However, ionosphere consists of electrons, ions and neutrals, of course, it can be modeled as a medium comprising of weak neutral plasma, hence, its physics can be grasped as plasma physics. Since the ionosphere plasma is highly magnetized under earth's magnetic field, therefore, it can be treated as an anisotropic medium. The ultraviolet radiation which impinges on the earth's atmosphere ionizes a fraction of neutral atmosphere, resulting into a mixture of charged (electrons and ions) and neutral particles. Since the collisions at altitudes above 80 km in the earth's atmosphere

are very rare, therefore, under such conditions the recombination rate of charged species is very slow and hence, a permanent ionized medium occurs, which is known as ionosphere.

The transmission, reflection, refraction, and diffraction of EM waves by ionosphere are the processes that can be understood via plasma physics. The ionosphere plasma also retains the equilibrium density of free electrons and ions because of the balance between photo-ionization and various loss mechanisms. However, the density of these electrons varies dramatically with altitude by the effects of sunrise and sunset [5]. Moreover, the ionosphere plasma is magnetized by the earth's magnetic field that forms the plasma to be as an anisotropic medium. The measurements based upon the artificial satellites immerse in the ionosphere plasma may be affected due to the interaction of communicating EM signals that are used for communication between the spacecraft and earth station. It is well known that the communicating signal radiated by the satellite may modify due to its interaction with the ionosphere plasma and due to the nature of body material (electric and magnetic susceptibilities or impedance) of waveguide used to guide the EM signal (radiated from the vehicle) to the earth station [6, 7]. With this the measurements based upon artificial satellite present in ionosphere communicating to an earth station may be affected drastically. The geometry and material used in complex body structure of an artificial satellite can also change the quality of an EM signal. It is understood that electric and magnetic susceptibilities of a material are related to permittivity and permeability parameters. Moreover, the characteristic impedance and speed of EM wave depend on any medium where detailed information of any medium is obtained by its refractive index.

The present work is based upon a theoretical model to investigate the effectiveness of the ionosphere plasma, earth's magnetic field, structure and nature of the body material (electric and magnetic susceptibilities or impedance) of an artifi-

cial satellite on an EM signal transmitting through the ionosphere. It is pertinent to mention that in order to model ionosphere plasma the whole system is supposed to be immersed in a cold plasma. The modeled problem have been combined to have a well known Helmholtz equation which is solved for the specified boundary conditions by employing Wiener-Hopf technique [8, 9]. Here, we have employed the magnetoionic theory that deals with the cold anisotropic plasma which is considered in this model. The temperature and pressure of plasma species (ions and electrons) are usually small and hence, are neglected. Under these circumstances such a plasma is treated as cold plasma. Sahin et al. [10] investigated the diffraction phenomenon in cold plasma. Yener and Serbest [11] also explored the diffraction of plane waves by an impedance loaded half-plane in cold plasma. Cinar and Büyükaksoy [12] studied the diffraction of the plane waves by an impedance loaded parallel-plate waveguide in the absence of cold plasma.

Keeping in view the aforementioned background, this thesis concerns largely with the effect of cold plasma permittivity on the scattering process of waveguide structures. This study is important mainly due to the worthwhile applications of scattering phenomena in structural design antennas and aircrafts.

1.2 STATE OF THE ART

This documents is mainly concerned about the wave scattering processes in the waveguide structure in the presence of cold plasma. Being fourth state of matter and larger part of universe the study of plasma is quite relevant and significant. The plasma contains a certain portion of free electrons whereas the atoms are partly ionized. The presence of negative and positive carriers of charge makes plasma electrically conductive and distinguishes it from gaseous state. The plasma that contains a very small part (approximately one percent) of the ionized particles is termed as cold (non-thermal) plasma. The cold plasma is

generated in a high-voltage electric field and the velocity of electron is strongly dependent to the temperature up to a thousand degrees of Celsius. Whilst their effect on the plasma temperature is low and final plasma temperature is close to the outward temperature. To quantify the results arising due to the effectiveness of ionosphere plasma, earth's magnetic field, structure and nature of body material of the radiator on the EM signal communicating to earth station propagating through ionosphere, a theoretical model has been devised. Lau and Biggs [13] is examined the effects of cold plasma on electron layer immersed in a cold background plasma. The mutual actions between guided electromagnetic waves and cold plasma in the presence of a static magnetic field were studied by Buchsbaum et al. [14]. Bardos and Barankova [15] examined the relation between a new type of radio frequency and cold plasma. Janis [16] developed a variational formulation for the impedances loaded antenna immersed in cold plasma. Tyukhtin [17] studied the diffraction of plane electromagnetic waves by a half-plane immersed in a parallel flow of cold plasma. Ikiz and Karoomerlioglu [18] investigated diffraction phenomenon by considering two impedances wedge in cold plasma.

In continuation to second part of this work, the wave scattering is a physical phenomenon in which waves are constrained to depart from the route in the medium through which they move. Mathematical analysis of scattering was the focus of attention for many researchers and scientists, for example [19, 20, 21]. The study was initiated by Ibn-al-Haitam in 10th century AD who computed the asymptotic field for diffraction of the wedge and arose the wave propagation theory referred as Poincare [22]. Sommerfeld [23] discussed the exact solution of diffraction from a plate by using the physical method of images on Reimann surfaces. Carslaw [24] utilized the parabolic coordinates and the results obtained by him were the same as achieved by Sommerfeld [23]. Levine and Schwinger [25, 26] used the integral equation in problem of diffraction followed by some related

studies containing the Wiener-Hopf type integral equations. Copson [27] studied the diffraction from a plane screen in the form of integral equation whose solution was obtained by Wiener-Hopf technique. Interestingly the obtained solution was consistent with the Summerfeld's problem [23]. It is worthwhile to comment that Copson [27] was the first one who used Wiener-Hopf technique to solve the problem of sound. The key feature of obtaining the solution via Wiener-Hopf technique is the kernel factorization. This factorization splits the function into a sum or product of two functions where one function is regular in the upper half-plane while the other in the lower half-plane. The detailed description regarding the kernel factorization can be found in [28, 29, 30, 31]. Sometime kernel factorization becomes very difficult and in such cases some alternative techniques are opted to get desired results. Bates and Mittra [32] have employed an integral representation for the factorization of a scalar function. Wiener-Hopf is a useful tool to handle two or three dimensional diffraction problems [33, 34, 35].

It is renowned that the problem having a geometry of planer boundaries with a sudden change in material properties of boundaries may lead to the solution by Wiener-Hopf technique [36, 37, 38, 39]. Büyükaksoy and Birbir [40, 41] considered the diffraction of E-polarized plane wave by the reactive step and radiation phenomenon that radiates from an impedance loaded parallel-plate waveguide radiator. Topsakal et.al. [42] used the Wiener-hopf technique to solve the problem of scattering of electromagnetic waves by a rectangular impedance cylinder. Cinar and Büyükoksoy [43] used the Wiener-Hopf technique for the problem of diffraction by a thick impedance half-plane with different end faces impedance. The diffraction by a rigid barrier with a soft or perfectly absorbent end face with Wiener-Hopf technique was studied by Mclver and Rawlins [44]. Rienstra [45] applied the Wiener-Hopf technique for the problem of sound radiation from semi-infinite duct. The solution to the sound radiation problem using Wiener-Hopf technique was due to Hassan and Rawlins [46]. Furthermore, the said

technique was successively used by Ayub et al [47, 48, 49, 50] and Nawaz et al. [51, 52, 53, 54] in their recent studies. A brief historical view of Wiener-Hopf technique was given by Lawrie and Abrahams [55]. As mentioned earlier that Wiener-Hopf technique is not always considered to be the easy task when kernel factor becomes complicated. Therefore, a hybrid method has recently been introduced to solve such complicated problems while bypassing the most difficult process of the matrix Wiener-Hopf factorization. This hybrid method is combination of Wiener-Hopf and Mode-Matching techniques that reduces the boundary-valued problem in terms of a modified Wiener-Hopf equation with second kind. The solution obtained from hybrid method contains an eigenfunction expansion of unknown complex coefficients. The expressions for these unknown coefficients are obtained as a system of infinite linear algebraic equations. Through a numerical procedure, this system can be solved approximately. This method was adopted to solve the E-polarized plane wave diffraction and radiation phenomenon in a waveguide by Büyükaksoy and Birbir [41]. Such methods were initially developed to tackle the problems governed by Helmholtz equation and waveguide boundaries described by Neumann (Rigid), Dirichlet (Soft) or Robin (Mixed) conditions. The solution of these problems contains the eigenfunction expansion. Ikiz et al. [56] used the name numerical-analytical method instead of hybrid method. The main objective of using this method is to modify the analytical methods which works well at high frequencies while numerical method works well at low frequencies.

Also the diffraction phenomenon was studied in a bifurcated waveguide using a dominant mode wave incident on a soft-hard half-plane amidst an infinite parallel-plate with hard boundary by Büyükaksoy and Polot [57]. Transmission and reflection coefficients are acquired in a bifurcated waveguide by Rawlin [58]. Pace and Mithra [59] studied the problem involving a trifurcated parallel-plate waveguide with an arbitrary spacing between the plates. Jones [60] considered

the waves scattering from the waveguide containing three semi-infinite parallel soft and equidistant plates. Asgher et al. [61] extended the Jones' problem [60] for point and line source scattering. Rawlin [62] also studied the radiation of a surface wave mode propagating in a semi-infinite cylindrical waveguide. Hassan and Rawlin [63] solved the problem of sound radiation from a waveguide (Semi-infinite duct) placed symmetrically within an infinite duct. Later on the radiation phenomenon was studied in a trifurcated parallel-plate waveguide by Rawlin and Hassan [64]. Morse and Feshbach [65] considered the problem of scattering in a perfectly conducting and an impedance loaded parallel-plate waveguide having the same impedances on lower and upper faces of the plates. Later on Johansen [66] considered the same geometry for different surface impedances using a coupled system of modified Wiener-Hopf equations. Büyükaksoy et al. [67] and Idemen [68] uncoupled the coupled system of modified Wiener-Hopf equations by using the week factorization method and obtained the exact solutions of the vector Wiener-Hopf equations. Abrahams [69] introduced a "pole removal technique" to uncouple the coupled system of modified Wiener-Hopf equations. This technique can be seen in some classical articles, to mention a few [70, 71, 72, 73].

1.3 AVANT GARDE

The main aspiration of this dissertation is to investigate that how a particular class of structural problems related to wave scattering may be solved while using different semi-analytic techniques. In particular when a cold plasma is immersed in the waveguide structure would be the topic of interest. Broadly speaking the present work can be seen as a continuation of ongoing studies, refer for instance to [1, 6, 10, 12]. The major part of this research is carried out in the following perspective:

(1) The derivation of governing Helmholtz equation in cold plasma from the well-known Maxwell equations.

(2) Inclusion of cold plasma permittivity values ϵ_1 and ϵ_2 in the given model.

(3) The use of Wiener-Hopf technique together with the Mode-Matching technique in order to yield a larger part of solutions to above model.

(4) The mathematical and numerical study related to the effect of cold plasma on scattering of E-polarized plane wave by step discontinuity.

(5) The discussion concerning the effect of cold plasma permittivity due to impedance loaded parallel-plate waveguide located in cold plasma.

(6) The consideration of radiation problem with an impedance loaded parallel-plate waveguide radiator.

(7) The study of problems involving the diffracted and transmitted fields.

(8) The graphical behavior of diffracted, transmitted and radiated field versus different physical parameters of our choice.

(9) In fact the major contribution towards the development of present study is to quantify the effects of ionosphere plasma on the communicating signals between earth station and an artificial satellite in the earth's atmosphere. In the process the standard Wiener-Hopf and somehow Mode-matching techniques are used to find appropriate solutions for such models. In fact the Wiener-Hopf technique with Mode Matching technique is used to show the effect of cold plasma permittivity in different waveguide structures. Briefly saying the Wiener-Hopf analysis and the effect of cold plasma permittivity in a waveguide are the major focus for this thesis.

1.4 DISSERTATION CATALOG

This thesis is summarized in the order below.

CHAPTER (2) begins with the review of generalized form of boundary-valued problems in cold plasma. As mentioned earlier this thesis is concerned mostly with the effect of cold plasma permittivity and scattering of waves in a waveguide structure. For this purpose, it contains some basic definitions and mathematical preliminaries which will be utilized in the succeeding chapters. A canonical problem is modeled in cold plasma and solved while using a modified Wiener-Hopf technique.

CHAPTER (3) consists of impedances loaded step problem in cold plasma. Here, a waveguide is designed in cold plasma containing by a two separated half-planes with different surface impedances and afterwards these half-planes were joined vertically by a hard step. Typically such kind of geometries can be used in constructing antennas. The contents of this chapter has already been submitted to the **Journal of Waves in Random and Complex Media** for possible publication.

In CHAPTER (4), the effect of cold plasma permittivity is analyzed on E-polarized plane wave diffraction by an impedance loaded parallel-plate waveguide in cold plasma. Also the effect of different parameters such as surface impedance and plate separation is observed. The model problem is solved by hybrid method i.e., Mode-Matching technique in conjunction with Fourier transform. These type of geometries in the ionosphere (plasma) are important in communication between the vehicles and the earth station. The contents of this chapter have been published in **Physica Scripta**, 89(8): Paper ID. e095207, (2014).

CHAPTER (5) deals with radiation phenomenon where an impedance loaded parallel-plate waveguide radiator in cold plasma is considered. This geometry is designed by a parallel plane and half-plane having all having different faces different surface impedances located in cold plasma. Here the effect of cold plasma permittivity is investigated on the radiation problem. The contents of

Chapter (5) are published in **Mathematical Methods in the Applied Sciences**, *DOI* : 10.1002/*mma*.3464.

CHAPTER (6) investigates the diffracted and transmitted fields from a waveguide located in cold plasma. The geometry of the problem is designed from the three half-planes where one half-plane is located between the other two in opposite direction. The surface material properties of the half-planes are characterized either by soft (Dirichlet type), hard (Neumann type) or impedances (Robin type). The solution to the underline problem is obtained with the help of hybrid method that reduces the boundary-valued problem to the modified Wiener-Hopf equation. This investigation has already been submitted to **New Journal of Physics** for possible publication.

CHAPTER 2

PRELIMINARIES

This chapter contains some of the mathematical preliminaries and compact reviews of the techniques which will be used in the subsequent chapters. These consist of Fourier transform [74], Wiener-Hopf technique [8, 57], Maliuzhinetz's function [75, 76, 77, 78, 79, 80] and Helmholtz equation in cold plasma [81]. Certainly these preliminaries will help to successful completion of thesis document.

2.1 ANALYTICAL PROPERTIES OF THE FOURIER TRANSFORM

The Fourier transform is a useful technique and plays an important role in solving a partial differential equation. This technique is applicable for the majority of the problem whether their domain is finite or infinite. Consider a function $h(x)$ defined for $x \in (-\infty, \infty)$. Then $h(x)$ can be written in the form as under

$$h(x) = h_+(x) + h_-(x), \tag{2.1}$$

where

$$h_+(x) = \begin{cases} h(x) & x > 0 \\ 0 & x < 0, \end{cases} \tag{2.2}$$

and

$$h_-(x) = \begin{cases} h(x) & x < 0 \\ 0 & x > 0. \end{cases} \tag{2.3}$$

$H(\alpha)$ represents the Fourier transform of $h(x)$ which is defined as under

$$H(\alpha) = \frac{1}{\sqrt{2\pi}} \int_{-\infty}^{\infty} h(x) e^{\iota \alpha x} dx, \tag{2.4}$$

where the integral in the above expression exists and h(x) is bounded for all x in the given domain. Use of equations (2.2) and (2.3) in equation (2.4) gives

$$H(\alpha) = \frac{1}{\sqrt{2\pi}} \int_{-\infty}^{\infty} [h_-(x) + h_+(x)] \, e^{\iota \alpha x} dx. \tag{2.5}$$

After simplification, equation (2.5) takes the form

$$H(\alpha) = \frac{1}{\sqrt{2\pi}} \int_{-\infty}^{0} h_-(x) e^{\iota \alpha x} dx + \frac{1}{\sqrt{2\pi}} \int_{0}^{\infty} h_+(x) e^{\iota \alpha x} dx, \tag{2.6}$$

that is

$$H(\alpha) = H_-(\alpha) + H_+(\alpha), \tag{2.7}$$

where

$$H_-(\alpha) = \frac{1}{\sqrt{2\pi}} \int_{-\infty}^{0} h_-(x) e^{\iota \alpha x} dx, \tag{2.8}$$

and

$$H_+(\alpha) = \frac{1}{\sqrt{2\pi}} \int_{0}^{\infty} h_+(x) e^{\iota \alpha x} dx. \tag{2.9}$$

The analytic properties of $H(\alpha)$ are the properties of $H_-(\alpha)$ and $H_+(\alpha)$. Initially, consider the properties of $H_+(\alpha)$ as follow:

If the function $h_+(x)$ is of exponential order, i.e.,

$$|h_+(x)| < M e^{\tau - x} \qquad \text{as} \quad x \to \infty, \tag{2.10}$$

then the function $H_+(\alpha)$ is a regular function of the complex variable $\alpha = \sigma + \iota\tau$ and $H_+(\alpha) \to 0$ as $|\alpha| \to \infty$ in the domain $\Im\mathfrak{m}(\alpha) > \tau_-$. Perceiving that

$$Me^{\tau_- x} e^{\iota\alpha x} = Me^{(\tau_- - \tau)x} e^{\iota\sigma x} \tag{2.11}$$

is bounded if $\tau > \tau_-$. Now taking the inverse Fourier transform of $H_+(\alpha)$, one obtains

$$h_+(x) = \frac{1}{\sqrt{2\pi}} \int_0^\infty H_+(\alpha) e^{-\iota\alpha x} d\alpha, \tag{2.12}$$

where integration will be taken over any straight line in the region $\Im\mathfrak{m}(\alpha) > \tau_-$ and parallel to $x-$axis in the complex $\alpha-$plane.

Now for the problem considered in this thesis, the strip of the analyticity can be calculated by considering the following cases.

(i) For $\tau_- < 0$ the function $h_+(x)$ decreases, the domain of the analyticity of $h_+(x)$ contains the real axis and equation (2.12) will be integrated along the positive real axis.

(ii) For $\tau_- > 0$ the function $h_+(x)$ increases but not faster than the exponential function with linear exponent, the domain of the analyticity of $h_+(x)$ lies above the real axis of the complex $\alpha-$plane and equation (2.12) will be integrated above the positive real axis.

Now consider the function $h_-(x)$ satisfies the exponential order condition, so one can write

$$|h_-(x)| < Me^{\tau_+ x} \qquad \text{as} \quad x \to \infty, \tag{2.13}$$

$$H_-(\alpha) = \int_0^\infty h_-(x) e^{\iota\alpha x} dx \tag{2.14}$$

is regular in the lower half plane $\Im\mathfrak{m}(\alpha) < \tau_+$.

Now taking into account the inverse Fourier transform of $H_-(\alpha)$ gives

$$h_-(x) = \frac{1}{\sqrt{2\pi}} \int_0^\infty H_-(\alpha) e^{-\iota\alpha x} d\alpha, \tag{2.15}$$

for $\tau_+ > 0$ the domain of analyticity of $H_-(\alpha)$ contains the negative real axis and for $\tau_+ < 0$, is below the negative real axis. Hence equation (2.15) is analytic in region $\tau_- < \Im\mathfrak{m}(\alpha) < \tau_+$ as shown in Fig. (2.1)

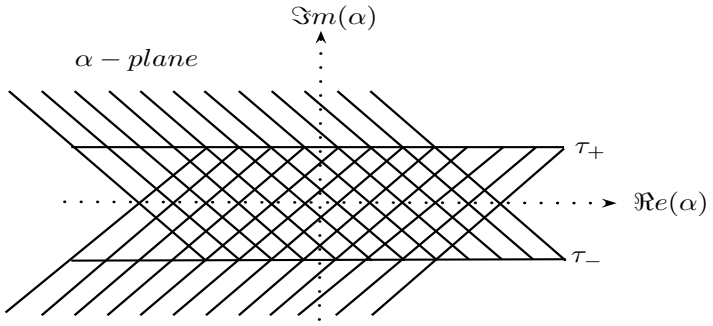

FIGURE 2.1. *Strip of analyticity*

2.2 WIENER-HOPF TECHNIQUE

Wiener-Hopf technique was introduced by N. Wiener and E. Hopf in 1931. Initially, this was used to solve singular integral equation of the form

$$f(x) = \phi(x) + \int_0^\infty K(x-y) f(y) dy, \qquad 0 < x < \infty, \tag{2.16}$$

where $\phi(x)$ and $K(x-y)$ are given known function while $f(y)$ is unknown function to be calculated. This equation had arisen in Hopf's work on Milne-Schwarzschild equation. This technique also reduces the problem of diffraction by a semi-infinite plate to the solution of singular integral equation. All physical phenomena are associated with ordinary or partial differential equations. These

partial differential equations may be solved by using certain method depending upon the geometry of the problem. The method of separation of variables is one of these methods that fails for certain geometries such as semi-infinite regions, waveguide structure with non planer boundaries etc. The detailed description of the technique is mentioned below.

2.2.1 GENERAL SCHEME OF WIENER-HOPF TECHNIQUE

In this technique it is required to determined the unknown function $F_-(\alpha)$ and $F_+(\alpha)$ of a complex variable α occurring in the below Wiener-Hopf equation. These functions are analytic in the half-planes $\mathfrak{Im}(\alpha) < \tau_+$ and $\mathfrak{Im}(\alpha) > \tau_-$, respectively, and approach to zero as $|\alpha| \to \infty$, satisfying the functional equation

$$\mathscr{A}(\alpha)F_+(\alpha) + \mathscr{B}(\alpha)F_-(\alpha) + \mathscr{C}(\alpha) = 0, \tag{2.17}$$

in the region $\tau_- < \mathfrak{Im}(\alpha) < \tau_+$. Here $\mathscr{A}(\alpha)$, $\mathscr{B}(\alpha)$ and $\mathscr{C}(\alpha)$ are the known functions regular in the strip $\tau_- < \mathfrak{Im}(\alpha) < \tau_+$ and $\mathscr{A}(\alpha)$ and $\mathscr{B}(\alpha)$ are non- zero in the strip. For the solution of the Wiener equation the main step is to replace

$$\frac{\mathscr{A}(\alpha)}{\mathscr{B}(\alpha)} = \frac{P_+(\alpha)}{P_-(\alpha)}, \tag{2.18}$$

where the functions $P_+(\alpha)$ and $P_-(\alpha)$ are non zero and regular, respectively, in the half-planes $\mathfrak{Im}(\alpha) > \tau_-$ and $\mathfrak{Im}(\alpha) < \tau_+$. On using equation (2.18) in equation (2.17), one can write

$$P_+(\alpha)F_+(\alpha) + P_-(\alpha)F_-(\alpha) + P_-(\alpha)\frac{\mathscr{C}(\alpha)}{\mathscr{B}(\alpha)} = 0. \tag{2.19}$$

The last term of the equation (2.19) can be decomposed as

$$P_-(\alpha)\frac{\mathscr{C}(\alpha)}{\mathscr{B}(\alpha)} = K_+(\alpha) + K_-(\alpha), \tag{2.20}$$

where the functions $K_+(\alpha)$ and $K_-(\alpha)$ are analytic in the half-planes $\Im\mathfrak{m}(\alpha) > \tau_-$ and $\Im\mathfrak{m}(\alpha) < \tau_-$, respectively. In the strip the following equation holds true

$$P_+(\alpha)F_+(\alpha) + K_+(\alpha) = -P_-(\alpha)F_-(\alpha) - K_-(\alpha) = S(\alpha). \tag{2.21}$$

The above equation is valid in the strip $\tau_- < \Im\mathfrak{m}(\alpha) < \tau_+$. The left-hand side of the equation (2.21) is regular in the half-plane $\Im\mathfrak{m}(\alpha) > \tau_-$ while the right-hand side of the equation (2.21) is regular in the half-plane $\Im\mathfrak{m}(\alpha) < \tau_+$. Hence by the analytic continuation principal one can define $S(\alpha)$ over the complex $\alpha - plane$. Let us suppose that

$$|P_+(\alpha)F_+(\alpha) + K_+(\alpha)| < |\alpha|^p \; as \quad \alpha \to \infty, \; \Im\mathfrak{m}(\alpha) > \tau_- \tag{2.22}$$

and

$$|P_-(\alpha)F_-(\alpha) + K_-(\alpha)| < |\alpha|^q \; as \;\; \alpha \to \infty, \; \Im\mathfrak{m}(\alpha) < \tau_+. \tag{2.23}$$

Then on using the extended Liouvillle's theorem which states that "If $S(\alpha)$ is an integral function such that $|S(\alpha)| < M|\alpha|^p$ as $\alpha \to \infty$ where M and p are constant then $S(\alpha)$ is a polynomial of degree less than or equal to $[p]$ where $[p]$ is the integral part of p." Here, $S(\alpha)$ represents a polynomial $P(\alpha)$ whose degree is less than or equal to the integral part of (p, q) i.e.,

$$F_+(\alpha) = \frac{P(\alpha) - K_+(\alpha)}{P_+(\alpha)} \tag{2.24}$$

and

$$F_-(\alpha) = \frac{-P(\alpha) - K_-(\alpha)}{P_-(\alpha)}. \tag{2.25}$$

The above equations determine $F_+(\alpha)$ and $F_-(\alpha)$ in term of $P(\alpha)$. Thus, the representation of equations (2.24) and (2.25) form a base to use the Wiener-Hopf technique. It is important to annotate that factorization of function expressed

in equation (2.18) and decomposition of function expressed in equation (2.20) is possible under certain conditions. The possibility of these representations is guaranteed by the following theorems.

2.3 ADDITIVE DECOMPOSITION THEOREM

Statement:

Let $F(\alpha)$ be a regular function in the region $\tau_- < \mathfrak{Im}(\alpha) < \tau_+$ and $F(\alpha) \to 0$ uniformly in the given region as $|\alpha| \to \infty$, then $F(\alpha)$ can be decomposed in the given region as under

$$F(\alpha) = F_-(\alpha) + F_+(\alpha), \tag{2.26}$$

where $F_+(\alpha)$ and $F_-(\alpha)$ are regular functions in the region $\mathfrak{Im}(\alpha) > \tau_-$ and $\mathfrak{Im}(\alpha) < \tau_+$, respectively.

Proof:

Consider a rectangle $P_1P_2P_3P_4$ bounded by the lines $\mathfrak{Im}(\alpha) = \tau'_-$, $\mathfrak{Im}(\alpha) = \tau'_+$, $\mathfrak{Re}(\alpha) = T$ and $\mathfrak{Re}(\alpha) = -T$ containing an arbitrary complex number $\alpha = \sigma + \iota\tau$ and lying in the given strip such that $\tau_- < \tau'_- < \mathfrak{Im}(\alpha) < \tau'_- < \tau_-$ as shown in the Fig. (2.2).

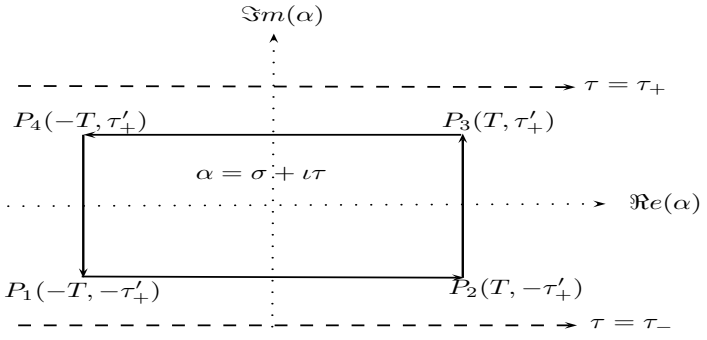

FIGURE 2.2. *Contour of integration*

According to Cauchy's integral formula, one can write

$$F(\alpha) = \frac{1}{2\pi\iota}\int_{-T+\iota\tau'_-}^{T+\iota\tau'_-}\frac{f(\zeta)}{\zeta-\alpha}d\zeta + \frac{1}{2\pi\iota}\int_{T+\iota\tau'_-}^{T+\iota\tau'_+}\frac{f(\zeta)}{\zeta-\alpha}d\zeta + \frac{1}{2\pi\iota}\int_{T+\iota\tau'_+}^{-T+\iota\tau'_+}\frac{f(\zeta)}{\zeta-\alpha}d\zeta + \frac{1}{2\pi\iota}\int_{-T+\iota\tau'_+}^{-T+\iota\tau'_-}\frac{f(\zeta)}{\zeta-\alpha}d\zeta. \tag{2.27}$$

On taking the limit $T \to \infty$, the second and fourth integrals on the right-hand side of equations (2.27) will tend to zero and hence equations (2.27) will take the form

$$F(\alpha) = F_-(\alpha) + F_+(\alpha), \tag{2.28}$$

where

$$F_-(\alpha) = -\frac{1}{2\pi\iota}\int_{-\infty+\iota\tau'_+}^{\infty+\iota\tau'_+}\frac{f(\zeta)}{\zeta-\alpha}d\zeta \tag{2.29}$$

and

$$F_+(\alpha) = \frac{1}{2\pi\iota}\int_{-\infty+\iota\tau'_-}^{\infty+\iota\tau'_-}\frac{f(\zeta)}{\zeta-\alpha}d\zeta. \tag{2.30}$$

$F_+(\alpha)$ and $F_-(\alpha)$ are regular functions in upper $\alpha - plane\ \Im\mathfrak{m}(\alpha) > \tau_-$ and in lower $\alpha - plane\ \Im\mathfrak{m}(\alpha) < \tau_+$, respectively. The arbitrary complex number $\alpha = \sigma + \iota\tau$ does not lie on the contour of integration.

2.4 MULTIPLICATIVE DECOMPOSITION THEOREM

Statement:

Let $\Psi(\alpha)$ be a non zero and regular function in the strip $\tau_- < \Im\mathfrak{m}(\alpha) < \tau_+$ and $\Psi(\alpha) \to 0$ uniformly as $|\alpha| \to \infty$ in the strip. Then $\Psi(\alpha)$ can be factorized in the given strip as

$$\Psi(\alpha) = \Psi_-(\alpha)\Psi_+(\alpha), \tag{2.31}$$

where the functions $\Psi_+(\alpha)$ and $\Psi_-(\alpha)$ are non-zero and regular in the half-planes $\Im\mathfrak{m}(\alpha) > \tau_-$ and $\Im\mathfrak{m}(\alpha) < \tau_+$, respectively.

Proof:

Let

$$F(\alpha) = \log \Psi(\alpha), \tag{2.32}$$

which satisfies all the condition of additive decomposition theorem. Thus, $F(\alpha)$ can be expressed as

$$F(\alpha) = F_-(\alpha) + F_+(\alpha), \tag{2.33}$$

where

$$F_+(\alpha) = \log \Psi_+(\alpha) \tag{2.34}$$

and

$$F_-(\alpha) = \log \Psi_-(\alpha). \tag{2.35}$$

Substituting the equations (2.32), (2.34) and (2.35) in equation (2.33) gives

$$\log \Psi(\alpha) = \log \Psi_+(\alpha) + \log \Psi_-(\alpha). \tag{2.36}$$

After simplification equation (2.36) takes the form

$$\Psi(\alpha) = \Psi_+(\alpha)\Psi_-(\alpha). \tag{2.37}$$

2.5 MALIUZHINETZ'S FUNCTION

Maliuzhinetz function plays a nobel role in the study of diffraction theory by an impedances half planes. The function denoted by $\mathscr{M}_\pi(z)$ and defined as

$$\mathscr{M}_\pi(z) = \exp\left[-\frac{1}{8\pi}\int_0^z \frac{\pi \sin t - 2\sqrt{2}\sin\frac{t}{2} + 2t}{\cos t}\, dt\right], \tag{2.38}$$

known as Maliuzhinetz's function introduced by Maliuzhinetz. Volakis and Senior [82] expressed the Maliuzhinetz's function for small and large complex arguments. For small arguments,

$$\mathscr{M}_\pi(z) = 1 - bz^2 + O(z^4), \tag{2.39}$$

where $b = \frac{1}{16}(1 + \frac{2}{\pi} - \sqrt{2})$. The small complex arguments approximation of Maliuzhinetz's function is, therefore,

$$\mathscr{M}_\pi(z) = 1 - 0.013900388z^2. \tag{2.40}$$

If $\mathfrak{Im}(z) >> 0$, then

$$\mathscr{M}_\pi(z) = 1.05302\left[\cos\frac{1}{4}(z - \iota\ln 2)\right]^{\frac{1}{2}} \qquad \mathfrak{Im}(z) > 8. \tag{2.41}$$

Equations (2.40) and (2.41) must be valid within the strip $0 < z < \frac{\pi}{2}$. For the remaining values of $\mathfrak{Re}(z)$ the $\mathscr{M}_\pi(z)$ relates to its value at the corresponding point within the strip

$$\mathscr{M}_\pi(z) = \left[\mathscr{M}_\pi\left(\frac{\pi}{2}\right)\right]^2 \frac{\cos(\frac{z}{4} - \frac{\pi}{8})}{\mathscr{M}_\pi(z - \pi)}, \tag{2.42}$$

$$\mathscr{M}_\pi(z) = \mathscr{M}_\pi(-z) \tag{2.43}$$

and

$$\bar{\mathscr{M}}_\pi(z) = \mathscr{M}_\pi(\bar{z}), \tag{2.44}$$

where bar complex conjugate. Maliuzhinetz's function is an even regular function of a complex variable z.

2.6 HELMHOLTZ EQUATION IN COLD PLASMA

In order to have a mathematical model for the problems in the subsequent chapters, we first derive the Helmholtz equation in cold plasma. For the reasons Fel-

son and Marcuvits [81] defined the tensor of dielectric permittivity for the cold plasma and expressed the electric field component in term of the magnetic field $H_z(x, y)$ by using the Maxwell's equations along with tensor of dielectric permittivity for the cold plasma as under:

The tensor of dielectric permittivity for the cold plasma is defined as

$$\epsilon = \begin{bmatrix} \epsilon_1 & -\iota\epsilon_2 & 0 \\ \iota\epsilon_2 & \epsilon_1 & 0 \\ 0 & 0 & \epsilon_z \end{bmatrix}, \tag{2.45}$$

with

$$\epsilon_1 = 1 - \left(\frac{\omega_p}{\omega}\right)^2 \left[1 - \left(\frac{\omega_c}{\omega}\right)^2\right]^{-1}, \tag{2.46}$$

$$\epsilon_2 = \left(\frac{\omega_p}{\omega}\right)^2 \left[\frac{\omega}{\omega_c} - \frac{\omega_c}{\omega}\right]^{-1} \tag{2.47}$$

and

$$\epsilon_z = 1 - \left(\frac{\omega_c}{\omega}\right)^2, \tag{2.48}$$

where

$$\omega_p^2 = \frac{N_e e^2}{m\epsilon_0} \tag{2.49}$$

and

$$\omega_c = \frac{|e|\,\mu_0 H_{dc}}{m}. \tag{2.50}$$

Here, e, N_e, m, ω, ω_c, ω_p and H_{dc} represent the electric charge, electron density, electron mass, operating, cyclotron, plasma frequencies and magnitude of the dc magnetic field vector, respectively.

The electric field component in term of the magnetic field are as follow

$$E_x = \frac{\iota\epsilon_1}{\omega\epsilon_0(\epsilon_1^2 - \epsilon_2^2)} \frac{\partial B_z}{\partial y} + \frac{\epsilon_2}{\omega\epsilon_0(\epsilon_1^2 - \epsilon_2^2)} \frac{\partial B_z}{\partial x}, \tag{2.51}$$

$$E_y = \frac{\epsilon_2}{\omega\epsilon_0(\epsilon_1^2-\epsilon_2^2)}\frac{\partial B_z}{\partial y} + \frac{\iota\epsilon_1}{\omega\epsilon_0(\epsilon_1^2-\epsilon_2^2)}\frac{\partial B_z}{\partial x}. \tag{2.52}$$

It is known that Maxwell's equations are valid in plasma so, one can write

$$\nabla \times \vec{E} = \frac{1}{c^2}\frac{\partial^2}{\partial t^2}\vec{B}, \tag{2.53}$$

where

$$\vec{E} = E_x i + E_y j + E_z k \text{ and } \vec{B} = B_x i + B_y j + B_z k\,. \tag{2.54}$$

Thus, using equations (2.51) and (2.52) in equation (2.53), one obtains the required Helmholtz's equation in cold plasma as follow

$$\frac{\partial^2}{\partial x^2}H_z(x,y) + \frac{\partial^2}{\partial y^2}H_z(x,y) + k_{eff}^2 H_z(x,y) = 0, \tag{2.55}$$

with

$$k_{\text{eff}}^2 = k^2\left(\frac{\epsilon_1^2-\epsilon_2^2}{\epsilon_1}\right), \quad k = \omega\sqrt{\epsilon_0\mu_0} \text{ and } B_z = e^{-\iota\omega t}H_z(x,y). \tag{2.56}$$

where the time dependence is assumed to be $e^{-\iota\omega t}$ and k_{eff} depends on k, ϵ_1 and ϵ_2.

2.7 CANONICAL PROBLEM IN COLD PLASMA

In this section we consider a prototype problem arising in cold plasma that concerned with wave scattering in waveguide designed by three semi-infinite plates. The material properties of these plates are impedance, rigid and soft. The rigid plate is defined in term of Neumann boundary condition whereas the soft plat are defined in term of Dirichlet condition. The Winer-Hopf technique along with Mode-Matching technique is used to obtain the approximate solution.

2.7.1 MATHEMATICAL MODEL OF THE PROBLEM

Here, we consider the scattering of a plane wave which is incident with angle θ_0 in the waveguide region in cold plasma formed by two half-planes S_1 define by

$\{(x,y,z)|\ x\in(-\infty,0),\ y=b,\ z\in(-\infty,\infty)\}$ and S_2 defined by $\{(x,y,z)|\ x\in(0,\infty),\ y=0,\ z\in(-\infty,\infty)\}$. The characteristic properties of the upper face of half-plane S_1 is characterized by surface impedance Z and the upper face of the half-plane S_1 is rigid. These two planes are combined by a soft vertical step of hight b as shown in Fig. (2.3):

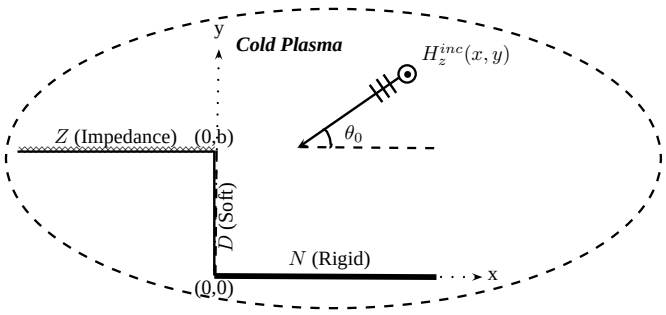

FIGURE 2.3. *The physical configuration of the waveguide structure in cold plasma*

The total field takes the form as under

$$H_z^T(x,y)=\begin{cases} H_z^1(x,y)+H_z^{inc}(x,y)+H_z^{ref}(x,y), & y\in(b,\infty)\\ H_z^2(x,y), & y\in(a,b)\end{cases} \tag{2.57}$$

where $H_z^{inc}(x,y)$ and $H_z^{ref}(x,y)$ stand for incident and reflected field, respectively, given by

$$H_z^{inc}(x,y)=e^{-\iota k_{\mathfrak{eff}}(x\cos\theta_0+y\sin\theta_0)} \tag{2.58}$$

and

$$H_z^{ref}(x,y)=-\frac{1-\eta\sin\theta_0}{1+\eta\sin\theta_0}e^{-\iota k_{\mathfrak{eff}}(x\cos\theta_0-(y-2b)\sin\theta_0)} \tag{2.59}$$

and $\{H_z^j \quad (j=1,2)\}$ satisfying the Helmholtz equation in cold plasma

$$\left[\frac{\partial^2}{\partial x^2}+\frac{\partial^2}{\partial y^2}+k_{\mathfrak{eff}}^2\right]\left[H_z^j(x,y)\right]=0, \tag{2.60}$$

with the following corresponding boundary conditions along with the continuity relations

$$\left(1+\frac{\eta}{\imath k_{\mathfrak{eff}}}\right)H_z^1(x,b)=0, \qquad x\in(-\infty,0), \tag{2.61}$$

$$\frac{\partial}{\partial y}H_z^2(x,0)=0, \qquad x\in(0,\infty), \tag{2.62}$$

$$H_z^2(0,y)=0, \qquad y\in(a,b), \tag{2.63}$$

$$H_z^1(x,\mathfrak{b})+H_z^{inc}(x,b)+H_z^{ref}(x,b)=H_z^2(x,b), \qquad x\in(0,\infty), \tag{2.64}$$

$$\frac{\partial}{\partial y}H_z^1(x,b)+\frac{\partial}{\partial y}H_z^{inc}(x,b)+\frac{\partial}{\partial y}H_z^{ref}(x,b)=\frac{\partial}{\partial y}H_z^2(x,b). \quad x\in(0,\infty). \tag{2.65}$$

The radiation and edge conditions for the uniqueness of the boundary-valued problem defined by the set of equations (2.60) - (2.65) are given by [83].

$$\sqrt{\rho}\left[\frac{\partial}{\partial\rho}H_z^1(x,y)-\imath k_{\mathfrak{eff}}H_z^1(x,y)\right]=0, \quad \rho=\sqrt{x^2+y^2}\to\infty \tag{2.66}$$

and

$$H_z^T(x,y)=\mathcal{O}(|x|^{\frac{1}{2}}), \quad \frac{\partial}{\partial y}H_z^T(x,y)=\mathcal{O}(|x|^{-\frac{1}{2}}), \quad |x|\to 0 \tag{2.67}$$

respectively.

2.7.2 FORMULATION OF WIENER-HOPF EQUATION

Since Helmholtz equation in cold plasma is satisfied by the field $H_z^1(x,y)$ in the region $x\in(-\infty,\infty)$ and $y\in(b,\infty)$ which gives

$$\frac{\partial^2}{\partial x^2}H_z^1(x,y)+\frac{\partial^2}{\partial y^2}H_z^1(x,y)+k_{\mathfrak{eff}}^2H_z^1(x,y)=0. \tag{2.68}$$

The Fourier transform of equation (2.68) with respect to x yields

$$\left[\frac{\partial^2}{\partial y^2}+(k_{\mathfrak{eff}}^2-\alpha^2)\right]F(\alpha,y)=0, \tag{2.69}$$

where

$$F(\alpha, y) = \int_{-\infty}^{\infty} H_z^1(x, y) e^{\iota \alpha x} dx. \tag{2.70}$$

Using additive decomposition theorem $F(\alpha, y)$ can be decomposed as

$$F(\alpha, y) = F_-(\alpha, y) + F_+(\alpha, y), \tag{2.71}$$

where

$$F_\pm(\alpha, y) = \pm \int_{0}^{\pm\infty} H_z^1(x, y) e^{\iota \alpha} dx. \tag{2.72}$$

It is assumed that $F_+(\alpha, y)$ and $F_-(\alpha, y)$ are regular functions of α in the half-plane $\Im\mathfrak{m}(\alpha) > \Im\mathfrak{m}(k_{\mathfrak{eff}} \cos\theta_0)$ and $\Im\mathfrak{m}(\alpha) < \Im\mathfrak{m}(k_{\mathfrak{eff}})$, respectively.

The general solution of equation (2.69) satisfying the radiation condition represented by equations (2.66) yields

$$F(\alpha, y) = A(\alpha) e^{\iota \mathfrak{L}(\alpha)(y-b)}, \tag{2.73}$$

where

$$\mathfrak{L}(\alpha) = \sqrt{k_{\mathfrak{eff}}^2 - \alpha^2}. \tag{2.74}$$

The square-root function $\mathfrak{L}(\alpha) = \sqrt{k_{\mathfrak{eff}}^2 - \alpha^2}$ is defined in the complex α-plane with branch cuts along $\alpha = k_{\mathfrak{eff}}$ to $\alpha = k_{\mathfrak{eff}} + \iota\infty$ and $\alpha = -k_{\mathfrak{eff}}$ to $\alpha = -k_{\mathfrak{eff}} - \iota\infty$ such that $\mathfrak{L}(0) = k_{\mathfrak{eff}}$ as shown in the Fig. (2.4).

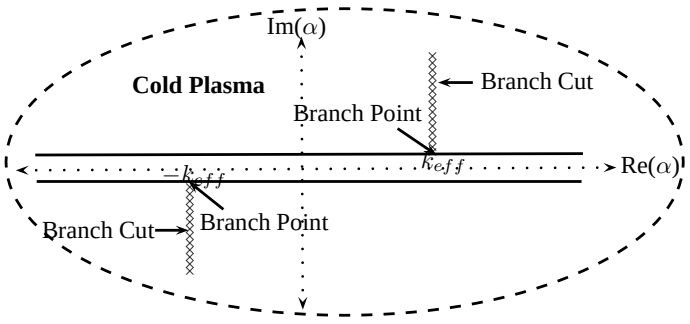

FIGURE 2.4. *The depiction of Branch cuts*

To find the unknown coefficient $A(\alpha)$, we can use the transformed form of boundary condition represented by equation (2.61) which gives

$$A(\alpha) = \frac{k_{\text{eff}}}{\mathfrak{L}(\alpha)} \mathscr{R}_+(\alpha)\chi(\eta,\alpha), \tag{2.75}$$

with

$$\mathscr{R}_+(\alpha) = F_+(\alpha,b) + \frac{\eta}{\imath k_{\text{eff}}} F_+'(\alpha,b) \tag{2.76}$$

and

$$\chi(\eta,\alpha) = \frac{\mathfrak{L}(\alpha)}{\eta\mathfrak{L}(\alpha) + k_{\text{eff}}} \ , \tag{2.77}$$

where the prime sign in equation (2.75) denotes the derivative with respect to y. Replacing equations (2.71) and (2.75) in equation (2.73), one gets

$$F_-(\alpha,y) + F_+(\alpha,y) = \frac{k_{\text{eff}}}{\mathfrak{L}(\alpha)} \mathscr{R}_+(\alpha)\chi_(\eta,\alpha) e^{\imath\mathfrak{L}(\alpha)(y-b)}. \tag{2.78}$$

In the region $x \in (0,\infty)$ and $y \in (a,b)$, $H_z^2(x,y)$ satisfies the Helmholtz equation in cold plasma gives

$$\frac{\partial^2}{\partial x^2} H_z^2(x,y) + \frac{\partial^2}{\partial y^2} H_z^2(x,y) + k_{\text{eff}}^2 H_z^2(x,y) = 0. \tag{2.79}$$

On multiplying equation (2.79) by $e^{\imath\alpha x}$ and integrating with respect to x from 0 to ∞, one obtains

$$\left[\frac{\partial^2}{\partial y^2} + \mathfrak{L}^2(\alpha)\right] \mathscr{G}_+(\alpha,y) = \mathfrak{f}(y), \tag{2.80}$$

with

$$\mathfrak{f}(y) = \frac{\partial}{\partial x} H_z^2(0,y) \tag{2.81}$$

and $\mathscr{G}_+(\alpha,y)$ is defined by

$$\mathscr{G}_+(\alpha,y) = \int_0^\infty H_z^2(x,y) e^{\imath\alpha x}\, dx, \tag{2.82}$$

which is a regular function in the half-plane.

The general solution of the non homogenous differential equation (2.80) can be obtained by using the method of variation of parameter as follow

$$\mathscr{G}_+(\alpha, y) = B(\alpha)\cos\mathfrak{L}(\alpha)y + C(\alpha)\sin\mathfrak{L}(\alpha)y + \frac{1}{\mathfrak{L}(\alpha)}\int_0^y \mathfrak{f}(t)\sin\mathfrak{L}(\alpha)(y-t)\,dt, \tag{2.83}$$

where $B(\alpha)$ and $C(\alpha)$ are the unknown spectral coefficients and $\mathfrak{L}(\alpha)$ is defined in equation (2.74).

Combining the transformed form of the boundary condition represented by the equation (2.62) and equation (2.83) gives

$$\mathscr{G}_+(\alpha, y) = B(\alpha)\cos\mathfrak{L}(\alpha)y + \frac{1}{\mathfrak{L}(\alpha)}\int_0^y \mathfrak{f}(t)\sin\mathfrak{L}(\alpha)(y-t)\,dt. \tag{2.84}$$

In the above expression $B(\alpha)$ can be obtained by adding the transformed form of equations (2.64) and $\frac{\eta}{\imath k_{\mathfrak{eff}}}$ time of (2.65) as under

$$B(\alpha) = \frac{\mathscr{R}_+(\alpha)}{\mathscr{W}(\alpha)} + \frac{1}{\mathscr{W}(\alpha)}\int_0^b \mathfrak{f}(t)\left(\frac{\sin\mathfrak{L}(\alpha)(b-t)}{\mathfrak{L}(\alpha)} + \frac{\eta}{\imath k_{\mathfrak{eff}}}\cos\mathfrak{L}(\alpha)(b-t)\right)dt, \tag{2.85}$$

where

$$\mathscr{W}(\alpha) = \cos\mathfrak{L}(\alpha)b - \frac{\eta}{\imath k_{\mathfrak{eff}}}\mathfrak{L}(\alpha)\sin\mathfrak{L}(\alpha)b. \tag{2.86}$$

Using equation (2.85) in equation (2.84), one gets

$$\begin{aligned}\mathscr{G}_+(\alpha, y) = &\frac{\cos\mathfrak{L}(\alpha)y}{\mathscr{W}(\alpha)}\left[\mathscr{R}_+(\alpha) - \int_0^b \mathfrak{f}(t)\left(\frac{\sin\mathfrak{L}(\alpha)(b-t)}{\mathfrak{L}(\alpha)} + \frac{\eta}{\imath k_{\mathfrak{eff}}}\cos\mathfrak{L}(\alpha)(b-t)\right)dt\right] \\ &+ \frac{1}{\mathfrak{L}(\alpha)}\int_0^y \mathfrak{f}(t)\sin\mathfrak{L}(\alpha)(b-t)\,dt.\end{aligned} \tag{2.87}$$

The left-hand side (i.e., $\mathscr{G}_+(\alpha, y)$) of the equation (2.87) is analytic in the upper half-plane $\mathfrak{Im}(\alpha) > \mathfrak{Im}(k_{\mathfrak{eff}}\cos\theta_0)$. However, the analyticity of the right-hand side

is violated by the appearance of simple poles lying at the zeros of $\mathscr{W}(\alpha)$, i.e., $\alpha = \pm\alpha_m$ satisfying

$$\mathscr{W}(\pm\alpha_m) = 0, \quad \Im\mathfrak{m}(\alpha_m) > \Im\mathfrak{m}(k_{eff}), \qquad m = 1,2,3.... \tag{2.88}$$

The poles in the equation (2.87) can be removed by using the condition that the residues of these poles are zero. Then from equation (2.87), it is found that

$$\mathscr{R}_+(\alpha_m) = \mathscr{D}_m\left(\frac{\sin\mathfrak{L}_m b}{\mathfrak{L}_m} + \frac{\eta}{\imath k_{\mathfrak{eff}}}\cos\mathfrak{L}_m b\right)\mathfrak{f}_m, \tag{2.89}$$

where $\mathfrak{f}_m$ is defined by

$$\mathfrak{f}(t) = \sum_{n=1}^{\infty}\mathfrak{f}_m\cos\mathfrak{L}_m t, \tag{2.90}$$

with

$$\mathfrak{L}_m = \sqrt{k_{\mathfrak{eff}}^2 - \alpha_m^2} \tag{2.91}$$

and

$$\mathscr{D}_m = \frac{\mathfrak{L}_m\sin\mathfrak{L}_m b}{2\alpha_m}\frac{\partial}{\partial\alpha}\mathscr{W}(\alpha_m). \tag{2.92}$$

Combining equations (2.87) and (2.78) with the help of the transformed domain of continuity relation given by equation (2.65), one can obtain

$$\begin{aligned}\imath k_{\mathfrak{eff}}\mathscr{R}_+(\alpha)\chi(\eta,\alpha) - \overset{\prime}{F}_-(\alpha,b) &= -\frac{2k_{\mathfrak{eff}}\sin\theta_0 e^{-\imath k_{\mathfrak{eff}} b\sin\theta_0}}{(\eta\sin\theta_0+1)(\alpha - k_{\mathfrak{eff}}\cos\theta_0)}\\ &+ \frac{\mathfrak{L}(\alpha)\sin\mathfrak{L}(\alpha)b}{\mathscr{W}(\alpha)}\left[\mathscr{R}_+(\alpha) - \int_0^b \mathfrak{f}(t)\left(\frac{\sin\mathfrak{L}(\alpha)(b-t)}{\mathfrak{L}(\alpha)} + \frac{\eta}{\imath k_{\mathfrak{eff}}}\cos\mathfrak{L}(\alpha)(b-t)\right)dt\right]\\ &+ \int_0^b \mathfrak{f}(t)\cos\mathfrak{L}(\alpha)(b-t)\,dt.\end{aligned} \tag{2.93}$$

After simplification the above expression can take the form

$$\frac{\iota k_{\mathfrak{eff}}\mathscr{R}_+(\alpha)\chi(\eta,\alpha)}{\mathscr{N}(\alpha)} - \overset{\prime}{F}_-(\alpha,b) = -\frac{2k_{\mathfrak{eff}}\sin\theta_0 e^{-\iota k_{\mathfrak{eff}} b\sin\theta_0}}{(\eta\sin\theta_0+1)(\alpha-k_{\mathfrak{eff}}\cos\theta_0)}$$
$$+\frac{1}{\mathscr{W}(\alpha)}\int_0^b \mathfrak{f}(t)\cos\mathfrak{L}(\alpha)t\,dt, \tag{2.94}$$

where

$$\mathscr{N}(\alpha) = \mathscr{W}(\alpha)e^{\iota\mathfrak{L}(\alpha)b}. \tag{2.95}$$

Using equation (2.90) in equation (2.94), one obtains the required Wiener-Hopf equation valid in the strip $\mathfrak{Im}(-k_{\mathfrak{eff}}) < \mathfrak{Im}(\alpha) < \mathfrak{Im}(k_{\mathfrak{eff}})$ as follows:

$$\frac{\iota k_{\mathfrak{eff}}\chi(\eta,\alpha)\mathscr{R}_+(\alpha)}{\mathscr{N}(\alpha)} - \overset{\prime}{F}_-(\alpha,b) = -\frac{2k_{\mathfrak{eff}}\sin\theta_0 e^{-\iota k_{\mathfrak{eff}} b\sin\theta_0}}{(\eta_2\sin\theta_0+1)(\alpha-k_{\mathfrak{eff}}\cos\theta_0)}$$
$$+\sum_{m=1}^{\infty}\frac{\mathfrak{L}_m\sin\mathfrak{L}_m b\mathfrak{f}_m}{\alpha^2-\alpha_m^2}. \tag{2.96}$$

2.7.3 SOLUTION OF WIENER-HOPF EQUATION

To solve the Wiener-Hopf equation, the kernel functions $\mathscr{N}(\alpha)$ and $\chi(\eta,\alpha)$ in equation (2.96) can be factorized by using the known results as following [8]:

$$\mathscr{N}_+(\alpha) = \left[\cos k_{\mathfrak{eff}}b + \iota\eta\sin k_{\mathfrak{eff}}b\right]^{\frac{1}{2}}$$
$$\times\exp\left[\frac{\mathfrak{L}(\alpha)b}{\pi}\ln\left(\frac{\alpha+\iota\mathfrak{L}(\alpha)}{k_{\mathfrak{eff}}}\right)+\frac{\iota\alpha b}{\pi}\left(1-C+\ln\left[\frac{2\pi}{k_{\mathfrak{eff}}b}\right]+\iota\frac{\pi}{2}\right)\right]\prod_{m=1}^{\infty}\left(1+\frac{\alpha}{\alpha_m}\right)e^{\frac{\iota\alpha b}{m\pi}}, \tag{2.97}$$

and

$$\mathscr{N}_-(\alpha) = \mathscr{N}_+(-\alpha). \tag{2.98}$$

In equation (2.97), C denotes the Euler-Mascheroni constant given by $C = 0.5772156649....$ Similarly the factor of $\chi(\eta,\alpha)$ can be expressed in the form of the Maliuzhinetz's function [82] as follows

$$\chi_{-}(\eta, k_{\mathfrak{eff}}\cos\theta) = \frac{4[\mathscr{M}_{\pi}(3\pi/2-\theta-\psi)\mathscr{M}_{\pi}(\pi/2-\theta+\psi)]^{2}\sin(\theta/2)}{\sqrt{\eta}[\mathscr{M}_{\pi}(\pi/2)]^{4}\times\left(1+\sqrt{2}\cos[\frac{3\pi/2-\theta-\psi}{2}]\right)\left(1+\sqrt{2}\cos[\frac{\pi/2-\theta+\psi}{2}]\right)} \tag{2.99}$$

and

$$\chi_{+}(\eta, k_{\mathfrak{eff}}\cos\theta) = \chi_{-}(\eta, -k_{\mathfrak{eff}}\cos\theta), \tag{2.100}$$

with $\mathscr{M}_{\pi}(z)$ and ψ are defined by

$$\mathscr{M}_{\pi}(z) = \exp\left[-\frac{1}{8\pi}\int_{0}^{z}\frac{\pi\sin u - 2\sqrt{2}\pi\sin(u/2)+2u}{\cos u}du\right] \tag{2.101}$$

and

$$\eta = \sin^{-1}\left(\frac{1}{\psi}\right). \tag{2.102}$$

Now, multiplying the Wiener-Hopf equation (2.96) on both sides with $\frac{\mathscr{N}_{-}(\alpha)}{\chi_{-}(\eta,\alpha)}$, one obtains

$$\frac{\iota k_{\mathfrak{eff}}\chi_{+}(\eta,\alpha)\mathscr{R}_{+}(\alpha)}{\mathscr{N}_{+}(\alpha)} - \frac{\mathscr{N}_{-}(\alpha)}{\chi_{-}(\eta,\alpha)}F'_{-}(\alpha,b) = -\frac{2k_{\mathfrak{eff}}\sin\theta_{0}e^{-\iota k_{\mathfrak{eff}}b\sin\theta_{0}}\mathscr{N}_{-}(\alpha)}{(\eta\sin\theta_{0}+1)(\alpha-k_{\mathfrak{eff}}\cos\theta_{0})\chi_{-}(\eta,\alpha)} + \sum_{m=1}^{\infty}\frac{\mathfrak{L}_{m}\sin\mathfrak{L}_{m}b\mathfrak{f}_{m}\mathscr{N}_{-}(\alpha)}{(\alpha^{2}-\alpha_{m}^{2})\chi_{-}(\eta,\alpha)}. \tag{2.103}$$

With the help of Cauchy's integral formula the terms at right-hand side of the equation (2.103) can be decomposed as

$$\begin{aligned}&\frac{2k_{\mathfrak{eff}}\sin\theta_{0}e^{-\iota k_{\mathfrak{eff}}b\sin\theta_{0}}\mathscr{N}_{-}(\alpha)}{(\eta\sin\theta_{0}+1)(\alpha-k_{\mathfrak{eff}}\cos\theta_{0})\chi_{-}(\eta_{2},\alpha)}\\ &=\frac{2k_{\mathfrak{eff}}\sin\theta_{0}e^{-\iota k_{\mathfrak{eff}}b\sin\theta_{0}}}{(\eta\sin\theta_{0}+1)(\alpha-k_{\mathfrak{eff}}\cos\theta_{0})}\left[\frac{\mathscr{N}_{-}(\alpha)}{\chi_{-}(\eta,\alpha)}-\frac{\mathscr{N}_{-}(k_{\mathfrak{eff}}\cos\theta_{0})}{\chi_{-}(\eta,k_{\mathfrak{eff}}\cos\theta_{0})}\right]\\ &+\frac{2k_{\mathfrak{eff}}\sin\theta_{0}e^{-\iota k_{\mathfrak{eff}}b\sin\theta_{0}}\mathscr{N}_{-}(k_{\mathfrak{eff}}\cos\theta_{0})}{(\eta\sin\theta_{0}+1)(\alpha-k_{\mathfrak{eff}}\cos\theta_{0})\chi_{-}(\eta,k_{\mathfrak{eff}}\cos\theta_{0})}\end{aligned} \tag{2.104}$$

and

$$\sum_{m=1}^{\infty}\frac{\mathfrak{L}_m\sin\mathfrak{L}_m b\mathscr{N}_-(\alpha)\mathfrak{f}_m}{(\alpha^2-\alpha_m^2)\chi_-(\eta,\alpha)}=\sum_{m=1}^{\infty}\frac{\mathfrak{L}_m\sin\mathfrak{L}_m b\mathfrak{f}_m}{(\alpha+\alpha_m)}$$
$$\times\left[\frac{\mathscr{N}_-(\alpha)}{(\alpha-\alpha_m)\chi_-(\eta,\alpha)}-\frac{\mathscr{N}_+(\alpha_m)}{2\alpha_m\chi_+(\eta,\alpha_m)}\right]+\sum_{m=1}^{\infty}\frac{\mathfrak{L}_m\sin\mathfrak{L}_m b\mathscr{N}_+(\alpha_m)\mathfrak{f}_m}{2\alpha_m(\alpha+\alpha_m)\chi_+(\eta,\alpha_m)}. \tag{2.105}$$

Now using equations (2.104) and (2.105) in equation (2.103), then placing the terms which are analytic in the upper half-plane ($\mathfrak{Im}(\alpha)>-k_{\mathfrak{eff}}$)and those which analytic in lower half-plane ($\mathfrak{Im}(\alpha)<k_{\mathfrak{eff}}$) at the right-hand side,which yields

$$\frac{\iota k_{\mathfrak{eff}}\chi_+(\eta,\alpha)\mathscr{R}_+(\alpha)}{\mathscr{N}_+(\alpha)}+\frac{2k_{\mathfrak{eff}}\sin\theta_0 e^{-\iota k_{\mathfrak{eff}}b\sin\theta_0}\mathscr{N}_-(k_{\mathfrak{eff}}\cos\theta_0)}{(\eta\sin\theta_0+1)(\alpha-k_{\mathfrak{eff}}\cos\theta_0)\chi_-(\eta,k_{\mathfrak{eff}}\cos\theta_0)}$$
$$-\sum_{m=1}^{\infty}\frac{\mathfrak{L}_m\sin\mathfrak{L}_m b\mathscr{N}_+(\alpha_m)\mathfrak{f}_m}{2\alpha_m(\alpha+\alpha_m)\chi_+(\eta,\alpha_m)}=\frac{\mathscr{N}_-(\alpha)}{\chi_-(\eta,\alpha)}\overset{\prime}{F}_-(\alpha,b)$$
$$-\frac{2k_{\mathfrak{eff}}\sin\theta_0 e^{-\iota k_{\mathfrak{eff}}b\sin\theta_0}}{(\eta\sin\theta_0+1)(\alpha-k_{\mathfrak{eff}}\cos\theta_0)}\left[\frac{\mathscr{N}_-(\alpha)}{\chi_-(\eta,\alpha)}-\frac{\mathscr{N}_-(k_{\mathfrak{eff}}\cos\theta_0)}{\chi_-(\eta,k_{\mathfrak{eff}}\cos\theta_0)}\right]$$
$$+\sum_{m=1}^{\infty}\frac{\mathfrak{L}_m\sin\mathfrak{L}_m b\mathfrak{f}_m}{(\alpha+\alpha_m)}\left[\frac{\mathscr{N}_-(\alpha)}{(\alpha-\alpha_m)\chi_-(\eta,\alpha)}-\frac{\mathscr{N}_+(\alpha_m)}{2\alpha_m\chi_+(\eta,\alpha_m)}\right]. \tag{2.106}$$

The required solution of Wiener-Hopf equation can be obtained by using analytical continuation principle complying the extended Liouville's theorem as under

$$\frac{\chi_+(\eta,\alpha)\mathscr{R}_+(\alpha)}{\mathscr{N}_+(\alpha)}=\frac{2\iota\sin\theta_0 e^{-\iota k_{\mathfrak{eff}}b\sin\theta_0}\mathscr{N}_-(k_{\mathfrak{eff}}\cos\theta_0)}{(\eta\sin\theta_0+1)(\alpha-k_{\mathfrak{eff}}\cos\theta_0)\chi_-(\eta,k_{\mathfrak{eff}}\cos\theta_0)}$$
$$-\sum_{m=1}^{\infty}\frac{\iota\mathfrak{L}_m\sin\mathfrak{L}_m b\mathscr{N}_+(\alpha_m)\mathfrak{f}_m}{2k_{\mathfrak{eff}}\alpha_m(\alpha+\alpha_m)\chi_+(\eta,\alpha_m)}. \tag{2.107}$$

Placing equation (2.89) into equation (2.107), gives

$$\frac{\mathscr{D}_n\chi_+(\eta,\alpha_n)}{\mathscr{N}_+(\alpha_n)}\left(\frac{\sin\mathfrak{L}_n b}{\mathfrak{L}_n}+\frac{\eta}{\iota k_{\mathfrak{eff}}}\cos\mathfrak{L}_n b\right)\mathfrak{f}_n$$
$$=\frac{2\iota\sin\theta_0 e^{-\iota k_{\mathfrak{eff}}b\sin\theta_0}\mathscr{N}_-(k_{\mathfrak{eff}}\cos\theta_0)}{(\eta\sin\theta_0+1)(\alpha_n-k_{\mathfrak{eff}}\cos\theta_0)\chi_-(\eta,k_{\mathfrak{eff}}\cos\theta_0)}$$
$$-\sum_{m=1}^{\infty}\frac{\iota\mathfrak{L}_m\sin\mathfrak{L}_m b\mathscr{N}_+(\alpha_m)\mathfrak{f}_m}{2k_{\mathfrak{eff}}\alpha_m(\alpha_n+\alpha_m)\chi_+(\eta,\alpha_m)}. \tag{2.108}$$

The above expression is system of infinite number of equation and these system of equation can be solved numerically after truncating after N terms.

2.7.4 THE DIFFRACTED FIELD

The required diffracted field $H_z^1(x,y)$ can be acquired by using the inverse Fourier transform of $F(\alpha,y)$. Thus from equation (2.78), one can get

$$H_z^1(x,y)=\frac{1}{2\pi}\int_{\mathscr{L}}\frac{k_{\mathfrak{eff}}\chi(\eta,\alpha)\mathscr{R}_+(\alpha)}{\mathfrak{L}(\alpha)}e^{\iota\mathfrak{L}(\alpha)(y-b)}e^{-\iota\alpha x}d\alpha. \tag{2.109}$$

Using the replacement of the function $\chi(\eta,\alpha)$ and the variables $\alpha=-k_{\mathfrak{eff}}\cos t$, $x=\rho\cos\theta$ and $y=\rho\sin\theta$ in the equation (2.109), one obtains

$$H_z^1(\rho,\theta)=\frac{1}{2\pi}\int_{\mathscr{L}}\frac{\mathscr{R}_+(-k_{\mathfrak{eff}}\cos t)}{1+\eta\sin t}e^{-\iota k_{\mathfrak{eff}}b\sin t+\iota k_{\mathfrak{eff}}\rho\cos(t-\theta)}k_{\mathfrak{eff}}\sin t\,dt. \tag{2.110}$$

The asymptotic evaluation of the integral in the equation (2.110) can be obtained via saddle-point technique. Here, saddle-point rests at $t=\theta$ which gives

$$\begin{aligned}H_z^1(\rho,\theta)=&\frac{\sin\theta e^{-\iota k\sqrt{(\epsilon_1^2-\epsilon_2^2)/\epsilon_1}\rho+\frac{\iota 3\pi}{4}-\iota k\sqrt{(\epsilon_1^2-\epsilon_2^2)/\epsilon_1}b\sin\theta}}{\sqrt{2\pi}\sqrt{k\rho\sqrt{(\epsilon_1^2-\epsilon_2^2)/\epsilon_1}}(1+\eta\sin\theta)}\\
&\times\left[\frac{2\iota\sin\theta_0 e^{-\iota k\sqrt{(\epsilon_1^2-\epsilon_2^2)/\epsilon_1}b\sin\theta_0}\mathscr{N}_-(k\sqrt{(\epsilon_1^2-\epsilon_2^2)/\epsilon_1}\cos\theta_0)\mathscr{N}_-(k\sqrt{(\epsilon_1^2-\epsilon_2^2)/\epsilon_1}\cos\theta)}{(\eta\sin\theta+1)(\cos\theta+\cos\theta_0)\chi_-(\eta,k\sqrt{(\epsilon_1^2-\epsilon_2^2)/\epsilon_1}\cos\theta_0)\chi_-(\eta,k\sqrt{(\epsilon_1^2-\epsilon_2^2)/\epsilon_1}\cos\theta)}\right.\\
&\left.-\sum_{m=1}^{\infty}\frac{\iota\mathfrak{L}_m\sin\mathfrak{L}_m b\mathscr{N}_+(\alpha_m)\mathscr{N}_-(k\sqrt{(\epsilon_1^2-\epsilon_2^2)/\epsilon_1}\cos\theta)\mathfrak{f}_m}{2k\sqrt{(\epsilon_1^2-\epsilon_2^2)/\epsilon_1}\alpha_m(\alpha_m-k\sqrt{(\epsilon_1^2-\epsilon_2^2)/\epsilon_1}\cos\theta)\chi_+(\eta,\alpha_m)\chi_-(\eta,k\sqrt{(\epsilon_1^2-\epsilon_2^2)/\epsilon_1}\cos\theta)}\right].\end{aligned} \tag{2.111}$$

2.7.5 COMPUTATIONAL RESULTS AND DISCUSSION

In this section, we have analyzed the numerical results for various physical parameters of interest by plotting graphs. Fig. (2.5) depicts the variation in the

diffracted field amplitude versus the truncation number "N". It is apparent that the effect of the truncation number is negligible for $N \geq 40$. Hence, the system containing infinite number of algebraic equations represented by the equation (2.108) can be managed to deal as finite. Where as the Fig. (2.6) has been plotted by varying the plate separations "b". The amplitude of the diffracted field decreases with increase in b. Fig. (2.7) depicts the variations of diffracted fields versus incident angle θ_0 ($0^o \leq \theta_0 \leq 90^o$). It is interesting to note that the value of diffracted field amplitude lies at 90^o when $\theta_0 = 90^o$. Where as this peak values moves to 120^o and 150^o for $\theta_0 = 60^o$ and $\theta_0 = 30^o$, respectively. As long as the angle of incident increases the center of diffracted field amplitude shifted towards 90^0. Fig. (2.8) shows the variation in the diffracted field amplitude versus the impedance "η". The variation in the diffracted field amplitude versus effect of cold plasma permittivity values for ϵ_1 and ϵ_2 have been analyzed in Figs. (2.9) and (2.10), respectively. Here it is noted that the amplitude of the diffracted field decreases by increasing the value of ϵ_1 where as slightly increases by increasing ϵ_2 but the effect of ϵ_2 is negligible as compare with ϵ_1.

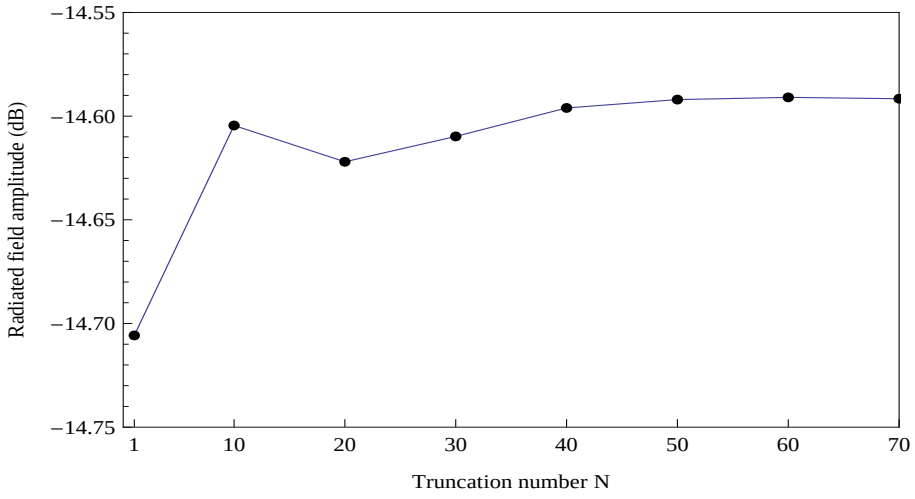

FIGURE 2.5. *Variation in the diffracted field amplitude versus "N" at $k = 5$, $\theta_0 = 90^o$, $\theta = 60^o$, $\eta = 0.3\iota$, $\epsilon_1 = 0.8$, $\epsilon_2 = 0.1$ and $b = 0.2\lambda$.*

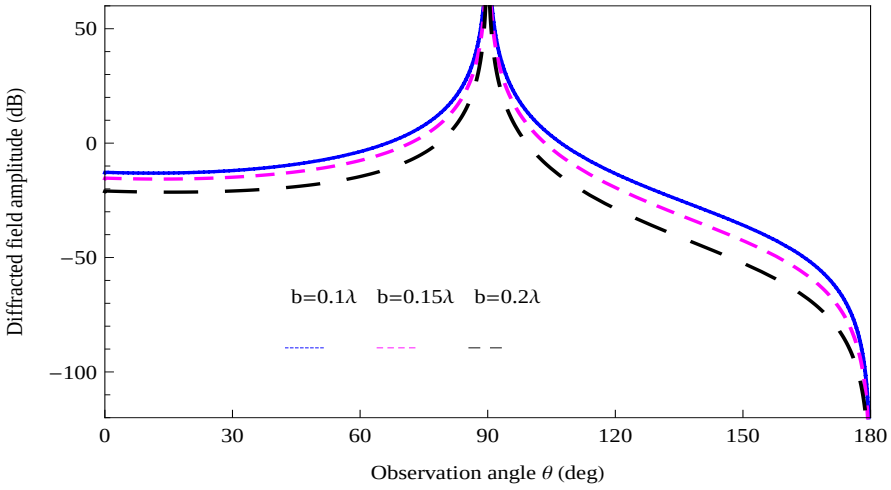

FIGURE 2.6. *Variation in the diffracted field amplitude versus "b" at* $k = 5$, $\theta_0 = 90^o$, $\eta = 0.7\iota$, $\epsilon_1 = 0.8$ *and* $\epsilon_2 = 0.1$.

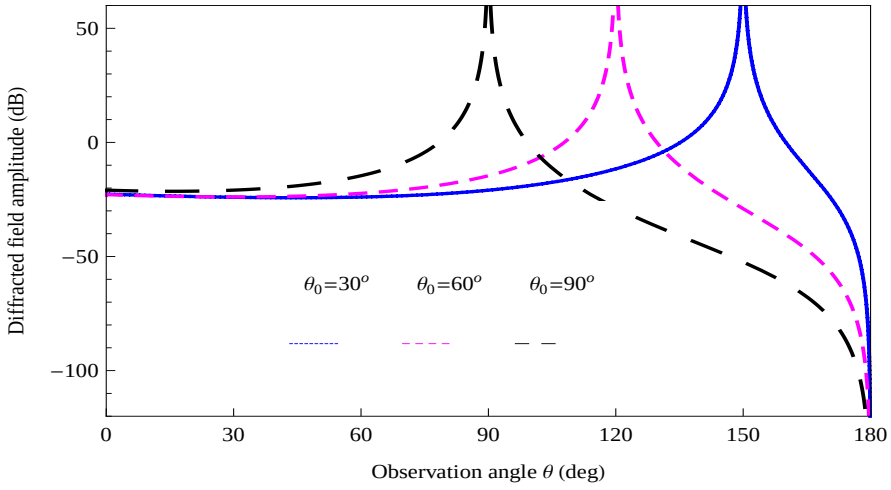

FIGURE 2.7. *Variation in the diffracted field amplitude versus "*θ_0*" at* $k = 5$, $\eta = 0.7\iota$, $\epsilon_1 = 0.8$, $\epsilon_2 = 0.1$ *and* $b = 0.2\lambda$.

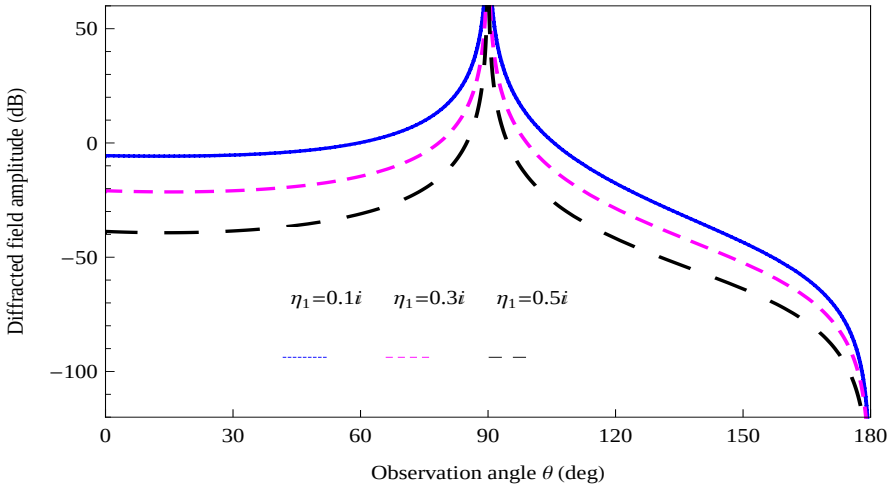

FIGURE 2.8. *Variation in the diffracted field amplitude versus "η" at $\theta_0 = 90^0$, $k = 5$, $\epsilon_1 = 0.8$, $\epsilon_2 = 0.1$ and $b = 0.2\lambda$.*

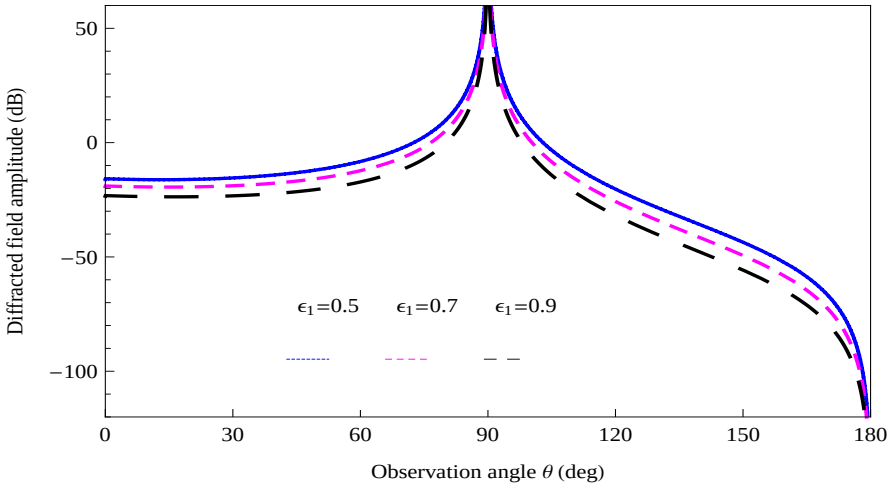

FIGURE 2.9. *Variation in the diffracted field amplitude versus "ϵ_1" at $k = 5$, $\theta_0 = 90^o$, $\eta = 0.7\iota$, $\epsilon_2 = 0.1$ and $b = 0.2\lambda$.*

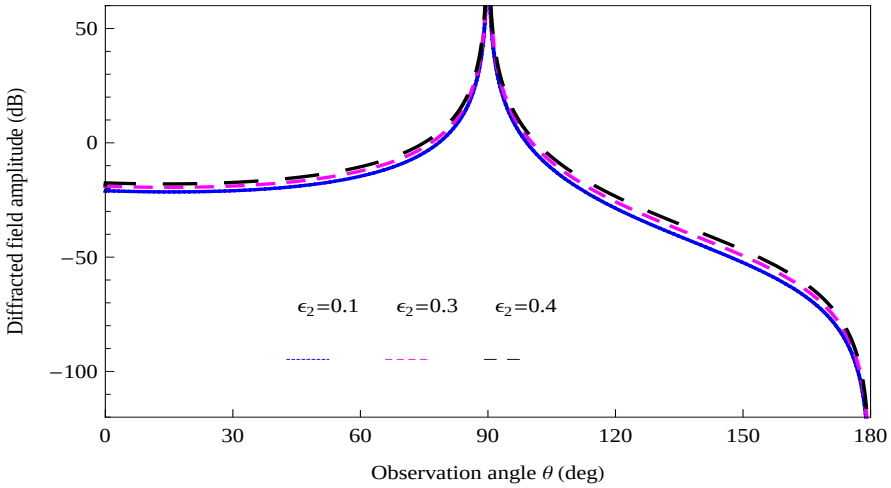

FIGURE 2.10. *Variation in the diffracted field amplitude versus "ϵ_2" at* $k = 5$, $\theta_0 = 90^o$, $\eta = 0.7\iota$, $\epsilon_1 = 0.8$ *and* $b = 0.2\lambda$.

CHAPTER 3

EFFECT OF COLD PLASMA PERMITTIVITY ON SCATTERING OF E-POLARIZED PLANE WAVE BY AN IMPEDANCE LOADED STEP

In this chapter, the scattering of E-polarized plane wave by two half-planes combined by a step of hight b is discussed. These types of geometries play a vital role in diffraction theory and many problems in science and engineering. Initially, Johansen [84] considered the problem of diffraction by two half-planes having same surfaces impedances combined by a step of hight h. After that Büyükaksoy and Birbir [85] studied the similar geometry for different impedances of the different surfaces. Yener and Serbest [11] considered the diffraction phenomenon in cold plasma considering by a single surface impedance half-plane. Here, in this chapter two half-planes of different surface impedances joined by rigid vertical step of hight b located in cold plasma is considered.

The contents of this chapter are organized in the following order. The boundary-valued problem is developed in Section (3.1) whereas Section (3.2) is dedicated to the formulation of Wiener-Hopf equation. The solution of Wiener-Hopf equation is obtained in Section (3.3). The diffracted field expression is shown in Section (3.4). Few numerical results for different parameters are plotted and discussed in the last Section (3.5).

3.1 MATHEMATICAL MODEL OF THE PROBLEM IN COLD PLASMA

Here, consider the scattering of a plane wave making an incident angle θ_0 in the region designed by two half-planes S_1 define by $\{(x,y,z)|\ x \in (-\infty,0),\ y=0,\ z \in (-\infty,\infty)\}$ and S_2 defined by $\{(x,y,z)|\ x \in (0,\infty),\ y=b,\ z \in (-\infty,\infty)\}$. The top faces of the half-planes S_1 and S_2 are characterized by the impedances Z_1 and Z_2, respectively. While vertical step surface is rigid as shown in Fig. (3.1):

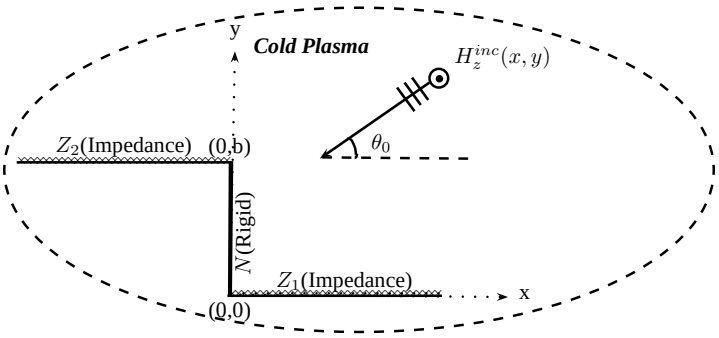

FIGURE 3.1. *Geometrical configuration of the waveguide structure in cold plasma*

The total field takes the form as under

$$H_z^T(x,y) = \begin{cases} H_z^1(x,y) + H_z^{inc}(x,y) + H_z^{ref}(x,y), & y \in (b,\infty) \\ H_z^2(x,y), & y \in (a,b) \end{cases} \tag{3.1}$$

where $H_z^{inc}(x,y)$ and $H_z^{ref}(x,y)$ stand for the incident and reflected fields, respectively, given by

$$H_z^{inc}(x,y) = e^{-\iota k_{\epsilon\mathfrak{f}\mathfrak{f}}(x\cos\theta_0 + y\sin\theta_0)} \tag{3.2}$$

and

$$H_z^{ref}(x,y) = -\frac{1-\eta_2\sin\theta_0}{1+\eta_2\sin\theta_0} e^{-\iota k_{\epsilon\mathfrak{f}\mathfrak{f}}(x\cos\theta_0 - (y-2b)\sin\theta_0)}, \tag{3.3}$$

with

$$k_{\epsilon\mathfrak{f}\mathfrak{f}} = k\sqrt{(\epsilon_1^2 - \epsilon_2^2)/\epsilon_1}. \tag{3.4}$$

$\{H_z^j \quad (j=1,2)\}$ satisfying the Helmholtz equation in cold plasma, i.e.,

$$\left[\frac{\partial^2}{\partial x^2}+\frac{\partial^2}{\partial y^2}+k_{\text{eff}}^2\right]\left[H_z^j(x,y)\right]=0, \tag{3.5}$$

with the following corresponding boundary conditions and continuity relations

$$\left(1+\frac{\eta_2}{\iota k_{\text{eff}}}\frac{\partial}{\partial y}\right)H_z^1(x,b)=0, \qquad x\in(-\infty,0) \tag{3.6}$$

$$\left(1+\frac{\eta_1}{\iota k_{\text{eff}}}\frac{\partial}{\partial y}\right)H_z^2(x,0)=0, \qquad x\in(0,\infty) \tag{3.7}$$

$$\frac{\partial}{\partial x}H_z^2(0,y)=0, \qquad y\in(0,b) \tag{3.8}$$

$$H_z^1(x,b)+H_z^{inc}(x,b)+H_z^{ref}(x,b)=H_z^2(x,b), \qquad x\in(0,\infty) \tag{3.9}$$

$$\frac{\partial}{\partial y}H_z^1(x,b)+\frac{\partial}{\partial y}H_z^{inc}(x,b)+\frac{\partial}{\partial y}H_z^{ref}(x,b)=\frac{\partial}{\partial y}H_z^2(x,b). \qquad x\in(0,\infty) \tag{3.10}$$

The radiation and edge conditions for the uniqueness of the boundary-valued problem defined by the set of equations (3.5) - (3.10) are given by

$$\sqrt{\rho}\left[\frac{\partial}{\partial\rho}H_z^1(x,y)-\iota k_{\text{eff}}H_z^1(x,y)\right]=0, \quad \rho=\sqrt{x^2+y^2}\to\infty \tag{3.11}$$

and

$$H_z^T(x,y)=\mathcal{O}(|x|^{\frac{1}{2}}), \quad \frac{\partial}{\partial y}H_z^T(x,y)=\mathcal{O}(|x|^{-\frac{1}{2}}), \quad |x|\to 0 \tag{3.12}$$

respectively.

3.2 FORMULATION OF WIENER-HOPF EQUATION

The Fourier transform of the Helmholtz equation in cold plasma which is satisfied by the field $H_z^1(x,y)$ in the domain $x\in(-\infty,\infty)$ and $y\in(b,\infty)$ leads to

$$\left[\frac{d^2}{dy^2}+(k_{\text{eff}}^2-\alpha^2)\right]F(\alpha,y)=0, \tag{3.13}$$

where $F(\alpha,y)$ is defined earlier.

Using the radiation condition represented by equation (3.11), the solution of equation (3.13) gives

$$F(\alpha, y) = A_1(\alpha) e^{\iota \mathfrak{L}(\alpha)(y-b)}, \tag{3.14}$$

where

$$\mathfrak{L}(\alpha) = \sqrt{k_{\mathfrak{eff}}^2 - \alpha^2} \tag{3.15}$$

and $A_1(\alpha)$ is the unknown spectral coefficient.

The square-root function $\mathfrak{L}(\alpha) = \sqrt{k_{\mathfrak{eff}}^2 - \alpha^2}$ represents the branch cuts along $\alpha = k_{\mathfrak{eff}}$ to $\alpha = k_{\mathfrak{eff}} + \iota\infty$ and $\alpha = -k_{\mathfrak{eff}}$ to $\alpha = -k_{\mathfrak{eff}} - \iota\infty$ such that $\mathfrak{L}(0) = k_{\mathfrak{eff}}$.

To find $A_1(\alpha)$, using the transformed form of the boundary condition represented by equation (3.6), one obtains

$$A_1(\alpha) = \frac{k_{\mathfrak{eff}} \mathscr{R}_+^1(\alpha)}{k_{\mathfrak{eff}} + \eta_2 \mathfrak{L}(\alpha)}, \tag{3.16}$$

with

$$\mathscr{R}_+^1(\alpha) = F_+(\alpha, b) + \frac{\eta_2}{\iota k_{\mathfrak{eff}}} \overset{\prime}{F}_+(\alpha, b), \tag{3.17}$$

where the prime sign in equation (3.17) represents the derivative with respect to y. Using the additive decomposition theorem and placing equation (3.16) in equation (3.14), one gets

$$F_-(\alpha, y) + F_+(\alpha, y) = \frac{k_{\mathfrak{eff}} \mathscr{R}_+^1(\alpha)}{k_{\mathfrak{eff}} + \eta_2 \mathfrak{L}(\alpha)} e^{\iota \mathfrak{L}(\alpha)(y-b)}. \tag{3.18}$$

The derivative of equation (3.18) with respect to y at $y = b$ takes the form

$$\overset{\prime}{F}_+(\alpha, b) = \frac{\iota k_{\mathfrak{eff}} \mathfrak{L}(\alpha) \mathscr{R}_+(\alpha)}{k_{\mathfrak{eff}} + \eta_2 \mathfrak{L}(\alpha)} - \overset{\prime}{F}_-(\alpha, b). \tag{3.19}$$

As the Helmholtz equation in cold plasma is satisfied by field $H_z^2(x, y)$ in equation (3.5) in the domain $x \in (0, \infty)$ and $y \in (a, b)$, multiplying this equation by $e^{\iota \alpha x}$ and

integrating the resultant equation with respect to x from 0 to ∞ leads to

$$\left[\frac{d^2}{dy^2} - \mathfrak{L}^2(\alpha)\right] \mathscr{G}_+(\alpha, y) = -\iota\alpha \mathfrak{g}(y), \tag{3.20}$$

where

$$\mathfrak{g}(y) = H_z^2(0, y) \tag{3.21}$$

and $\mathscr{G}_+(\alpha, y)$ defined by

$$\mathscr{G}_+(\alpha, y) = \int_0^\infty H_z^2(x, y) e^{\iota\alpha x} dx, \tag{3.22}$$

is a regular function in the half-plane.

Owing the method of variation of parameter the solution of non homogenous differential equation (3.20) gives

$$\mathscr{G}_+(\alpha, y) = C_1(\alpha)\cos\mathfrak{L}(\alpha)y + C_2(\alpha)\sin\mathfrak{L}(\alpha)y - \frac{\iota\alpha}{\mathfrak{L}(\alpha)}\int_0^y \mathfrak{g}(t)\sin\mathfrak{L}(\alpha)(b-t)dt, \tag{3.23}$$

where $C_1(\alpha)$ and $C_2(\alpha)$ are the unknown spectral coefficients.

To find $C_1(\alpha)$ one can apply the transformed form of the boundary condition represented by the equation (3.7), to get

$$C_1(\alpha) = -\frac{\eta_1}{\iota k_{\mathfrak{eff}}}\mathfrak{L}(\alpha)C_2(\alpha). \tag{3.24}$$

Substituting equation (3.24) in equation (3.23) yields

$$\begin{aligned}\mathscr{G}_+(\alpha, y) = &\left[\sin\mathfrak{L}(\alpha)y - \frac{\eta_1}{\iota k_{\mathfrak{eff}}}\mathfrak{L}(\alpha)\cos\mathfrak{L}(\alpha)y\right] C_2(\alpha) \\ &- \frac{\iota\alpha}{\mathfrak{L}(\alpha)}\int_0^y \mathfrak{g}(t)\sin\mathfrak{L}(\alpha)(b-t)dt.\end{aligned} \tag{3.25}$$

$C_2(\alpha)$ can be obtained by adding the transformed form of equations (3.9) and $\frac{\eta_1}{\iota k_{\mathfrak{eff}}}$ time of (3.10)

$$C_2(\alpha) = \frac{\mathscr{R}_+^1(\alpha)}{\mathscr{W}_1(\alpha)} + \frac{1}{\mathscr{W}_1(\alpha)} \int_0^b \mathfrak{f}(t) \left(\frac{\sin \mathfrak{L}(\alpha)(b-t)}{\mathfrak{L}(\alpha)} + \frac{\eta_1}{\iota k_{\mathfrak{eff}}} \cos \mathfrak{L}(\alpha)(b-t) \right) dt, \tag{3.26}$$

where

$$\mathscr{W}_1(\alpha) = \left(\frac{\eta_2 - \eta_1}{\iota k_{\mathfrak{eff}}} \right) \cos \mathfrak{L}(\alpha) b + \left(1 - \frac{\eta_1 \eta_2}{k_{\mathfrak{eff}}^2} \mathfrak{L}^2(\alpha) \right) \frac{\sin \mathfrak{L}(\alpha) b}{\mathfrak{L}(\alpha)}. \tag{3.27}$$

Using equation (3.26) in equation (3.25), one gets

$$\begin{aligned} \mathscr{G}_+(\alpha, y) &= \frac{\sin \mathfrak{L}(\alpha) y - \frac{\eta_1}{\iota k_{\mathfrak{eff}}} \mathfrak{L}(\alpha) \cos \mathfrak{L}(\alpha) y}{\mathfrak{L}(\alpha) \mathscr{W}_1(\alpha)} \\ &\times \left[\mathscr{R}_+^1(\alpha) + \iota \alpha \int_0^b \mathfrak{g}(t) \left(\frac{\sin \mathfrak{L}(\alpha)(b-t)}{\mathfrak{L}(\alpha)} + \frac{\eta_2}{\iota k_{\mathfrak{eff}}} \cos \mathfrak{L}(\alpha)(b-t) \right) dt \right] \\ &- \frac{\iota \alpha}{\mathfrak{L}(\alpha)} \int_0^y \mathfrak{g}(t) \sin \mathfrak{L}(\alpha)(b-t) dt. \end{aligned} \tag{3.28}$$

The left-hand side (i.e., $\mathscr{G}_+(\alpha, y)$) of the equation (3.28) is analytic in the upper half-plane $\mathfrak{Im}(\alpha) > \mathfrak{Im}(k_{\mathfrak{eff}} \cos \theta_0)$. However, the analyticity of the right-hand side is desecrated by the appearance of simple poles lying at the zeros of $\mathscr{W}_1(\alpha)$, i.e., $\alpha = \pm \alpha_m$ satisfying

$$\mathscr{W}_1(\pm \alpha_m) = 0, \quad \mathfrak{Im}(\alpha_m) > \mathfrak{Im}(k_{\mathfrak{eff}}), \qquad m = 1, 2, 3.... \tag{3.29}$$

The poles in the equation (3.28) can be removed by applying the condition that the residues of these poles are zero. Then from equation (3.28), it is found that

$$\mathscr{R}_+^1(\alpha_m) = \mathscr{D}_m^1 \left(\frac{\eta_2}{\iota k_{eff}} \mathfrak{L}_m \sin \mathfrak{L}_m b - \cos \mathfrak{L}_m b \right) \mathfrak{g}_m, \tag{3.30}$$

where $\mathfrak{g}_m$ is denoted by

$$\mathfrak{g}_m = \frac{1}{\mathscr{D}_m^1}\int_0^b \mathfrak{g}(t)\left(\frac{\sin\mathfrak{L}_m t}{\mathfrak{L}_m} - \frac{\eta_1}{\iota k_{\mathfrak{eff}}}\cos\mathfrak{L}_m t\right)dt, \tag{3.31}$$

with

$$\mathfrak{L}_m = \sqrt{k_{\mathfrak{eff}}^2 - \alpha_m^2} \tag{3.32}$$

and

$$\mathscr{D}_m^1 = \frac{\iota\mathfrak{L}_m}{2}\left(\frac{\cos\mathfrak{L}_m b}{\mathfrak{L}_m} + \frac{\eta_1}{\iota k_{\mathfrak{eff}}}\sin\mathfrak{L}_m b\right)\frac{d}{d\alpha}\mathscr{W}_1(\alpha_m). \tag{3.33}$$

Hence, considering equations (3.19) and (3.28) in the transformed domain of continuity relation given by equation (3.10) together, one can write

$$\begin{aligned}
&\iota k_{\mathfrak{eff}}\mathscr{R}_+^1(\alpha)\chi(\eta_2,\alpha) - \overset{\prime}{F}_-(\alpha,b) = -\frac{2k_{\mathfrak{eff}}\sin\theta_0 e^{-\iota k_{\mathfrak{eff}} b\sin\theta_0}}{(\eta_2\sin\theta_0+1)(\alpha - k_{\mathfrak{eff}}\cos\theta_0)}\\
&+\frac{\cos\mathfrak{L}b + \frac{\eta_1}{\iota k_{\mathfrak{eff}}}\mathfrak{L}\sin\mathfrak{L}b}{\mathscr{W}_1(\alpha)}\left[\mathscr{R}_+^1(\alpha) + \iota\alpha\int_0^b \mathfrak{g}(t)\left(\frac{\sin\mathfrak{L}(b-t)}{\mathfrak{L}(\alpha)} + \frac{\eta_2}{\iota k_{\mathfrak{eff}}}\cos\mathfrak{L}(b-t)\right)dt\right]\\
&-\iota\alpha\int_0^b \mathfrak{g}(t)\cos\mathfrak{L}(b-t)\,dt,
\end{aligned} \tag{3.34}$$

where

$$\chi(\eta_j,\alpha) = \frac{\mathfrak{L}(\alpha)}{\eta_j\mathfrak{L}(\alpha) + k_{\mathfrak{eff}}}. \tag{3.35}$$

After simplification, equation (3.34) takes the form

$$\begin{aligned}
&\frac{\chi(\eta_2,\alpha)\mathscr{R}_+^1(\alpha)}{\chi(\eta_1,\alpha)\mathscr{N}^1(\alpha)} + \overset{\prime}{F}_-(\alpha,b) = \frac{2k_{\mathfrak{eff}}\sin\theta_0 e^{-\iota k_{\mathfrak{eff}} b\sin\theta_0}}{(\eta_2\sin\theta_0+1)(\alpha - k_{\mathfrak{eff}}\cos\theta_0)}\\
&+\frac{\iota\alpha}{\mathscr{W}_1(\alpha)}\int_0^b \mathfrak{g}(t)\left(\frac{\sin\mathfrak{L}(\alpha)t}{\mathfrak{L}(\alpha)} - \frac{\eta_1}{\iota k_{\mathfrak{eff}}}\cos\mathfrak{L}(\alpha)t\right)dt,
\end{aligned} \tag{3.36}$$

where

$$\mathscr{N}^1(\alpha) = \mathscr{W}_1(\alpha)e^{\iota\mathfrak{L}(\alpha)b}. \tag{3.37}$$

Owing to equation (3.31), $\mathfrak{g}(t)$ can be expanded into a series of eigen-functions as under

$$\mathfrak{g}(t) = \sum_{m=1}^{\infty} \mathfrak{g}_m \left(\frac{\sin \mathfrak{L}_m t}{\mathfrak{L}_m} - \frac{\eta_1}{\iota k_{\mathfrak{eff}}} \cos \mathfrak{L}_m t \right). \tag{3.38}$$

Using equation (3.38) in equation (3.36), one obtains the required Wiener-Hopf equation valid in the strip $\mathfrak{Im}(-k_{\mathfrak{eff}}) < \mathfrak{Im}(\alpha) < \mathfrak{Im}(k_{\mathfrak{eff}})$ as follows:

$$\begin{aligned} &\frac{\chi(\eta_2,\alpha)\mathscr{R}^1_+(\alpha)}{\chi(\eta_1,\alpha)\mathscr{N}^1(\alpha)} + \overset{\prime}{F}_-(\alpha,b) = \frac{2k_{\mathfrak{eff}} \sin\theta_0 e^{-\iota k_{\mathfrak{eff}} b \sin\theta_0}}{(\eta_2 \sin\theta_0 + 1)(\alpha - k_{\mathfrak{eff}} \cos\theta_0)} \\ &- \sum_{m=1}^{\infty} \frac{\iota\alpha \mathfrak{L}_m \mathfrak{g}_m}{\alpha^2 - \alpha_m^2} \left(\frac{\cos \mathfrak{L}_m b}{\mathfrak{L}_m} + \frac{\eta_1}{\iota k_{eff}} \sin \mathfrak{L}_m b \right). \end{aligned} \tag{3.39}$$

3.3 SOLUTION OF WIENER-HOPF EQUATION

To solve the Wiener-Hopf equation the kernel functions $\mathscr{N}^1(\alpha)$ and $\chi(\eta_j,\alpha)$ in equation (3.39) can be factorized by applying the known results as following:

$$\begin{aligned} \mathscr{N}^1_+(\alpha) &= \left[\left(\frac{\eta_2 - \eta_1}{\iota k_{\mathfrak{eff}}} \right) \cos k_{\mathfrak{eff}} b + (1 - \eta_1\eta_2) \frac{\sin k_{\mathfrak{eff}} b}{k_{\mathfrak{eff}}} \right]^{\frac{1}{2}} \\ &\times \exp\left[\frac{\mathfrak{L}(\alpha) b}{\pi} \ln\left(\frac{\alpha + \iota\mathfrak{L}(\alpha)}{k_{\mathfrak{eff}}} \right) + \frac{\iota\alpha b}{\pi} \left(1 - C + \ln\left[\frac{2\pi}{k_{\mathfrak{eff}} b} \right] + \iota\frac{\pi}{2} \right) \right] \prod_{m=1}^{\infty} \left(1 + \frac{\alpha}{\alpha_m} \right) e^{\frac{\iota\alpha b}{m\pi}}, \end{aligned} \tag{3.40}$$

and

$$\mathscr{N}^1_-(\alpha) = \mathscr{N}^1_+(-\alpha). \tag{3.41}$$

Similarly the factor of $\chi(\eta_j,\alpha)$ can be expressed in form of the Maliuzhinetz's function as discussed in earlier.

Now, multiplying the Wiener-Hopf equation (3.39) on both sides by $\frac{\chi_-(\eta_1,\alpha)\mathscr{N}^1_-(\alpha)}{\chi_-(\eta_2,\alpha)}$, one obtains

$$\frac{\chi_+(\eta_2,\alpha)\mathscr{R}^1_+(\alpha)}{\mathscr{N}^1_+(\alpha)\chi_+(\eta_1,\alpha)}+\frac{\chi_-(\eta_1,\alpha)\mathscr{N}^1_-(\alpha)}{\chi_-(\eta_2,\alpha)}F'_-(\alpha,b)$$
$$=\frac{2k_{\mathfrak{eff}}\sin\theta_0 e^{-\iota k_{\mathfrak{eff}}b\sin\theta_0}\chi_-(\eta_1,\alpha)\mathscr{N}^1_-(\alpha)}{(\eta_2\sin\theta_0+1)(\alpha-k_{\mathfrak{eff}}\cos\theta_0)\chi_-(\eta_2,\alpha)}$$
$$-\sum_{m=1}^{\infty}\frac{\iota\alpha\mathfrak{g}_m\mathfrak{L}_m\chi_-(\eta_1,\alpha)\mathscr{N}^1_-(\alpha)}{(\alpha^2-\alpha_m^2)\chi_-(\eta_2,\alpha)}\left(\frac{\cos\mathfrak{L}_m b}{\mathfrak{L}_m}+\frac{\eta_1}{\iota k_{eff}}\sin\mathfrak{L}_m b\right). \tag{3.42}$$

With the aid of Cauchy's integral formula the terms on right-hand of the equation (3.42) can be decomposed as

$$\frac{2k_{\mathfrak{eff}}\sin\theta_0 e^{-\iota k_{\mathfrak{eff}}b\sin\theta_0}\chi_-(\eta_1,\alpha)\mathscr{N}^1_-(\alpha)}{(\eta_2\sin\theta_0+1)(\alpha-k_{\mathfrak{eff}}\cos\theta_0)\chi_-(\eta_2,\alpha)}=\frac{2k_{\mathfrak{eff}}\sin\theta_0 e^{-\iota k_{\mathfrak{eff}}b\sin\theta_0}}{(\eta_2\sin\theta_0+1)(\alpha-k_{\mathfrak{eff}}\cos\theta_0)}$$
$$\times\left[\frac{\chi_-(\eta_1,\alpha)\mathscr{N}^1_-(\alpha)}{\chi_-(\eta_2,\alpha)}-\frac{\chi_-(\eta_1,k_{\mathfrak{eff}}\cos\theta_0)\mathscr{N}^1_-(k_{\mathfrak{eff}}\cos\theta_0)}{\chi_-(\eta_2,k_{\mathfrak{eff}}\cos\theta_0)}\right]$$
$$+\frac{2k_{\mathfrak{eff}}\sin\theta_0 e^{-\iota k_{\mathfrak{eff}}b\sin\theta_0}\chi_-(\eta_4,k_{\mathfrak{eff}}\cos\theta_0)\mathscr{N}^1_-(k_{\mathfrak{eff}}\cos\theta_0)}{(\eta_1\sin\theta_0+1)(\alpha-k_{\mathfrak{eff}}\cos\theta_0)\chi_-(\eta_2,k_{\mathfrak{eff}}\cos\theta_0)} \tag{3.43}$$

and

$$\sum_{m=1}^{\infty}\frac{\iota\alpha\mathfrak{L}_m\mathfrak{g}_m\chi_-(\eta_1,\alpha)\mathscr{N}^1_-(\alpha)}{(\alpha^2-\alpha_m^2)\chi_-(\eta_2,\alpha)}\left(\frac{\cos\mathfrak{L}_m b}{\mathfrak{L}_m}+\frac{\eta_1}{\iota k_{eff}}\sin\mathfrak{L}_m b\right)$$
$$=\sum_{m=1}^{\infty}\frac{\iota\mathfrak{L}_m}{(\alpha+\alpha_m)}\left(\frac{\cos\mathfrak{L}_m b}{\mathfrak{L}_m}+\frac{\eta_2}{\iota k_{eff}}\sin\mathfrak{L}_m b\right)$$
$$\times\left[\frac{\alpha\mathfrak{g}_m\chi_-(\eta_1,\alpha)\mathscr{N}^1_-(\alpha)}{(\alpha-\alpha_m)\chi_-(\eta_2,\alpha)}-\frac{\alpha_m\mathfrak{g}_m\chi_+(\eta_1,\alpha_m)\mathscr{N}^1_+(\alpha_m)}{2\alpha_m\chi_+(\eta_2,\alpha_m)}\right]$$
$$+\sum_{m=1}^{\infty}\frac{\iota\mathfrak{L}_m\alpha_m\mathfrak{g}_m\chi_+(\eta_1,\alpha_m)\mathscr{N}^1_+(\alpha_m))}{2\alpha_m\chi_+(\eta_1,\alpha_m)(\alpha+\alpha_m)}\left(\frac{\cos\mathfrak{L}_m b}{\mathfrak{L}_m}+\frac{\eta_1}{\iota k_{eff}}\sin\mathfrak{L}_m b\right). \tag{3.44}$$

On using equations (3.43) and (3.44) in equation (3.42), and then separating the terms which are analytic in the upper half-plane ($\mathfrak{Im}(\alpha) > -k_{\mathfrak{eff}}$) at left-hand side and those which are analytic in lower half-plane ($\mathfrak{Im}(\alpha) < k_{\mathfrak{eff}}$) at the right-hand

side yields

$$\frac{\chi_+(\eta_2,\alpha)\mathscr{R}^1_+(\alpha)}{\mathscr{N}^1_+(\alpha)\chi_+(\eta_1,\alpha)} - \frac{2k_{\mathfrak{eff}}\sin\theta_0 e^{-\iota k_{\mathfrak{eff}} b\sin\theta_0}\chi_-(\eta_1,k_{\mathfrak{eff}}\cos\theta_0)\mathscr{N}^1_-(k_{\mathfrak{eff}}\cos\theta_0)}{(\eta_2\sin\theta_0+1)(\alpha-k_{\mathfrak{eff}}\cos\theta_0)\chi_-(\eta_2,k_{\mathfrak{eff}}\cos\theta_0)}$$
$$+\sum_{m=1}^{\infty}\frac{\iota\alpha_m\mathfrak{L}_m\mathfrak{g}_m\chi_+(\eta_1,\alpha_m)\mathscr{N}^1_+(\alpha_m))}{2\alpha_m\chi_+(\eta_2,\alpha_m)(\alpha+\alpha_m)}\left(\frac{\cos\mathfrak{L}_m b}{\mathfrak{L}_m}+\frac{\eta_1}{\iota k_{\mathfrak{eff}}\sin\mathfrak{L}_m b}\right)$$
$$=-\frac{\chi_-(\eta_1,\alpha)\mathscr{N}^1_-(\alpha)}{\chi_-(\eta_2,\alpha)}F'_-(\alpha,b)+\frac{2k_{\mathfrak{eff}}\sin\theta_0 e^{-\iota k_{\mathfrak{eff}} b\sin\theta_0}}{(\eta_2\sin\theta_0+1)(\alpha-k_{\mathfrak{eff}}\cos\theta_0)}$$
$$\times\left[\frac{\chi_-(\eta_1,\alpha)\mathscr{N}^1_-(\alpha)}{\chi_-(\eta_2,\alpha)}-\frac{\chi_-(\eta_1,k_{\mathfrak{eff}}\cos\theta_0)\mathscr{N}^1_-(k_{\mathfrak{eff}}\cos\theta_0)}{\chi_-(\eta_2,k_{\mathfrak{eff}}\cos\theta_0)}\right]$$
$$-\sum_{m=1}^{\infty}\frac{\iota\mathfrak{L}_m}{(\alpha+\alpha_m)}\left(\frac{\cos\mathfrak{L}_m b}{\mathfrak{L}_m}+\frac{\eta_1}{\iota k_{eff}}\sin\mathfrak{L}_m b\right)$$
$$\times\left[\frac{\alpha\mathfrak{g}_m\chi_-(\eta_1,\alpha)\mathscr{N}^1_-(\alpha)}{(\alpha-\alpha_m)\chi_-(\eta_2,\alpha)}-\frac{\alpha_m\mathfrak{g}_m\chi_+(\eta_1,\alpha_m)\mathscr{N}^1_+(\alpha_m)}{2\alpha_m\chi_+(\eta_2,\alpha_m)}\right]. \tag{3.45}$$

The required solution of Wiener-Hopf equation can be obtained by using analytical continuation principle complying the extended Liouville's theorem as under

$$\frac{\chi_+(\eta_2,\alpha)\mathscr{R}^1_+(\alpha)}{\chi_+(\eta_1,\alpha)\mathscr{N}^1_+(\alpha)}=\frac{2k_{\mathfrak{eff}}\sin\theta_0 e^{-\iota k_{\mathfrak{eff}} b\sin\theta_0}\chi_-(\eta_1,k_{\mathfrak{eff}}\cos\theta_0)\mathscr{N}^1_-(k_{\mathfrak{eff}}\cos\theta_0)}{(\eta_2\sin\theta_0+1)(\alpha-k_{\mathfrak{eff}}\cos\theta_0)\chi_-(\eta_2,k_{\mathfrak{eff}}\cos\theta_0)}$$
$$-\sum_{m=1}^{\infty}\frac{\iota\alpha_m\mathfrak{L}_m\mathfrak{g}_m\ \chi_+(\eta_1,\alpha_m)\mathscr{N}^1_+(\alpha_m)}{2\alpha_m(\alpha+\alpha_m)\chi_+(\eta_2,\alpha_m)}\left(\frac{\cos\mathfrak{L}_m b}{\mathfrak{L}_m}+\frac{\eta_1}{\iota k_{\mathfrak{eff}}}\sin\mathfrak{L}_m b\right). \tag{3.46}$$

While placing equation (3.30) in equation (3.46) at $\alpha=\alpha_m$, one can obtain

$$\frac{\chi_+(\eta_2,\alpha_n)\mathscr{D}^1_n}{\chi_+(\eta_1,\alpha_n)\mathscr{N}^1_+(\alpha_n)}\left(\frac{\eta_2}{\iota k_{eff}}\mathfrak{L}_n\sin\mathfrak{L}_n b-\cos\mathfrak{L}_n b\right)\mathfrak{g}_n$$
$$=\frac{2k_{\mathfrak{eff}}\sin\theta_0 e^{-\iota k_{\mathfrak{eff}} b\sin\theta_0}\chi_-(\eta_1,k_{\mathfrak{eff}}\cos\theta_0)\mathscr{N}^1_-(k_{\mathfrak{eff}}\cos\theta_0)}{(\eta_2\sin\theta_0+1)(\alpha_n-k_{\mathfrak{eff}}\cos\theta_0)\chi_-(\eta_2,k_{\mathfrak{eff}}\cos\theta_0)}$$
$$-\sum_{m=1}^{\infty}\frac{\iota\alpha_m\mathfrak{L}_m\mathfrak{g}_m\chi_+(\eta_1,\alpha_m)\mathscr{N}^1_+(\alpha_m)}{2\alpha_m(\alpha_n+\alpha_m)\chi_+(\eta_2,\alpha_m)}\left(\frac{\cos\mathfrak{L}_m b}{\mathfrak{L}_m}+\frac{\eta_1}{\iota k_{\mathfrak{eff}}}\sin\mathfrak{L}_m b\right). \tag{3.47}$$

The above expression is the system of infinite number of algebraic equations that can be solved numerically by truncating after N terms.

3.4 THE DIFFRACTED FIELD

The diffracted field $H_z^1(x,y)$ is acquired by taking the inverse Fourier transform of $F(\alpha,y)$. On using equation (3.18), one gets

$$H_z^1(x,y)=\frac{1}{2\pi}\int_{\mathscr{L}}\frac{k_{\mathfrak{eff}}\mathscr{R}_+^1(\alpha)}{k_{\mathfrak{eff}}+\eta_2\mathfrak{L}(\alpha)}e^{\iota\mathfrak{L}(\alpha)(y-b)}e^{-\iota\alpha x}d\alpha. \tag{3.48}$$

Now placing the variables $\alpha=-k_{\mathfrak{eff}}\cos t,\ x=\rho\cos\theta$ and $y=\rho\sin\theta$ in the equation (3.48) gives

$$H_z^1(\rho,\theta)=\frac{1}{2\pi}\int_{\mathscr{L}}\frac{\mathscr{R}_+^1(-k_{\mathfrak{eff}}\cos t)}{1+\eta_2\sin t}e^{-\iota k_{\mathfrak{eff}}b\sin t+\iota k_{\mathfrak{eff}}\rho\cos(t-\theta)}k_{\mathfrak{eff}}\sin t\,dt. \tag{3.49}$$

The asymptotic evaluation of the integral in the equation (3.49) can be obtained via saddle-point technique. Here, saddle-point rests at $t=\theta$, which gives

$$H_z^1(\rho,\theta)=\frac{k_{\mathfrak{eff}}\sin\theta\mathscr{R}_+^1(-k_{\mathfrak{eff}}\cos\theta)}{\sqrt{2\pi k_{\mathfrak{eff}}\rho}(1+\eta_2\sin\theta)}e^{\iota k_{\mathfrak{eff}}\rho-\frac{\iota\pi}{4}-\iota k_{\mathfrak{eff}}b\sin\theta}. \tag{3.50}$$

On taking into account equations (3.4) and (3.46), the diffracted field takes the form

$$\begin{aligned}
H_z^1(\rho,\theta)=&-\frac{k\sqrt{(\epsilon_1^2-\epsilon_2^2)/\epsilon_1}\sin\theta e^{\iota k\sqrt{(\epsilon_1^2-\epsilon_2^2)/\epsilon_1}\rho-\frac{\iota\pi}{4}-\iota k\sqrt{(\epsilon_1^2-\epsilon_2^2)/\epsilon_1}b\sin\theta}}{\sqrt{2\pi k\rho\sqrt{(\epsilon_1^2-\epsilon_2^2)/\epsilon_1}(1+\eta_1\sin\theta)}}\\
&\times\left[\left(\frac{2k\sqrt{(\epsilon_1^2-\epsilon_2^2)/\epsilon_1}\sin\theta_0 e^{-\iota k\sqrt{(\epsilon_1^2-\epsilon_2^2)/\epsilon_1}b\sin\theta_0}\chi_-(\eta_1,k_{\mathfrak{eff}}\cos\theta_0)}{(\eta_2\sin\theta_0+1)(k\sqrt{(\epsilon_1^2-\epsilon_2^2)/\epsilon_1}\cos\theta+k\sqrt{(\epsilon_1^2-\epsilon_2^2)/\epsilon_1}\cos\theta_0)}\right)\times\right.\\
&\left(\frac{\mathscr{N}_-^1(k\sqrt{(\epsilon_1^2-\epsilon_2^2)/\epsilon_1}\cos\theta_0)\chi_-(\eta_1,k\sqrt{(\epsilon_1^2-\epsilon_2^2)/\epsilon_1}\cos\theta)\mathscr{N}_-^1(k\sqrt{(\epsilon_1^2-\epsilon_2^2)/\epsilon_1}\cos\theta)}{\chi_-(\eta_2,k\sqrt{(\epsilon_1^2-\epsilon_2^2)/\epsilon_1}\cos\theta_0)\chi_-(\eta_2,k\sqrt{(\epsilon_1^2-\epsilon_2^2)/\epsilon_1}\cos\theta)}\right)\\
&-\sum_{m=1}^{\infty}\left(\frac{\iota\alpha_m\mathfrak{L}_m\mathfrak{g}_m\ \chi_+(\eta_1,\alpha_m)\mathscr{N}_+^1(\alpha_m)\chi_-(\eta_1,k\sqrt{(\epsilon_1^2-\epsilon_2^2)/\epsilon_1}\cos\theta)}{2\alpha_m(k\sqrt{(\epsilon_1^2-\epsilon_2^2)/\epsilon_1}\cos\theta-\alpha_m)\chi_+(\eta_2,\alpha_m))}\right)\\
&\left.\times\frac{\mathscr{N}_-^1(k\sqrt{(\epsilon_1^2-\epsilon_2^2)/\epsilon_1}\cos\theta)}{\chi_-(\eta_2,k\sqrt{(\epsilon_1^2-\epsilon_2^2)/\epsilon_1}\cos\theta}\left(\frac{\cos\mathfrak{L}_m b}{\mathfrak{L}_m}+\frac{\eta_1}{\iota k\sqrt{(\epsilon_1^2-\epsilon_2^2)/\epsilon_1}}\sin\mathfrak{L}_m b\right)\right].
\end{aligned} \tag{3.51}$$

3.5 COMPUTATIONAL RESULTS AND DISCUSSION

This section is devoted to analyze the numerical results for various physical parameters of interest. Fig. (3.2) shows the variation in the diffracted field amplitude versus the truncation number "N". It is clear that the effect of the truncation number is negligible for $N \geq 15$. Hence, the infinite system of algebraic equations in equation (3.47) can be managed to deal as finite. Fig. (3.3) explores the effect of separation "b" between the parallel plates on the diffracted field amplitude which shows that the diffracted field amplitude also depend upon the plate separation. While Fig. (3.4) represents the variation in diffracted field amplitude versus the incident angle "θ_0" ($0^o \leq \theta_0 \leq 90^o$). It is interesting to note that the value of diffracted field amplitude lies at 90^o when $\theta_0 = 90^o$. Whereas this peak values moves to 120^o and 150^o for $\theta_0 = 60^o$ and $\theta_0 = 30^o$, respectively. The effect of wall impedance η_1 on the amplitude of the diffracted field is shown in Fig. (3.5). Fig. (3.6) shows the variation in the diffracted field amplitude with wall impedance η_2. The effect of cold plasma permittivity has been analyzed in Figs. (3.7) and (3.8). Here, we have found that the increase in cold plasma permittivity decreases the diffracted field amplitude. In other words the diffracted field amplitude decreases with increasing ion number density in cold plasma or by decreasing plasma frequency. Here, in this problem it is observed that the diffracted field is highly effected with ϵ_1 while slightly with ϵ_2. Also it is noted that the diffracted field amplitude decreases with increase in permittivity value ϵ_1 while in case of ϵ_2 diffracted field amplitude decreases with increasing ϵ_2.

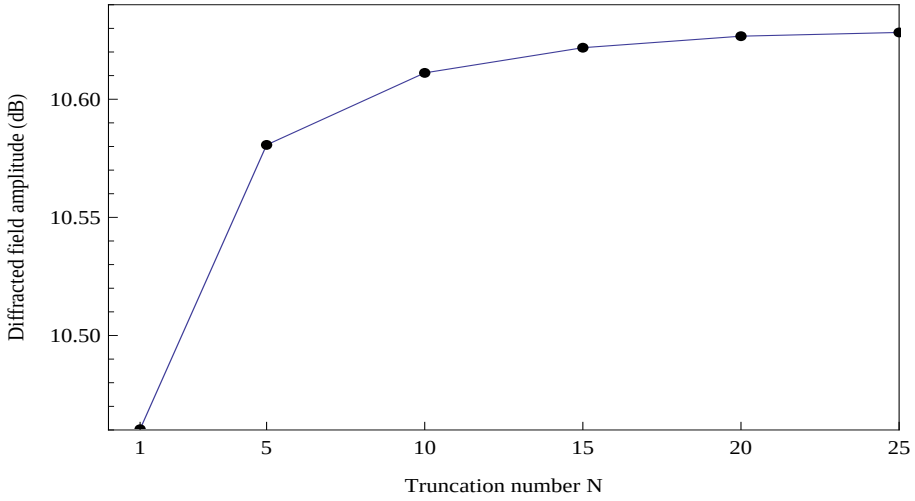

FIGURE 3.2. *Variation in the diffracted field amplitude versus "N" at* $k = 5$, $\theta_0 = 90^o$, $\theta = 60^o$, $\eta_1 = 0.3\iota$, $\eta_2 = 0.5\iota$, $\epsilon_1 = 0.8$, $\epsilon_2 = 0.1$ *and* $b = 0.2\lambda$.

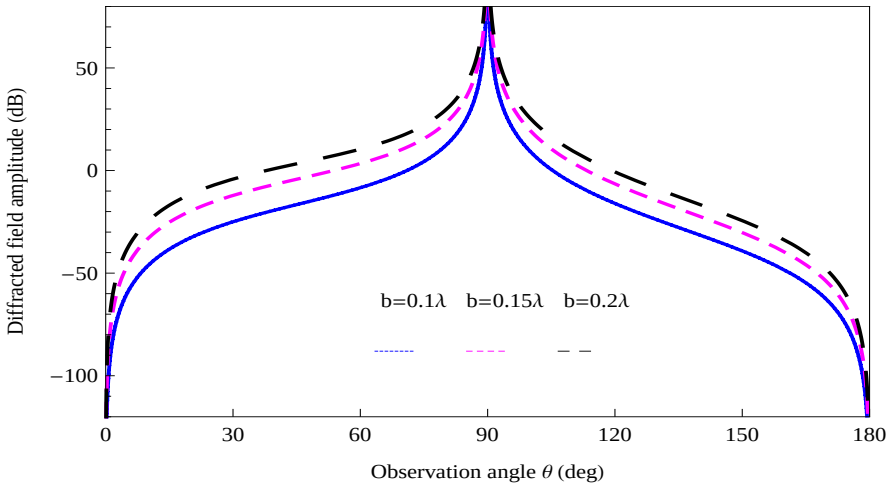

FIGURE 3.3. *Variation in the diffracted field amplitude versus "b" at* $k = 5$, $\theta_0 = 90^o$, $\eta_1 = 0.7\iota$, $\eta_2 = 0.5\iota$, $\epsilon_1 = 0.8$ *and* $\epsilon_2 = 0.1$.

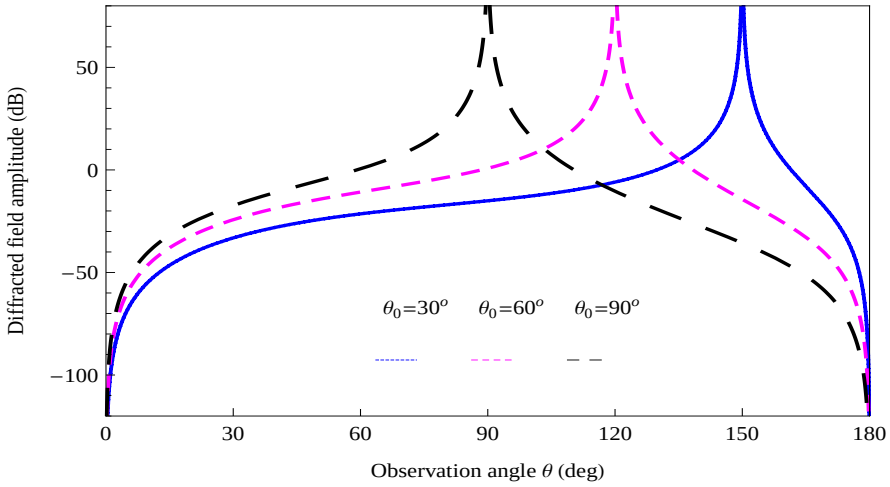

FIGURE 3.4. *Variation in the diffracted field amplitude versus "θ_0" at* $k = 5$, $\eta_1 = 0.7\iota$, $\eta_2 = 0.5\iota$, $\epsilon_1 = 0.8$, $\epsilon_2 = 0.1$ *and* $b = 0.2\lambda$.

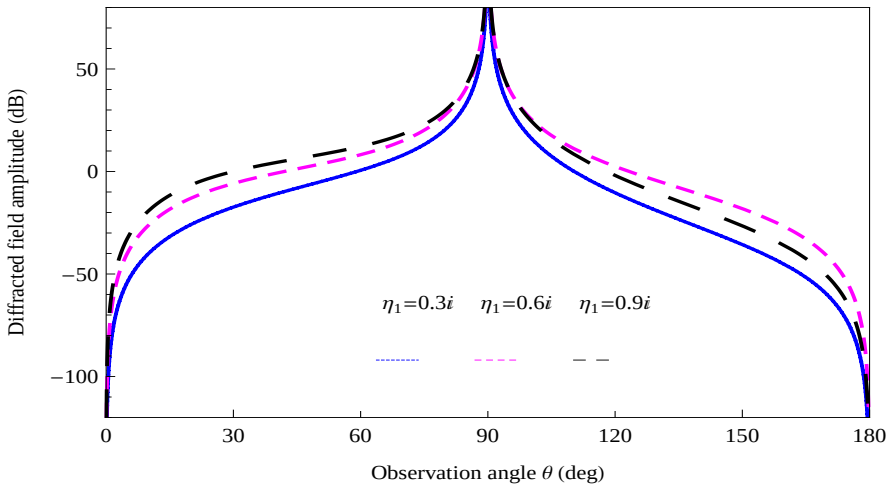

FIGURE 3.5. *Variation in the diffracted field amplitude versus "η_1" at* $\theta_0 = 90^0$, $k = 5$, $\eta_2 = 0.5\iota$, $\epsilon_1 = 0.8$, $\epsilon_2 = 0.1$ *and* $b = 0.2\lambda$.

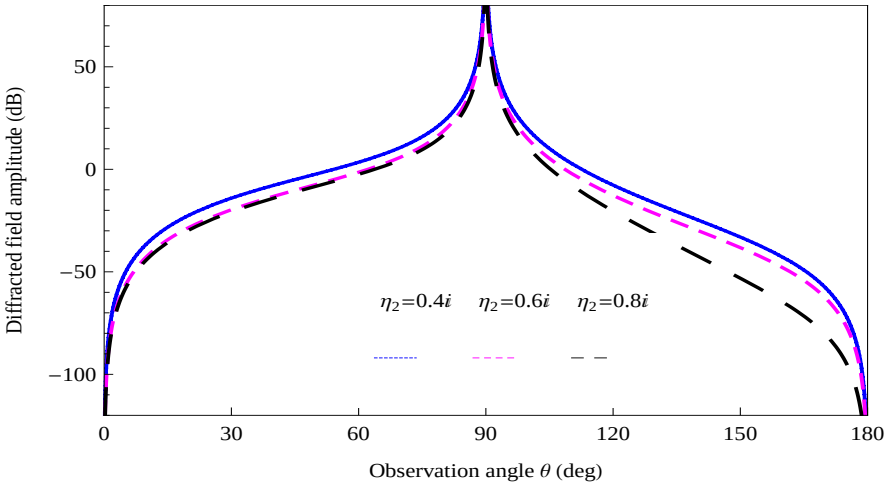

FIGURE 3.6. *Variation in the diffracted field amplitude versus "η_2" at $k = 5$, $\theta_0 = 90^0$, $\eta_1 = 0.3\iota$, $\epsilon_1 = 0.8$, $\epsilon_2 = 0.1$ and $b = 0.2\lambda$.*

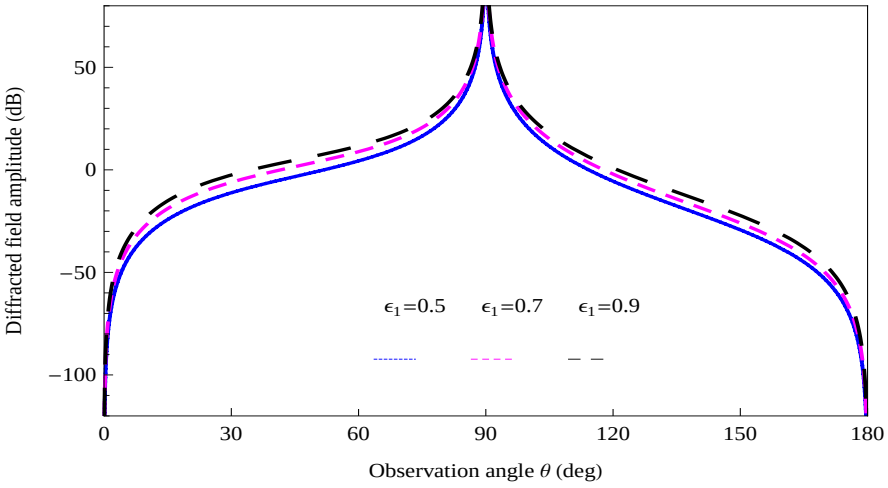

FIGURE 3.7. *Variation in the diffracted field amplitude versus "ϵ_1" at $k = 5$, $\theta_0 = 90^o$, $\eta_1 = 0.7\iota$, $\eta_2 = 0.5\iota$ $\epsilon_2 = 0.1$ and $b = 0.2\lambda$.*

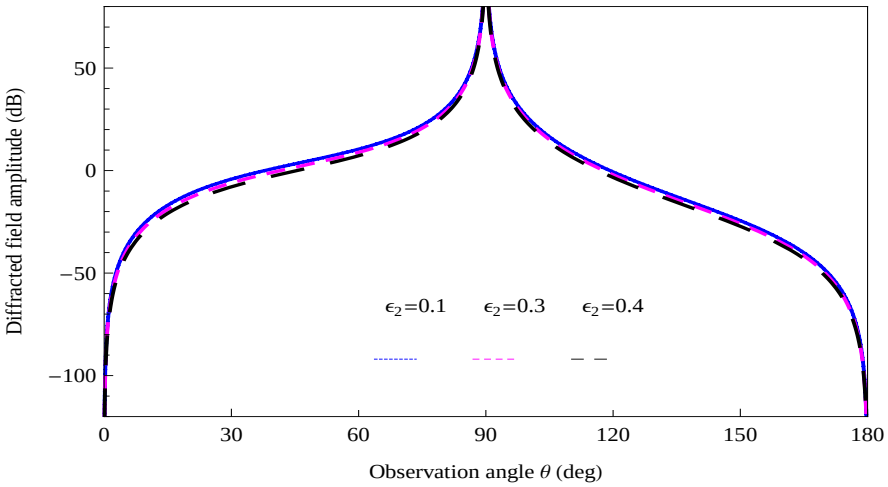

FIGURE 3.8. *Variation in the diffracted field amplitude versus "ϵ_2" at $k = 5$, $\theta_0 = 90^o$, $\eta_1 = 0.7\iota$, $\eta_2 = 0.5\iota$ $\epsilon_1 = 0.8$ and $b = 0.2\lambda$.*

CHAPTER 4

E-POLARIZED PLANE WAVE DIFFRACTION BY AN IMPEDANCE LOADED PARALLEL-PLATE WAVEGUIDE LOCATED IN COLD PLASMA

This chapter comprises the consideration of the diffraction of E-polarized plane wave by a waveguide designed by an infinite plane and a parallel half-plane having a different surface impedances in cold plasma. It plays an important role in diffraction theory and many problems in science and engineering. Initially, Büyükaksoy and Cinar [70] studied the problem of diffraction of a plane wave by a waveguide designed by an infinite plane and half-plane. The upper faces of the left and right part of the plane having different surface impedances. While the half-plane is parallel to the plane and perfectly conducting. This problem was solved with the help of matrix Wiener-Hopf equations. After that Cinar and Büyükaksoy [12] considered the same geometry but for different surface impedances of the half-plane instead of perfectly conducting half-plane. The solution of the problem was obtained by a hybrid method. Here, in this chapter the same geometry is considered in cold plasma.

This chapter is compiled with the subsequent order. Section (4.1) is dedicated to formulate boundary-valued problem governing the wave propagation in waveg-

uide located in cold plasma. Section (4.2) contains the formulation of Wiener-Hopf equation from the related model. The solution of the said Winer-Hopf equation is obtained in Section (4.3). Whereas Section (4.4) is devoted to the determination of infinite unknown coefficients. The diffracted field expression is presented in Section (4.5). Finally graphical results for different parameters are discussed in Section (4.6). The contents of this chapter have been published in **Physica Scripta**, 89(8): Paper ID. e095207, (2014).

4.1 MATHEMATICAL MODEL OF THE PROBLEM IN COLD PLASMA

Consider a waveguide constructed by a half-plane defined by $S_1 = \{(x, y, z)|\ x \in (-\infty, 0),\ y = b,\ z \in (-\infty, \infty)\}$ and an infinite plane defined by $S_2 = \{(x, y, z)|\ x \in (-\infty, \infty),\ y = 0,\ z \in (-\infty, \infty)\}$ designed in cold plasma. The surface impedances of the upper and lower faces of the half-plane S_1 are assumed to be $Z_1 = \eta_1 Z_0$ and $Z_2 = \eta_2 Z_0$, respectively. The surface impedances of the left and right upper faces of the plane S_2 are assumed to be $Z_3 = \eta_3 Z_0$ and $Z_4 = \eta_4 Z_0$, respectively, as shown in Fig. (4.1)

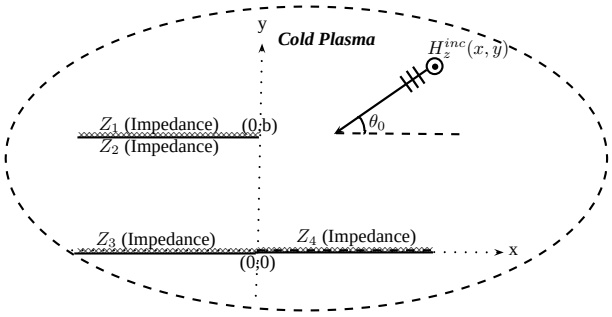

FIGURE 4.1. *Geometrical configuration of a waveguide structure in cold plasma*

For analysis purpose, it is convenient to express the total field as follows:

$$H_z^T(x,y) = \begin{cases} H_z^{inc}(x,y) + H_z^{ref}(x,y) + H_z^1(x,y), & y \in (b,\infty) \\ H_z^2(x,y)\mathscr{H}(-x) + H_z^3(x,y)\mathscr{H}(x), & y \in (0,b) \end{cases} \tag{4.1}$$

where $\mathscr{H}(x)$ represents the Heaviside unit step function. $H_z^{inc}(x,y)$ and $H_z^{ref}(x,y)$ denotes the incident and reflected fields, respectively, defined as below

$$H_z^{inc}(x,y) = e^{-\iota k_{\mathfrak{eff}}(x\cos\theta_0 + y\sin\theta_0)} \tag{4.2}$$

and

$$H_z^{ref}(x,y) = \frac{\eta_1\sin\theta_0 - 1}{\eta_1\sin\theta_0 + 1} e^{-\iota k_{\mathfrak{eff}}(x\cos\theta_0 - (y-2b)\sin\theta_0)}, \tag{4.3}$$

where

$$k_{\mathfrak{eff}} = k\sqrt{\frac{\epsilon_1^2 - \epsilon_2^2}{\epsilon_1}} \quad \text{and} \quad k = \omega\sqrt{\epsilon_0\mu_0}. \tag{4.4}$$

Now, $H_z^j(x,y)$, $(j = 1,2,3)$ are scattered fields satisfying the Helmholtz equation in cold plasma as under

$$\left[\frac{\partial^2}{\partial x^2} + \frac{\partial^2}{\partial y^2} + k_{\mathfrak{eff}}^2\right]\left[H_z^j(x,y)\right] = 0, \qquad j = 1,2,3 \tag{4.5}$$

with the following corresponding boundary conditions and continuity relations

$$\left(1 + \frac{\eta_1}{\iota k_{\mathfrak{eff}}}\frac{\partial}{\partial y}\right) H_z^1(x,b) = 0, \qquad x \in (-\infty, 0) \tag{4.6}$$

$$\left(1 - \frac{\eta_2}{\iota k_{\mathfrak{eff}}}\frac{\partial}{\partial y}\right) H_z^2(x,b) = 0, \qquad x \in (-\infty, 0) \tag{4.7}$$

$$\mathscr{H}(-x)\left(1 + \frac{\eta_3}{\iota k_{\mathfrak{eff}}}\frac{\partial}{\partial y}\right) H_z^2(x,0) + \mathscr{H}(x)\left(1 + \frac{\eta_4}{\iota k_{\mathfrak{eff}}}\frac{\partial}{\partial y}\right) H_z^3(x,0) = 0, \quad x \in (-\infty,\infty) \tag{4.8}$$

$$H_z^1(x,b) + H_z^{inc}(x,b) + H_z^{ref}(x,b) - H_z^3(x,b) = 0, \qquad x \in (0,\infty) \tag{4.9}$$

$$\frac{\partial}{\partial y}H_z^1(x,b) + \frac{\partial}{\partial y}H_z^{inc}(x,b) + \frac{\partial}{\partial y}H_z^{ref}(x,b) - \frac{\partial}{\partial y}H_z^3(x,b) = 0, \quad x \in (0,\infty) \tag{4.10}$$

$$H_z^2(0,y) - H_z^3(0,y) = 0, \qquad y \in (0,b) \tag{4.11}$$

$$\frac{\partial}{\partial x}H_z^2(0,y) - \frac{\partial}{\partial x}H_z^3(0,y) = 0, \qquad y \in (0,b). \tag{4.12}$$

For the uniqueness of the boundary-value problem defined by the set of equations (4.6) - (4.12). One can take the radiation and edge conditions, respectively, as follow

$$\sqrt{\rho}\left[\frac{\partial}{\partial \rho}H_z^1(x,y) - \iota k_{\mathfrak{eff}}H_z^1(x,y)\right] = 0, \;\; \rho = \sqrt{x^2+y^2} \to \infty \tag{4.13}$$

and

$$H_z^T(x,y) = \mathcal{O}(|x|^{\frac{1}{2}}), \;\; \frac{\partial}{\partial y}H_z^T(x,y) = \mathcal{O}(|x|^{-\frac{1}{2}}), \quad |x| \to 0. \tag{4.14}$$

4.2 FORMULATION OF WIENER-HOPF EQUATION

The Fourier transform of the Helmholtz equation in cold plasma is satisfied by the field $H_z^1(x,y)$ in the region $x \in (-\infty,\infty)$ and $y \in (b,\infty)$ gives

$$\left[\frac{d^2}{dy^2} + \mathfrak{L}^2(\alpha)\right]F(\alpha,y) = 0, \tag{4.15}$$

where $F(\alpha,y)$ is defined as earlier.

The general solution of equation (4.15) satisfying the radiation condition represented by equations (4.13) yields

$$F(\alpha,y) = A_2(\alpha)e^{\iota\mathfrak{L}(\alpha)(y-b)}, \tag{4.16}$$

where

$$\mathfrak{L}(\alpha) = \sqrt{k_{\mathfrak{eff}}^2 - \alpha^2}. \tag{4.17}$$

To find the unknown spectral coefficient $A_2(\alpha)$, using the boundary condition represented by the equation (4.6) in the transformed domain, one obtains

$$A_2(\alpha) = \frac{\mathscr{R}_+^2(\alpha)}{1 + \frac{\eta_1}{k_{\mathfrak{eff}}}\mathfrak{L}(\alpha)}, \tag{4.18}$$

with

$$\mathscr{R}_+^2(\alpha) = F_+(\alpha, b) + \frac{\eta_1}{\iota k_{\mathfrak{eff}}} \overset{\prime}{F}_+(\alpha, b). \tag{4.19}$$

Using the additive decomposition theorem and placing equation (4.48) in equation (4.16), one obtains

$$F_-(\alpha, y) + F_+(\alpha, y) = \frac{\mathscr{R}_+^2(\alpha)}{1 + \frac{\eta_1}{k_{\mathfrak{eff}}}\mathfrak{L}(\alpha)} e^{\iota\mathfrak{L}(\alpha)(y-b)}. \tag{4.20}$$

The derivative of equation (4.20) with respect to at $y = b$ takes the form

$$\overset{\prime}{F}_+(\alpha, b) = \frac{\iota\mathfrak{L}(\alpha)\mathscr{R}_+^2(\alpha)}{1 + \frac{\eta_1}{k_{\mathfrak{eff}}}\mathfrak{L}(\alpha)} - \overset{\prime}{F}_-(\alpha, b). \tag{4.21}$$

As the Helmholtz equation in cold plasma is satisfied by field $H_z^2(x, y)$ in the waveguide region $x \in (0, \infty)$ and $y \in (a, b)$, multiplying this equation by $e^{\iota\alpha x}$ and integrating the resultant equation with respect to x from 0 to ∞ gives

$$\left[\frac{d^2}{dy^2} - \mathfrak{L}^2(\alpha)\right] \mathscr{G}_+(\alpha, y) = \mathfrak{f}(t) - \iota\alpha\mathfrak{g}(t), \tag{4.22}$$

where

$$\mathfrak{f}(y) - \iota\alpha\mathfrak{g}(y) = \frac{\partial}{\partial x} H_z^3(0, y) - \iota\alpha H_z^3(0, y) \tag{4.23}$$

and $\mathscr{G}_+(\alpha, y)$ defined by

$$\mathscr{G}_+(\alpha, y) = \int_0^\infty H_z^3(x, y) e^{\iota\alpha x} dx, \tag{4.24}$$

is a regular function in the half-plane.

Owing the method of variation of parameter the solution of non-homogenous differential equation (3.20) yields

$$\mathscr{G}_+(\alpha,y) = C_5(\alpha)\cos\mathfrak{L}(\alpha)y + C_6(\alpha)\sin\mathfrak{L}(\alpha)y + \frac{1}{\mathfrak{L}(\alpha)}\int_0^y (\mathfrak{f}(t)-\iota\alpha\mathfrak{g}(t))\sin\mathfrak{L}(\alpha)(b-t)dt. \tag{4.25}$$

Here $C_5(\alpha)$ and $C_6(\alpha)$ are the unknown spectral coefficients.

To find $C_5(\alpha)$, one uses the transformed form of the boundary condition represented by the equation (4.7) which gives

$$C_5(\alpha) = -\frac{\eta_4}{\iota k_{\mathfrak{eff}}}\mathfrak{L}(\alpha)C_6(\alpha). \tag{4.26}$$

Placing equation (4.26) in equation (4.25) yields

$$\mathscr{G}_+(\alpha,y) = \left[\sin\mathfrak{L}(\alpha)y - \frac{\eta_4}{\iota k_{\mathfrak{eff}}}\mathfrak{L}(\alpha)\cos\mathfrak{L}(\alpha)y\right]C_6(\alpha) + \frac{1}{\mathfrak{L}(\alpha)}\int_0^y (\mathfrak{f}(t)-\iota\alpha\mathfrak{g}(t))\sin\mathfrak{L}(\alpha)(b-t)dt. \tag{4.27}$$

$C_6(\alpha)$ can be obtained by adding the transformed form of equations (4.9) and $\frac{\eta_1}{\iota k_{\mathfrak{eff}}}$ time of (4.10) as under

$$C_6(\alpha) = \frac{\mathscr{R}_+^2(\alpha)}{\mathfrak{L}(\alpha)\mathscr{W}_2(\alpha)} - \frac{1}{\mathfrak{L}(\alpha)\mathscr{W}_2(\alpha)}\int_0^b (\mathfrak{f}(t)-\iota\alpha\mathfrak{g}(t))\left(\frac{\sin\mathfrak{L}(\alpha)(b-t)}{\mathfrak{L}(\alpha)} + \frac{\eta_1}{\iota k_{\mathfrak{eff}}}\cos\mathfrak{L}(\alpha)(b-t)\right)dt, \tag{4.28}$$

where

$$\mathscr{W}_2(\alpha) = \left(\frac{\eta_1-\eta_4}{\iota k_{\mathfrak{eff}}}\right)\cos\mathfrak{L}(\alpha)b + \left(1-\frac{\eta_1\eta_4}{k_{\mathfrak{eff}}^2}\mathfrak{L}^2(\alpha)\right)\frac{\sin\mathfrak{L}(\alpha)b}{\mathfrak{L}(\alpha)}. \tag{4.29}$$

Using equation (4.28) in equation (4.27), one gets

$$\mathscr{G}_+(\alpha,y)=\frac{\sin\mathfrak{L}(\alpha)y-\frac{\eta_4}{\iota k_{\mathfrak{eff}}}\mathfrak{L}(\alpha)\cos\mathfrak{L}(\alpha)y}{\mathfrak{L}(\alpha)\mathscr{W}_2(\alpha)}$$
$$\times\left[\mathscr{R}^2_+(\alpha)-\int_0^b(\mathfrak{f}(t)-\iota\alpha\mathfrak{g}(t))\left(\frac{\sin\mathfrak{L}(\alpha)(b-t)}{\mathfrak{L}(\alpha)}+\frac{\eta_1}{\iota k_{\mathfrak{eff}}}\cos\mathfrak{L}(\alpha)(b-t)\right)dt\right]$$
$$+\frac{1}{\mathfrak{L}(\alpha)}\int_0^y(\mathfrak{f}(t)-\iota\alpha\mathfrak{g}(t))\sin\mathfrak{L}(\alpha)(b-t)dt. \tag{4.30}$$

The left-hand side (i.e., $\mathscr{G}_+(\alpha,y)$) of the equation (4.30) is analytic in the upper half-plane $\mathfrak{Im}(\alpha)>\mathfrak{Im}(k_{\mathfrak{eff}}\cos\theta_0)$. However, the analyticity of the right-hand side is desecrated by the appearance of simple poles placing at the zeros of $\mathscr{W}_2(\alpha)$, i.e., $\alpha=\pm\alpha_m$ satisfying

$$\mathscr{W}_2(\pm\alpha_m)=0,\qquad \mathfrak{Im}(\alpha_m)>\mathfrak{Im}(k_{\mathfrak{eff}}),\qquad m=1,2,3.... \tag{4.31}$$

The poles in the equation (4.30) can be removed by applying the condition that the residues of these poles are zero. Then from equation (4.30), one gets

$$\mathscr{R}^2_+(\alpha_m)=\mathscr{D}^2_m\left(\frac{\eta_1}{\iota k_{eff}}\mathfrak{L}_m\sin\mathfrak{L}_m b-\cos\mathfrak{L}_m b\right)(\mathfrak{f}_m-\iota\alpha_m\mathfrak{g}_m), \tag{4.32}$$

where $\mathfrak{f}_m$ and $\mathfrak{g}_m$ are denoted by

$$\begin{bmatrix}\mathfrak{f}_m\\ \mathfrak{g}_m\end{bmatrix}=\frac{1}{\mathscr{D}^2_m}\int_0^b\begin{bmatrix}\mathfrak{f}(t)\\ \mathfrak{g}(t)\end{bmatrix}\left[\frac{\sin\mathfrak{L}_m t}{\mathfrak{L}_m}-\frac{\eta_4}{\iota k_{\mathfrak{eff}}}\cos\mathfrak{L}_m t\right]dt, \tag{4.33}$$

with

$$\mathfrak{L}_m=\sqrt{k^2_{\mathfrak{eff}}-\alpha^2_m} \tag{4.34}$$

and

$$\mathscr{D}^2_m=-\frac{\mathfrak{L}_m}{2\alpha_m}\left(\frac{\cos\mathfrak{L}_m b}{\mathfrak{L}_m}+\frac{\eta_4}{\iota k_{\mathfrak{eff}}}\sin\mathfrak{L}_m b\right)\frac{\partial}{\partial\alpha}\mathscr{W}_2(\alpha_m). \tag{4.35}$$

Hence, considering equation (4.21) and transformed domain of continuity relation given by equation (4.10), one can write

$$\iota\mathscr{R}_+^2(\alpha)\chi(\eta_1,\alpha)-\overset{\prime}{F}_-(\alpha,b)=-\frac{2k_{\mathfrak{eff}}\sin\theta_0 e^{-\iota k_{\mathfrak{eff}}b\sin\theta_0}}{(\eta_1\sin\theta_0+1)(\alpha-k_{\mathfrak{eff}}\cos\theta_0)}$$
$$+\int_0^b(\mathfrak{f}(t)-\iota\alpha\mathfrak{g}(t))\cos\mathfrak{L}(b-t)\,dt+\frac{\cos\mathfrak{L}b+\frac{\eta_4}{\iota k_{\mathfrak{eff}}}\mathfrak{L}\sin\mathfrak{L}b}{\mathscr{W}_2(\alpha)}$$
$$\times\left[\mathscr{R}_+^2(\alpha)-\int_0^b(\mathfrak{f}(t)-\iota\alpha\mathfrak{g}(t))\left(\frac{\sin\mathfrak{L}(b-t)}{\mathfrak{L}(\alpha)}+\frac{\eta_1}{\iota k_{\mathfrak{eff}}}\cos\mathfrak{L}(b-t)\right)dt\right], \tag{4.36}$$

where

$$\chi(\eta_j,\alpha)=\frac{\mathfrak{L}(\alpha)}{\eta_j\mathfrak{L}(\alpha)+k_{\mathfrak{eff}}}. \tag{4.37}$$

After simplification, equation (5.33) takes the form

$$\frac{\chi(\eta_1,\alpha)\mathscr{R}_+^2(\alpha)}{\chi(\eta_4,\alpha)\mathscr{N}^2(\alpha)}+\overset{\prime}{F}_-(\alpha,b)=\frac{2k_{\mathfrak{eff}}\sin\theta_0 e^{-\iota k_{\mathfrak{eff}}b\sin\theta_0}}{(\eta_1\sin\theta_0+1)(\alpha-k_{\mathfrak{eff}}\cos\theta_0)}$$
$$-\frac{1}{\mathscr{W}_2(\alpha)}\int_0^b(\mathfrak{f}(t)-\iota\alpha\mathfrak{g}(t))\left(\frac{\sin\mathfrak{L}(\alpha)t}{\mathfrak{L}(\alpha)}-\frac{\eta_4}{\iota k_{\mathfrak{eff}}}\cos\mathfrak{L}(\alpha)t\right)dt, \tag{4.38}$$

where

$$\mathscr{N}^2(\alpha)=\mathscr{W}_2(\alpha)e^{\iota\mathfrak{L}(\alpha)b}. \tag{4.39}$$

Owing to equation (4.33), $\mathfrak{f}(t)$ and $\mathfrak{g}(t)$ can be expanded into a series of eigenfunctions as under

$$\begin{bmatrix}\mathfrak{f}(t)\\ \mathfrak{g}(t)\end{bmatrix}=\sum_{m=1}^{\infty}\begin{bmatrix}\mathfrak{f}_m\\ \mathfrak{g}_m\end{bmatrix}\left[\frac{\sin\mathfrak{L}_m t}{\mathfrak{L}_m}-\frac{\eta_4}{\iota k_{\mathfrak{eff}}}\cos\mathfrak{L}_m t\right]. \tag{4.40}$$

Using equation (4.40) in equation (4.38), one obtains the required Wiener-Hopf equation valid in the strip $\mathfrak{Im}(-k_{\mathfrak{eff}}) < \mathfrak{Im}(\alpha) < \mathfrak{Im}(k_{\mathfrak{eff}})$ as follows:

$$\frac{\chi(\eta_1,\alpha)\mathscr{R}_+^2(\alpha)}{\chi(\eta_4,\alpha)\mathscr{N}^2(\alpha)} + \overset{\prime}{F}_-(\alpha,b) = \frac{2k_{\mathfrak{eff}}\sin\theta_0 e^{-\iota k_{\mathfrak{eff}} b\sin\theta_0}}{(\eta_1\sin\theta_0+1)(\alpha-k_{\mathfrak{eff}}\cos\theta_0)} + \sum_{m=1}^{\infty}\frac{(\mathfrak{f}_m-\iota\alpha\mathfrak{g}_m)\mathfrak{L}_m}{\alpha^2-\alpha_m^2}\left(\frac{\cos\mathfrak{L}_m b}{\mathfrak{L}_m}+\frac{\eta_4}{\iota k_{\mathfrak{eff}}}\sin\mathfrak{L}_m b\right). \tag{4.41}$$

4.3 SOLUTION OF WIENER-HOPF EQUATION

To solve the Wiener-Hopf equation the kernel functions $\mathscr{N}^2(\alpha)$ and $\chi(\eta_j,\alpha))$ in equation (4.41) can be factorized by applying the known results as follows

$$\mathscr{N}_+^2(\alpha) = \left[\left(\frac{\eta_1-\eta_4}{\iota k_{\mathfrak{eff}}}\right)\cos k_{\mathfrak{eff}} b + (1-\eta_1\eta_4)\frac{\sin k_{\mathfrak{eff}} b}{k_{\mathfrak{eff}}}\right]^{\frac{1}{2}} \times \exp\left[\frac{\mathfrak{L}(\alpha)b}{\pi}\ln\left(\frac{\alpha+\iota\mathfrak{L}(\alpha)}{k_{\mathfrak{eff}}}\right)+\frac{\iota\alpha b}{\pi}\left(1-C+\ln\left[\frac{2\pi}{k_{\mathfrak{eff}}b}\right]+\iota\frac{\pi}{2}\right)\right]\prod_{m=1}^{\infty}\left(1+\frac{\alpha}{\alpha_m}\right)e^{\frac{\iota\alpha b}{m\pi}} \tag{4.42}$$

and

$$\mathscr{N}_-^2(\alpha) = \mathscr{N}_+^2(-\alpha). \tag{4.43}$$

Now, on multiplying the Wiener-Hopf equation (4.41) on both sides with $\frac{\chi_-(\eta_4,\alpha)\mathscr{N}_-^2(\alpha)}{\chi_-(\eta_1,\alpha)}$, one obtains

$$\frac{\chi_+(\eta_1,\alpha)\mathscr{R}_+^2(\alpha)}{\mathscr{N}_+^2(\alpha)\chi_+(\eta_4,\alpha)} + \frac{\overset{\prime}{F}_-(\alpha,b)\chi_-(\eta_4,\alpha)\mathscr{N}_-^2(\alpha)}{\chi_-(\eta_1,\alpha)} = \frac{2k_{\mathfrak{eff}}\sin\theta_0 e^{-\iota k_{\mathfrak{eff}} b\sin\theta_0}\chi_-(\eta_4,\alpha)\mathscr{N}_-^2(\alpha)}{(\eta_1\sin\theta_0+1)(\alpha-k_{\mathfrak{eff}}\cos\theta_0)\chi_-(\eta_1,\alpha)} + \sum_{m=1}^{\infty}\frac{(\mathfrak{f}_m-\iota\alpha\mathfrak{g}_m)\mathfrak{L}_m\chi_-(\eta_4,\alpha)\mathscr{N}_-^2(\alpha)}{(\alpha^2-\alpha_m^2)\chi_-(\eta_1,\alpha)}\left(\frac{\cos\mathfrak{L}_m b}{\mathfrak{L}_m}+\frac{\eta_4}{\iota k_{\mathfrak{eff}}}\sin\mathfrak{L}_m b\right). \tag{4.44}$$

With help of cauchy's integral formula the terms on the right-hand side of equation (4.44) can be decomposed as

$$\frac{2k_{\mathfrak{eff}}\sin\theta_0 e^{-\iota k_{\mathfrak{eff}} b\sin\theta_0}\chi_-(\eta_4,\alpha)\mathscr{N}_-^2(\alpha)}{(\eta_1\sin\theta_0+1)(\alpha-k_{\mathfrak{eff}}\cos\theta_0)\chi_-(\eta_1,\alpha)} = \frac{2k_{\mathfrak{eff}}\sin\theta_0 e^{-\iota k_{\mathfrak{eff}} b\sin\theta_0}}{(\eta_1\sin\theta_0+1)(\alpha-k_{\mathfrak{eff}}\cos\theta_0)}$$
$$\times\left[\frac{\chi_-(\eta_4,\alpha)\mathscr{N}_-^2(\alpha)}{\chi_-(\eta_1,\alpha)} - \frac{\chi_-(\eta_4,k_{\mathfrak{eff}}\cos\theta_0)\mathscr{N}_-^2(k_{\mathfrak{eff}}\cos\theta_0)}{\chi_-(\eta_1,k_{\mathfrak{eff}}\cos\theta_0)}\right]$$
$$+\frac{2k_{\mathfrak{eff}}\sin\theta_0 e^{-\iota k_{\mathfrak{eff}} b\sin\theta_0}\chi_-(\eta_4,k_{\mathfrak{eff}}\cos\theta_0)\mathscr{N}_-^2(k_{\mathfrak{eff}}\cos\theta_0)}{(\eta_1\sin\theta_0+1)(\alpha-k_{\mathfrak{eff}}\cos\theta_0)\chi_-(\eta_1,k_{\mathfrak{eff}}\cos\theta_0)} \tag{4.45}$$

and

$$\sum_{m=1}^{\infty}\frac{\mathfrak{L}_m(\mathfrak{f}_m-\iota\alpha\mathfrak{g}_m)\chi_-(\eta_4,\alpha)\mathscr{N}_-^2(\alpha)}{(\alpha^2-\alpha_m^2)\chi_-(\eta_1,\alpha)}\left(\frac{\cos\mathfrak{L}_m b}{\mathfrak{L}_m}+\frac{\eta_4}{\iota k_{\mathfrak{eff}}}\sin\mathfrak{L}_m b\right]$$
$$=\sum_{m=1}^{\infty}\frac{\mathfrak{L}_m}{(\alpha+\alpha_m)}\left(\frac{\cos\mathfrak{L}_m b}{\mathfrak{L}_m}+\frac{\eta_4}{\iota k_{\mathfrak{eff}}}\sin\mathfrak{L}_m b\right)$$
$$\times\left[\frac{(\mathfrak{f}_m-\iota\alpha\mathfrak{g}_m)\chi_-(\eta_4,\alpha)\mathscr{N}_-^2(\alpha)}{(\alpha-\alpha_m)\chi_-(\eta_1,\alpha)}+\frac{(\mathfrak{f}_m+\iota\alpha_m\mathfrak{g}_m)\chi_+(\eta_4,\alpha_m)\mathscr{N}_+^2(\alpha_m)}{2\alpha_m\chi_+(\eta_1,\alpha_m)}\right]$$
$$-\sum_{m=1}^{\infty}\frac{\mathfrak{L}_m(\mathfrak{f}_m+\iota\alpha_m\mathfrak{g}_m)\chi_+(\eta_4,\alpha_m)\mathscr{N}_+^2(\alpha_m))}{2\alpha_m\chi_+(\eta_1,\alpha_m)(\alpha+\alpha_m)}\left(\frac{\cos\mathfrak{L}_m b}{\mathfrak{L}_m}+\frac{\eta_4}{\iota k_{\mathfrak{eff}}}\sin\mathfrak{L}_m b\right). \tag{4.46}$$

Now using equations (4.45) and (4.46) in equation (4.44), then placing the terms which are analytic in the upper half-plane ($\mathfrak{Im}(\alpha) > -k_{\mathfrak{eff}}$) at the left-hand side and those which analytic in lower half-plane ($\mathfrak{Im}(\alpha) < k_{\mathfrak{eff}}$) at the right-hand side, gives

$$\frac{\chi_+(\eta_1,\alpha)\mathscr{R}_+^2(\alpha)}{\mathscr{N}_+^2(\alpha)\chi_+(\eta_4,\alpha)} - \frac{2k_{\mathfrak{eff}}\sin\theta_0 e^{-\iota k_{\mathfrak{eff}} b\sin\theta_0}\chi_-(\eta_4,k_{\mathfrak{eff}}\cos\theta_0)\mathscr{N}_-^2(k_{\mathfrak{eff}}\cos\theta_0)}{(\eta_1\sin\theta_0+1)(\alpha-k_{\mathfrak{eff}}\cos\theta_0)\chi_-(\eta_1,k_{\mathfrak{eff}}\cos\theta_0)}$$
$$+\sum_{m=1}^{\infty}\frac{\mathfrak{L}_m(\mathfrak{f}_m+\iota\alpha_m\mathfrak{g}_m)\chi_+(\eta_4,\alpha_m)\mathscr{N}_+^2(\alpha_m)}{2\alpha_m\chi_+(\eta_1,\alpha_m)(\alpha+\alpha_m)}\left(\frac{\cos\mathfrak{L}_m b}{\mathfrak{L}_m}+\frac{\eta_4}{\iota k_{eff}}\sin\mathfrak{L}_m b\right)$$
$$=-\frac{F'_-(\alpha,b)\chi_-(\eta_4,\alpha)\mathscr{N}_-^2(\alpha)}{\chi_-(\eta_1,\alpha)}+\sum_{m=1}^{\infty}\frac{\mathfrak{L}_m}{(\alpha+\alpha_m)}\left(\frac{\cos\mathfrak{L}_m b}{\mathfrak{L}_m}+\frac{\eta_4}{\iota k_{\mathfrak{eff}}}\sin\mathfrak{L}_m b\right)$$
$$\times\left[\frac{(\mathfrak{f}_m-\iota\alpha\mathfrak{g}_m)\chi_-(\eta_4,\alpha)\mathscr{N}_-^2(\alpha)}{(\alpha-\alpha_m)\chi_-(\eta_1,\alpha)}+\frac{(\mathfrak{f}_m+\iota\alpha_m\mathfrak{g}_m)\chi_+(\eta_4,\alpha_m)\mathscr{N}_+^2(\alpha_m)}{2\alpha_m\chi_+(\eta_1,\alpha_m)}\right]$$
$$+\sum_{m=1}^{\infty}\frac{\mathfrak{L}_m}{(\alpha+\alpha_m)}\left(\frac{\cos\mathfrak{L}_m b}{\mathfrak{L}_m}+\frac{\eta_4}{\iota k_{\mathfrak{eff}}}\sin\mathfrak{L}_m b\right)$$
$$\times\left[\frac{(\mathfrak{f}_m-\iota\alpha\mathfrak{g}_m)\chi_-(\eta_4,\alpha)\mathscr{N}_-^2(\alpha)}{(\alpha-\alpha_m)\chi_-(\eta_1,\alpha)}+\frac{(\mathfrak{f}_m+\iota\alpha_m\mathfrak{g}_m)\chi_+(\eta_4,\alpha_m)\mathscr{N}_+^2(\alpha_m)}{2\alpha_m\chi_+(\eta_1,\alpha_m)}\right]. \tag{4.47}$$

The required solution of Wiener-Hopf equation can be obtained by using analytical continuation principle following the extended Liouville's theorem gives

$$\frac{\chi_+(\eta_1,\alpha)\mathscr{K}^2_+(\alpha)}{\chi_+(\eta_4,\alpha)\mathscr{N}_+(\alpha)} = \frac{2k_{\mathfrak{eff}}\sin\theta_0 e^{-\iota k_{\mathfrak{eff}} b\sin\theta_0}\chi_-(\eta_4,k_{\mathfrak{eff}}\cos\theta_0)\mathscr{N}^2_-(k_{\mathfrak{eff}}\cos\theta_0)}{(\eta_1\sin\theta_0+1)(\alpha-k_{\mathfrak{eff}}\cos\theta_0)\chi_-(\eta_1,k_{\mathfrak{eff}}\cos\theta_0)}$$
$$-\sum_{m=1}^{\infty}\frac{(\mathfrak{f}_m+\iota\alpha_m\mathfrak{g}_m)\mathfrak{L}_m}{2\alpha_m(\alpha+\alpha_m)}\left(\frac{\cos\mathfrak{L}_m b}{\mathfrak{L}_m}+\frac{\eta_4}{\iota k_{\mathfrak{eff}}}\sin\mathfrak{L}_m b\right)\frac{\chi_+(\eta_4,\alpha_m)\mathscr{N}^2_+(\alpha_m)}{\chi_+(\eta_1,\alpha_m)}. \tag{4.48}$$

4.4 DETERMINATION OF THE UNKNOWN COEFFICIENTS

The equation (4.48) contains infinite number of unknown coefficients. To find out these unknown coefficients one uses method of Mode-Matching technique with the Fourier transform [70]. The Mode-Matching technique enables us to declare the field components defined in the waveguide region in terms of normal modes, as

$$H^2_z(x,y) = \sum_{m=1}^{\infty} a_n\left(\frac{\sin\zeta_n y}{\zeta_n}-\frac{\eta_3}{\iota k_{\mathfrak{eff}}}\cos\zeta_n y\right)e^{-\iota\beta_n x}, \tag{4.49}$$

where

$$\beta_n=\sqrt{k^2_{\mathfrak{eff}}-\zeta^2_n},\quad \Im\mathfrak{m}(\beta_n)>\Im\mathfrak{m}(k_{\mathfrak{eff}}),\quad n=1,2,3,.... \tag{4.50}$$

To find β_n and ζ_n, placing equations (4.49) in equation (4.7) gives

$$\frac{(\eta_3+\eta_2)}{\iota k_{\mathfrak{eff}}}\cos\zeta_n b-(1+\frac{\eta_2\eta_3}{k^2_{\mathfrak{eff}}}\zeta^2_n)\frac{\sin\zeta_n y}{\zeta_n}=0,\qquad n=1,2,3,.... \tag{4.51}$$

Using equations (4.40) and (4.49) in equation (4.23), then multiplying the resulting equation by $(\frac{\sin\mathfrak{L}_j y}{\mathfrak{L}_j}-\frac{\eta_4}{\iota k_{\mathfrak{eff}}}\cos\mathfrak{L}_j y)$ and integrating with respect to y from $y=0$ to $y=b$, one obtains

$$\mathfrak{f}_m-\iota\alpha_m\mathfrak{g}_m=-\frac{\iota}{\mathscr{D}^2_m}\sum_{n=1}^{\infty}\mathfrak{a}_n(\alpha+\beta_n)\Delta_{nm}, \tag{4.52}$$

where Δ_{nm} is

$$\Delta_{nm} = \frac{(\eta_3 - \eta_4)}{\iota k_{\text{eff}}(\zeta_n^2 - \mathfrak{L}_m^2)} + \frac{(\eta_2 + \eta_1)\mathfrak{L}_m \zeta_n}{\iota k_{\text{eff}}(\zeta_n^2 - \mathfrak{L}_m^2)} \left(\frac{\cos \zeta_n b}{\zeta_n} + \frac{\eta_3}{\iota k_{\text{eff}}} \sin \zeta_n b \right) \times \left(\frac{\cos \mathfrak{L}_m b}{\mathfrak{L}_m} + \frac{\eta_4}{\iota k_{\text{eff}}} \sin \mathfrak{L}_m b \right). \tag{4.53}$$

Placing equation (4.52) in equation (4.32), then using the resulting equation in equation (4.48) to yield

$$\sum_{n=1}^{\infty} \mathscr{A}_n(\alpha_j)\mathfrak{a}_n = I(\alpha_j), \qquad j = 1, 2, 3, ..., \tag{4.54}$$

where

$$\begin{aligned} \mathscr{A}_n(\alpha_j) = & -\iota \left(\frac{\eta_1}{k_{\text{eff}}} \mathfrak{L}_j \sin \mathfrak{L}_j b - \cos \mathfrak{L}_m b \right) (\alpha_j + \beta_n)\Delta_{nj} \\ & - \frac{\iota \mathscr{N}_+^2(\alpha_j)\chi_+(\eta_4, \alpha_j)}{\chi_+(\eta_1, \alpha_j)} \sum_{m=1}^{\infty} \frac{\mathfrak{L}_m(\beta_n - \alpha_m)\Delta_{nm}}{2\alpha_m \mathscr{D}_m^2(\alpha_j + \alpha_m)} \\ & \left(\frac{\cos \mathfrak{L}_m b}{\mathfrak{L}_m} + \frac{\eta_4}{\iota k} \sin \mathfrak{L}_m b \right) \frac{\chi_+(\eta_4, \alpha_m)\mathscr{N}_+^2(\alpha_m)}{\chi_+(\eta_1, \alpha_m)}, \end{aligned} \tag{4.55}$$

and

$$I(\alpha_j) = \frac{2k_{\text{eff}} \sin\theta_0 e^{-\iota k_{\text{eff}} b \sin\theta_0} \chi_-(\eta_4, k_{\text{eff}} \cos\theta_0) \mathscr{N}_-^2(k_{\text{eff}} \cos\theta_0) \mathscr{N}_+^2(\alpha_j) \chi_+(\eta_4, \alpha_j)}{(\eta_1 \sin\theta_0 + 1)(\alpha_j - k_{\text{eff}} \cos\theta_0)\chi_+(\eta_1, \alpha_j)\chi_-(\eta_1, k_{\text{eff}} \cos\theta_0)}. \tag{4.56}$$

The infinite system of algebraic equations represented by equation (4.54) is solved numerically. To solve this infinite system of algebraic equations we have truncated it after first N terms in order to obtain required diffracted field.

4.5 THE DIFFRACTED FIELD

The diffracted field $H_z^1(x, y)$ is acquired redby taking the inverse Fourier transform of $F(\alpha, y)$. By using equation (4.20), one obtains

$$H_z^1(x, y) = \frac{1}{2\pi} \int_{\mathscr{L}} \frac{\mathscr{R}_+^2(\alpha)}{1 + \frac{\eta_1}{k_{\text{eff}}} \mathfrak{L}(\alpha)} e^{\iota \mathfrak{L}(\alpha)(y-b)} e^{-\iota \alpha x} d\alpha. \tag{4.57}$$

Using the change of variables $\alpha = -k_{\mathfrak{eff}}\cos t$, $x = \rho\cos\theta$ and $y = \rho\sin\theta$ in the equation (4.57), one yields

$$H_z^1(\rho,\theta) = \frac{1}{2\pi}\int_{\mathscr{L}} \frac{\mathscr{R}_+^2(-k_{\mathfrak{eff}}\cos t)\,k_{\mathfrak{eff}}\sin t}{1+\eta_1\sin t}\, e^{-\iota k_{\mathfrak{eff}}\sin t + \iota k_{\mathfrak{eff}}\rho\cos(t-\theta)}\,dt. \tag{4.58}$$

The asymptotic evaluation of the integral in the equation (4.58) can be obtained via saddle-point technique. Here, saddle-point rests at $t=\theta$ whose contribution is

$$H_z^1(\rho,\theta) = P_1\,(P_2+P_2), \tag{4.59}$$

where

$$P_1 = \left(\frac{k\sqrt{(\epsilon_1^2-\epsilon_2^2)/\epsilon_1}\sin\theta\, e^{\iota k\rho\sqrt{(\epsilon_1^2-\epsilon_2^2)/\epsilon_1}-\iota\frac{\pi}{4}-\iota k\sqrt{(\epsilon_1^2-\epsilon_2^2)/\epsilon_1}b\sin\theta}}{\sqrt{2\pi k\rho}(1+\eta_1\sin t)}\right) \times\left(\frac{\chi_-(\eta_4,k\sqrt{(\epsilon_1^2-\epsilon_2^2)/\epsilon_1}\cos\theta_0)\mathscr{N}_-(k\sqrt{(\epsilon_1^2-\epsilon_2^2)/\epsilon_1}\cos\theta_0)}{\chi_-(\eta_1,k\sqrt{(\epsilon_1^2-\epsilon_2^2)/\epsilon_1}\cos\theta_0)}\right), \tag{4.60}$$

$$P_2 = \left(\frac{2k\sqrt{(\epsilon_1^2-\epsilon_2^2)}\sin\theta_0 e^{-\iota k\sqrt{(\epsilon_1^2-\epsilon_2^2)/\epsilon_1}b\sin\theta_0}\mathscr{N}_-(k\sqrt{(\epsilon_1^2-\epsilon_2^2)/\epsilon_1}\cos\theta_0)}{\sqrt{\epsilon_1}(\eta_1\sin\theta_0+1)(\cos\theta+\cos\theta_0)}\right) \times\left(\frac{\chi_-(\eta_4,k\sqrt{(\epsilon_1^2-\epsilon_2^2)/\epsilon_1}\cos\theta_0)}{\chi_-(\eta_1,k\sqrt{\times(\epsilon_1^2-\epsilon_2^2)/\epsilon_1}\cos\theta_0)}\right) \tag{4.61}$$

and

$$P_3 = \sum_{m=1}^{\infty}\left(\frac{(\mathfrak{f}_m+\iota\alpha_m\mathfrak{g}_m)\mathfrak{L}_m}{2\alpha_m(\alpha_m-(k\sqrt{(\epsilon_1^2-\epsilon_2^2)/\epsilon_1}\cos\theta))}\frac{\chi_+(\eta_4,\alpha_m)\mathscr{N}_+(\alpha_m)}{\chi_+(\eta_1,\alpha_m)}\right) \times\left(\frac{\cos\mathfrak{L}_m b}{\mathfrak{L}_m}+\frac{\eta_4}{\iota k\sqrt{(\epsilon_1^2-\epsilon_2^2)/\epsilon_1}}\sin\mathfrak{L}_m b\right). \tag{4.62}$$

4.6 COMPUTATIONAL RESULTS AND DISCUSSION

In this section, we have analyzed and potted the numerical results for various physical parameters of interest. Fig. (4.2) depicts the variation in the diffracted field amplitude versus the truncation number "N". It is apparent that the effect of the truncation number is negligible for $N \geq 80$. Hence, the infinite system of algebraic equations in equation (4.54) can be managed to deal as finite. Fig. (4.3) explores the effect of separation between the parallel plates on the diffracted field amplitude. The amplitude of the diffracted field decreases with the increase of wall impedance $|\eta_1|$ as shown in Fig. (4.4). Figs. (4.5) and (4.6) show that the diffracted field amplitude is not affected by impedances η_2 and η_3, which is similar to the result obtained by Cinar and Büyükaksoy [12]. Fig. (4.7) shows the variation in the diffracted field amplitude with wall impedance η_4. The effect of cold plasma permittivity values ϵ_1 and ϵ_2 has been analyzed in Fig. (4.8) and (4.9), respectively. Here, we have found that the increase in cold plasma permittivity value ϵ_1 highly decreases the diffracted field amplitude while the effect of ϵ_1 is negligibly small. In other words the diffracted field amplitude decreases with increasing ion number density in cold plasma or by decreasing plasma frequency. Here, in this problem it is observed that the diffracted field is highly effected with ϵ_1 while slightly with ϵ_2.

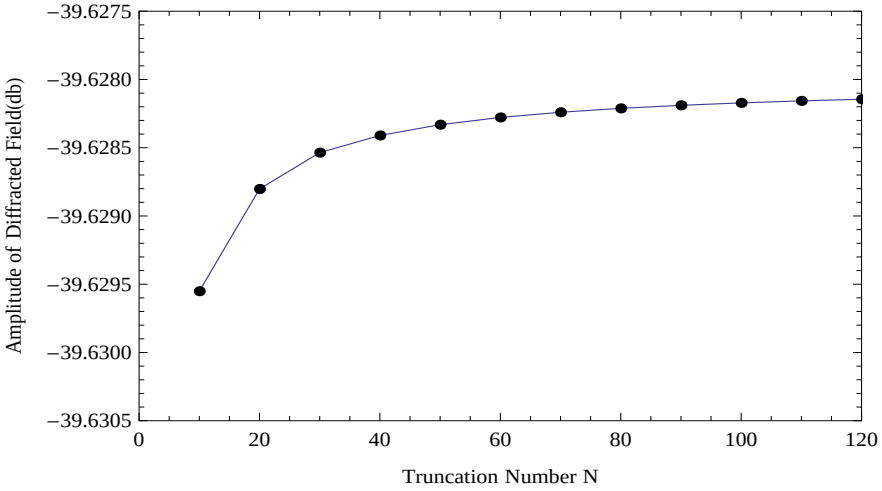

FIGURE 4.2. *Variation in the diffracted field amplitude versus truncation number "N" at* $\theta_0 = 90^o$, $\theta = 45^o$, $k = 5$, $\eta_1 = 0.3\iota$, $\eta_2 = 0.9\iota$, $\eta_3 = 0.6\iota$, $\eta_4 = 0.4\iota$, $\epsilon_1 = 0.8$, $\epsilon_2 = 0.0$ *and* $b = 0.2\lambda$.

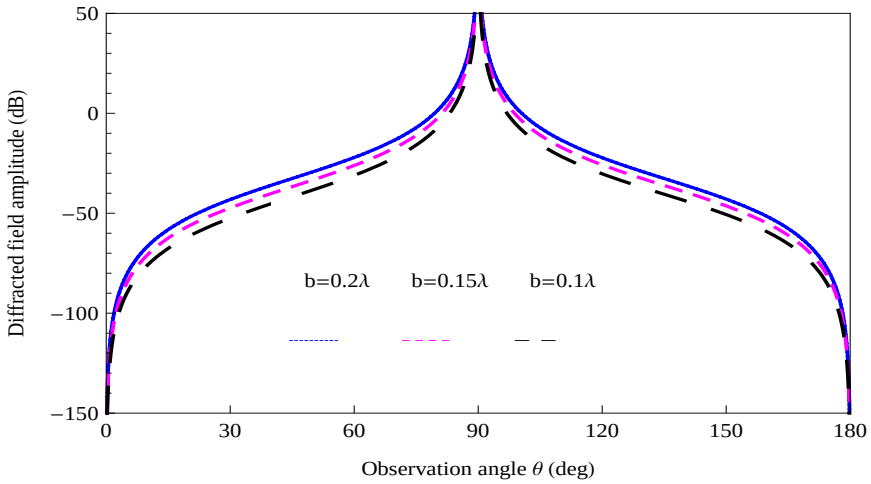

FIGURE 4.3. *Variation in the diffracted field amplitude versus "b" at* $\theta_0 = 90^o$, $k = 5$, $\eta_1 = 0.6\iota$, $\eta_2 = 0.4\iota$, $\eta_3 = 0.7\iota$, $\eta_4 = 0.5\iota$, $\epsilon_1 = 0.8$ *and* $\epsilon_2 = 0$.

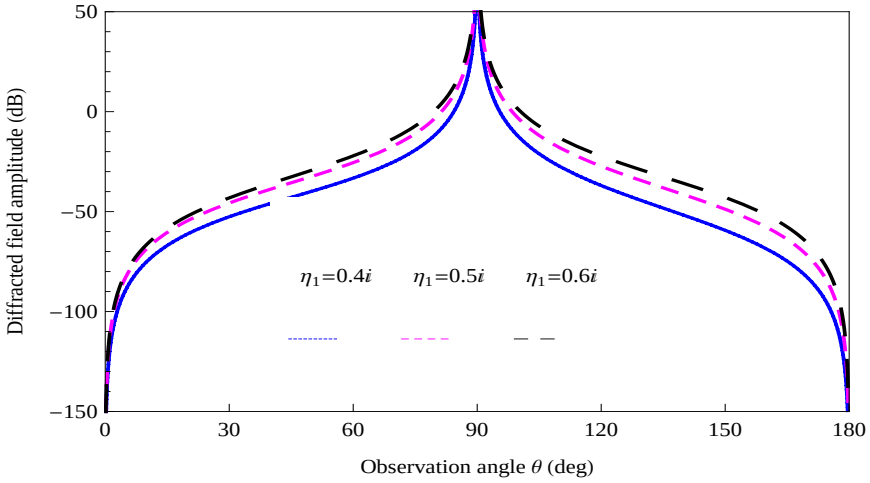

FIGURE 4.4. *Variation in the diffracted field amplitude versus "η_1" at $\phi_0 = 90^o$, $k = 5$, $\eta_2 = 0.4\iota$, $\eta_3 = 0.7\iota$, $\eta_4 = 0.5\iota$, $t\epsilon_1 = 0.8$, $\epsilon_2 = 0$ and $b = 0.2\lambda$.*

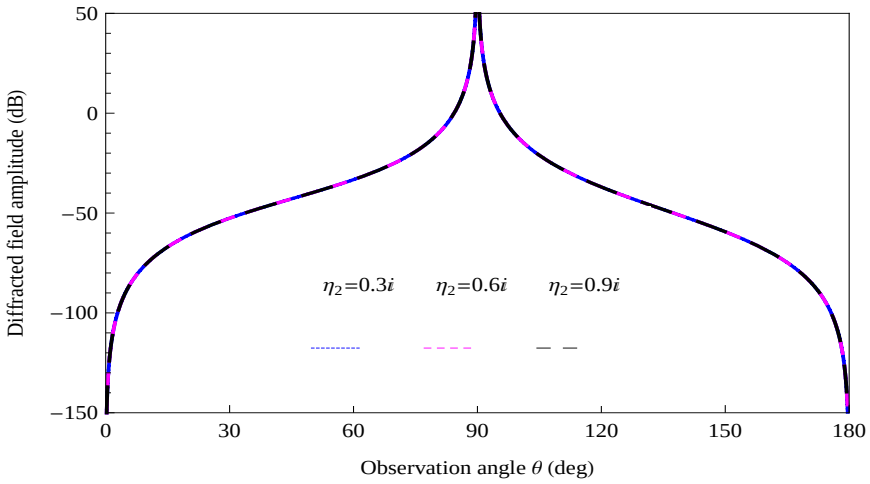

FIGURE 4.5. *Variation in the diffracted field amplitude versus "η_2" at $\theta_0 = 90^o$, $k = 5$, $\eta_1 = 0.4\iota$, $\eta_3 = 0.7\iota$, $\eta_4 = 0.5\iota$, $\epsilon_1 = 0.8$, $\epsilon_2 = 0$ and $b = 0.2\lambda$.*

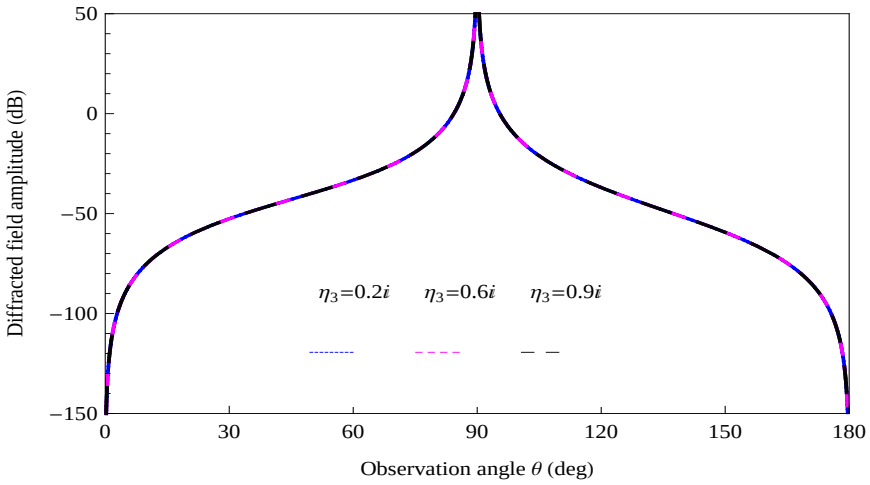

FIGURE 4.6. *Variation in the diffracted field amplitude versus "η_3" at $\theta_0 = 90^o$, $k = 5$, $\eta_1 = 0.4\iota$, $\eta_2 = 0.3\iota$, $\eta_4 = 0.5\iota$, $\epsilon_1 = 0.8$, $\epsilon_2 = 0$ and $b = 0.2\lambda$.*

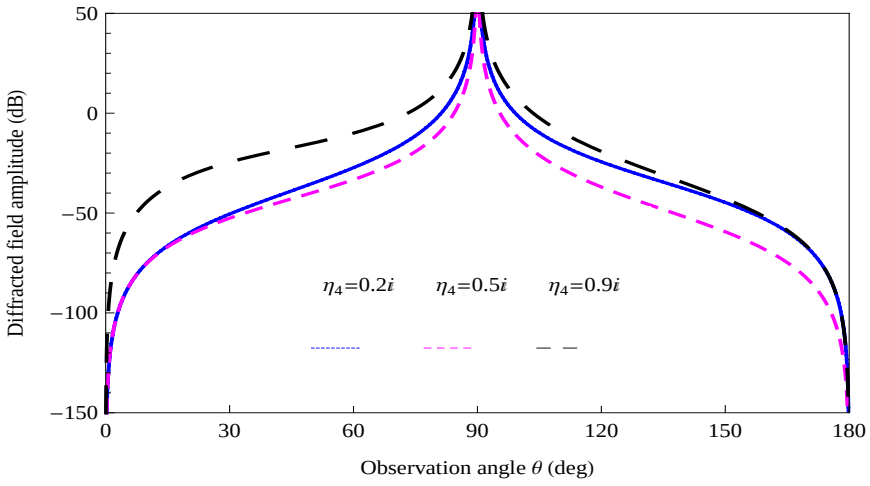

FIGURE 4.7. *Variation in the diffracted field amplitude versus "η_4" at $\theta_0 = 90^o$,$k = 5$, $\eta_1 = 0.4\iota$, $\eta_2 = 0.3\iota$, $\eta_3 = 0.5\iota$, $\epsilon_1 = 0.8$, $\epsilon_2 = 0$ and $b = 0.2\lambda$.*

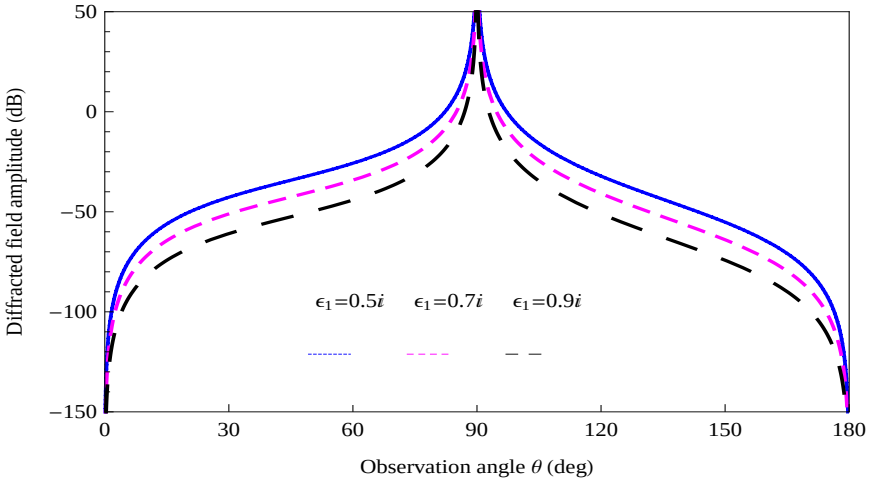

FIGURE 4.8. *Variation in the diffracted field amplitude versus "ϵ_1" at $\theta_0 = 90^o$, $k = 5$, $\eta_1 = 0.4\iota$, $\eta_2 = 0.3\iota$, $\eta_3 = 0.5\iota$, $\eta_4 = 0.7$, $\epsilon_2 = 0$ and $b = 0.2\lambda$.*

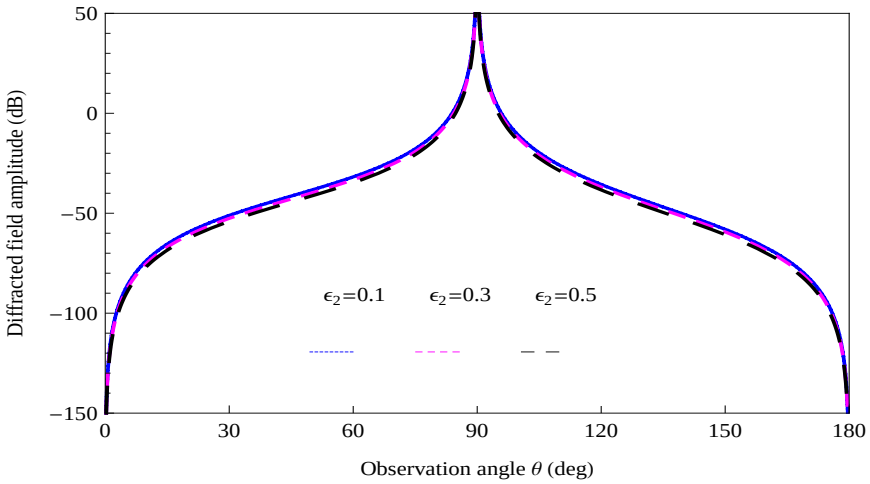

FIGURE 4.9. *Variation in the diffracted field amplitude versus "ϵ_2" at $\theta_0 = 90^o$, $k = 5$, $\eta_1 = 0.4\iota$, $\eta_2 = 0.3\iota$, $\eta_3 = 0.5\iota$, $\eta_4 = 0.7$, $\epsilon_1 = 0.9$ and $b = 0.2\lambda$.*

CHAPTER 5

EFFECT OF COLD PLASMA PERMITTIVITY ON THE RADIATION OF THE DOMINANT TEM-WAVE BY AN IMPEDANCE LOADED PARALLEL-PLATE WAVEGUIDE RADIATOR

In this chapter, the aim is to determine the effect of cold plasma permittivity and other parameters on the radiation phenomenon. For this purpose an impedance coated parallel-plate waveguide radiator located in cold plasma is considered. This radiation phenomenon was initially considered by Rulf and Hurd [86]. According to them, the presence of surface impedances $+Z_1$ on the upper and $-Z_1$ on the lower faces is the merely combination of impedances that converts the boundary-valued problem into a scalar Wiener-Hopf equation. After that Büyükaksoy and Birbir [41] generalized the problem for different upper and lower faces surface impedances and solved by the hybrid method consisting of Fourier transform with Mode Matching technique.

The section wise summery of this chapter is arranged as follow. Section (5.1) consists of boundary-valued problem for radiation phenomenon obtained from the geometry of the problem. Using this mathematical model, the Wiener-Hopf

equation is formulated in Section (5.2) while the solution of Wiener-Hopf equation is obtained in Section (5.3). In Section (5.4) the infinite number of unknown coefficients are determined. The mathematical expression for the radiated field is obtained in Section (5.5) whereas the numerical results are shown in Section (5.6). The contents of this chapter are published in **Mathematical Methods in the Applied Sciences**, DOI : 10.1002/mma.3464.

5.1 MATHEMATICAL MODEL OF THE PROBLEM

Here, we consider the radiation of the dominant transverse electromagnetic wave (TEM-wave) which is incident from the left in the parallel-plate waveguide region formed by two-part impedance plane S_1 define by $\{(x,y,z)|\ x \in (-\infty,\infty),\ y = 0,\ z \in (-\infty,\infty)\}$ and a parallel impedance half-plane S_2 defined by $\{(x,y,z)|\ x \in (-\infty,0),\ y = b,\ z \in (-\infty,\infty)\}$. The left and right parts of the plane S_1 are coated by the impedances Z_1 and Z_2, respectively. The surface impedance of the lower and upper faces of the half-plane S_2 are assumed to be Z_3 and Z_4, respectively, as shown in Fig. (5.1).

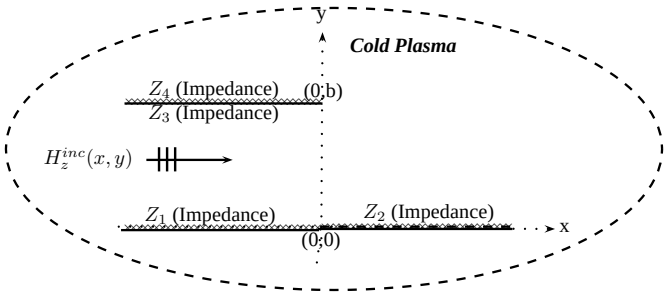

FIGURE 5.1. *Geometry of the impedance loaded parallel-plate waveguide radiator located in cold plasma*

The total field can be expressed as follows:

$$H_z^T(x,y) = \begin{cases} H_z^1(x,y), & y \in (b,\infty) \\ \left[H_z^{inc}(x,y) + H_z^2(x,y)\right]\mathscr{H}(-x) + H_z^3(x,y)\mathscr{H}(x), & y \in (0,b), \end{cases} \tag{5.1}$$

where $\mathscr{H}(x)$ denotes the Heaviside unit step function, $H_z^{inc}(x,y)$ is the incident field given by

$$H_z^{inc}(x,y) = e^{\iota k_{\text{eff}} x}, \tag{5.2}$$

with

$$k_{\text{eff}} = k\sqrt{\frac{\epsilon_1^2 - \epsilon_2^2}{\epsilon_1}} \quad \text{and} \quad k = \omega\sqrt{\epsilon_0\mu_0}. \tag{5.3}$$

$H_z^j \quad (j = 1,2,3)$ are the scattered fields satisfy the Helmholtz's equation in cold plasma

$$\left[\frac{\partial^2}{\partial x^2} + \frac{\partial^2}{\partial y^2} + k_{\text{eff}}^2\right]\left[H_z^j(x,y)\right] = 0, \tag{5.4}$$

with the following corresponding boundary conditions and continuity relations

$$\left(\eta_4 k_{\text{eff}} + \frac{\partial}{\partial y}\right) H_z^1(x,b) = 0, \qquad x \in (-\infty, 0), \tag{5.5}$$

$$\left(\eta_3 k_{\text{eff}} - \frac{\partial}{\partial y}\right) H_z^2(x,b) = 0, \qquad x \in (-\infty, 0), \tag{5.6}$$

$$\mathscr{H}(-x)\left(\eta_1 k_{\text{eff}} + \frac{\partial}{\partial y}\right) H_z^2(x,0) + \mathscr{H}(x)\left(\eta_2 k_{\text{eff}} + \frac{\partial}{\partial y}\right) H_z^3(x,0) = 0, \quad x \in (-\infty, \infty), \tag{5.7}$$

$$H_z^1(x,b) = H_z^3(x,b), \qquad x \in (0,\infty), \tag{5.8}$$

$$\frac{\partial}{\partial y} H_z^1(x,b) = \frac{\partial}{\partial y} H_z^3(x,b), \qquad x \in (0,\infty), \tag{5.9}$$

$$H_z^{inc}(0,y) + H_z^2(0,y) = H_z^3(0,y), \qquad y \in (0,b), \tag{5.10}$$

$$\frac{\partial}{\partial x} H_z^{inc}(0,y) + \frac{\partial}{\partial x} H_z^2(0,y) = \frac{\partial}{\partial x} H_z^3(0,y), \qquad y \in (0,b). \tag{5.11}$$

The radiation and edge conditions are discussed as earlier.

5.2 FORMULATION OF WIENER-HOPF EQUATION

Fourier transform of the Helmholtz equation in cold plasma is satisfied by the field $H_z^1(x,y)$ in the waveguide region $x \in (-\infty,\infty)$ and $y \in (b,\infty)$ gives

$$\left[\frac{d^2}{dy^2} + (k_{\text{eff}}^2 - \alpha^2)\right] F(\alpha, y) = 0, \tag{5.12}$$

With the help of radiation condition solution of equation (5.12) leads to

$$F(\alpha, y) = A_3(\alpha) e^{\iota \mathfrak{L}(\alpha)(y-b)}, \tag{5.13}$$

where

$$\mathfrak{L}(\alpha) = \sqrt{k_{\mathfrak{eff}}^2 - \alpha^2}. \tag{5.14}$$

To find the unknown coefficient $A_3(\alpha)$, using the transformed domain of the boundary condition represented by the equation (5.5), one obtains

$$A_3(\alpha) = \frac{\mathscr{R}_+^3(\alpha)}{\eta_4 k_{\mathfrak{eff}} + \iota \mathfrak{L}(\alpha)}, \tag{5.15}$$

with

$$\mathscr{R}_+^3(\alpha) = \eta_4 k_{\mathfrak{eff}} F_+(\alpha, b) + \overset{\prime}{F}_+(\alpha, b), \tag{5.16}$$

where the prime sign in equation (5.16) denotes the derivative with respect to y. On using the additive decomposition theorem and equation (5.15) in equation (5.13), one gets

$$F_+(\alpha, y) + F_-(\alpha, y) = \frac{\mathscr{R}_+^3(\alpha)}{\eta_4 k_{\mathfrak{eff}} + \iota \mathfrak{L}(\alpha)} e^{\iota \mathfrak{L}(\alpha)(y-b)}. \tag{5.17}$$

The derivative of equation (5.17) with respect to y at $y = b$ takes the form

$$\overset{\prime}{F}_+(\alpha, b) = \frac{\iota \mathfrak{L}(\alpha) \mathscr{R}_+^3(\alpha)}{\eta_4 k_{\mathfrak{eff}} + \iota \mathfrak{L}(\alpha)} - \overset{\prime}{F}_-(\alpha, b). \tag{5.18}$$

As in equation (5.4), the Helmholtz equation in cold plasma is satisfied by field $H_z^2(x, y)$ in the waveguide region $x \in (0, \infty)$ and $y \in (a, b)$, multiplying this equation by $e^{\iota \alpha x}$ and integrating the resultant equation with respect to x from 0 to ∞ yields

$$\left[\frac{d^2}{dy^2} - \mathfrak{L}^2(\alpha) \right] \mathscr{G}_+(\alpha, y) = \mathfrak{f}(t) - \iota \alpha \mathfrak{g}(t), \tag{5.19}$$

where

$$\mathfrak{f}(y) - \iota\alpha\mathfrak{g}(y) = \frac{\partial}{\partial x} H_z^3(0, y) - \iota\alpha H_z^3(0, y) \tag{5.20}$$

and $\mathscr{G}_+(\alpha, y)$ defined by

$$\mathscr{G}_+(\alpha, y) = \int_0^\infty H_z^3(x, y) e^{\iota\alpha x} dx, \tag{5.21}$$

is a regular function in the half-plane.

Owing the method of variation of parameter the solution of the non-homogenous differential equation (5.19) gives

$$\begin{aligned}\mathscr{G}_+(\alpha, y) &= C_7(\alpha)\cos\mathfrak{L}(\alpha)y + C_8(\alpha)\sin\mathfrak{L}(\alpha)y \\ &+ \frac{1}{\mathfrak{L}(\alpha)}\int_0^y (\mathfrak{f}(t) - \iota\alpha\mathfrak{g}(t))\sin\mathfrak{L}(\alpha)(b-t)dt,\end{aligned} \tag{5.22}$$

where $C_7(\alpha)$ and $C_8(\alpha)$ are the unknown spectral coefficients.

To find $C_8(\alpha)$ applying the transformed form of the boundary condition represented by the equation (5.7), one gets

$$C_8(\alpha) = -\frac{\eta_2 k_{\mathfrak{eff}}}{\mathfrak{L}(\alpha)} C_7(\alpha). \tag{5.23}$$

Placing equation (5.23) in equation (5.22) yields

$$\begin{aligned}\mathscr{G}_+(\alpha, y) &= \left[\cos\mathfrak{L}(\alpha)y - \eta_2 k_{\mathfrak{eff}}\frac{\sin\mathfrak{L}(\alpha)y}{\mathfrak{L}(\alpha)}\right] C_7(\alpha) \\ &+ \frac{1}{\mathfrak{L}(\alpha)}\int_0^y (\mathfrak{f}(t) - \iota\alpha\mathfrak{g}(t))\sin\mathfrak{L}(\alpha)(b-t)dt.\end{aligned} \tag{5.24}$$

$C_7(\alpha)$ can be obtained by adding the transformed form of equation (5.9) and $\eta_4 k_{\mathfrak{eff}}$ times of equation (5.8) gives

$$C_7(\alpha) = \frac{\mathscr{R}^2_+(\alpha)}{\mathscr{W}_3(\alpha)} - \frac{1}{\mathfrak{L}(\alpha)\mathscr{W}_3(\alpha)} \int_0^b ((\mathfrak{f}(t) - \iota\alpha\mathfrak{g}(t)) \left(\eta_4 k_{\mathfrak{eff}} \sin\mathfrak{L}(\alpha)(b-t) + \mathfrak{L}(\alpha)\cos\mathfrak{L}(\alpha)(b-t)\right) dt, \quad (5.25)$$

where $$\mathscr{W}_3(\alpha) = (\eta_4 - \eta_2) k_{\mathfrak{eff}} \cos\mathfrak{L}(\alpha) b - (1 + \eta_2\eta_4 k^2_{\mathfrak{eff}}) \frac{\sin\mathfrak{L}(\alpha) b}{\mathfrak{L}(\alpha)}. \quad (5.26)$$

Substituting equation (5.25) in equation (5.24) gives

$$\mathscr{G}_+(\alpha, y) = \frac{\mathfrak{L}(\alpha)\cos\mathfrak{L}(\alpha) y - k_{\mathfrak{eff}}\eta_2 \sin\mathfrak{L}(\alpha) y}{\mathfrak{L}(\alpha)\mathscr{W}_3(\alpha)} \times \left\{ \mathscr{R}^3_+(\alpha) - \int_0^b (\mathfrak{f}(t) - \iota\alpha\mathfrak{g}(t)) \left(\cos\mathfrak{L}(\alpha)(b-t) + k_{\mathfrak{eff}}\eta_4 \frac{\sin\mathfrak{L}(\alpha)(b-t)}{\mathfrak{L}(\alpha)}\right) dt \right\} + \frac{1}{\mathfrak{L}(\alpha)} \int_0^y (\mathfrak{f}(t) - \iota\alpha\mathfrak{g}(t)) \sin\mathfrak{L}(\alpha)(y-t) dt. \quad (5.27)$$

The left-hand side (i.e., $\mathscr{G}_+(\alpha, y)$) of the equation (5.27) is analytic in the region $\mathfrak{Im}(\alpha) > \mathfrak{Im}(k_{\mathfrak{eff}} \cos\theta_0)$. However, the analyticity of the right-hand side is desecrated due to the appearance of simple poles lying at the zeros of $\mathscr{W}_3(\alpha)$, i.e., $\alpha = \pm\alpha_m$ satisfying

$$\mathscr{W}_3(\pm\alpha_m) = 0, \quad \mathfrak{Im}(\alpha_m) > \mathfrak{Im}(k_{eff}), \quad m = 1, 2, 3.... \quad (5.28)$$

The poles in the equation (5.27) can be removed by enforcing the condition that residues of these poles are zero. Then from equation (5.27), one obtains

$$\mathscr{R}^3_+(\alpha_m) = \mathscr{D}^3_m(\mathfrak{f}_m - \iota\alpha_m\mathfrak{g}_m) \left(\cos\mathfrak{L}_m b + k_{\mathfrak{eff}}\eta_4 \frac{\sin\mathfrak{L}_m b}{\mathfrak{L}_m}\right), \quad (5.29)$$

where $\mathfrak{f}_m$ and $\mathfrak{g}_m$ are denoted by

$$\begin{bmatrix} \mathfrak{f}_m \\ \mathfrak{g}_m \end{bmatrix} = \frac{1}{\mathscr{D}_m^3} \int_0^b \begin{bmatrix} \mathfrak{f}(t) \\ \mathfrak{g}(t) \end{bmatrix} \left[\cos \mathfrak{L}_m t - \eta_2 k_{\mathfrak{eff}} \frac{\sin \mathfrak{L}_m t}{\mathfrak{L}_m} \right] dt, \tag{5.30}$$

with

$$\mathfrak{L}_m = \sqrt{k_{\mathfrak{eff}}^2 - \alpha_m^2}\,, \tag{5.31}$$

and

$$\mathscr{D}_m^3 = \frac{1}{2\alpha_m} \left(\cos \mathfrak{L}_m b - \eta_2 k_{\mathfrak{eff}} \frac{\sin \mathfrak{L}_m b}{\mathfrak{L}_m} \right) \frac{\partial}{\partial \alpha} \mathscr{W}_3(\alpha_m). \tag{5.32}$$

Hence, considering equation (5.17) and the Fourier transform of the continuity relation given by equation (5.8), one can write

$$\begin{aligned} &\frac{\mathscr{R}_+^3(\alpha)}{\eta_4 k_{\mathfrak{eff}} + \imath \mathfrak{L}(\alpha)} - F_-(\alpha, b) = \frac{\mathfrak{L}(\alpha) \cos \mathfrak{L}(\alpha) b - k_{\mathfrak{eff}} \eta_2 \sin \mathfrak{L}(\alpha) b}{\mathfrak{L}(\alpha) \mathscr{W}_3(\alpha)} \\ &\times \left\{ \mathscr{R}_+^3(\alpha) - \int_0^b (\mathfrak{f}(t) - \imath \alpha \mathfrak{g}(t)) \left(\cos \mathfrak{L}(\alpha)(b-t) + k_{\mathfrak{eff}} \eta_4 \frac{\sin \mathfrak{L}(\alpha)(b-t)}{\mathfrak{L}(\alpha)} \right) dt \right\} \\ &+ \frac{1}{\mathfrak{L}(\alpha)} \int_0^b (\mathfrak{f}(t) - \imath \alpha \mathfrak{g}(t)) \sin \mathfrak{L}(\alpha)(b-t)\, dt. \end{aligned} \tag{5.33}$$

After simplification the above expression takes the form

$$\begin{aligned} &\frac{\eta_2 \chi(\frac{\imath}{\eta_4}, \alpha) \mathscr{R}_+^3(\alpha)}{\eta_4 \chi(\frac{\imath}{\eta_2}, \alpha) \mathscr{N}^3(\alpha)} + F_-(\alpha, b) \\ &= \frac{1}{\mathscr{W}_3(\alpha)} \int_0^b [\mathfrak{f}(t) - \imath \alpha \mathfrak{g}(t)] \left[\cos \mathfrak{L}(\alpha) t - k_{\mathfrak{eff}} \eta_2 \frac{\sin \mathfrak{L}(\alpha) t}{\mathfrak{L}(\alpha)} \right] dt, \end{aligned} \tag{5.34}$$

with

$$\chi(\eta_j, \alpha) = \frac{\mathfrak{L}(\alpha)}{\eta_j \mathfrak{L}(\alpha) + k_{\mathfrak{eff}}} \quad \text{and} \quad \mathscr{N}^3(\alpha) = \mathscr{W}_3(\alpha) e^{\imath \mathfrak{L}(\alpha) b}, \tag{5.35}$$

and $\mathfrak{f}(t)$ and $\mathfrak{g}(t)$ are expanded into a series of eigen-functions as

$$\begin{bmatrix} \mathfrak{f}(t) \\ \mathfrak{g}(t) \end{bmatrix} = \sum_{m=1}^{\infty} \begin{bmatrix} \mathfrak{f}_m \\ \mathfrak{g}_m \end{bmatrix} \left[\cos \mathfrak{L}_m t - \eta_2 k_{\mathfrak{eff}} \frac{\sin \mathfrak{L}_m t}{\mathfrak{L}_m} \right]. \tag{5.36}$$

Using equation (5.36) into equation (5.34), one gets the required Wiener-Hopf equation valid within the strip $\mathfrak{Im}(-k_{\mathfrak{eff}}) < \mathfrak{Im}(\alpha) < \mathfrak{Im}(k_{\mathfrak{eff}})$ as follow:

$$\frac{\eta_2 \chi(\frac{\iota}{\eta_4}, \alpha) \mathscr{R}_+^3(\alpha)}{\eta_4 \chi(\frac{\iota}{\eta_2}, \alpha) \mathscr{N}^3(\alpha)} + F_-(\alpha, b) = \sum_{m=1}^{\infty} \frac{\mathfrak{f}_m - \iota \alpha \mathfrak{g}_m}{\alpha^2 - \alpha_m^2} \left(\cos \mathfrak{L}_m b - k_{\mathfrak{eff}} \eta_2 \frac{\sin \mathfrak{L}_m b}{\mathfrak{L}_m} \right). \tag{5.37}$$

5.3 SOLUTION OF WIENER-HOPF EQUATION

To obtain the required solution of Wiener-Hopf equation the kernel functions $\mathscr{N}^3(\alpha)$ and $\chi(\eta_j, \alpha))$ in equation (5.37) can be factorized by applying the known results as follows

$$\begin{aligned} \mathscr{N}_+^3(\alpha) &= \left[k_{\mathfrak{eff}} \left(\eta_4 - \eta_2 \right) \cos k_{\mathfrak{eff}} b - k_{\mathfrak{eff}} (1 + \eta_2 \eta_4) \sin k_{\mathfrak{eff}} b \right]^{\frac{1}{2}} \\ &\times \exp \left[\frac{\mathfrak{L}(\alpha) b}{\pi} \ln \left(\frac{\alpha + \iota \mathfrak{L}(\alpha)}{k_{\mathfrak{eff}}} \right) + \frac{\iota \alpha b}{\pi} \left(1 - C + \ln [\frac{2\pi}{k_{\mathfrak{eff}} b}] + \iota \frac{\pi}{2} \right) \right] \prod_{m=1}^{\infty} \left(1 + \frac{\alpha}{\alpha_m} \right) e^{\frac{\iota \alpha b}{m \pi}} \end{aligned} \tag{5.38}$$

and

$$\mathscr{N}_-^3(\alpha) = \mathscr{N}_+^3(-\alpha), \tag{5.39}$$

where the factors of $\chi(\eta_j, \alpha)$ and C are discussed in earlier chapters.
Now, multiplying the Wiener-Hopf equation (5.37) on both sides with $\frac{\chi_-(\frac{\iota}{\eta_2}, \alpha)\, \mathscr{N}_-^3(\alpha)}{\chi_-(\frac{\iota}{\eta_4}, \alpha)}$, one obtains

$$\begin{aligned} &\frac{\eta_2 \chi_+(\frac{\iota}{\eta_4}, \alpha) \mathscr{R}_+^3(\alpha)}{\eta_4 \chi_+(\frac{\iota}{\eta_2}, \alpha) \mathscr{N}_+^3(\alpha)} + \frac{\chi_-(\frac{\iota}{\eta_2}, \alpha) \mathscr{N}_-^3(\alpha)}{\chi_-(\frac{\iota}{\eta_4}, \alpha)} F_-(\alpha, b) \\ &= \frac{\chi_-(\frac{\iota}{\eta_2}, \alpha) \mathscr{N}_-^3(\alpha)}{\chi_-(\frac{\iota}{\eta_4}, \alpha)} \sum_{m=1}^{\infty} \frac{\mathfrak{f}_m - \iota \alpha \mathfrak{g}_m}{\alpha^2 - \alpha_m^2} \left(\cos \mathfrak{L}_m b + k_{\mathfrak{eff}} \eta_2 \frac{\sin \mathfrak{L}_m b}{\mathfrak{L}_m} \right) \end{aligned} \tag{5.40}$$

With help of cauchy integral formula the terms on right-hand of the equation (5.40) can be decomposed as

$$\begin{aligned}
&\frac{\chi_-(\frac{\iota}{\eta_2},\alpha)\mathscr{N}_-^3(\alpha)}{\chi_-(\frac{\iota}{\eta_4},\alpha)}\sum_{m=1}^{\infty}\frac{\mathfrak{f}_m-\iota\alpha\mathfrak{g}_m}{\alpha^2-\alpha_m^2}\left(\cos\mathfrak{L}_m b+k_{\mathfrak{eff}}\eta_2\frac{\sin\mathfrak{L}_m b}{\mathfrak{L}_m}\right)\\
&=\sum_{m=1}^{\infty}\frac{1}{\alpha+\alpha_m}\left(\cos\mathfrak{L}_m b+k_{\mathfrak{eff}}\eta_2\frac{\sin\mathfrak{L}_m b}{\mathfrak{L}_m}\right)\\
&\left[\frac{(\mathfrak{f}_m-\iota\alpha\mathfrak{g}_m)\chi_-(\frac{\iota}{\eta_2},\alpha)\mathscr{N}_-^3(\alpha)}{(\alpha-\alpha_m)\chi_-(\frac{\iota}{\eta_4},\alpha)}+\frac{(\mathfrak{f}_m+\iota\alpha\mathfrak{g}_m)\chi_+(\frac{\iota}{\eta_2},\alpha)\mathscr{N}_+^3(\alpha)}{2\alpha_m\chi_+(\frac{\iota}{\eta_4},\alpha)}\right]\\
&-\sum_{m=1}^{\infty}\left(\cos\mathfrak{L}_m b+k_{\mathfrak{eff}}\eta_2\frac{\sin\mathfrak{L}_m b}{\mathfrak{L}_m}\right)\frac{(\mathfrak{f}_m+\iota\alpha\mathfrak{g}_m)\chi_+(\frac{\iota}{\eta_2},\alpha)\mathscr{N}_+^3(\alpha)}{2\alpha_m(\alpha+\alpha_m)\chi_+(\frac{\iota}{\eta_4},\alpha)}.
\end{aligned}\tag{5.41}$$

Now using equation (5.41) in equation (5.40) and then placing all those terms on the left-hand side which are analytic in the region ($\mathfrak{Im}(\alpha) > -k_{\mathfrak{eff}}$) and the terms which are analytic in the region ($\mathfrak{Im}(\alpha) < k_{\mathfrak{eff}}$) on the right-hand side which yields

$$\begin{aligned}
&\frac{\eta_2\chi_+(\frac{\iota}{\eta_4},\alpha)\mathscr{R}_+(\alpha)}{\eta_4\chi_+(\frac{\iota}{\eta_2},\alpha)\mathscr{N}_+(\alpha)}+\sum_{m=1}^{\infty}\left(\cos\mathfrak{L}_m b+k_{\mathfrak{eff}}\eta_2\frac{\sin\mathfrak{L}_m b}{\mathfrak{L}_m}\right)\frac{(\mathfrak{f}_m+\iota\alpha\mathfrak{g}_m)\chi_+(\frac{\iota}{\eta_2},\alpha)\mathscr{N}_+(\alpha)}{2\alpha_m(\alpha+\alpha_m)\chi_+(\frac{\iota}{\eta_4},\alpha)}\\
&=-\frac{\chi_-(\frac{\iota}{\eta_2},\alpha)\mathscr{N}_-(\alpha)}{\chi_-(\frac{\iota}{\eta_4},\alpha)}F_-(\alpha,b)+\sum_{m=1}^{\infty}\frac{1}{\alpha+\alpha_m}\left(\cos\mathfrak{L}_m b+k_{\mathfrak{eff}}\eta_2\frac{\sin\mathfrak{L}_m b}{\mathfrak{L}_m}\right)\\
&\left[\frac{(\mathfrak{f}_m-\iota\alpha\mathfrak{g}_m)\chi_-(\frac{\iota}{\eta_2},\alpha)\mathscr{N}_-(\alpha)}{(\alpha-\alpha_m)\chi_-(\frac{\iota}{\eta_4},\alpha)}+\frac{(\mathfrak{f}_m+\iota\alpha\mathfrak{g}_m)\chi_+(\frac{\iota}{\eta_2},\alpha)\mathscr{N}_+(\alpha)}{2\alpha_m\chi_+(\frac{\iota}{\eta_4},\alpha)}\right].
\end{aligned}\tag{5.42}$$

The required solution of Wiener-Hopf equation can be obtained by using analytical continuation principle following Liouville's theorem gives

$$\begin{aligned}
&\frac{\eta_2\chi_+(\frac{\iota}{\eta_4},\alpha)\mathscr{R}_+^3(\alpha)}{\eta_4\chi_+(\frac{\iota}{\eta_2},\alpha)\mathscr{N}_+^3(\alpha)}=\\
&-\sum_{m=1}^{\infty}\frac{(\mathfrak{f}_m+\iota\alpha_m\mathfrak{g}_m)}{2\alpha_m(\alpha+\alpha_m)}\left(\cos\mathfrak{L}_m b-k_{\mathfrak{eff}}\eta_2\frac{\sin\mathfrak{L}_m b}{\mathfrak{L}_m}\right)\frac{\chi_+(\frac{\iota}{\eta_2},\alpha_m)\mathscr{N}_+^3(\alpha_m)}{\chi_+(\frac{\iota}{\eta_4},\alpha_m)}.
\end{aligned}\tag{5.43}$$

5.4 DETERMINATION OF THE UNKNOWN COEFFICIENTS

The equation(5.43) contains infinite number of unknown coefficients. In order to determine these unknown coefficients we employ the well-known Mode-Matching technique along with the Fourier transform. The Mode-Matching technique is a standard method to handle the waveguide structures. This technique has been used extensively [87, 88] to analyze the scattered field at the junction. In this investigation the Mode-Matching technique enables us to declare the field component defined in the waveguide region in terms of normal modes as

$$H_z^2(x,y) = \sum_{n=1}^{\infty} a_n \left(\cos\zeta_n y - k_{\mathfrak{eff}}\eta_1 \frac{\sin\zeta_n y}{\zeta_n} \right) e^{-\iota\beta_n x}, \tag{5.44}$$

where

$$\beta_n = \sqrt{k_{\mathfrak{eff}}^2 - \zeta_n^2}, \quad \Im\mathfrak{m}(\beta_n) > \Im\mathfrak{m}(k_{\mathfrak{eff}}), \quad n = 1,2,3,.... \tag{5.45}$$

β_n's and ζ_n's can be obtained by using equations (5.6) together with (5.44) as under

$$k_{\mathfrak{eff}}(\eta_1+\eta_3)\cos\zeta_n b + (\zeta_n^2 - k_{\mathfrak{eff}}^2\eta_1\eta_3)\frac{\sin\zeta_n y}{\zeta_n} = 0, \qquad n = 0,1,2,3,.... \tag{5.46}$$

Placing the continuity relations represented by the equations (5.10) and (5.11) in equation (5.20), one yields

$$\mathfrak{f}(y) - \iota\alpha\mathfrak{g}(y) = \iota(k_{\mathfrak{eff}} - \alpha) + \frac{\partial}{\partial x}H_z^2(0,y) - \iota\alpha H_z^2(0,y). \tag{5.47}$$

Substituting equations (5.44) and (5.30) in equation (5.47), then multiplying the resulting equation by $(\frac{\sin\mathfrak{L}_j y}{\mathfrak{L}_j} - \frac{\eta_4}{\iota k_{\mathfrak{eff}}}\cos\mathfrak{L}_j y)$ and integrating from $y = 0$ to $y = b$, one obtains

$$\mathfrak{f}_m - \iota\alpha_m\mathfrak{g}_m = \frac{\iota(k_{\mathfrak{eff}} - a)}{\mathscr{D}_m^3\mathfrak{L}_m^2}\left(k_{\mathfrak{eff}}\eta_2\cos\mathfrak{L}_m b + \mathfrak{L}_m\sin\mathfrak{L}_m b - k_{\mathfrak{eff}}\eta_2\right)$$
$$-\frac{\iota}{\mathscr{D}_m^3}\sum_{n=1}^{\infty}\mathfrak{a}_n(\alpha+\beta_n)\Delta_{nm}, \tag{5.48}$$

where Δ_{nm} is

$$\Delta_{nm} = \frac{k_{\text{eff}}(\eta_2-\eta_1)}{\zeta_n^2-\mathfrak{L}_m^2} - \frac{k_{\text{eff}}(\eta_3+\eta_4)}{\zeta_n^2-\mathfrak{L}_m^2}\left(\cos\zeta_n b - k_{\text{eff}}\eta_1\frac{\sin\zeta_n b}{\zeta_n}\right) \times\left(\cos\mathfrak{L}_m b - k_{\text{eff}}\eta_2\frac{\sin\mathfrak{L}_m b}{\mathfrak{L}_m}\right). \tag{5.49}$$

Substituting equation (5.48) into equation (5.29) and then using the resulting equation into equation (5.43) to yield

$$\sum_{n=1}^{\infty}\mathscr{A}_n(\alpha_j)\mathfrak{a}_n = I(\alpha_j), \qquad j=1,2,3,... \tag{5.50}$$

where

$$\mathscr{A}_n(\alpha_j) = -\iota(\alpha_j+\beta_n)\Delta_{nj}\left(\cos\mathfrak{L}_j b + k_{\text{eff}}\eta_4\frac{\sin\mathfrak{L}_j b}{\mathfrak{L}_j}\right) + \frac{\iota\eta_4^2\mathscr{N}_+^3(\alpha_j)\chi_+(\frac{\iota}{\eta_2},\alpha_j)}{\eta_2^2\chi_+(\frac{\iota}{\eta 4},\alpha_j)}\sum_{m=1}^{\infty}\frac{(\beta_n-\alpha_m)\Delta_{nm}}{2\alpha_m\mathscr{D}_m^3(\alpha_j+\alpha_m)} \times\left(\cos\mathfrak{L}_m b + k_{\text{eff}}\eta_4\frac{\sin\mathfrak{L}_m b}{\mathfrak{L}_m}\right)\frac{\chi_+(\frac{\iota}{\eta_2},\alpha_m)\mathscr{N}_+^3(\alpha_m)}{\chi_+(\frac{\iota}{\eta 4},\alpha_m)} \tag{5.51}$$

and

$$I(\alpha_j) = \iota(k_{\text{eff}}-\alpha_j)\left(\cos\mathfrak{L}_j b + k_{\text{eff}}\eta_4\frac{\sin\mathfrak{L}_j b}{\mathfrak{L}_j}\right)\left(\frac{\sin\mathfrak{L}_j b}{\mathfrak{L}_j} + k_{\text{eff}}\eta_2\frac{\cos\mathfrak{L}_j b}{\mathfrak{L}_j} - \frac{k_{\text{eff}}\eta_2}{\mathfrak{L}_j^2}\right) + \frac{\eta_4^2\chi_+(\frac{\iota}{\eta_2},\alpha_j)\mathscr{N}_+^3(\alpha_j)}{\eta_2^2\chi_+(\frac{\iota}{\eta 4},\alpha_j)}\sum_{m=1}^{\infty}\frac{\iota(k_{\text{eff}}+\alpha_m)}{2\alpha_m\mathscr{D}_m^3(\alpha_j+\alpha_m)}\left(\frac{\sin\mathfrak{L}_m b}{\mathfrak{L}_m} + k_{\text{eff}}\eta_2\frac{\cos\mathfrak{L}_m b}{\mathfrak{L}_m} - \frac{\eta_2 k_{\text{eff}}}{\mathfrak{L}_m^2}\right) \times\left(\cos\mathfrak{L}_m b + k_{\text{eff}}\eta_2\frac{\sin\mathfrak{L}_m b}{\mathfrak{L}_m}\right)\frac{\chi_+(\frac{\iota}{\eta_2},\alpha_m)\mathscr{N}_+^3(\alpha_m)}{\chi_+(\frac{\iota}{\eta 4},\alpha_m)}. \tag{5.52}$$

The infinite system of algebraic equations represented by equation (5.50) is solved numerically. To solve this infinite system of algebraic equations we have truncated it after first N terms in order to obtain required radiated field.

5.5 RADIATED FIELD

The radiated field $H_z^1(x,y)$ is obtained by taking the inverse Fourier transform of $F(\alpha,y)$. By using equation (5.17), one obtains

$$H_z^1(x,y)=\frac{1}{2\pi}\int_{\mathscr{L}}\frac{\mathscr{R}_+^3(\alpha)}{\eta_4 k_{\mathfrak{eff}}+\iota\mathfrak{L}(\alpha)}e^{\iota\mathfrak{L}(\alpha)(\alpha)(y-b)}e^{-\iota\alpha x}d\alpha. \tag{5.53}$$

Using the change of variables $\alpha=-k_{\mathfrak{eff}}\cos\ t$, $x=\rho\cos\theta$ and $y=\rho\sin\theta$ in the equation (5.53), one obtains

$$H_z^1(\rho,\theta)=\frac{1}{2\pi}\int_{\mathscr{L}}\frac{\mathscr{R}_+^3(-k_{\mathfrak{eff}}\cos t)k_{\mathfrak{eff}}\sin t}{\eta_2+\iota\sin t}e^{-\iota k_{\mathfrak{eff}}\sin t+\iota k_{\mathfrak{eff}}\rho\cos(t-\theta)}dt. \tag{5.54}$$

The integral in equation (5.53) can be evaluated asymptotically through the saddle point technique. Here, saddle point occurs at $t=\theta$. On taking into account equations (5.3) and (5.43), the radiated field takes the form:

$$\begin{aligned}
&H_z^1(\rho,\theta)=\\
&-\frac{\eta_2^2 k\sqrt{(\epsilon_1^2-\epsilon_2^2)/\epsilon_1}\sin\theta e^{\iota k\rho\sqrt{(\epsilon_1^2-\epsilon_2^2)/\epsilon_1}-\iota\frac{\pi}{4}}\chi_-(\frac{\iota}{\eta_2},k\sqrt{(\epsilon_1^2-\epsilon_2^2)/\epsilon_1}\cos\theta)}{\sqrt{2\pi k\rho}(\eta_2+\sin t)\eta_4^2\chi_-(\frac{\iota}{\eta_4},k\sqrt{(\epsilon_1^2-\epsilon_2^2)/\epsilon_1}\cos\theta)}\\
&\times\left[\left(\sum_{m=1}^{\infty}\frac{(\mathfrak{f}_m+\iota\alpha_m\mathfrak{g}_m)\chi_+(\frac{\iota}{\eta_2},\alpha_m)\mathscr{N}_+^3(\alpha_m)\mathscr{N}_-^3(k\sqrt{(\epsilon_1^2-\epsilon_2^2)/\epsilon_1}\cos\theta)}{2\alpha_m(\alpha_m-(k\sqrt{(\epsilon_1^2-\epsilon_2^2)/\epsilon_1}\cos\theta))\chi_+(\frac{\iota}{\eta_4},\alpha_m)}\right)\right.\\
&\left.\times\left(\cos\mathfrak{L}_m b-\eta_2 k\sqrt{(\epsilon_1^2-\epsilon_2^2)/\epsilon_1}\frac{\sin\mathfrak{L}_m b}{\mathfrak{L}_m}\right)\right].
\end{aligned} \tag{5.55}$$

5.6 COMPUTATIONAL RESULTS AND DISCUSSION

In this section, we have presented some useful numerical results to show the effects of various physical parameters of interest on the radiated field amplitude. Actually the solution of Wiener-Hopf equation contains a set of infinitely many constants satisfying an infinite system of algebraic equations. To solve this

infinite system of algebraic equations we have truncated it after N terms in order to obtain the required radiated field. Fig. (5.2) illustrates the variation in the radiated field amplitude versus the truncation number "N". It is apparent that the effect of the truncation number is negligible for $N > 20$. Hence, the infinite system of algebraic equations in equation (5.50) can be managed to deal as finite. Fig. (5.3) shows the variation in the radiated field amplitude with increasing plate separation parameter b. Clearly, the radiated (diffracted) field amplitude enhances when we increase the ratio b/λ. Physically, such an increase in the diffracted field amplitude is due to the fact that plate separation parameter b becomes comparable to the wavelength λ of the incident wave. The amplitude will be maximum for $b/\lambda = 1$. Figs. (5.4) and (5.5) shows the variation in the radiated field amplitude with impedances η_1 and η_2 both for inductive and capacitative cases. Fig. (5.4) shows that in case of η_1 (for capacitative and inductive cases) the amplitude decreases with increasing impedance where as for η_2 (See Fig. (5.5)) for capacitative case the amplitude decreases and for inductive case it rises. Fig. (5.6) explores the effect of η_3 (both for capacitative and inductive cases) wherein the amplitude decreases with increasing impedance, however, the case is different for the variation of η_4 as shown in Fig. (5.7). These impedance dependent variations are actually related to the magnetic and electric susceptibilities of the waveguide surfaces. Actually, the surface impedances Z_j $(j = 1,2,3,4)$ are normalized by Z_0 i.e., $Z_j = \eta_4 Z_0$. Here $Z_0 = \sqrt{\mu_0/\epsilon_0}$ is the characteristic impedance of surrounding medium and μ_0 and ϵ_0 are, respectively, the magnetic permeability and dielectric permittivity of the free space. Since the surface impedances of a conductive medium (plasma) are imaginary in magnitude, that is, $Z = \sqrt{i\omega\mu/(\sigma + i\omega\epsilon)}$, where σ is conductivity of cold plasma, so in the present model it would be taken as complex. Z in the normalized form is $\eta = \sqrt{i\omega\mu/(\sigma + i\omega\epsilon)}/Z_0$, which for free space becomes unity. Fig. (5.8) demonstrates the effect of cold plasma permittivity ϵ_1 on the radiation

phenomenon. The radiated field amplitude is effected drastically in the presence of an anisotropic plasma medium. The field amplitude enhances with increasing plasma permittivity ϵ_1, actually for fixed number densities of ions and electrons in cold plasma, the parameter increases with the increase in incident wave frequency ω, i.e., $\epsilon_1 \approx 1 - (\frac{\omega_p}{\omega})^2$ (for high frequency signal). The electric field of such a high frequency signal oscillates the electrons about the cold ionic centers and such oscillating electrons then radiate enormously thereby increasing the amplitude of the radiated field. Fig. (5.9) demonstrates the effect of parameter ϵ_2 on the radiated field amplitude. Clearly, the amplitude of the radiated field diminishes with the increase in parameter ϵ_2. Actually, the increase in the parameter ϵ_2 leads to the decrease in the signal frequency for which the electron oscillation under the low frequency of incident wave diminishes the radiated amplitude. The results obtained in this work can be a useful knot in order to improve the radiated signal quality transmitted by an artificial satellite in the ionosphere for communication means to an earth station.

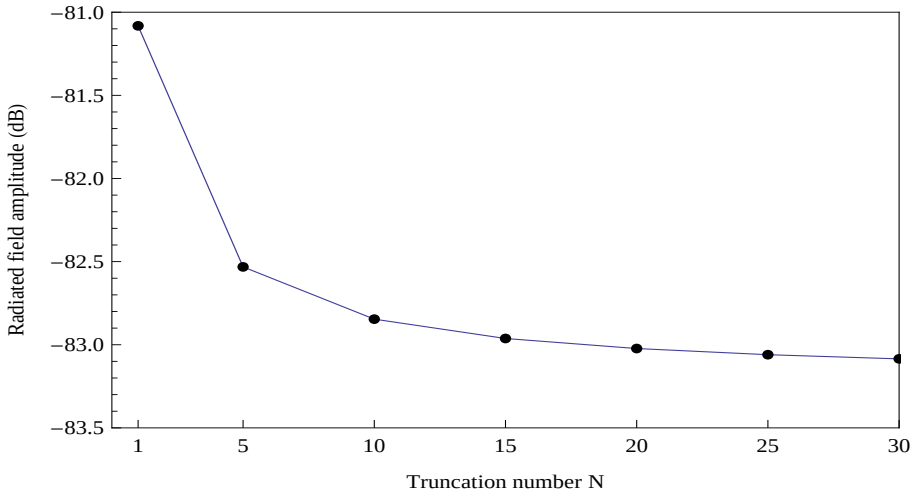

FIGURE 5.2. *Variation in the radiated field amplitude versus truncation number "N". The other parameters are* $\theta = 45^o$ $\eta_1 = 0.2$, $\eta_2 = 0.5$, $\eta_3 = 0.3$, $\eta_4 = 0.6$, $\epsilon_1 = 0.8$, $\epsilon_2 = 0$, $k = 5$ *and* $b = 0.2\lambda$.

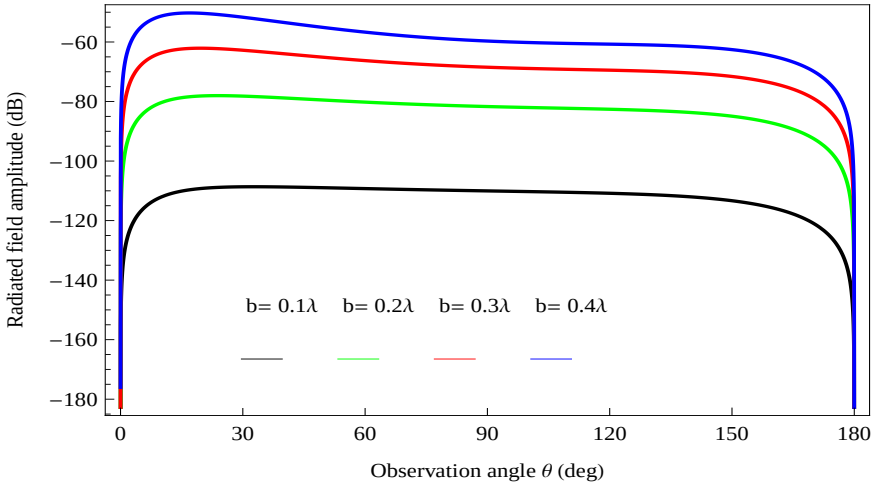

FIGURE 5.3. *Variation in the radiated field amplitude versus "b". The other parameters are* $k = 5$, $\eta_1 = 0.5$, $\eta_2 = 0.3$, $\eta_3 = 0.6$, $\eta_4 = 0.7$, $\epsilon_1 = 0.8$ *and* $\epsilon_2 = 0$.

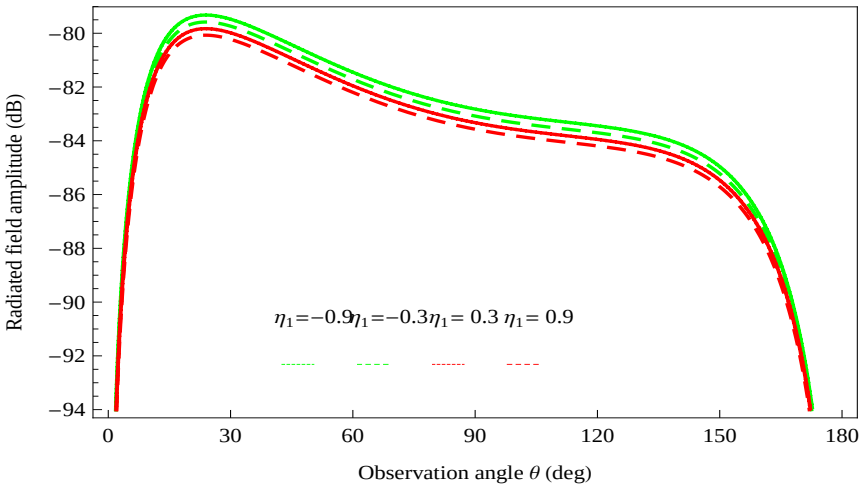

FIGURE 5.4. *Variation in the radiated field amplitude versus "*η_1*". The other parameters are* $k = 5$, $\eta_2 = 0.3$, $\eta_3 = 0.6$, $\eta_4 = 0.5$, $\epsilon_1 = 0.8$, $\epsilon_2 = 0$ *and* $b = 0.2\lambda$.

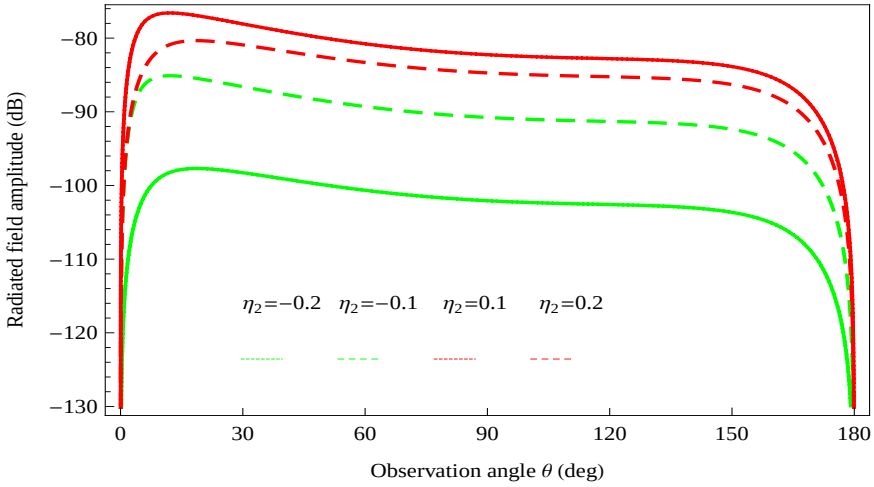

FIGURE 5.5. *Variation in the radiated field amplitude versus "η_2". The other parameters are* $k = 5$, $\eta_1 = 0.7$, $\eta_3 = 0.6$, $\eta_4 = 0.4$, $\epsilon_1 = 0.8$, $\epsilon_2 = 0$ *and* $b = 0.2\lambda$.

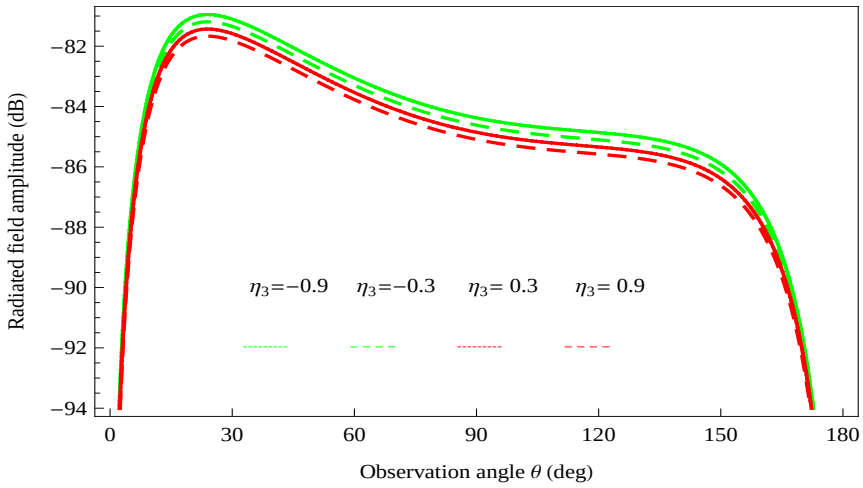

FIGURE 5.6. *Variation in the radiated field amplitude versus "η_3". The other parameters are* $k = 5$ $\eta_1 = 0.5$, $\eta_2 = 0.3$, $\eta_4 = 0.4$, $\epsilon_1 = 0.8$, $\epsilon_2 = 0$ *and* $b = 0.2\lambda$.

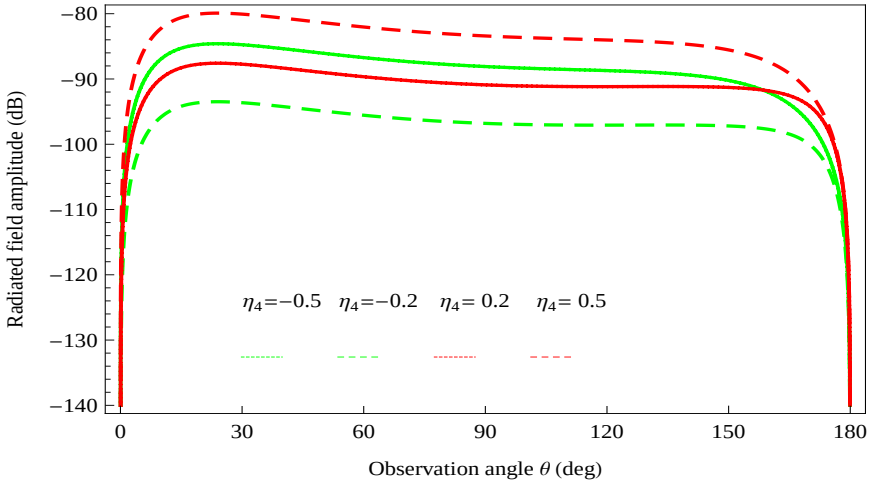

FIGURE 5.7. *Variation in the radiated field amplitude versus "η_4". The other parameters are* $k = 5$, $\eta_1 = 0.5$, $\eta_2 = 0.3$, $\eta_3 = 0.6$, $\epsilon_1 = 0.8$, $\epsilon_2 = 0$ *and* $b = 0.2\lambda$.

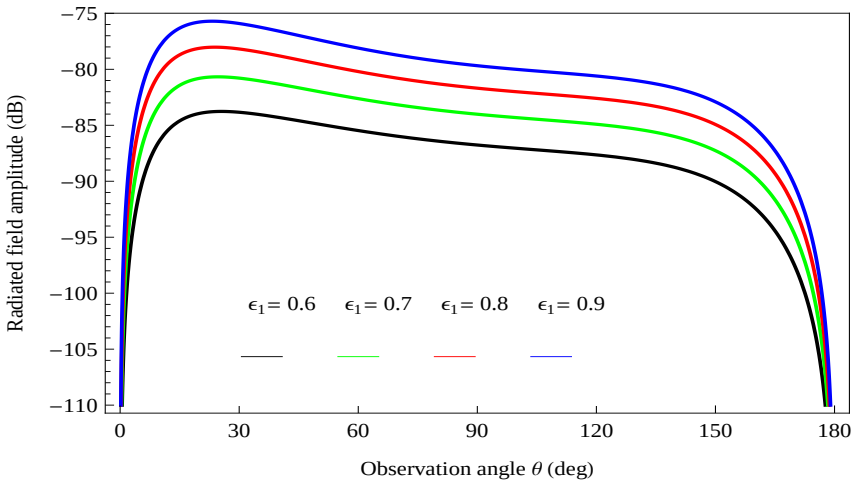

FIGURE 5.8. *Variation in the radiated field amplitude versus "ϵ_1". The other parameters are* $k = 5$, $\eta_1 = 0.5$, $\eta_2 = 0.3$, $\eta_3 = 0.6$, $\eta_4 = 0.7$, $\epsilon_2 = 0$ *and* $b = 0.2\lambda$.

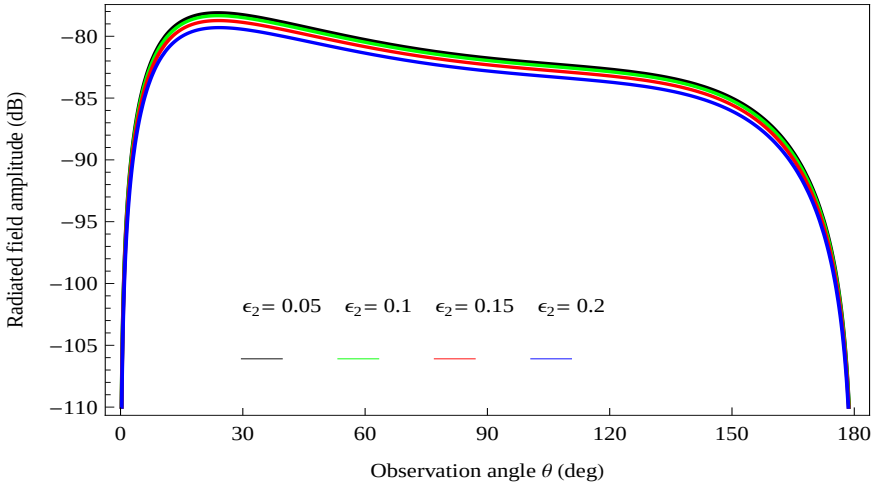

FIGURE 5.9. *Variation in the radiated field amplitude versus "ϵ_2". The other parameters are* $k = 5$, $\eta_1 = 0.5$, $\eta_2 = 0.3$, $\eta_3 = 0.6$, $\eta_4 = 0.7$, $\epsilon_1 = 0.8$ *and* $b = 0.2\lambda$.

CHAPTER 6

DIFFRACTED AND TRANSMITTED FIELDS BY AN IMPEDANCE LOADED WAVEGUIDE LOCATED IN COLD PLASMA

In this chapter, the problem of diffraction of plane wave by an impedance loaded waveguide designed in cold plasma is considered. The structure of waveguide is constructed from three parallel impedance loaded half-planes such that one amidst in the opposite direction. Such type of problem was initially considered by Weinstein [89, 90] and Boersma [91] for the case of two half-planes characteristic by either soft (Dirichlet) or rigid (Neumann) surface material properties of all faces of the half-planes. After that Cinar and Büyükaksoy [85] generalized the problem for surface impedance (Robin) and each face of the half-planes is loaded by different impedances. Here, the case is considered for soft, rigid and impedance surface material properties of the waveguide located in cold plasma as shown in Fig. (6.1).

The chapter is arranged as follows. In the next Section (6.1) mathematical model of the problem in cold plasma is stated. The Wiener-Hopf equation is formulated in Section (6.2) whereas the solution of Wiener-Hopf equation is developed in Section (6.3). The unknown coefficients are obtained with the help of Mode-Matching technique in Section (6.4). The diffracted and transmitted fields are

considered in Section (6.5). In the end the Section (6.6) is devoted to numerical results and discussions.

6.1 MATHEMATICAL MODEL OF THE PROBLEM IN COLD PLASMA

In this chapter consider an incident time harmonic wave propagating in cold plasma and making an incident angle θ_0. On striking the waveguide surface the incident field generates reflected and transmitted fields. Let ω denotes the angular frequency and k be the wave number. The geometry of the problem is formed by three parallel half-planes represented by S_1={$(x,y,z)|\ x \in (-\infty,0),\ y = b,\ z \in (-\infty,\infty)$}, S_2={$(x,y,z)|\ x \in (-\infty,0),\ y = -b,\ z \in (-\infty,\infty)$} and S_3={$(x,y,z)|\ x \in (0,\infty),\ y = 0,\ z \in (-\infty,\infty)$}, respectively. The material property of waveguide surface impedance of the upper and lower faces of the half-planes S_1 and S_2 are assumed to be Z_1 and Z_2, respectively, as shown in the Fig. (6.1)

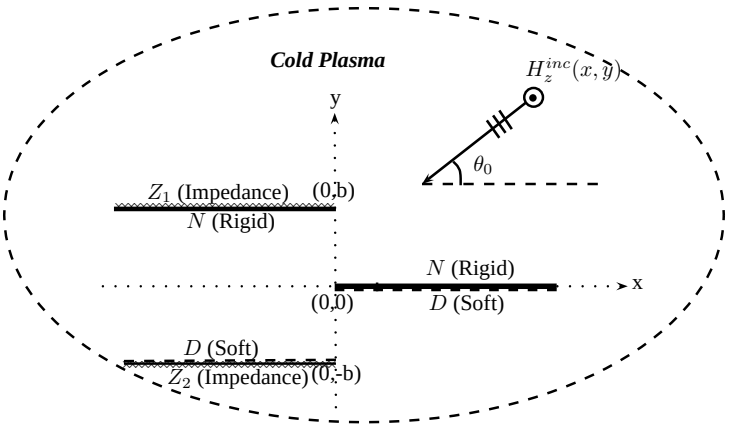

FIGURE 6.1. *The physical configuration of the waveguide located in cold plasma*

The total field can be expressed as follows:

$$H_z^T(x,y) = \begin{cases} H_z^1(x,y) + H_z^{inc}(x,y) + H_z^{ref}(x,y), & y \in (b,\infty) \\ H_z^3(x,y)\mathscr{H}(-x) + H_z^2(x,y)\mathscr{H}(x), & y \in (0,b) \\ H_z^3(x,y)\mathscr{H}(-x) + H_z^4(x,y)\mathscr{H}(x), & y \in (-b,0) \\ H_z^5(x,y), & y \in (-\infty,-b). \end{cases} \tag{6.1}$$

where $\mathscr{H}(x)$, $H_z^{inc}(x,y)$ and $H_z^{ref}(x,y)$ stand for Heaviside unit step function, incident and reflected fields, respectively, which are already defined in Chapter (4). $\{H_z^j \quad (j=1,2,3,4,5)\}$ are the scattered fields satisfy the Helmholtz equation in cold plasma as under

$$\left[\frac{\partial^2}{\partial x^2}+\frac{\partial^2}{\partial y^2}+k_{\text{eff}}^2\right]\left[H_z^j(x,y)\right]=0, \tag{6.2}$$

with the following corresponding boundary conditions and continuity relations

$$\left(1+\frac{\eta_1}{\iota k_{\text{eff}}}\frac{\partial}{\partial y}\right)H_z^1(x,b)=0, \qquad x\in(-\infty,0) \tag{6.3}$$

$$\frac{\partial}{\partial y}H_z^2(x,0)=0, \qquad x\in(0,\infty) \tag{6.4}$$

$$\frac{\partial}{\partial y}H_z^3(x,b)=0, \qquad x\in(-\infty,0) \tag{6.5}$$

$$H_z^2(x,-b)=0, \qquad x\in(-\infty,0) \tag{6.6}$$

$$H_z^4(x,0)=0, \qquad x\in(0,\infty) \tag{6.7}$$

$$\left(1-\frac{\eta_2}{\iota k_{\text{eff}}}\frac{\partial}{\partial y}\right)H_z^5(x,-b)=0, \qquad x\in(-\infty,0) \tag{6.8}$$

$$H_z^1(x,b)+H_z^{inc}(x,b)+H_z^{ref}(x,b)=H_z^2(x,b), \qquad x\in(0,\infty) \tag{6.9}$$

$$\frac{\partial}{\partial y}H_z^1(x,b)+\frac{\partial}{\partial y}H_z^{inc}(x,b)+\frac{\partial}{\partial y}H_z^{ref}(x,b)=\frac{\partial}{\partial y}H_z^2(x,b), \qquad x\in(0,\infty) \tag{6.10}$$

$$H_z^3(0,y)=H_z^2(0,y), \qquad x\in(0,b) \tag{6.11}$$

$$\frac{\partial}{\partial x}H_z^3(0,y)=\frac{\partial}{\partial x}H_z^2(0,y), \qquad x\in(0,b) \tag{6.12}$$

$$H_z^3(0,y)=H_z^4(0,y), \qquad x\in(-b,0) \tag{6.13}$$

$$\frac{\partial}{\partial x}H_z^3(0,y)=\frac{\partial}{\partial x}H_z^4(0,y), \qquad x\in(-b,0) \tag{6.14}$$

$$H_z^4(x,-b)=H_z^5(x,-b), \qquad x\in(0,\infty) \tag{6.15}$$

$$\frac{\partial}{\partial y}H_z^4(x,-b) = \frac{\partial}{\partial y}H_z^5(x,-b), \qquad x \in (0,\infty). \tag{6.16}$$

6.2 FORMULATION OF WIENER-HOPF EQUATION

Since Helmholtz equation in cold plasma is satisfied by the field $H_z^1(x,y)$ in the waveguide region $x \in (-\infty,\infty)$ and $y \in (b,\infty)$ whose Fourier transform gives

$$\left[\frac{d^2}{dy^2} + (k_{\text{eff}}^2 - \alpha^2)\right] F(\alpha,y) = 0. \tag{6.17}$$

Using the radiation condition the general solution of equation (6.17) is as under

$$F(\alpha,y) = A_4(\alpha)e^{\iota\mathfrak{L}(\alpha)(y-b)}. \tag{6.18}$$

To find the unknown spectral coefficient $A_4(\alpha)$, using the transformed domain of the boundary condition represented by equation (6.3) gives

$$A_4(\alpha) = \frac{k_{\text{eff}}}{\mathfrak{L}(\alpha)}\mathscr{R}_+^4(\alpha)\chi(\eta_1,\alpha), \tag{6.19}$$

where

$$\mathscr{R}_+^4(\alpha) = F_+(\alpha,b) + \frac{\eta_1}{\iota k_{\text{eff}}}\overset{\prime}{F}_+(\alpha,b) \tag{6.20}$$

and $\chi(\eta_1,\alpha)$ are defined in previous chapter.

Using the additive decomposition theorem and substituting equation (6.19) in equation (6.18), one can write

$$F_-(\alpha,y) + F_+(\alpha,y) = \frac{k_{\text{eff}}}{\mathfrak{L}(\alpha)}\mathscr{R}_+^4(\alpha)\chi(\eta_1,\alpha)e^{\iota\mathfrak{L}(\alpha)(y-b)}. \tag{6.21}$$

The derivative of equation (6.21) with respect to y at $y = b$ takes the form

$$\overset{\prime}{F}_+(\alpha,b) = \iota k_{\text{eff}}\mathscr{R}_+^4(\alpha)\chi(\eta_1,\alpha) - \overset{\prime}{F}_-(\alpha,b). \tag{6.22}$$

As the Helmholtz equation in cold plasma is satisfied by field $H_z^2(x,y)$ in equation (6.2) in the waveguide region $x \in (0,\infty)$ and $y \in (0,b)$, on multiplying this equation by $e^{\iota\alpha x}$ and then integrating the resultant equation with respect to x from 0 to ∞, one gets

$$\left[\frac{d^2}{dy^2} + \mathfrak{L}^2(\alpha)\right] \mathscr{G}_+(\alpha,y) = \mathfrak{f}(y) - \iota\alpha\mathfrak{g}(y), \tag{6.23}$$

where $\mathscr{G}_+(\alpha,y)$, $\mathfrak{f}(y)$ and $\mathfrak{g}(y)$ are also defined as earlier.

The general solution of the non-homogenous differential equation (6.23) can be obtained by using the method of variation of parameter yields

$$\mathscr{G}_+(\alpha,y) = C_9(\alpha)\cos\mathfrak{L}(\alpha)y + C_{10}(\alpha)\sin\mathfrak{L}(\alpha)y + \frac{1}{\mathfrak{L}(\alpha)}\int_0^y \mathfrak{f}(t)\sin\mathfrak{L}(\alpha)(b-t)\,dt, \tag{6.24}$$

where $C_9(\alpha)$ and $C_{10}(\alpha)$ are the unknown spectral coefficients.

Using the transformed form of boundary condition given by the equation (6.4), one gets

$$\mathscr{G}_+(\alpha,y) = C_9(\alpha)\cos\mathfrak{L}(\alpha)y + \frac{1}{\mathfrak{L}(\alpha)}\int_0^y [\mathfrak{f}(t) - \iota\alpha\mathfrak{g}(t)]\sin\mathfrak{L}(\alpha)(y-t)\,dt. \tag{6.25}$$

The transformed form of the continuity relation represented by the equations (6.9) and (6.18), respectively, gives

$$F_+(\alpha,b) + \frac{2i\eta_1\sin\theta_0 e^{-\iota k_{\mathfrak{eff}} b\sin\theta_0}}{(1+\eta_1\sin\theta_0)(\alpha - k_{\mathfrak{eff}}\cos\theta_0)} = \mathscr{G}_+(\alpha,b) \tag{6.26}$$

and

$$\overset{\prime}{F}_+(\alpha,b) + \frac{2k_{\mathfrak{eff}}\sin\theta_0 e^{-\iota k_{\mathfrak{eff}} b\sin\theta_0}}{(1+\eta_1\sin\theta_0)(\alpha - k_{\mathfrak{eff}}\cos\theta_0)} = \overset{\prime}{\mathscr{G}}_+(\alpha,b). \tag{6.27}$$

Adding equation (6.26) and $\frac{\eta_1}{ik_{\mathfrak{eff}}}$ times of equation (6.27), one can obtain

$$\mathscr{G}_+(\alpha,b) + \frac{\eta_1}{ik_{\mathfrak{eff}}}\overset{\prime}{\mathscr{G}}_+(\alpha,b) = \mathscr{R}_+^4(\alpha). \tag{6.28}$$

$C_9(\alpha)$ can be obtained by placing equation (6.25) in equation (6.28) which yields

$$C_9(\alpha) = \frac{\mathscr{R}_+^4(\alpha)}{\mathscr{W}_4(\alpha)} - \frac{1}{\mathscr{W}_4(\alpha)} \int_0^b (\mathfrak{f}(y) - \imath\alpha\mathfrak{g}(y)) \left(\frac{\sin \mathfrak{L}(\alpha)(b-t)}{\mathfrak{L}(\alpha)} + \frac{\eta_1}{\imath k_{\mathfrak{eff}}} \cos \mathfrak{L}(\alpha)(b-t) \right) dt, \tag{6.29}$$

with

$$\mathscr{W}_4(\alpha) = \cos \mathfrak{L}(\alpha) b - \frac{\eta_1}{\imath k_{\mathfrak{eff}}} \mathfrak{L}(\alpha) \sin \mathfrak{L}(\alpha) b. \tag{6.30}$$

Placing equation (6.29) in equation (6.25) gives

$$\begin{aligned} \mathscr{G}_+(\alpha, y) = & \frac{1}{\mathfrak{L}(\alpha)} \int_0^y (\mathfrak{f}(y) - \imath\alpha\mathfrak{g}(y)) \sin \mathfrak{L}(\alpha)(y-t)\, dt + \\ & \frac{\cos \mathfrak{L}(\alpha) y}{\mathscr{W}_4(\alpha)} \left\{ \mathscr{R}_+^4(\alpha) - \int_0^b (\mathfrak{f}(y) - \imath\alpha\mathfrak{g}(y)) \left(\frac{\sin \mathfrak{L}(\alpha)(b-t)}{\mathfrak{L}(\alpha)} + \frac{\eta_1}{\imath k_{\mathfrak{eff}}} \cos \mathfrak{L}(\alpha)(b-t) \right) dt \right\}. \end{aligned} \tag{6.31}$$

The left-hand side (i.e., $\mathscr{G}_+(\alpha, y)$) of the equation (6.31) is analytic in the upper half-plane $\mathfrak{Im}(\alpha) > \mathfrak{Im}(k_{\mathfrak{eff}} \cos\theta_0)$. However, the analyticity of the right-hand side is desecrated by the appearance of simple poles placing at the zeros of $\mathscr{W}_4(\alpha)$, i.e., $\alpha = \pm\alpha_m$ satisfying

$$\mathscr{W}_4(\pm\alpha_m) = 0, \quad \mathfrak{Im}(\alpha_m) > \mathfrak{Im}(k_{\mathfrak{eff}}), \qquad m = 1, 2, 3.... \tag{6.32}$$

The poles in the equation (6.31) can be removed by imposing the condition that residues of these poles are zero. Then from equation (6.31), one obtains

$$\mathscr{R}_+^4(\alpha_m) = \int_0^b (\mathfrak{f}(t) - \imath\alpha_m\mathfrak{g}(t)) \left(\frac{\sin \mathfrak{L}_m(b-t)}{\mathfrak{L}_m} + \frac{\eta_1}{\imath k_{\mathfrak{eff}}} \cos \mathfrak{L}_m(b-t) \right) dt. \tag{6.33}$$

After simplifying equation (6.34), one gets

$$\mathscr{R}_{+}^{4}(\alpha_m) = \left(\frac{\sin \mathfrak{L}_m b}{\mathfrak{L}_m} + \frac{\eta_1}{\iota k_{\mathfrak{eff}}} \cos \mathfrak{L}_m b\right) \int_0^b (\mathfrak{f}(t) - \iota \alpha_m \mathfrak{g}(t)) \cos \mathfrak{L}_m t \, dt. \tag{6.34}$$

$\mathfrak{f}(t)$ and $\mathfrak{g}(t)$ can be express in the form of eigen-functions as follows:

$$\mathfrak{f}(t) - \iota \alpha \mathfrak{g}(t) = \sum_{n=1}^{\infty} (\mathfrak{f}_n - \iota \alpha \mathfrak{g}_n) \cos \mathfrak{L}_n t. \tag{6.35}$$

Substituting equation (6.35) in equation (6.34) leads to

$$\mathscr{R}_{+}^{4}(\alpha_m) = \left(\frac{\sin \mathfrak{L}_m b}{\mathfrak{L}_m} + \frac{\eta_1}{\iota k_{\mathfrak{eff}}} \cos \mathfrak{L}_m b\right) \int_0^b \sum_{n=1}^{\infty} (\mathfrak{f}_n - \iota \alpha_m \mathfrak{g}_n) \cos \mathfrak{L}_n t \cos \mathfrak{L}_m t \, dt. \tag{6.36}$$

After simplifying the equation (6.36), one can write

$$\mathscr{R}_{+}^{4}(\alpha_m) = \mathfrak{D}_m^4 (\mathfrak{f}_m - \iota \alpha \mathfrak{g}_m) \left(\frac{\sin \mathfrak{L}_m b}{\mathfrak{L}_m} + \frac{\eta_1}{i k_{\mathfrak{eff}}} \cos \mathfrak{L}_m b\right), \tag{6.37}$$

with

$$\mathfrak{L}_m = \sqrt{k_{\mathfrak{eff}}^2 - \alpha_m^2} \tag{6.38}$$

and

$$\mathfrak{D}_m^4 = \frac{\mathfrak{L}_m \sin \mathfrak{L}_m b}{2\alpha_m} \frac{\partial}{\partial \alpha} \mathscr{W}_4(\alpha_m). \tag{6.39}$$

The Fourier transform of the continuity relation given by equation (6.18) gives

$$\overset{\prime}{F}_{+}(\alpha, b) + \frac{2 k_{\mathfrak{eff}} \sin\theta_0 e^{-\iota k_{\mathfrak{eff}} b \sin\theta_0}}{(1 + \eta_1 \sin\theta_0)(\alpha - k_{\mathfrak{eff}} \cos\theta_0)} = \overset{\prime}{\mathscr{G}}_{+}(\alpha, b). \tag{6.40}$$

While placing equations (6.22) and (6.31) in equation (6.40) yields

$$\iota k_{\mathfrak{eff}}\mathscr{R}_{+}^{4}(\alpha)\chi(\eta_1,\alpha)-\overset{\prime}{F}_{-}(\alpha,b)+\frac{2k_{\mathfrak{eff}}\sin\theta_0 e^{-\iota k_{\mathfrak{eff}}b\sin\theta_0}}{(1+\eta_1\sin\theta_0)(\alpha-k_{\mathfrak{eff}}\cos\theta_0)}$$
$$=\frac{-\mathfrak{L}(\alpha)(\alpha)\sin\mathfrak{L}(\alpha)b\mathscr{R}_{+}^{4}(\alpha)}{\mathscr{W}_4(\alpha)}+\frac{1}{\mathscr{W}_4(\alpha)}\int_0^b[\mathfrak{f}(t)-\iota\alpha\mathfrak{g}(t)]\cos\mathfrak{L}(\alpha)t\,dt. \tag{6.41}$$

Rearranging equations (6.41), one gets

$$\frac{\iota\eta_1\chi(\eta_1,\alpha)\mathscr{R}_{+}^{4}(\alpha)}{\mathscr{N}^4(\alpha)}+\overset{\prime}{F}_{-}(\alpha,b)=\frac{2k_{\mathfrak{eff}}\sin\theta_0 e^{-\iota k_{\mathfrak{eff}}b\sin\theta_0}}{(1+\eta_1\sin\theta_0)(\alpha-k_{\mathfrak{eff}}\cos\theta_0)}$$
$$-\frac{1}{\mathscr{W}_4(\alpha)}\int_0^b(\mathfrak{f}(t)-\iota\alpha\mathfrak{g}(t))\cos\mathfrak{L}(\alpha)t\,dt, \tag{6.42}$$

where

$$\mathscr{N}^4(\alpha)=\mathscr{W}_4(\alpha)e^{\iota\mathfrak{L}(\alpha)b}. \tag{6.43}$$

Using equation (6.35) into equation (6.42), one obtains

$$\frac{\iota\eta_1\chi(\eta_1,\alpha)\mathscr{R}_{+}^{4}(\alpha)}{\mathscr{N}^4(\alpha)}+\overset{\prime}{F}_{-}(\alpha,b)=\frac{2k_{\mathfrak{eff}}\sin\theta_0 e^{-\iota k_{\mathfrak{eff}}b\sin\theta_0}}{(1+\eta_1\sin\theta_0)(\alpha-k_{\mathfrak{eff}}\cos\theta_0)}$$
$$-\frac{1}{\mathscr{W}_4(\alpha)}\int_0^b\sum_{m=1}^{\infty}(\mathfrak{f}_m+\iota\alpha\mathfrak{g}_m)\cos\mathfrak{L}_m t\cos\mathfrak{L}(\alpha)t\,dt. \tag{6.44}$$

After simplifying the equation (6.44), one can obtain the required Wiener-Hopf equation valid within the strip $\mathfrak{Im}(k_{\mathfrak{eff}}\cos\theta_0)<\mathfrak{Im}(\alpha)<\mathfrak{Im}(k_{\mathfrak{eff}})$ as follows:

$$\frac{\iota\eta_1\chi(\eta_1,\alpha)\mathscr{R}_{+}^{4}(\alpha)}{\mathscr{N}(\alpha)}+\overset{\prime}{F}_{-}(\alpha,b)=\frac{2k_{\mathfrak{eff}}\sin\theta_0 e^{-\iota k_{\mathfrak{eff}}b\sin\theta_0}}{(1+\eta_1\sin\theta_0)(\alpha-k_{\mathfrak{eff}}\cos\theta_0)}$$
$$-\sum_{m=1}^{\infty}\frac{\mathfrak{f}_m-\iota\alpha\mathfrak{g}_m}{\alpha^2-\alpha_m^2}(\mathfrak{L}_m\sin\mathfrak{L}_m b). \tag{6.45}$$

In order to calculate the transmitted field, the Fourier transform of the Helmholtz equation in cold plasma in the waveguide region $x\in(-\infty,\infty)$ and $y\in(-\infty,-b)$

results into

$$\left[\frac{d^2}{dy^2} + (k_{\text{eff}}^2 - \alpha^2)\right]\Psi(\alpha, y) = 0, \tag{6.46}$$

where

$$\Psi(\alpha, y) = \int_{-\infty}^{\infty} H_z^5(x, y) e^{\iota\alpha x} dx. \tag{6.47}$$

Using the radiation condition the general solution of equation (6.46) is as under

$$\Psi(\alpha, y) = A_5(\alpha) e^{-\iota\mathfrak{L}(\alpha)(y+b)}. \tag{6.48}$$

To find the unknown coefficient $A_5(\alpha)$, using the boundary condition represented by equation (6.8) in the transformed domain, one obtains

$$A_5(\alpha) = \frac{k_{\text{eff}}\mathscr{R}_+^5(\alpha)\chi(\eta_2, \alpha)}{\mathfrak{L}(\alpha)}, \tag{6.49}$$

where

$$\mathscr{R}_+^5(\alpha) = \Psi_+(\alpha, -b) - \frac{\eta_2}{\iota k_{\text{eff}}}\Psi_+'(\alpha, -b). \tag{6.50}$$

Using the additive decomposition theorem and equation (6.49) in equation (6.48), it is found that

$$\Psi_+(\alpha, y) + \Psi_-(\alpha, y) = \frac{k_{\text{eff}}\mathscr{R}_+^4(\alpha)\chi(\eta_2, \alpha)}{\mathfrak{L}(\alpha)} e^{-\iota\mathfrak{L}(\alpha)(y+b)}, \tag{6.51}$$

whereas the derivative of equation (6.51) with respect to y at $y = b$ takes the form

$$\Psi_+'(\alpha, -b) = -\iota k_{\text{eff}}\mathscr{R}_+^4(\alpha)\chi(\eta_2, \alpha) - \Psi_-'(\alpha, -b). \tag{6.52}$$

From equation (6.2), we observe that $H_z^4(x, y)$ satisfies the Helmholtz equation in cold plasma in the waveguide region $x \in (0, \infty)$ and $y \in (-b, 0)$. After multiplying

by $e^{\iota\alpha x}$ and integrating with respect to x from 0 to ∞, takes the form as under

$$\left[\frac{d^2}{dy^2} + \mathfrak{L}^2(\alpha)\right] G_+(\alpha, y) = \mathfrak{p}(y) + \iota\mathfrak{q}(y), \tag{6.53}$$

with

$$\mathfrak{p}(y) = \frac{\partial}{\partial x} H_z^4(0, y), \quad \mathfrak{q}(y) = H_z^4(0, y) \tag{6.54}$$

and $G_+(\alpha, y)$ defined by

$$G_+(\alpha, y) = \int_0^\infty H_z^4(x, y) e^{\iota\alpha x} dx, \tag{6.55}$$

is a regular function in the half-plane.

The general solution of the non-homogenous differential equation (6.53) can be obtained by using the method of variation of parameter yields

$$G_+(\alpha, y) = C_{11}(\alpha)\cos\mathfrak{L}(\alpha)y + C_{12}(\alpha)\sin\mathfrak{L}(\alpha)y + \frac{1}{\mathfrak{L}(\alpha)}\int_{-b}^{y} (\mathfrak{p}(t) + \iota\mathfrak{q}(t))\sin\mathfrak{L}(\alpha)(y-t)dt. \tag{6.56}$$

To find $C_{11}(\alpha)$ using the transform form of the boundary condition represented by equation (6.7) gives

$$C_{11}(\alpha) = \frac{1}{\mathfrak{L}(\alpha)}\int_{-b}^{0} (\mathfrak{p}(t) - \iota\alpha\mathfrak{q}(t))\sin\mathfrak{L}(\alpha)t dt. \tag{6.57}$$

Substituting equations (6.57) in equations (6.56), one obtains

$$G_+(\alpha, y) = C_{12}(\alpha)\sin\mathfrak{L}(\alpha)y + \frac{\cos\mathfrak{L}(\alpha)y}{\mathfrak{L}(\alpha)}\int_{-b}^{0} (\mathfrak{p}(t) - \iota\alpha\mathfrak{q}(t))\sin\mathfrak{L}t dt$$
$$+ \frac{1}{\mathfrak{L}(\alpha)}\int_{-b}^{y} (\mathfrak{p}(t) - \iota\alpha\mathfrak{g}(y))\sin\mathfrak{L}(\alpha)(y-t)dt. \tag{6.58}$$

The transformed form of the continuity relations represented by the equations (6.15) and (6.16), respectively, are as below

$$\Psi_+(\alpha,-b) = G_+(\alpha,-b) \tag{6.59}$$

and

$$\overset{\prime}{\Psi}_+(\alpha,-b) = \overset{\prime}{G}_+(\alpha,-b). \tag{6.60}$$

Subtracting equation (6.59) and $\frac{\eta_2}{\imath k_{\mathfrak{eff}}}$ times of equation (6.60) yields

$$G_+(\alpha,-b) - \frac{\eta_2}{\imath k_{\mathfrak{eff}}}\overset{\prime}{G}_+(\alpha,-b) = \mathscr{R}^5_+(\alpha). \tag{6.61}$$

To find $C_{12}(\alpha)$ placing equation (6.58) in equation (6.61), one obtains

$$C_{12}(\alpha) = \frac{-\mathscr{R}^5_+(\alpha)}{\mathscr{W}_5(\alpha)} + \frac{\cos\mathfrak{L}(\alpha)y - \frac{\eta_2}{\imath k_{\mathfrak{eff}}}\mathfrak{L}(\alpha)\sin\mathfrak{L}(\alpha)b}{\mathfrak{L}(\alpha)\mathscr{W}_5(\alpha)}\int_{-b}^{0}(\mathfrak{p}(t)-\imath\alpha\mathfrak{q}(t))\sin\mathfrak{L}(\alpha)t\,dt, \tag{6.62}$$

where

$$\mathscr{W}_5(\alpha) = \sin\mathfrak{L}(\alpha)b + \frac{\eta_2}{\imath k_{\mathfrak{eff}}}\mathfrak{L}(\alpha)\cos\mathfrak{L}(\alpha)b. \tag{6.63}$$

Using equation (6.62) in (6.58) yields

$$\begin{aligned} G_+(\alpha,y) &= \frac{-\mathscr{R}^5_+(\alpha)}{\mathscr{W}_5(\alpha)}\sin\mathfrak{L}(\alpha)y \\ &+ \frac{\cos\mathfrak{L}(\alpha)b - \frac{\eta_2}{\imath k_{\mathfrak{eff}}}\mathfrak{L}\sin\mathfrak{L}(\alpha)b}{\mathfrak{L}(\alpha)\mathscr{W}_5(\alpha)}\sin\mathfrak{L}(\alpha)y\int_{-b}^{0}(\mathfrak{p}(t)-\imath\alpha\mathfrak{q}(t))\sin\mathfrak{L}(\alpha)t\,dt \\ &+ \frac{\cos\mathfrak{L}y}{\mathfrak{L}(\alpha)}\int_{-b}^{0}(\mathfrak{p}(t)-\imath\alpha\mathfrak{q}(t))\sin\mathfrak{L}t\,dt + \frac{1}{\mathfrak{L}(\alpha)}\int_{-b}^{y}(\mathfrak{f}(t)-\imath\alpha\mathfrak{g}(t))\sin\mathfrak{L}(y-t)\,dt. \end{aligned} \tag{6.64}$$

Rearranging equation (6.64) takes the form

$$G_+(\alpha,y)=\frac{-\mathscr{R}_+^5(\alpha)}{\mathscr{W}_5(\alpha)}\sin\mathfrak{L}(\alpha)y+\frac{1}{\mathfrak{L}(\alpha)}\int_{-b}^{y}(\mathfrak{p}(t)-\iota\alpha\mathfrak{q}(t))\sin\mathfrak{L}(\alpha)(y-t)dt$$
$$+\frac{\sin\mathfrak{L}(\alpha)(y+b)+\frac{\eta_2}{\iota k_{\mathfrak{eff}}}\mathfrak{L}(\alpha)\cos\mathfrak{L}(\alpha)(y+b)}{\mathfrak{L}(\alpha)\mathscr{W}_5(\alpha)}\int_{-b}^{0}(\mathfrak{p}(t)-\iota\alpha\mathfrak{q}(t))\sin\mathfrak{L}(\alpha)tdt. \tag{6.65}$$

The left-hand side (i.e., $G_+(\alpha,y)$) of the equation (6.65) is analytic in the upper half-plane $\mathfrak{Im}(\alpha)>\mathfrak{Im}(k_{\mathfrak{eff}}\cos\theta_0)$. However, the analyticity of the right-hand side is violated by the appearance of simple poles placing at the zeros of $\mathscr{W}_5(\alpha)$, i.e., $\alpha=\pm\alpha_m$ satisfying

$$\mathscr{W}_5(\pm\nu_m)=0,\qquad \mathfrak{Im}(\nu_m)>\mathfrak{Im}(k_{\mathfrak{eff}}),\qquad m=1,2,3.... \tag{6.66}$$

The poles in the equation (6.65) can be removed by imposing the condition that residues of these poles are zero. Then from equation (6.65), one obtains

$$\mathscr{R}_+^5(\nu_m)=-\left(\frac{\cos L_m b}{L_m}+\frac{\eta_2}{\iota k_{\mathfrak{eff}}}\sin L_m b\right)\int_{-b}^{0}(\mathfrak{p}(t)-\iota\alpha\mathfrak{q}(t))\sin L_m t dt, \tag{6.67}$$

where

$$L_m=\sqrt{k_{\mathfrak{eff}}^2-\nu_m^2}, \tag{6.68}$$

$\mathfrak{p}(t)$ and $\mathfrak{q}(t)$ can be expanded into a series of eigen-functions as follows:

$$\mathfrak{p}(t)-\iota\alpha\mathfrak{q}(t)=\sum_{n=1}^{\infty}(\mathfrak{p}_n-\iota\alpha\mathfrak{q}_n)\sin L_n t. \tag{6.69}$$

Using equation (6.69) in equation (6.67) yields

$$\mathscr{R}_{+}^{5}(\alpha_m) = -\left(\frac{\cos L_m b}{L_m} + \frac{\eta_2}{\imath k_{\mathfrak{eff}}} \sin L_m b\right) \int_{-b}^{0} \sum_{n=1}^{\infty} (\mathfrak{p}_n - \imath \alpha_m \mathfrak{q}_n) \sin L_n t \sin L_m t \, dt. \tag{6.70}$$

After simplification, equation (6.70) gives

$$\mathscr{R}_{+}^{4}(\alpha_m) = \mathfrak{D}_m^5 (\mathfrak{p}_m + \imath \mathfrak{q}_m) \left(\frac{\cos L_m b}{L_m} + \frac{\eta_2}{\imath k_{\mathfrak{eff}}} \sin L_m b\right), \tag{6.71}$$

$$\mathfrak{D}_m^5 = \frac{L_m \cos L_m b}{2\nu_m} \frac{\partial}{\partial \alpha} \mathscr{W}_5(\nu_m). \tag{6.72}$$

Using equations (6.52) and (6.65) in equation (6.60) yields

$$\begin{aligned} -\imath k_{\mathfrak{eff}} \mathscr{R}_{+}^{5}(\alpha) \chi(\eta_2, \alpha) - \overset{\prime}{\Psi}_{-}(\alpha, -b) &= -\frac{\mathfrak{L}(\alpha) \mathscr{R}_{+}^{5}(\alpha)}{\mathscr{W}_5(\alpha)} \cos \mathfrak{L}(\alpha) b \\ -\frac{1}{\mathscr{W}_5(\alpha)} \int_{-b}^{0} (\mathfrak{p}(t) - \imath \alpha \mathfrak{q}(t)) \sin \mathfrak{L}(\alpha) t \, dt. & \end{aligned} \tag{6.73}$$

After simplifying equations (6.73), one can obtain

$$\frac{k_{\mathfrak{eff}} \chi(\eta_2, \alpha) \mathscr{R}_{+}^{5}(\alpha)}{\mathscr{N}^5(\alpha)} - \overset{\prime}{\Psi}_{-}(\alpha, -b) = -\frac{1}{\mathscr{W}_5(\alpha)} \int_{-b}^{0} (\mathfrak{p}(t) - \imath \alpha \mathfrak{q}(t)) \sin \mathfrak{L}(\alpha) t \, dt, \tag{6.74}$$

where

$$\mathscr{N}^5(\alpha) = \mathscr{W}_5(\alpha) e^{\imath \mathfrak{L}(\alpha) b}. \tag{6.75}$$

Using equation (6.69) into equation (6.74), one obtains the required Wiener-Hopf equation valid in the strip $\mathfrak{Im}(-k_{\mathfrak{eff}}) < \mathfrak{Im}(\alpha) < \mathfrak{Im}(k_{\mathfrak{eff}})$ as follows:

$$\frac{k_{\mathfrak{eff}} \chi(\eta_2, \alpha) \mathscr{R}_{+}^{5}(\alpha)}{\mathscr{N}^5(\alpha)} - \overset{\prime}{\Psi}_{-}(\alpha, -b) = -\frac{1}{\mathscr{W}_5(\alpha)} \int_{0}^{b} \sum_{m=1}^{\infty} (\mathfrak{p}_m - \imath \alpha \mathfrak{q}_m) \sin L_m t \sin \mathfrak{L}(\alpha) t \, dt. \tag{6.76}$$

From the above expression, one can write

$$\frac{k_{\text{eff}}\chi(\eta_2,\alpha)\mathscr{R}^5_+(\alpha)}{\mathscr{N}^5(\alpha)} - \overset{\prime}{\Psi}_-(\alpha,-b) = \sum_{m=1}^{\infty} \frac{\mathfrak{p}_m - \iota\alpha\mathfrak{q}_m}{\alpha^2-\nu_m^2}\,(L_m\cos L_m b)\,. \tag{6.77}$$

6.3 SOLUTION OF WIENER-HOPF EQUATION

To solve the Wiener-Hopf equations the kernel functions $\mathscr{N}^4(\alpha)$, $\mathscr{N}^5(\alpha)$ and $\chi(\eta_j,\alpha))$ in equations (6.45) and (6.77) can be factorized by applying the known results as following:

$$\mathscr{N}^4(\alpha) = \mathscr{N}^4_+(\alpha)\mathscr{N}^4_-(\alpha), \tag{6.78}$$

$$\mathscr{N}^5(\alpha) = \mathscr{N}^5_+(\alpha)\mathscr{N}^5_-(\alpha), \tag{6.79}$$

where

$$\begin{aligned}\mathscr{N}^4_+(\alpha) &= \left[\cos k_{\text{eff}} b + \iota\eta_1 \sin k_{\text{eff}} b\right]^{\frac{1}{2}} \\ &\times \exp\left[\frac{\mathfrak{L}(\alpha)b}{\pi}\ln\left(\frac{\alpha+\iota\mathfrak{L}(\alpha)}{k_{\text{eff}}}\right) + \frac{\iota\alpha b}{\pi}\left(1-C+\ln\left[\frac{2\pi}{k_{\text{eff}}b}\right]+\iota\frac{\pi}{2}\right)\right]\prod_{m=1}^{\infty}\left(1+\frac{\alpha}{\alpha_m}\right)e^{\frac{\iota\alpha b}{m\pi}}\end{aligned} \tag{6.80}$$

and

$$\begin{aligned}\mathscr{N}^5_+(\alpha) &= \left[\sin k_{\text{eff}} b - \iota\eta_2 \cos k_{\text{eff}} b\right]^{\frac{1}{2}} \\ &\times \exp\left[\frac{\mathfrak{L}(\alpha)b}{\pi}\ln\left(\frac{\alpha+\iota\mathfrak{L}(\alpha)}{k_{\text{eff}}}\right) + \frac{\iota\alpha b}{\pi}\left(1-C+\ln\left[\frac{2\pi}{k_{\text{eff}}b}\right]+\iota\frac{\pi}{2}\right)\right]\prod_{m=1}^{\infty}\left(1+\frac{\alpha}{\alpha_m}\right)e^{\frac{\iota\alpha b}{m\pi}},\end{aligned} \tag{6.81}$$

such that

$$\mathscr{N}^4_-(\alpha) = \mathscr{N}^4_+(-\alpha), \tag{6.82}$$

$$\mathscr{N}^5_-(\alpha) = \mathscr{N}^5_+(-\alpha). \tag{6.83}$$

As mention before, the factor of $\chi(\eta_j,\alpha)$ can be written in terms of the Maliuzhinetz's function.

Now, multiplying the Wiener-Hopf equation (6.45) on both sides with $\frac{\mathscr{N}^4_-(\alpha)}{\chi_-(\eta_1,\alpha)}$, one obtains

$$\frac{\iota\eta_1\chi_+(\eta_1,\alpha)\mathscr{R}_+(\alpha)}{\mathscr{N}_+^4(\alpha)}+\frac{\mathscr{N}_-^4(\alpha)\overset{\prime}{F}_-(\alpha,b)}{\chi_-(\eta_1,\alpha)}=\frac{2k_{\mathfrak{eff}}\sin\theta_0 e^{-\iota k_{\mathfrak{eff}}b\sin\theta_0}\mathscr{N}_-^4(\alpha)}{(1+\eta_1\sin\theta_0)(\alpha-k_{\mathfrak{eff}}\cos\theta_0)\chi_-(\eta_1,\alpha)}$$
$$-\sum_{m=1}^{\infty}\frac{\mathfrak{L}_m\sin\mathfrak{L}_m b(\mathfrak{f}_m-\iota\alpha\mathfrak{g}_m)\mathscr{N}_-^4(\alpha)}{(\alpha^2-\alpha_m^2)\chi_-(\eta_1,\alpha)}. \tag{6.84}$$

With the help of cauchy's integral formula the terms on right-hand of the equation (6.84) can be decomposed as

$$\begin{aligned}&\frac{2k_{\mathfrak{eff}}\sin\theta_0 e^{-\iota k_{\mathfrak{eff}}\sin\theta_0}\mathscr{N}_-^4(\alpha)}{(1+\eta_1\sin\theta_0)(\alpha-k_{\mathfrak{eff}}\cos\theta_0)\chi_-(\eta_1,\alpha)}\\&=\frac{2k_{\mathfrak{eff}}\sin\theta_0 e^{-\iota k_{\mathfrak{eff}}b\sin\theta_0}}{(1+\eta_1\sin\theta_0)(\alpha-k_{\mathfrak{eff}}\cos\theta_0)}\left[\frac{\mathscr{N}_-^4(\alpha)}{\chi_-(\eta,\alpha)}-\frac{\mathscr{N}_-^4(k_{\mathfrak{eff}}\cos\theta_0)}{\chi_-(\eta_1,k_{\mathfrak{eff}}\cos\theta_0)}\right]\\&+\frac{2k_{\mathfrak{eff}}\sin\theta_0 e^{-\iota k_{\mathfrak{eff}}b\sin\theta_0}}{(1+\eta_1\sin\theta_0)(\alpha-k_{\mathfrak{eff}}\cos\theta_0)}\frac{\mathscr{N}_-^4(k_{\mathfrak{eff}}\cos\theta_0)}{\chi_-(\eta_1,k_{\mathfrak{eff}}\cos\theta_0)}\end{aligned} \tag{6.85}$$

and

$$\begin{aligned}&\sum_{m=1}^{\infty}\frac{\mathfrak{L}_m\sin\mathfrak{L}_m b(\mathfrak{f}_m-\iota\alpha\mathfrak{g}_m)\mathscr{N}_-^4(\alpha)}{(\alpha^2-\alpha_m^2)\chi_-(\eta_1,\alpha)}=-\sum_{m=1}^{\infty}\frac{\mathfrak{L}_m\sin\mathfrak{L}_m b(\mathfrak{f}_m+\iota\alpha_m\mathfrak{g}_m)\mathscr{N}_+^4(\alpha_m)}{2\alpha_m(\alpha+\alpha_m)\chi_+(\eta_1,\alpha_m)}\\&+\sum_{m=1}^{\infty}\frac{\mathfrak{L}_m\sin\mathfrak{L}_m b}{\alpha+\alpha_m}\left[\frac{(\mathfrak{f}_m-\iota\alpha\mathfrak{g}_m)\ \mathscr{N}_-^4(\alpha)}{(\alpha-\alpha_m)\chi_-(\eta,\alpha)}+\frac{(\mathfrak{f}_m+\iota\alpha_m\mathfrak{g}_m)\ \mathscr{N}_+^4(\alpha_m)}{2\alpha_m\chi_+(\eta_1,\alpha_m)}\right].\end{aligned} \tag{6.86}$$

Now using equations (6.85) and (6.86) in equation (6.84), then placing the terms which are analytic in the upper half-plane ($\mathfrak{Im}(\alpha) > -k_{\mathfrak{eff}}$) at the left-hand side and those which analytic in lower half-plane ($\mathfrak{Im}(\alpha) < k_{\mathfrak{eff}}$) at the right-hand side which gives

$$\begin{aligned}&\frac{\iota\eta_1\chi_+(\eta_1,\alpha)\mathscr{R}_+^4(\alpha)}{\mathscr{N}_+^4(\alpha)}-\frac{2k_{\mathfrak{eff}}\sin\theta_0 e^{-\iota k_{\mathfrak{eff}}b\sin\theta_0}\mathscr{N}_-^4(k_{\mathfrak{eff}}\cos\theta_0)}{(1+\eta_1\sin\theta_0)(\alpha-k_{\mathfrak{eff}}\cos\theta_0)\chi_-(\eta_1,k_{\mathfrak{eff}}\cos\theta_0)}\\&+\sum_{m=1}^{\infty}\frac{(\mathfrak{f}_m+\iota\alpha_m\mathfrak{g}_m)\mathfrak{L}_m\sin\mathfrak{L}_m b\mathscr{N}_+^4(\alpha_m)}{2\alpha_m(\alpha+\alpha_m)\chi_+(\eta_1,\alpha_m)}=-\frac{F_-(\alpha,b)\mathscr{N}_-^4(\alpha)}{\chi_-(\eta_1,\alpha)}\\&+\frac{2k_{\mathfrak{eff}}\sin\theta_0 e^{-\iota k_{\mathfrak{eff}}b\sin\theta_0}}{(1+\eta_1\sin\theta_0)(\alpha-k_{\mathfrak{eff}}\cos\theta_0)}\left[\frac{\mathscr{N}_-^4(\alpha)}{\chi_-(\eta_1,\alpha)}-\frac{\mathscr{N}_-^4(k_{\mathfrak{eff}}\cos\theta_0)}{\chi_-(\eta_1,k_{\mathfrak{eff}}\cos\theta_0)}\right]\\&+\sum_{m=1}^{\infty}\frac{\mathfrak{L}_m\sin\mathfrak{L}_m b}{\alpha+\alpha_m}\left[\frac{(\mathfrak{f}_m-\iota\alpha\mathfrak{g}_m)\mathscr{N}_-^4(\alpha)}{(\alpha-\alpha_m)\chi_-(\eta_1,\alpha)}+\frac{(\mathfrak{f}_m+\iota\alpha_m\mathfrak{g}_m)\ \mathscr{N}_+^4(\alpha_m)}{2\alpha_m\chi_+(\eta_1,\alpha_m)}\right].\end{aligned} \tag{6.87}$$

The required solution of Wiener-Hopf equation for the diffracted can be obtained by using analytical continuation principle following extended Liouville's theorem yields

$$\frac{\iota\eta_1\chi_+(\eta_1,\alpha)\mathscr{R}_+(\alpha)}{\mathscr{N}_+^4(\alpha)} = \frac{2k_{\mathfrak{eff}}\sin\theta_0 e^{-\iota k_{\mathfrak{eff}}b\sin\theta_0}\mathscr{N}_-^4(k_{\mathfrak{eff}}\cos\theta_0)}{(1+\eta_1\sin\theta_0)(\alpha-k_{\mathfrak{eff}}\cos\theta_0)\chi_-(\eta_1,k_{\mathfrak{eff}}\cos\theta_0)} - \sum_{m=1}^{\infty}\frac{(\mathfrak{f}_m+\iota\alpha_m\mathfrak{g}_m)\mathfrak{L}_m\sin\mathfrak{L}_m b\mathscr{N}_+^4(\alpha_m)}{2\alpha_m(\alpha+\alpha_m)\chi_+(\eta_1,\alpha_m)}. \tag{6.88}$$

Now, multiplying the Wiener-Hopf equation (6.77) on both sides with $\frac{\mathscr{N}_-^5(\alpha)}{\chi_-(\eta_2,\alpha)}$, one obtains

$$\frac{k_{\mathfrak{eff}}\chi_+(\eta_2,\alpha)\mathscr{R}_+^4(\alpha)}{\mathscr{N}_+^5(\alpha)} - \frac{\mathscr{N}_-^5(\alpha)\Psi'_-(\alpha,b)}{\chi_-(\eta_2,\alpha)} = \sum_{m=1}^{\infty}\frac{L_m\sin L_m b(\mathfrak{p}_m-\iota\alpha\mathfrak{q}_m)\mathscr{N}_-^5(\alpha)}{(\alpha^2-\nu_m^2)\chi_-(\eta_2,\alpha)}. \tag{6.89}$$

With the aid of cauchy's integral formula the terms at the right-hand of the equation (6.89) can be decomposed as

$$\sum_{m=1}^{\infty}\frac{L_m\cos L_m b(\mathfrak{p}_m-\iota\alpha\mathfrak{q}_m)\mathscr{N}_-^5(\alpha)}{(\alpha^2-\nu_m^2)\chi_-(\eta_2,\alpha)} = -\sum_{m=1}^{\infty}\frac{(\mathfrak{p}_m+\iota\nu_m\mathfrak{q}_m)L_m\cos L_m b\mathscr{N}_+^5(\upsilon_m)}{2\upsilon_m(\alpha+\upsilon_m)\chi_+(\eta_2,\nu_m)} + \sum_{m=1}^{\infty}\frac{L_m\cos L_m b}{\alpha+\nu_m}\left[\frac{(\mathfrak{p}_m-\iota\alpha\mathfrak{q}_m)\,\mathscr{N}_-^5(\alpha)}{(\alpha-\upsilon_m)\chi_-(\eta_2,\alpha)} + \frac{(\mathfrak{p}_m+\iota\nu_m\mathfrak{q}_m)\,\mathscr{N}_+^5(\nu_m)}{2\nu_m\chi_+(\eta_2,\nu_m)}\right]. \tag{6.90}$$

Now substituting equation (6.90) in equation (6.89), then placing the terms which are analytic in the upper half-plane ($\mathfrak{Im}(\alpha) > -k_{\mathfrak{eff}}$) at the left-hand side and those which analytic in lower half-plane ($\mathfrak{Im}(\alpha) < k_{\mathfrak{eff}}$) at the right-hand side which gives

$$\frac{k\chi_+(\eta_2,\alpha)\mathscr{R}_+^5(\alpha)}{\mathscr{N}_+^4(\alpha)} + \sum_{m=1}^{\infty}\frac{(\mathfrak{p}_m+\iota\upsilon_m\mathfrak{q}_m)L_m\cos L_m b\mathscr{N}_+^5(\upsilon_m)}{2\upsilon_m(\alpha+\upsilon_m)\chi_+(\eta_2,\upsilon_m)} = \frac{F_-(\alpha,b)Q_-(\alpha)}{\chi_-(\eta_2,\alpha)} + \sum_{m=1}^{\infty}\frac{L_m\cos L_m b}{\alpha+\upsilon_m}\left[\frac{(\mathfrak{p}_m-\iota\alpha\mathfrak{q}_m)\,\mathscr{N}_-^5(\alpha)}{(\alpha-\upsilon_m)\chi_-(\eta_2,\alpha)} + \frac{(\mathfrak{p}_m+\iota\upsilon_m\mathfrak{q}_m)\,\mathscr{N}_+^5(\upsilon_m)}{2\upsilon_m\chi_+(\eta_2,\upsilon_m)}\right]. \tag{6.91}$$

The required solution of Wiener-Hopf equation for the transmitted can be obtained by using analytical continuation principle following extended Liouville's

theorem, the above expression gives

$$\frac{k\chi_+(\eta_1,\alpha)\mathscr{R}_+^5(\alpha)}{\mathscr{N}_+^5(\alpha)} = -\sum_{m=1}^{\infty}\frac{(\mathfrak{p}_m+\iota\upsilon_m\mathfrak{q}_m)L_m\cos L_m b\mathscr{N}_+^5(\upsilon_m)}{2\upsilon_m(\alpha+\upsilon_m)\chi_+(\eta_2,\upsilon_m)}. \tag{6.92}$$

6.4 DETERMINATION OF THE UNKNOWN COEFFICIENTS

The significant distinction of this sort of formulation from the one used by Cigar and Büyükaksoy [12], was the simultaneous use of Mode-Matching technique with the Fourier transform. The Mode-Matching technique enables us to express the field components defined in the waveguide region in terms of normal modes as

$$H_z^2(x,y) = \sum_{m=1}^{\infty} a_n \sin\zeta_n(y+b)e^{-\iota\beta_n x}. \tag{6.93}$$

With the help of boundary conditions represented by equations (6.5) and (6.6) β_n 's and ζ_n's are obtained from

$$\zeta_n\cos\zeta_n b = 0, \qquad n = 1,2,3,..., \tag{6.94}$$

which gives

$$\zeta_n = (2n+1)\frac{\pi}{4b}, \quad \beta_n = \sqrt{k_{\mathfrak{eff}}^2-\zeta_n^2}, \quad \Im\mathfrak{m}(\beta_n) > \Im\mathfrak{m}(k_{\mathfrak{eff}}), \quad n = 1,2,.... \tag{6.95}$$

From continuity relations represented by equations (6.11) and (6.12) gives

$$\mathfrak{f}(y) - \iota\alpha\mathfrak{g}(y) = -\iota\sum_{n=1}^{\infty} a_n(\alpha+\beta_n)\sin\zeta_n(y+b). \tag{6.96}$$

Using equation (6.35) into equation (6.96) gives

$$\sum_{m=1}^{\infty}(\mathfrak{f}_m - \iota\alpha\mathfrak{g}_m)\cos\mathfrak{L}_m t = -\iota\sum_{n=1}^{\infty} a_n(\alpha+\beta_n)\sin\zeta_n(y+b). \tag{6.97}$$

Multiplying equation (6.97) by $\cos \mathfrak{L}_s t$ and integrating with respect y from $y = 0$ to $y = b$, one obtains

$$\mathfrak{f}_s - \iota\alpha \mathfrak{g}_s = -\frac{\iota}{\mathscr{D}_s^4} \sum_{n=1}^{\infty} \frac{\zeta_n \cos \mathfrak{L}_s b}{\zeta_n^2 - \mathfrak{L}_s^2} \mathfrak{a}_n (\alpha + \beta_n), \tag{6.98}$$

Using equation (6.98) in equation (6.37) gives

$$\mathscr{R}_+^4(\alpha_m) = -\iota \left(\frac{\sin \mathfrak{L}_m b}{\mathfrak{L}_m} + \frac{\eta_1}{i k_{\mathfrak{eff}}} \cos \mathfrak{L}_m b \right) \sum_{n=1}^{\infty} \frac{\zeta_n \cos \mathfrak{L}_m b}{\zeta_n^2 - \mathfrak{L}_m^2} \mathfrak{a}_n (\alpha_m + \beta_n) \tag{6.99}$$

Substituting equations (6.99) and (6.98) in equation (6.45) at $\alpha = \alpha_s$ leads to

$$\begin{aligned}
&\frac{\eta_1 \chi_+(\eta_1, \alpha_s)}{\mathscr{N}_+^4(\alpha_s)} \left(\frac{\sin \mathfrak{L}_s b}{\mathfrak{L}_s} + \frac{\eta_1}{i k_{\mathfrak{eff}}} \cos \mathfrak{L}_s b \right) \sum_{n=1}^{\infty} \frac{\zeta_n \sin \mathfrak{L}_s b}{\zeta_n^2 - \mathfrak{L}_s^2} \mathfrak{a}_n (\alpha_s + \beta_n) \\
&= \frac{2k \sin\theta_0 e^{-ik_{eff} b \sin\theta_0} \mathscr{N}_-(k_{\mathfrak{eff}} \cos\theta_0)}{(1 + \eta_1 \sin\theta_0)(\alpha_s - k_{\mathfrak{eff}} \cos\theta_0) \chi_-(\eta_1, k_{\mathfrak{eff}} \cos\theta_0)} \\
&+ \sum_{m=1}^{\infty} \frac{\iota \mathfrak{L}_m \sin \mathfrak{L}_m b \mathscr{N}_+^4(\alpha_m)}{\mathscr{N}_m^4(\alpha_s + \alpha_m) 2\alpha_m \chi_+(\eta_1, \alpha_m)} \sum_{n=1}^{\infty} \frac{\zeta_n \sin \mathfrak{L}_m b}{\zeta_n^2 - \mathfrak{L}_m^2} \mathfrak{a}_n (\beta_n - \alpha_m).
\end{aligned} \tag{6.100}$$

The above expression can be written as under

$$\sum_{n=1}^{\infty} \mathscr{A}_n(\alpha_s) \mathfrak{a}_n = I(\alpha_s), \qquad s = 1, 2, 3, \ldots \tag{6.101}$$

where

$$\begin{aligned}
\mathscr{A}_n(\alpha_s) &= \frac{\eta_1 \chi_+(\eta_1, \alpha_s)}{\mathscr{N}_+(\alpha_s)} \left(\frac{\sin \mathfrak{L}_s b}{\mathfrak{L}_s} + \frac{\eta_1}{i k_{\mathfrak{eff}}} \cos \mathfrak{L}_j b \right) \frac{\zeta_n \sin \mathfrak{L}_s b}{\zeta_n^2 - \mathfrak{L}_s^2} (\alpha_s + \beta_n) \\
&+ \sum_{m=1}^{\infty} \frac{\iota \mathfrak{L}_m \sin \mathfrak{L}_m b \mathscr{N}_+^4(\alpha_m) \zeta_n \sin \mathfrak{L}_m b (\beta_n - \alpha_m)}{2\mathscr{N}_m^4 \alpha_m (\alpha_j + \alpha_m) \chi_+(\eta_1, \alpha_m)(\zeta_n^2 - \mathfrak{L}_m^2)}
\end{aligned} \tag{6.102}$$

and

$$I(\alpha_s) = \frac{2k_{eff} \sin\theta_0 e^{-\iota k_{\mathfrak{eff}} b \sin\theta_0} \mathscr{N}_-(k_{\mathfrak{eff}} \cos\theta_0)}{(1 + \eta_1 \sin\theta_0)(\alpha_s - k_{\mathfrak{eff}} \cos\theta_0) \chi_-(\eta_1, k_{\mathfrak{eff}} \cos\theta_0)} \,. \tag{6.103}$$

The infinite system of algebraic equation in equation (6.101) will be solved numerically. To solve this system we truncate the infinite system of algebraic equations after the first N terms.

Now for transmitted field one can consider continuity relations represented by equations (6.13) and (6.14) as under

$$\mathfrak{p}(y) - \iota\alpha\mathfrak{q}(y) = -\iota\sum_{n=1}^{\infty}\mathfrak{a}_n(\alpha+\beta_n)\sin\zeta_n(y+b). \tag{6.104}$$

Using equation (6.69) into equation (6.104), gives

$$\sum_{m=1}^{\infty}(\mathfrak{p}_m - \iota\alpha\mathfrak{q}_m)\sin L_m t \;= -\iota\sum_{n=1}^{\infty}\mathfrak{a}_n(\alpha+\beta_n)\sin\zeta_n(y+b). \tag{6.105}$$

Multiplying equation (6.105) by $\sin L_s y$ and integrating from $y=-b$ to $y=0$, one obtains

$$\mathfrak{p}_s - \iota\alpha\mathfrak{q}_s = \frac{-\iota}{\mathscr{D}_s^5}\int_{-b}^{0}\sum_{n=1}^{\infty}\mathfrak{a}_n(\alpha+\beta_n)\sin\zeta_n(y+b)\sin L_s y\,dy, \tag{6.106}$$

simplification of which gives

$$\mathfrak{p}_s - \iota\alpha_s\mathfrak{q}_j = -\frac{\iota}{\mathscr{D}_m^5}\sum_{n=1}^{\infty}\mathfrak{a}_n(\alpha+\beta_n)\Delta_{ns}, \tag{6.107}$$

where Δ_{ns} is given by

$$\Delta_{ns} = \frac{1}{\zeta_n^2 - L_s^2}\left(L_s\sin\zeta_n b - \zeta_n\sin L_s b\right). \tag{6.108}$$

6.5 THE DIFFRACTED AND TRANSMITTED FIELDS

The diffracted field $H_z^1(x,y)$ is acquired by taking the inverse Fourier transform of $F(\alpha,y)$. While using equation (6.21), one gets

$$H_z^1(x,y) = \frac{1}{2\pi}\int_{\mathscr{L}}\frac{k_{\mathfrak{eff}}}{\mathfrak{L}(\alpha)}\mathscr{R}_+^4(\alpha)\chi(\eta_1,\alpha)e^{\iota\mathfrak{L}(\alpha)(y-b)}e^{-\iota\alpha x}d\alpha. \tag{6.109}$$

Using the replacement of function $\chi(\eta_1,\alpha)$ and variables $\alpha=-k_{\mathfrak{eff}}\cos t,\ x=\rho\cos\theta$ and $y=\rho\sin\theta$, equation (6.109) takes the form

$$H_z^1(\rho,\theta)=\frac{1}{2\pi}\int_{\mathscr{L}}\frac{\mathscr{R}_+^4(-k_{\mathfrak{eff}}\cos t)k_{\mathfrak{eff}}\sin t}{1+\eta_1\sin t}e^{-\iota k_{\mathfrak{eff}}\sin t+\iota k_{\mathfrak{eff}}\rho\cos(t-\theta)}dt. \tag{6.110}$$

The integral in equation (6.110) can be evaluated asymptotically through the saddle point technique. Here, saddle point occurs at $t=\theta$.

On taking into account equation (6.88), the diffracted field takes following form

$$\begin{aligned}H_z^1(\rho,\theta)=&\frac{k\sqrt{(\epsilon_1^2-\epsilon_2^2)/\epsilon_1}e^{\iota k\rho\sqrt{(\epsilon_1^2-\epsilon_2^2)/\epsilon_1}-\iota\frac{\pi}{4}-\iota k\sqrt{(\epsilon_1^2-\epsilon_2^2)/\epsilon_1}b\sin\theta}\sin\theta}{\sqrt{2\pi k\rho}(1+\eta_1\sin\theta)}\\ &\times\left[\frac{2\iota\sin\theta_0 e^{-ik\sqrt{(\epsilon_1^2-\epsilon_2^2)/\epsilon_1}b\sin\theta_0}\mathscr{N}_-^4(k\sqrt{(\epsilon_1^2-\epsilon_2^2)/\epsilon_1}\cos\theta_0)}{\eta_1(1+\sin\theta_0)(\cos\theta+\cos\theta_0)\chi_-(\eta_1,k_{\mathfrak{eff}}\cos\theta_0)}+\right.\\ &\left.\sum_{m=1}^{\infty}\frac{\iota\mathfrak{L}_m\sin\mathfrak{L}_m b\mathscr{N}_+^4(\alpha_m)(\mathfrak{f}_m+\iota\alpha_m\mathfrak{g}_m)}{2\eta_1\alpha_m(\alpha_m-k\sqrt{(\epsilon_1^2-\epsilon_2^2)/\epsilon_1}\cos\theta)\chi_+(\eta_1,\alpha_m)}\right]\frac{\mathscr{N}_-^4(k\sqrt{(\epsilon_1^2-\epsilon_2^2)/\epsilon_1}\cos\theta)}{\chi_-(\eta_1,k\sqrt{(\epsilon_1^2-\epsilon_2^2)/\epsilon_1}\cos\theta)}.\end{aligned} \tag{6.111}$$

The transmitted field $H_z^5(x,y)$ is obtained by taking the inverse Fourier transform of $\psi(\alpha,y)$. While using equation (6.51), one gets

$$H_z^5(x,y)=\frac{1}{2\pi}\int_{\mathscr{L}}\frac{k_{\mathfrak{eff}}\mathscr{R}_+^5(\alpha)\chi(\eta_2,\alpha)}{\mathfrak{L}(\alpha)}e^{-\iota\mathfrak{L}(y+b)}e^{-\iota\alpha x}d\alpha. \tag{6.112}$$

Using the replacement of function $\chi(\eta_2,\alpha)$ and change of variables $\alpha=-k_{\mathfrak{eff}}\cos t$, $x=\rho\cos\theta$ and $y=\rho\sin\theta$, equation (6.112) takes the form

$$H_z^5(\rho,\theta)=\frac{1}{2\pi}\int_{\mathscr{L}}\frac{\mathscr{R}_+^5(-k_{\mathfrak{eff}}\cos t)k_{\mathfrak{eff}}\sin t}{1+\eta_2\sin t}e^{-\iota k_{\mathfrak{eff}}\sin t+\iota k_{\mathfrak{eff}}\rho\cos(t+\theta)}dt. \tag{6.113}$$

The integral in equation (6.113) can be evaluated asymptotically through the saddle point technique. Here, saddle point occurs at $t=2\pi-\theta$. Taking into account

equation (6.92), the transmitted field takes the form:

$$H_z^5(\rho,\theta) = -\frac{\sqrt{(\epsilon_1^2-\epsilon_2^2)/\epsilon_1}\sin\theta e^{\iota k\rho\sqrt{(\epsilon_1^2-\epsilon_2^2)/\epsilon_1}-\frac{\iota\pi}{4}-\iota kb\sqrt{(\epsilon_1^2-\epsilon_2^2)/\epsilon_1}\sin\theta}}{\sqrt{2\pi k\rho}(1-\eta_2\sin\theta)}$$
$$\times\frac{\mathcal{N}_-^5(k\sqrt{(\epsilon_1^2-\epsilon_2^2)/\epsilon_1}\cos\theta)}{\chi_-(\eta_1,k\sqrt{(\epsilon_1^2-\epsilon_2^2)/\epsilon_1}\cos\theta)}\sum_{m=1}^{\infty}\frac{L_m\cos L_m b\mathcal{N}_+^5(\upsilon_m)(\mathfrak{p}_m+\iota\mathfrak{q}_m)}{2\upsilon_m(\upsilon_m-k_{\mathfrak{eff}}\cos\theta)\chi_+(\eta_2,\upsilon_m)}. \quad (6.114)$$

6.6 COMPUTATIONAL RESULTS AND DISCUSSION

In this section, we evaluate the numerical results for various physical parameters of interest. It is obvious to see that the diffracted and transmitted fields represented by the equations (6.111) and (6.114) contain infinite series. Fig. (6.2) shows the variation of the modulus of the diffracted field versus the truncation number "N". It is observed that the effect of the truncation number is negligible for $N \geq 100$. Hence, the infinite system of algebraic equations in equation (6.101) can be managed to deal as finite. Fig. (6.3) deals with variation of modulus of the transmitted field with respect to truncation number N and the result is obtained that the effect of the truncation number is negligible for $N \geq 80$. Fig. (6.4) depicts the variation in the diffracted field versus impedance η_1. It is apparent that the diffracted field decreases with increasing of surface impedance η_1. Whereas Figs. (6.5) and (6.6) show variation in the diffracted field versus the cold plasma permittivity values ϵ_1 and ϵ_2, respectively. It is interesting to note that the diffracted field highly decreases by increasing ϵ_1 but slightly increases with increasing ϵ_2. Also Fig. (6.7) explores the effect of surface impedance over the transmitted field. It is observed that the transmitted field also decreases with increasing η_2. The effect of cold plasma permittivity values ϵ_1 and ϵ_2 over the transmitted are shown in Figs. (6.8) and (6.9), respectively. It is observed here that the transmitted field highly decreases while increasing ϵ_1 whereas it increases slightly by increasing ϵ_2. In other words the diffracted and transmitted fields amplitude decreases with

increasing ion number density in cold plasma or by decreasing plasma frequency.

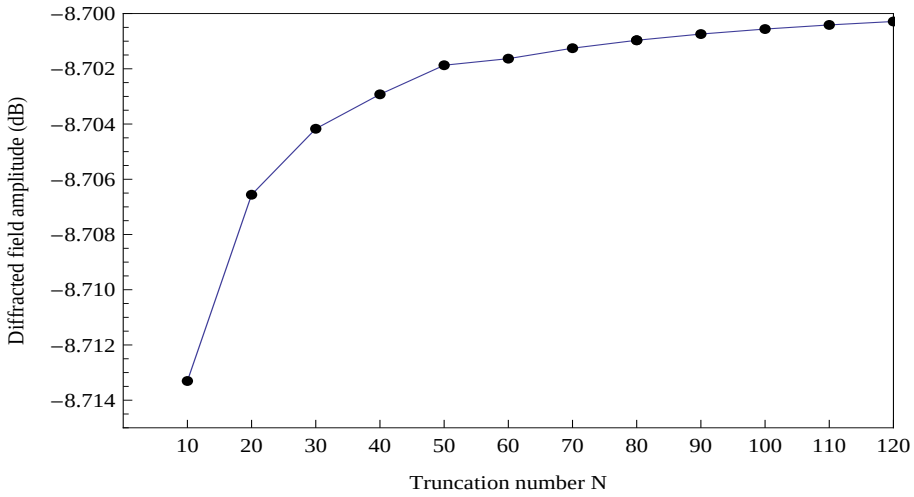

FIGURE 6.2. *Variation in the diffracted field amplitude versus "N" at* $k = 5$, $\theta_0 = 45^o$, $\theta = 90^0$, $\eta_1 = 0.2\iota$, $\epsilon_1 = 0.8$, $\epsilon_2 = 0.1$, $b = 0.2\lambda$.

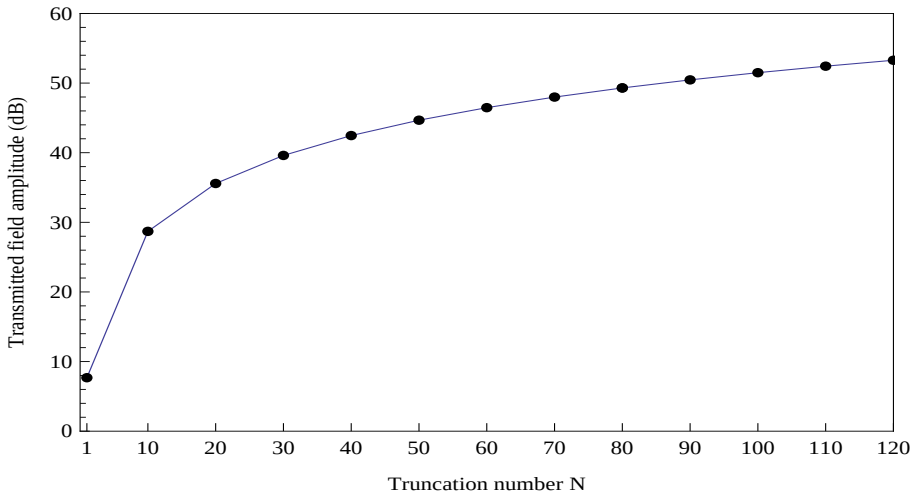

FIGURE 6.3. *Variation in the transmitted field amplitude versus "N" at* $k = 5$, $\theta_0 = 45^o$, $\theta = 90^0$, $\eta_5 = 0.4\iota$, $\epsilon_1 = 0.5$, $\epsilon_2 = 0.1$, $b = 0.2\lambda$.

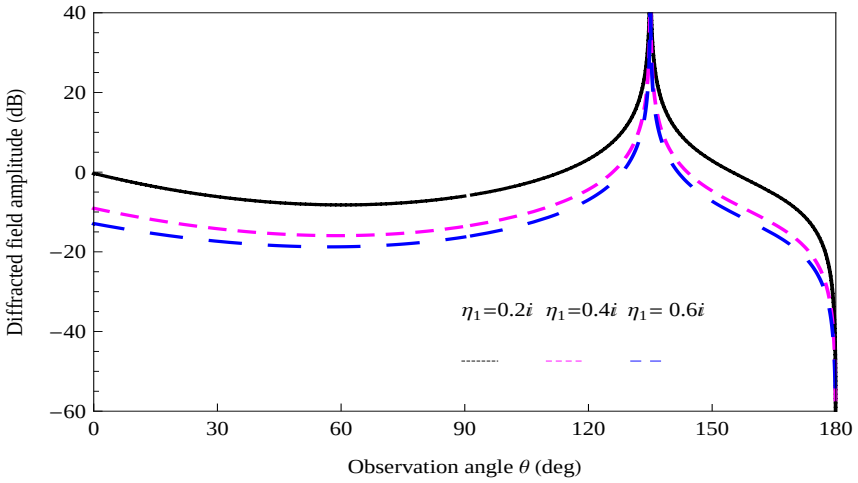

FIGURE 6.4. *Variation in the diffracted field amplitude versus "θ_1" at $\theta_0 = 45^0$, $k = 5$, $\epsilon_1 = 0.8$, $\epsilon_2 = 0.1$ and $b = 0.2\lambda$.*

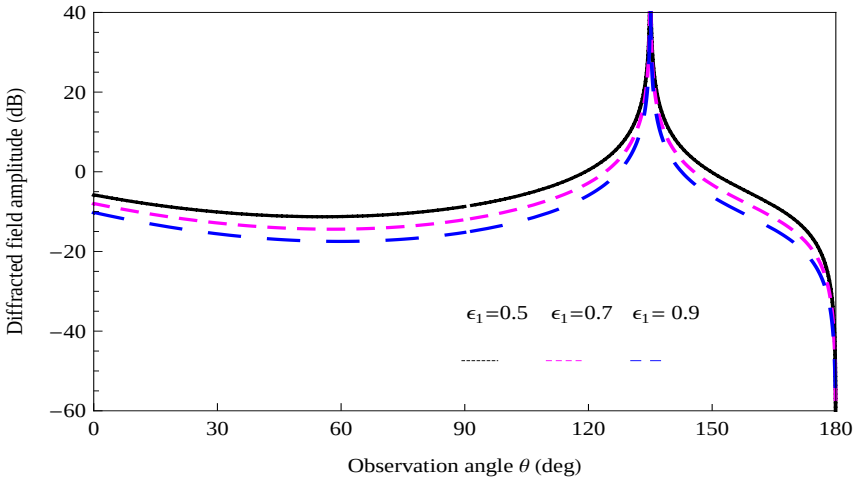

FIGURE 6.5. *Variation in the diffracted field amplitude versus "ϵ_1" at $k = 5$, $\theta_0 = 45^0$, $\eta_1 = 0.2\iota$, $\epsilon_2 = 0.1$ and $b = 0.2\lambda$.*

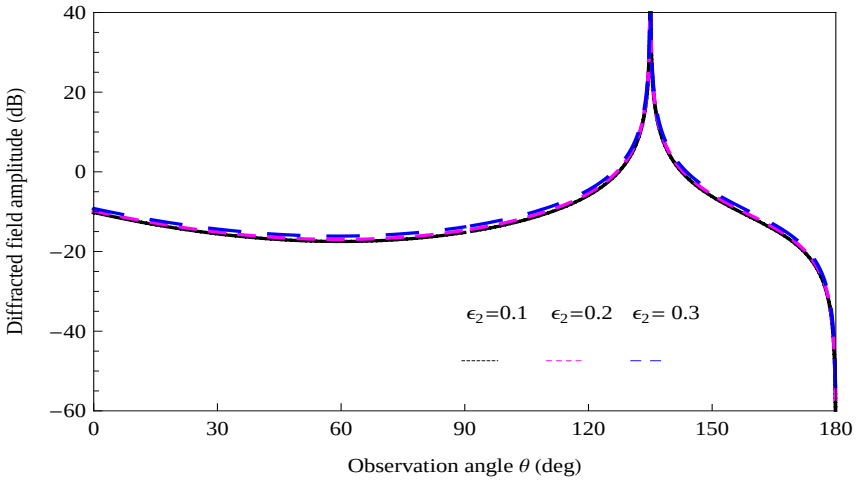

FIGURE 6.6. *Variation in the diffracted field amplitude versus "ϵ_2" at $k = 5$, $\theta_0 = 45^0$, $\eta_1 = 0.2\imath$, $\epsilon_1 = 0.8$ and $b = 0.2\lambda$.*

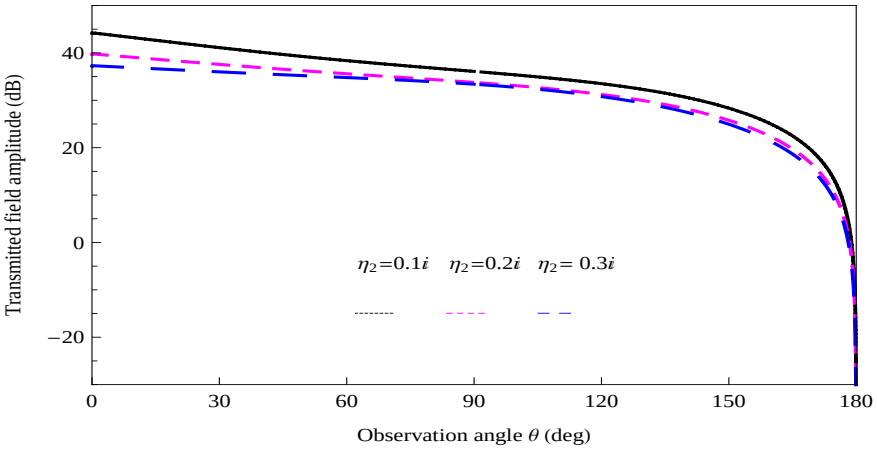

FIGURE 6.7. *Variation in the transmitted field amplitude versus "η_2" at $k = 5$, $\theta_0 = 45^o$, $\epsilon_1 = 0.8$, $\epsilon_2 = 0.1$ and $b = 0.2\lambda$.*

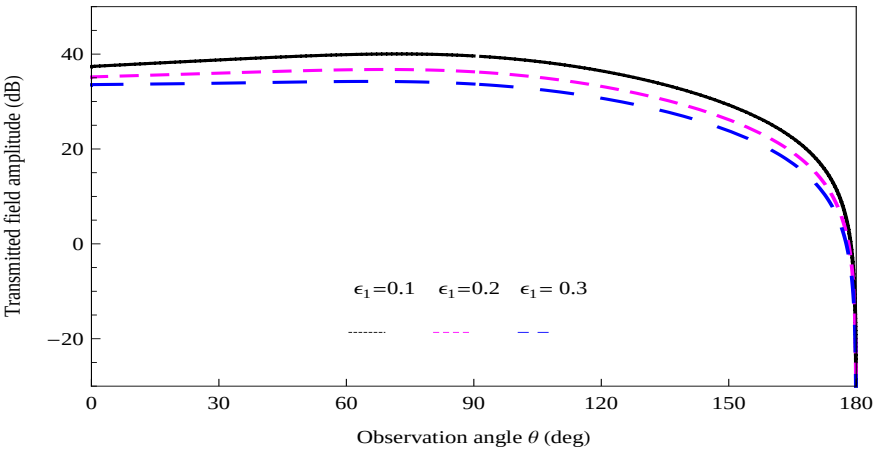

FIGURE 6.8. *Variation in the transmitted field amplitude versus "ϵ_1" at $k = 5$, $\eta_2 = 0.2\imath$, $\epsilon_2 = 0.1$ and $b = 0.2\lambda$.*

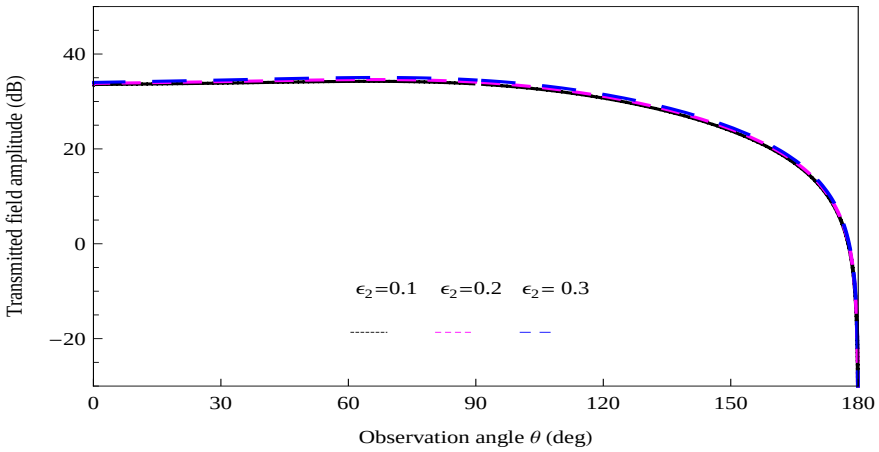

FIGURE 6.9. *Variation in the transmitted field amplitude versus "ϵ_2" at $k = 5$, $\eta_2 = 0.2\iota$, $\epsilon_1 = 0.8$ and $b = 0.2\lambda$.*

CHAPTER 7

CONCLUSION AND PERSPECTIVES

The study of plasma in wave scattering problems have been of significant interest in recent years due to a variety of associated applications in diverse domains. The particular application includes, the construction of antennas, communication between the vehicles and earth station, radio communication etc. We have investigated theoretically the effectiveness of ionosphere plasma, earth's magnetic field, structure and nature of the body material used as an artificial satellite. For analysis purpose the whole system was supposed to be immersed in a cold plasma. The underlying model problems present that how a particular class of boundary-valued problems related to wave scattering in cold plasma may be solved by using different semi-analytic techniques. The solutions to the problems have been focused using Wiener-Hopf technique together with the Mode-Matching technique.

In a first attempt, the model problem describing the effect of cold plasma on scattering of E-polarized plane wave by step discontinuity has been considered. For this purpose the Helmholtz equation in cold plasma has been retrieved from Maxwell's equations in the canonical problem. Then with the help of Fourier transform followed by the Wiener-Hopf technique the diffracted field expression was obtained successfully. It is concluded that the effect of the truncation number is negligible after 15 truncation term. Moreover the diffracted field amplitude

increases with the length of vertical plate. The analysis has also been performed for other parameters of interest such as incident angle and surface impedances. It is depicted that the amplitude of diffracted field increases while increasing the permittivity value ϵ_1. In other words amplitude increases by either decreasing electron number density (plasma frequency) or by increasing ion number density. Whereas in contrast to ϵ_1 the amplitude of diffracted field decreases with increase of the permittivity value ϵ_2. It has been noted that the diffracted field is greatly effected due to permittivity value ϵ_1 as compared with that of permittivity value ϵ_2. Moreover the results in the absence of cold plasma can be computed while taking $\epsilon_1 = 1$ and $\epsilon_2 = 0$ With this we may conclude that the existing model with out cold plasma's effects can be reduced from this model. This analysis has been carried out in Chapter (3).

Further, we have studied the effect of cold plasma permittivity by an impedance loaded parallel-plate waveguide. From the computed results it has been observed that diffracted field is mostly affected by varying the plate separations, whereas the variation of impedances η_2 and η_3 have negligibly small effects on the obtained diffracted field. These results are much consistent with that of already existing results in literature, for example [12]. Moreover the diffracted field amplitude decreases with increasing the permittivity values ϵ_1 and ϵ_2. Again the diffracted field is generally affected due to permittivity value ϵ_1 than that of ϵ_2. In this case the truncated parameter takes higher value in order to get appropriate results. These observations are related to Chapter (4) of this dissertation.

The effect of cold plasma permittivity on the radiation of the dominant TEM-wave by an impedance loaded parallel plate has been examined in Chapter (5). For the reason, the waveguide radiator with impedance loaded parallel-plate is considered. The Wiener-Hopf technique enables to obtain the radiated field while computing the unknown complex coefficients with the help of Mode-Matching technique. It has been concluded that the radiated field amplitude had impres-

sive variation against all physical parameters such as plate separation b, surface impedances η_1, η_2, η_3 and η_4 and permittivity values ϵ_1 and ϵ_2 for both reactive and capacitive cases. Moreover the radiated field amplitude for both cases (Reactive and Capacitive) decreases with the increasing of permittivity values ϵ_1 and ϵ_2. Likewise diffracted field, the radiated field has largely been affected due to permittivity value ϵ_1 instead of ϵ_2. Further the amplitude of radiated field is effected drastically in the presence of an ionosphere plasma medium. This observation can be depicted while ignoring the effect of cold plasma in the expression obtained for radiated field. It has also been observed throughout that the radiated field showed impedance dependant variations. These variations are actually related to the magnetic and electric susceptibilities of the waveguide surfaces. We conclude that these results can be used to improve the radiated signal quality transmitted by an artificial satellite in the ionosphere.

Finally, we have examined diffracted and transmitted fields due to an impedance loaded waveguide located in cold plasma. The ultimate objective was to study the effect of cold plasma permittivity on the diffracted and transmitted fields. Again hybrid methods such as Wiener-Hopf technique and Mode-Matching technique were opted to get the desired expressions of diffracted and transmitted fields. It is worthwhile to comment that up to 100 number of truncation terms are needed to achieve the better accuracy of the obtained solution. By this we can say that whilst computing diffracted and transmitted field one requires higher number of truncated terms as compared to problem of diffraction and radiation. The diffracted and transmitted fields have similar behavior (inverse proportionality) for both impedance parameters η_1 and η_2. A similar proportionality is observed when diffracted and transmitted fields were observed with respect to both permittivity values ϵ_1 and ϵ_2.

In addition, while solving field problems, there are mainly three types of techniques: experimental, analytical, and numerical. Experiments are expensive,

time consuming, and usually do not allow much flexibility in parameter variation. However analytical and numerical methods are much flexible. Numerical methods have become popular with the development of the computing capabilities, and although they give approximate solutions, have sufficient accuracy for engineering purposes. But as a particular choice in this thesis we have preferred analytical methods over numerical methods. As an argument we seek that the implication of numerical techniques restrict such models up to low frequency regime whereas the analytical/hybrid methods used here in do not have limitations for a specific range of frequency problems. So we have a preference to use hybrid methods which operate well for both low frequency problems as well as high frequency problems.

7.1 FUTURE DIRECTIONS AND OPEN QUESTIONS

The analysis to the proposed problems related to the effect of cold plasma and wave scattering requires further attention for more realistic models, for example, by taking into account non-linear higher order boundaries, modeling different physical edge conditions and computing related power expressions. Moreover, in view of their application for acoustic scattering, underwater acoustics, structural acoustics, electromagnetic wave scattering, the low-frequency approximations need due attention. The problems of coupled wave scattering with cold plasma effects finds many applications in a broad area of physics and engineering. For the problems involving planar boundaries such as soft, rigid or impedance, their solution can be obtained via standard Wiener-Hopf technique In such cases the obtained eigenfunctions in terms of either reflected, transmitted or radiated fields satisfy the usual orthogonal properties and required no more complications. Also these eigenfunctions are linearly independent. It would be of interest to consider more complicated boundary conditions on the faces of waveguide. Therefore for non-planar boundaries (flexible), the eigenfunctions

will no more be orthogonal as well as linearly independent. All such problems will lead to in some form of infinite sum. Obviously calculating an infinite sum is impractical (but still possible) but mathematical solutions will require higher order of accuracy. The demonstration of such an application of plasma physics and wave scattering will determine that how a particular class of model problems may be solved. The Wiener-Hopf technique will no longer exist to yield solution of these problems. Of course, for such type of problems, one have to develop appropriate orthogonality relations instead of usual ones. After that the matched eigenfunctions expansion may lead to the solution of problem. The eigenfunctions expansion with dependant sums will require the use of some extra conditions. Therefore some extra conditions in terms of edge conditions will be necessary to use. Otherwise the uniqueness and the convergence of the modeled problems will be questionable. The overall process will be the blend of analytic as well as numerical approaches. Further, while obtaining expressions for the power transferred through the boundaries as well as fluid would be an interesting and realistic choice. The present model could be extended to aforementioned studies with the help of some related investigations, refer for instance to [92, 93, 94, 95, 96].

BIBLIOGRAPHY

[1] S. L. Dvorak, R. W. Ziolkowski and D. G. Dudley, "Ultra-wide-band electromagnetic pulse propagation in a homogeneous cold plasma", *Radio Science*. 32: pp. 239–250 (1997). [cited at p. 1, 7]

[2] A. D. Avdeev, "On the special function of the problem of diffraction by a wedge in an anisotropic plasma", *Radio Tekhnika 1 Elektronika*. 39: pp. 885–892 (1994). [cited at p. 1]

[3] M. K. Tippet and R. W. Ziolkowski, "A bidirectional wave transformation of the cold plasma equations", *Journal of Mathematical Physics.* 32: pp. 488–492 (1991). [cited at p. 1]

[4] H. Rishbeth and M. Mendillo, "Patterns of f2-layer variability", *J. Math. Phys*. 32: pp. 488–492 (1991). [cited at p. 1]

[5] A. Nina, V. Cadez, V. Streckovic and D. Sulic, *Sect. b, beam interact. mater. Atoms. Nucl. Instrum. Methods Phys.* 279: pp. 110–113 (2012). [cited at p. 2]

[6] M. Grabner and V. Kvicera, "Refractive index measurements in the lowest troposphere in the czech republic", *J. Atoms. Solar-Terr. Phys.* 68: pp. 1334–1339 (2006). [cited at p. 2, 7]

[7] H. Rishbeth, "the ionospheric e layer and f layer dynamos", *J. Atoms. Solar-Terr. Phys.* 59: pp. 1873–1880 (1997). [cited at p. 2]

[8] B. Noble, *Methods based on the Wiener–Hopf technique*, Pergamon Press, London (1958). [cited at p. 3, 11, 29]

[9] R. Mittra and S. W. Lee, *Analytical Techniques in the theory of guided waves*, The macmillan Co, Newyork (1971). [cited at p. 3]

[10] I. Sahin, A. H. Serbest and M. A. Lyalinov, "Diffraction of plane waves by an impedance half-plane in cold plasma", *IEEE.* 38: pp. 569–572 (1998). [cited at p. 3, 7]

[11] H. Yener and A. H. Serbest, "Diffraction of plane waves by an impedance half-plane in cold plasma", *J. of Electromagn. Waves and Appl.* 16: pp.995–1005 (2002). [cited at p. 3, 37]

[12] G. Cinar and A. Büyükaksoy, "A hybrid method for the solution of plane wave diffraction by an impedance loaded parallel-plate waveguide", *PIER.* 60: pp. 293–310 (2006). [cited at p. 3, 7, 53, 66, 105, 116]

[13] Y. Y. Lau and R. J. Briggs, "Effects of cold plama on the negative mass instability of a relativistic electron layer", *Physics of Fluids.* 14(5) pp. 967–976 (1971). [cited at p. 4]

[14] S. J. Buchsbaum, L. Mower and S. C. Brown, "Interaction between cold plasmas and guidede electromagnetic waves", *Physics of Fluids.* 3(5): pp. 806–819 (1960). [cited at p. 4]

[15] L. Bardos and H. Barankova, "Radio frequency hollow cathode source for large area cold atmospheric plama applications", *Surface and Coatings Technology.* 133-134: pp. 523–527 (2000). [cited at p. 4]

[16] J. Galejs, "Impedance of a finite insulated cylindrical antenna in a cold plasma with a longitudinal magnetic field", *IEEE Traksactions on Antenna and Propagation.* ap-14(6): pp. 727–736 (1966). [cited at p. 4]

[17] A. V. Tyukhtin, "Diffraction of electromagnetic waves by a half-plane located in a moving cold plasma", *Radiophysics and Quantum Electronics.* 41(4): pp.314–328 (1998) [cited at p. 4]

[18] T. Ikiz and F. Karaomerlioglu, "Diffraction of plane waves by a two-impedance wedge in cold plasma", *J. Electromagn Waves and appl.* 18: pp. 1361–1372 (2004) [cited at p. 4]

[19] H. Ammari and H. Kang, F. Santosa, "Scattering of electromagnatic waves by thin dielectric struc- tures", *SAIM Journal on Mathematical Analysis.* 38: pp. 1329-1342 (2006). [cited at p. 4]

[20] H. Ammari and A. Khelifi, "Electromagnetic scattering by small dielectric inhomogeneties", *J. Math. Pures Appl.* 82: pp. 749–842 (2003). [cited at p. 4]

[21] H. Ammari and C. Latiri-Grous, "Electromagnetic scattering on an absorbing plane", *Integr. Equ. Oper. Theory.* 39: pp. 159-181 (2001). [cited at p. 4]

[22] H. Poincare, "Sur la polarization per diffraction", *Acta Math.* 16: pp. 297-339 (1892). [cited at p. 4]

[23] A. Sommerfeld, "Mathematische theorie der diffraction", *Math. Ann*. 47: pp.317–374 (1896). [cited at p. 4, 5]

[24] H. S. Carslaw, "Diffraction of waves by a wedge of any angle", *Proc. Lond. Math. Soc.*18:(2),291 (1919). [cited at p. 4]

[25] H. Levine and Schwinger, "On the theory of diffraction by an aperture in an infinite plane screen.I." *J. Phys. Rev.*, 74: 958 (1948). [cited at p. 4]

[26] H. Levine and Schwinger, "On the theory of diffraction by an aperture in an infinite plane screen.II." *J. Phys. Rev.*, 75: 1423 (1949). [cited at p. 4]

[27] E. T. Copson, "Diffraction by a plane screen", *Quart. J.Math.* 17: pp. 277-289 (1946). [cited at p. 5]

[28] A. D. Rawlins and W. E. Williams *Q. J. Mech. Appl. Math.* 34(1)(1981). [cited at p. 5]

[29] W. E. Williams, Proc. Camb. Phil.Soc. 55,195 (1959). [cited at p. 5]

[30] V. G. Daniele, "On the solution of two coupled wierner hopf equation", *SIAM J. Appl. Math.* 44: (1984). [cited at p. 5]

[31] A. D. Rawlins, "A note on Wiener-Hopf matrix factorization" *Q. J. Mech. Appl Math.* 38,433 (1985). [cited at p. 5]

[32] C. P. Bates and R. Mittra, "A factorization procedure for Wiener-Hopf kernels", *IEEE Trans on Antennas Propagat.* 26: pp. 614–616 (1978). [cited at p. 5]

[33] R. Nawaz, M. Afzal and M. Ayub, "Acoustic propagation in two-dimensional waveguide for membrane bounded ducts", *Communication in Non-Linear Science and Numerical Simulation.* 20(2): pp. 421-433 (2015). [cited at p. 5]

[34] M. Ayub, R. Nawaz and A. Naeem, "Line source diffraction by a slit in a moving fluid", *Canadian Journal of Physics.* 87(11): pp. 1139–1149 (2009). [cited at p. 5]

[35] M. Ayub, R. Nawaz and A. Naeem, "Diffraction of an impulsive line source with wake", *Physica Scripta*. 82: 045402(10PP) (2010). [cited at p. 5]

[36] P. R. Brazier-Smith, "The acoustic properties of two co-planar half-plane plates", *Proc. R. Soc. A.* 409: pp. 115–139 (1987). [cited at p. 5]

[37] A. N. Norris and G. R. Wickham, "Acoustic diffraction from the junction of two flat plates", *Proc. R. Soc. A.* 451: pp. 631–655 (1995). [cited at p. 5]

[38] P. A. Cannell, "Edge scattering of aerodynamic sound by a lightly loaded elastic half-plane", *Proc. R. Soc. Lond.* A-347: pp. 213–238 (1975). [cited at p. 5]

[39] D. P. Warren, J. B, Lawrie and I. M. Mohamed, "Acoustic scattering in waveguides with discontinuities in height and material property", *Wave Motion.* 36: pp. 119–142 (2002). [cited at p. 5]

[40] A. Büyükaksoy and F. Birbir, "Plane wave diffraction by a reactive step", *Int. J. Engng Sci.*, 35: pp. 311–319 (1997). [cited at p. 5]

[41] A. Büyükaksoy anf F. Birbir, "Analysis of an impedance loaded parallel-plate waveguide radiator", *Journal of Electromagnetic Waves and Applications.* 12: pp. 1509–1526 (1998). [cited at p. 5, 6, 71]

[42] E. Topsakal, A. Büyükaksoy and M. Idemen, "Scattering of electromagnatic waves by a rectangular impedance cylinder", *Wave Motion.* 31: pp. 273–296 (2000). [cited at p. 5]

[43] G. Cinar and A. Büyükaksoy, "Diffraction by a thick impedance half plane with a different end faces impedance", *Electromagetics.* 22: pp. 565–580 (2002). [cited at p. 5]

[44] P. Mclver and A. D. Rawlins, "Diffraction by a rigid barrier with a soft or perfectly absorbent end face", *Wave Motion.* 22: pp. 387–402 (1995). [cited at p. 5]

[45] S. W. Rienstra, "Acoustic radiation from semi-infinite annular in a uniform subsonis mean flow", *Journal of Sound and Vibration.* 92(2): pp. 267–288 (1984). [cited at p. 5]

[46] M. Hassan and A. D. Rawlins, "Sound radiation in a planar trifurcated lined duct", *Wave Motion.* 29: pp. 157–74 (1999). [cited at p. 5]

[47] M. Ayub, A. Naeem and R. Nawaz, "Sound due to an impulsive line source", *Computer and Mathematics with Applications.* 60(12): pp. 3123–3129 (2010). [cited at p. 6]

[48] M. Ayub, M. Ramzan and A. B. Mann, "Line source and point source diffraction by a reactive step", *Journal of Modern Optics.*, 56(7): pp. 893-902 (2009). [cited at p. 6]

[49] M. Ayub, M. H. Tiwana and A. B. Mann, "Wiener-Hopf analysis of an acoustic plane wave in a trifurcated waveguide", *Archive of Applied Mechanics.* 81: pp. 701–713 (2011). [cited at p. 6]

[50] M. Ayub, M. Ramzan and A. B. Mann, "Magnetic line source diffraction by an impedance step", *IEEE trans. on Antennas Propagat.* 57(4): pp. 1289–1293 (2009). [cited at p. 6]

[51] R. Nawaz, A. Wahab and A. Rasheed, "An intermediate range solution to a diffraction problem with impedance conditions", Journal of Modern Optics 61 (16), pp. 1324–1332 (2014). [cited at p. 6]

[52] R. Nawaz, "A note on acoustic diffraction by an absorbing finite strip". *Indian J. of Pure and Appl. Math.* 43(6): pp. 571-589 (2012). [cited at p. 6]

[53] R. Nawaz, A. Naeem, M. Ayub and A. Javaid, "Point source diffraction by a slit in a moving fluid", *Waves in Random and Complex Media*. 24(4): pp. 357-375 (2014). [cited at p. 6]

[54] R. Nawaz and M. Ayub, "An exact and asymptotic analysis of a diffraction problem", *Meccanica*. 48: pp. 653-662 (2012). [cited at p. 6]

[55] J. B. Lawrie and I. D. Abrahams, "A brief historical perspective of the Wiener-Hopf technique", *J*. Eng. Math. 59: pp. 351–358 (2007). [cited at p. 6]

[56] T. Ikiz, S. Koshikawa, K. Kobashi, E. I. Veliev and A. H. Serbest, "Solution of plane wave diffraction by an impedance strip using a Numerical-analytical Method: E-Polarized Case", *J*. Electromagn. Waves and Appl. 15(3): pp.315–340 (2001). [cited at p. 6]

[57] A. Büyükaksoy and B. Polot, "A bifurcated waveguide problem", *ARI.* 51: pp.196–102 (1999). [cited at p. 6, 11]

[58] A. Rawlins, "A bifurcated circular waveguide problem", *IMA J.Appl. Math.* 54: pp.59–81 (1995). [cited at p. 6]

[59] J. R. Pace and R. Mittra, "The trifurcated waveguide", *R*adio Science. 1: pp.117–122 (1965). [cited at p. 6]

[60] D. S. Jones, "Diffraction by three semi-infinite planes", *P*roc. R. Soc. London. 404: pp.299–321 (1986). [cited at p. 6, 7]

[61] S. Asghar, M. Ayub and B. Ahmad, "Point source diffraction by three half planes in a moving fluid", *W*ave Motion. 15: pp.201–220 (1992). [cited at p. 7]

[62] A. D. Rawlin, "Two waveguide trifurcation problem", *Math. Proc. Camb. Phil. Soc.* 121: pp.555–573 (1997). [cited at p. 7]

[63] M. Hassan and A. D. Rawlin, "Two problem of waveguide carrying mean fluid flow", *J. Sound and Vib.* 216(4): pp. 713–738 (1998). [cited at p. 7]

[64] A. D. Rawlin and M. Hassan, "Wave propagation in a waveguide", *ZAMM Z. Angrew. Math. Mech.*, 83(5): pp. 333–343 (2003). [cited at p. 7]

[65] P. M. Morse and H. Feshbach, *Methods of theoretical physics* Mc Graw-Hill, New York, 1953. [cited at p. 7]

[66] E. L. Johansen, "Scattering coefficient for wall impedances change in waveguides", *IRE Transaction on Microwave Theory and Techniques.* pp.26–29 (1967). [cited at p. 7]

[67] A. Büyükaksoy, E. Topsakal and M. Idemen, "Plane wave diffractionby a pair of parallel soft and hord overlapping half-planes", *W*ave Motion. 20(3): pp.273–282 (1994). [cited at p. 7]

[68] M. Idemen, "A new method to obtain exact solutions of vector Wiener-Hopf equations", *Z*AMM Z. Angew. Math. Mech. 59: pp.656–658 (1979). [cited at p. 7]

[69] I. D. Abrahams, "Scattering of sound wavesby two pallalel semi-infinite screens", *W*ave Motion. 9: pp.289–300 (1987). [cited at p. 7]

[70] A. Büyükaksoy and G. Cinar, "Solution of matrix Wiener-Hopf equation conected with a plane wave diffraction by an impedance loaded parallel-plate waveguide", *M*ath. Mech. Appl. Sci. 28(14): pp.1633–1645 (2005). [cited at p. 7, 53, 63]

[71] A. Büyükaksoy and A. Demer, "Radiation of sound from a semi-infinite duct inserted axially into a larger tube with wall impedance discontinuity", *ZAMM M. Angew. Math. Mech.* 86(7): pp.563–571 (2006). [cited at p. 7]

[72] A. Büyükaksoy, I. H. Tayyar ang G. Uzgoren, "Influance of ajunction of perfectly conducting and impedance parallel plate semi-infinite waveguides to the domi-

nent mode propagation", *First european conference on antennas and propagation, Eu CAP Nice France (2006).* [cited at p. 7]

[73] I. H. Tayyar, A. Büyükaksoy and A. Isikyer, "Wiener-Hopf analysis of the parallel-plate waveguide with opposing rectangular dielectric-filled grooves", Can. J. Physics. 869: pp.733–745 (2008). [cited at p. 7]

[74] E. C. Titchmarch, *Theory of Fourier Integral*, Oxford University Press, 1937. [cited at p. 11]

[75] G. D. Maliuzhinets, "Excitation, reflection and emission of surface waves from a wedge with given face impedances", *Sov. Phy. Dokl.* 3: pp.752–755 (1958). [cited at p. 11]

[76] O. M. Bucci, "On a function occuring in the theory of scattering from an impedance half plane", *Report, Institute, Universitario Navale, Napoli, Italy*, (1974). [cited at p. 11]

[77] G. D. Maliuzhinets, "Das sommerfelds integral and die losung von beugungsaufgaben in winkelgebieten", *Ann. Phy.* 6: pp.107–112 (1960). [cited at p. 11]

[78] G. D. Maliuzhinets, "Inversion formula for the summerfeld integral", *Sov. Phy. Dokl.* 3: pp.52–56 (1958). [cited at p. 11]

[79] J. Lin Hu, S. Lin and W. Wang, "Calculation of Maliuzhinetz function in complex region", *IEEE trans. on Antennas Propagat.* 44(8): pp.1195–1196 (1996). [cited at p. 11]

[80] A. Osipov and V. Stein, "The theory and numerical computation of maliuzhinetz'special function", *DLR Institute of Radio Frequency Technology 1999*. [cited at p. 11]

[81] L. B. Felson and N. Marcuvitz, *Radiation and Scattering of Waves*, Prentice Hall, Englewood Cliffs, 1973. [cited at p. 11, 21]

[82] J. L. Volakis and T. B. A. Senior, "Simple expressions for a function occuring in diffraction theory", *IEEE trans. on Antennas Propagat.* 33: pp. 678–680 (1985). [cited at p. 20, 29]

[83] A. D. Rawlins "The solution of a mixed boundary problem in the theory of diffraction by a semi-infinite plane" *R Soc Lond A*: pp. 469–484 (1975). [cited at p. 24]

[84] E. L. Johansen, "Surface wave scattering by a step", *IEEE Transactions on Antennas and Propagation.* AP-15: pp. 442–448 (1967). [cited at p. 37]

[85] A. Büyükaksoy and G. Cinar, "Plane wave diffraction by a reactive step", *Int. J. Engg Sci.* 35(4): pp. 311–319 (1997). [cited at p. 37, 89]

[86] B. Rulf and R. A. Hurd, "Radiation from an open waveguide with reactive walls", *IEEE Trans. Antennas and Propagat.* AP-26(5): (1978). [cited at p. 71]

[87] R. Nawaz and J. B. Lawree, "Scattering of a fluid-structure coupled wave at a flanged junction between two flexible waveguides", *Journal of Acoustic Society of America* 134(3): pp. 1939–1949 (2013). [cited at p. 80]

[88] M. Afzal, R. Nawaz, M.Ayub and A. Wahab, "Acoustic scattering in a flexiable wave guide involving in step discontinity", *PLoS ONE* 9(8):e103807 (2014). [cited at p. 80]

[89] L. A. Weinsrein, "Rigorous solution of the problem of an open-ended parallel-plate waveguide", *Izv. Akad. Nauk., Ser. Fiz.* 12: pp. 144–165 (1948). [cited at p. 89]

[90] L. A. Weinsrein, "On the theory of diffraction by two parallel half-planes", *Izv. Akad. Nauk., Ser. Fiz.* 12: pp. 166–180 (1948). [cited at p. 89]

[91] J. Boersma, "Diffraction by two parallel half-planes", *Q. J. Mech. Math.* 28: pp. 405-425 (1975). [cited at p. 89]

[92] J. B. Lawrie and Idil M. M. Guled, "On tuning a reactive silencer by varying the position of an internal membrane", *J. Acoust. Soc. Am*, 120(2): (2006). [cited at p. 119]

[93] J. B. Lawrie and R. Kirby, "Mode matching without root finding: Application to a dissipative silencer", *J. Acoust. Soc. Am*, 119: pp. 2050–2061 (2006). [cited at p. 119]

[94] Y. D. Kaplunov, I. V. Kirillova and Y. A. Postnova, "Dispersion of waves in a plane acoustic layer with fexible elastic walls", *Acoustical Physics*, 50: pp. 694–698 (2004). [cited at p. 119]

[95] J. B. Lawrie, "On eigenfunction expansions associated with wave propagation along ducts with wave-bearing boundaries", *IMA Jl Appl Math*, 72: pp. 376–394 (2002). [cited at p. 119]

[96] R. Alonso, L. Borcea and J. Garnier, "Wave propagation in waveguides with rough boundaries", *Communications in Mathematical Sciences*. 11: pp. 233–267 (2012). [cited at p. 119]

PhD

by Tufail Ahmad Khan

ABSTRACT

A number of diffraction problems having a practical application in science and engineering can be solved through Wiener-Hopf and Mode Matching techniques. Whilst using these techniques, this dissertation addresses a class of boundary-value problems related to the effect of cold plasma and wave scattering. These problems find applications in a broad area of physics and engineering. The envisaged mathematical model is governed by the Helmholtz equation in cold plasma along with soft, hard and impedance boundary conditions. The diffracted, scattered, transmitted and radiated fields are obtained for waveguide structures located in cold plasma. The numerical analysis is made in its factual perspective by using different material properties of the waveguide. It is revealed that the amplitude of obtained field is affected drastically in the presence of an ionosphere plasma medium. Likewise it is observed that the field showed impedance dependent variations that are actually related to the magnetic and electric susceptibilities of the waveguide surfaces. We conclude that such types of results can be used to improve the radiated signal quality transmitted by an artificial satellite in the ionosphere.

Contents

Abstract i

Contents ii

List of Figures v

1 Introduction 1

1.1 Motivation 1

1.2 State of the art 3

1.3 Avant garde 7

1.4 Dissertation catalog 9

2 Preliminaries 11

2.1 Analytical properties of the Fourier transform 11

2.2 Wiener-Hopf technique 14

2.2.1 General scheme of Wiener-Hopf technique 15

2.3 Additive decomposition theorem 17

2.4 Multiplicative decomposition theorem 18

2.5 Maliuzhinetz's function 19

2.6 Helmholtz equation in cold plasma 20

2.7 Canonical problem in cold plasma 22
2.7.1 Mathematical model of the problem 22
2.7.2 Formulation of Wiener-Hopf equation 24
2.7.3 Solution of Wiener-Hopf equation 29
2.7.4 The diffracted field 32
2.7.5 Computational results and discussion 32

3 EFFECT OF COLD PLASMA PERMITTIVITY ON SCATTERING OF E-POLARIZED PLANE WAVE BY AN IMPEDANCE LOADED STEP 37
3.1 Mathematical model of the problem in cold plasma 38
3.2 Formulation of Wiener-Hopf equation 39
3.3 Solution of Wiener-Hopf equation 44
3.4 The diffracted field 47
3.5 Computational results and discussion 48

4 E-POLARIZED PLANE WAVE DIFFRACTION BY AN IMPEDANCE LOADED PARALLEL-PLATE WAVEGUIDE LOCATED IN COLD PLASMA 53
4.1 Mathematical model of the problem in cold plasma 54
4.2 Formulation of Wiener-Hopf equation 56
4.3 Solution of Wiener-Hopf equation 61
4.4 Determination of the unknown coefficients 63
4.5 The diffracted field 64
4.6 Computational results and discussion 66

5 EFFECT OF COLD PLASMA PERMITTIVITY ON THE RADIATION OF THE DOMINANT TEM-WAVE BY AN IMPEDANCE LOADED PARALLEL-PLATE WAVEGUIDE RADIATOR 71
5.1 Mathematical model of the problem 72
5.2 Formulation of Wiener-Hopf equation 73
5.3 Solution of Wiener-Hopf equation 78

5.4 Determination of the unknown coefficients 80
5.5 Radiated field 82
5.6 Computational results and discussion 82

6 DIFFRACTED AND TRANSMITTED FIELDS BY AN IMPEDANCE LOADED WAVEGUIDE LOCATED IN COLD PLASMA 89

6.1 Mathematical model of the problem in cold plasma 90
6.2 Formulation of Wiener-Hopf equation 92
6.3 Solution of Wiener-Hopf equation 102
6.4 Determination of the unknown coefficients 105
6.5 The diffracted and transmitted fields 107
6.6 Computational results and discussion 109

7 CONCLUSION AND PERSPECTIVES 115

7.1 Future directions and open questions 118

BIBLIOGRAPHY 121

LIST OF FIGURES

2.1 Strip of analyticity 14

2.2 Contour of integration 17

2.3 The physical configuration of the waveguide structure in cold plasma 23

2.4 The depiction of Branch cuts 25

2.5 Variation in the diffracted field amplitude versus "N" at $k = 5$, $\theta_0 = 90^o$, $\theta = 60^o$, $\eta = 0.3\iota$, $\epsilon_1 = 0.8$, $\epsilon_2 = 0.1$ and $b = 0.2\lambda$. 33

2.6 Variation in the diffracted field amplitude versus "b" at $k = 5$, $\theta_0 = 90^o$, $\eta = 0.7\iota$, $\epsilon_1 = 0.8$ and $\epsilon_2 = 0.1$. 34

2.7 Variation in the diffracted field amplitude versus "θ_0" at $k = 5$, $\eta = 0.7\iota$, $\epsilon_1 = 0.8$, $\epsilon_2 = 0.1$ and $b = 0.2\lambda$. 34

2.8 Variation in the diffracted field amplitude versus "η" at $\theta_0 = 90^0$, $k = 5$, $\epsilon_1 = 0.8$, $\epsilon_2 = 0.1$ and $b = 0.2\lambda$. 35

2.9 Variation in the diffracted field amplitude versus "ϵ_1" at $k = 5$, $\theta_0 = 90^o$, $\eta = 0.7\iota$, $\epsilon_2 = 0.1$ and $b = 0.2\lambda$. 35

2.10 Variation in the diffracted field amplitude versus "ϵ_2" at $k = 5$, $\theta_0 = 90^o$, $\eta = 0.7\iota$, $\epsilon_1 = 0.8$ and $b = 0.2\lambda$. 36

3.1 Geometrical configuration of the waveguide structure in cold plasma 38

3.2 Variation in the diffracted field amplitude versus "N" at $k = 5$, $\theta_0 = 90^o$, $\theta = 60^o$, $\eta_1 = 0.3\iota$, $\eta_2 = 0.5\iota$, $\epsilon_1 = 0.8$, $\epsilon_2 = 0.1$ and $b = 0.2\lambda$. 49

3.3 Variation in the diffracted field amplitude versus "b" at $k = 5$, $\theta_0 = 90^o$, $\eta_1 = 0.7\iota$, $\eta_2 = 0.5\iota$, $\epsilon_1 = 0.8$ and $\epsilon_2 = 0.1$. 49

3.4 Variation in the diffracted field amplitude versus "θ_0" at $k = 5$, $\eta_1 = 0.7\iota$, $\eta_2 = 0.5\iota$, $\epsilon_1 = 0.8$, $\epsilon_2 = 0.1$ and $b = 0.2\lambda$. 50

3.5 Variation in the diffracted field amplitude versus "η_1" at $\theta_0 = 90^0$, $k = 5$, $\eta_2 = 0.5\iota$, $\epsilon_1 = 0.8$, $\epsilon_2 = 0.1$ and $b = 0.2\lambda$. 50

3.6 Variation in the diffracted field amplitude versus "η_2" at $k = 5$, $\theta_0 = 90^0$, $\eta_1 = 0.3\iota$, $\epsilon_1 = 0.8$, $\epsilon_2 = 0.1$ and $b = 0.2\lambda$. 51

3.7 Variation in the diffracted field amplitude versus "ϵ_1" at $k = 5$, $\theta_0 = 90^o$, $\eta_1 = 0.7\iota$, $\eta_2 = 0.5\iota$ $\epsilon_2 = 0.1$ and $b = 0.2\lambda$. 51

3.8 Variation in the diffracted field amplitude versus "ϵ_2" at $k = 5$, $\theta_0 = 90^o$, $\eta_1 = 0.7\iota$, $\eta_2 = 0.5\iota$ $\epsilon_1 = 0.8$ and $b = 0.2\lambda$. 52

4.1 Geometrical configuration of a waveguide structure in cold plasma . 54

4.2 Variation in the diffracted field amplitude versus truncation number "N" at$\theta_0 = 90^o$, $\theta = 45^o$, $k = 5$, $\eta_1 = 0.3\iota$, $\eta_2 = 0.9\iota$, $\eta_3 = 0.6\iota$, $\eta_4 = 0.4\iota$, $\epsilon_1 = 0.8$, $\epsilon_2 = 0.0$ and $b = 0.2\lambda$. 67

4.3 Variation in the diffracted field amplitude versus "b" at $\theta_0 = 90^o$, $k = 5$, $\eta_1 = 0.6\iota$, $\eta_2 = 0.4\iota$, $\eta_3 = 0.7\iota$, $\eta_4 = 0.5\iota$, $\epsilon_1 = 0.8$ and $\epsilon_2 = 0$. 67

4.4 Variation in the diffracted field amplitude versus "η_1" at $\phi_0 = 90^o$, $k = 5$, $\eta_2 = 0.4t\iota$, $\eta_3 = 0.7\iota$, $\eta_4 = 0.5\iota$, $t\epsilon_1 = 0.8$, $\epsilon_2 = 0$ and $b = 0.2\lambda$. 68

4.5 Variation in the diffracted field amplitude versus "η_2" at $\theta_0 = 90^o$, $k = 5$, $\eta_1 = 0.4\iota$, $\eta_3 = 0.7\iota$, $\eta_4 = 0.5\iota$, $\epsilon_1 = 0.8$, $\epsilon_2 = 0$ and $b = 0.2\lambda$. 68

4.6 Variation in the diffracted field amplitude versus "η_3" at $\theta_0 = 90^o$, $k = 5$, $\eta_1 = 0.4\iota$, $\eta_2 = 0.3\iota$, $\eta_4 = 0.5\iota$, $\epsilon_1 = 0.8$, $\epsilon_2 = 0$ and $b = 0.2\lambda$. 69

4.7 Variation in the diffracted field amplitude versus "η_4" at $\theta_0 = 90^o$,$k = 5$, $\eta_1 = 0.4\iota$, $\eta_2 = 0.3\iota$, $\eta_3 = 0.5\iota$, $\epsilon_1 = 0.8$, $\epsilon_2 = 0$ and $b = 0.2\lambda$. 69

4.8 Variation in the diffracted field amplitude versus "ϵ_1" at $\theta_0 = 90^o$, $k = 5$, $\eta_1 = 0.4\iota$, $\eta_2 = 0.3\iota$, $\eta_3 = 0.5\iota$, $\eta_4 = 0.7$, $\epsilon_2 = 0$ and $b = 0.2\lambda$. 70

4.9 Variation in the diffracted field amplitude versus "ϵ_2" at $\theta_0 = 90^o$, $k = 5$, $\eta_1 = 0.4\iota$, $\eta_2 = 0.3\iota$, $\eta_3 = 0.5\iota$, $\eta_4 = 0.7$, $\epsilon_1 = 0.9$ and $b = 0.2\lambda$. 70

5.1 Geometry of the impedance loaded parallel-plate waveguide radiator located in cold plasma 72

5.2 Variation in the radiated field amplitude versus truncation number "N". The other parameters are $\theta = 45^o$ $\eta_1 = 0.2$, $\eta_2 = 0.5$, $\eta_3 = 0.3$, $\eta_4 = 0.6$, $\epsilon_1 = 0.8$, $\epsilon_2 = 0$, $k = 5$ and $b = 0.2\lambda$. 84

5.3 Variation in the radiated field amplitude versus "b". The other parameters are $k = 5$, $\eta_1 = 0.5$, $\eta_2 = 0.3$, $\eta_3 = 0.6$, $\eta_4 = 0.7$, $\epsilon_1 = 0.8$ and $\epsilon_2 = 0$. . . 85

5.4 Variation in the radiated field amplitude versus "η_1". The other parameters are $k = 5$, $\eta_2 = 0.3$, $\eta_3 = 0.6$, $\eta_4 = 0.5$, $\epsilon_1 = 0.8$, $\epsilon_2 = 0$ and $b = 0.2\lambda$. 85

5.5 Variation in the radiated field amplitude versus "η_2". The other parameters are $k = 5$, $\eta_1 = 0.7$, $\eta_3 = 0.6$, $\eta_4 = 0.4$, $\epsilon_1 = 0.8$, $\epsilon_2 = 0$ and $b = 0.2\lambda$. 86

5.6 Variation in the radiated field amplitude versus "η_3". The other parameters are $k = 5$ $\eta_1 = 0.5$, $\eta_2 = 0.3$, $\eta_4 = 0.4$, $\epsilon_1 = 0.8$, $\epsilon_2 = 0$ and $b = 0.2\lambda$. 86

5.7 Variation in the radiated field amplitude versus "η_4". The other parameters are $k = 5$, $\eta_1 = 0.5$, $\eta_2 = 0.3$, $\eta_3 = 0.6$, $\epsilon_1 = 0.8$, $\epsilon_2 = 0$ and $b = 0.2\lambda$. 87

5.8 Variation in the radiated field amplitude versus "ϵ_1". The other parameters are $k = 5$, $\eta_1 = 0.5$, $\eta_2 = 0.3$, $\eta_3 = 0.6$, $\eta_4 = 0.7$, $\epsilon_2 = 0$ and $b = 0.2\lambda$. 87

5.9 Variation in the radiated field amplitude versus "ϵ_2". The other parameters are $k = 5$, $\eta_1 = 0.5$, $\eta_2 = 0.3$, $\eta_3 = 0.6$, $\eta_4 = 0.7$, $\epsilon_1 = 0.8$ and $b = 0.2\lambda$. 88

6.1 The physical configuration of the waveguide located in cold plasma . 90

6.2 Variation in the diffracted field amplitude versus "N" at $k = 5$, $\theta_0 = 45^o$, $\theta = 90^0$, $\eta_1 = 0.2\iota$, $\epsilon_1 = 0.8$, $\epsilon_2 = 0.1$, $b = 0.2\lambda$. 110

6.3 Variation in the transmitted field amplitude versus "N" at $k = 5$, $\theta_0 = 45^o$, $\theta = 90^0$, $\eta_5 = 0.4\iota$, $\epsilon_1 = 0.5$, $\epsilon_2 = 0.1$, $b = 0.2\lambda$. 110

6.4 Variation in the diffracted field amplitude versus "θ_1" at $\theta_0 = 45^0$, $k = 5$, $\epsilon_1 = 0.8$, $\epsilon_2 = 0.1$ and $b = 0.2\lambda$. 111

6.5 Variation in the diffracted field amplitude versus "ϵ_1" at $k = 5$, $\theta_0 = 45^0$, $\eta_1 = 0.2\iota$, $\epsilon_2 = 0.1$ and $b = 0.2\lambda$. 111

6.6 Variation in the diffracted field amplitude versus "ϵ_2" at $k = 5$, $\theta_0 = 45^0$, $\eta_1 = 0.2\iota$, $\epsilon_1 = 0.8$ and $b = 0.2\lambda$. 112

6.7 Variation in the transmitted field amplitude versus "η_2" at $k = 5$, $\theta_0 = 45^o$, $\epsilon_1 = 0.8$, $\epsilon_2 = 0.1$ and $b = 0.2\lambda$. 112

6.8 Variation in the transmitted field amplitude versus "ϵ_1" at $k = 5$, $\eta_2 = 0.2\iota$, $\epsilon_2 = 0.1$ and $b = 0.2\lambda$. 112

6.9 Variation in the transmitted field amplitude versus "ϵ_2" at $k = 5$, $\eta_2 = 0.2\iota$, $\epsilon_1 = 0.8$ and $b = 0.2\lambda$. 113

CHAPTER 1

INTRODUCTION

1.1 MOTIVATION

The problems involving wave scattering in cold plasma have been of great interest to scientists and engineers. The study of the propagation of electromagnetic (EM) waves through the earth's ionosphere is of deep interest and importance providing with a natural mean of radio communication [1, 2, 3]. Ionosphere consists of ions and electrons formed by solar photo-ionization and soft x-ray radiation [4]. Such ions and electrons, of course, form weak neutral plasma and hence, the physics of ionosphere can be coined in terms of plasma physics. Earth's ionosphere has been divided into four broad regions, namely, D, E, F, and topside regions. For radio communications the region of interest is F-region lying above the height of 150 km. The F-region contains an important reflecting layer for communication signals arriving from an earth station. However, ionosphere consists of electrons, ions and neutrals, of course, it can be modeled as a medium comprising of weak neutral plasma, hence, its physics can be grasped as plasma physics. Since the ionosphere plasma is highly magnetized under earth's magnetic field, therefore, it can be treated as an anisotropic medium. The ultraviolet radiation which impinges on the earth's atmosphere ionizes a fraction of neutral atmosphere, resulting into a mixture of charged (electrons and ions) and neutral particles. Since the collisions at altitudes above 80 km in the earth's atmosphere

are very rare, therefore, under such conditions the recombination rate of charged species is very slow and hence, a permanent ionized medium occurs, which is known as ionosphere.

The transmission, reflection, refraction, and diffraction of EM waves by ionosphere are the processes that can be understood via plasma physics. The ionosphere plasma also retains the equilibrium density of free electrons and ions because of the balance between photo-ionization and various loss mechanisms. However, the density of these electrons varies dramatically with altitude by the effects of sunrise and sunset [5]. Moreover, the ionosphere plasma is magnetized by the earth's magnetic field that forms the plasma to be as an anisotropic medium. The measurements based upon the artificial satellites immerse in the ionosphere plasma may be affected due to the interaction of communicating EM signals that are used for communication between the spacecraft and earth station. It is well known that the communicating signal radiated by the satellite may modify due to its interaction with the ionosphere plasma and due to the nature of body material (electric and magnetic susceptibilities or impedance) of waveguide used to guide the EM signal (radiated from the vehicle) to the earth station [6, 7]. With this the measurements based upon artificial satellite present in ionosphere communicating to an earth station may be affected drastically. The geometry and material used in complex body structure of an artificial satellite can also change the quality of an EM signal. It is understood that electric and magnetic susceptibilities of a material are related to permittivity and permeability parameters. Moreover, the characteristic impedance and speed of EM wave depend on any medium where detailed information of any medium is obtained by its refractive index.

The present work is based upon a theoretical model to investigate the effectiveness of the ionosphere plasma, earth's magnetic field, structure and nature of the body material (electric and magnetic susceptibilities or impedance) of an artifi-

cial satellite on an EM signal transmitting through the ionosphere. It is pertinent to mention that in order to model ionosphere plasma the whole system is supposed to be immersed in a cold plasma. The modeled problem have been combined to have a well known Helmholtz equation which is solved for the specified boundary conditions by employing Wiener-Hopf technique [8, 9]. Here, we have employed the magnetoionic theory that deals with the cold anisotropic plasma which is considered in this model. The temperature and pressure of plasma species (ions and electrons) are usually small and hence, are neglected. Under these circumstances such a plasma is treated as cold plasma. Sahin et al. [10] investigated the diffraction phenomenon in cold plasma. Yener and Serbest [11] also explored the diffraction of plane waves by an impedance loaded half-plane in cold plasma. Cinar and Büyükaksoy [12] studied the diffraction of the plane waves by an impedance loaded parallel-plate waveguide in the absence of cold plasma.

Keeping in view the aforementioned background, this thesis concerns largely with the effect of cold plasma permittivity on the scattering process of waveguide structures. This study is important mainly due to the worthwhile applications of scattering phenomena in structural design antennas and aircrafts.

1.2 STATE OF THE ART

This documents is mainly concerned about the wave scattering processes in the waveguide structure in the presence of cold plasma. Being fourth state of matter and larger part of universe the study of plasma is quite relevant and significant. The plasma contains a certain portion of free electrons whereas the atoms are partly ionized. The presence of negative and positive carriers of charge makes plasma electrically conductive and distinguishes it from gaseous state. The plasma that contains a very small part (approximately one percent) of the ionized particles is termed as cold (non-thermal) plasma. The cold plasma is

generated in a high-voltage electric field and the velocity of electron is strongly dependent to the temperature up to a thousand degrees of Celsius. Whilst their effect on the plasma temperature is low and final plasma temperature is close to the outward temperature. To quantify the results arising due to the effectiveness of ionosphere plasma, earth's magnetic field, structure and nature of body material of the radiator on the EM signal communicating to earth station propagating through ionosphere, a theoretical model has been devised. Lau and Biggs [13] is examined the effects of cold plasma on electron layer immersed in a cold background plasma. The mutual actions between guided electromagnetic waves and cold plasma in the presence of a static magnetic field were studied by Buchsbaum et al. [14]. Bardos and Barankova [15] examined the relation between a new type of radio frequency and cold plasma. Janis [16] developed a variational formulation for the impedances loaded antenna immersed in cold plasma. Tyukhtin [17] studied the diffraction of plane electromagnetic waves by a half-plane immersed in a parallel flow of cold plasma. Ikiz and Karoomerlioglu [18] investigated diffraction phenomenon by considering two impedances wedge in cold plasma.

In continuation to second part of this work, the wave scattering is a physical phenomenon in which waves are constrained to depart from the route in the medium through which they move. Mathematical analysis of scattering was the focus of attention for many researchers and scientists, for example [19, 20, 21]. The study was initiated by Ibn-al-Haitam in 10th century AD who computed the asymptotic field for diffraction of the wedge and arose the wave propagation theory referred as Poincare [22]. Sommerfeld [23] discussed the exact solution of diffraction from a plate by using the physical method of images on Reimann surfaces. Carslaw [24] utilized the parabolic coordinates and the results obtained by him were the same as achieved by Sommerfeld [23]. Levine and Schwinger [25, 26] used the integral equation in problem of diffraction followed by some related

studies containing the Wiener-Hopf type integral equations. Copson [27] studied the diffraction from a plane screen in the form of integral equation whose solution was obtained by Wiener-Hopf technique. Interestingly the obtained solution was consistent with the Summerfeld's problem [23]. It is worthwhile to comment that Copson [27] was the first one who used Wiener-Hopf technique to solve the problem of sound. The key feature of obtaining the solution via Wiener-Hopf technique is the kernel factorization. This factorization splits the function into a sum or product of two functions where one function is regular in the upper half-plane while the other in the lower half-plane. The detailed description regarding the kernel factorization can be found in [28, 29, 30, 31]. Sometime kernel factorization becomes very difficult and in such cases some alternative techniques are opted to get desired results. Bates and Mittra [32] have employed an integral representation for the factorization of a scalar function. Wiener-Hopf is a useful tool to handle two or three dimensional diffraction problems [33, 34, 35].

It is renowned that the problem having a geometry of planer boundaries with a sudden change in material properties of boundaries may lead to the solution by Wiener-Hopf technique [36, 37, 38, 39]. Büyükaksoy and Birbir [40, 41] considered the diffraction of E-polarized plane wave by the reactive step and radiation phenomenon that radiates from an impedance loaded parallel-plate waveguide radiator. Topsakal et.al. [42] used the Wiener-hopf technique to solve the problem of scattering of electromagnetic waves by a rectangular impedance cylinder. Cinar and Büyükoksoy [43] used the Wiener-Hopf technique for the problem of diffraction by a thick impedance half-plane with different end faces impedance. The diffraction by a rigid barrier with a soft or perfectly absorbent end face with Wiener-Hopf technique was studied by Mclver and Rawlins [44]. Rienstra [45] applied the Wiener-Hopf technique for the problem of sound radiation from semi-infinite duct. The solution to the sound radiation problem using Wiener-Hopf technique was due to Hassan and Rawlins [46]. Furthermore, the said

technique was successively used by Ayub et al [47, 48, 49, 50] and Nawaz et al. [51, 52, 53, 54] in their recent studies. A brief historical view of Wiener-Hopf technique was given by Lawrie and Abrahams [55]. As mentioned earlier that Wiener-Hopf technique is not always considered to be the easy task when kernel factor becomes complicated. Therefore, a hybrid method has recently been introduced to solve such complicated problems while bypassing the most difficult process of the matrix Wiener-Hopf factorization. This hybrid method is combination of Wiener-Hopf and Mode-Matching techniques that reduces the boundary-valued problem in terms of a modified Wiener-Hopf equation with second kind. The solution obtained from hybrid method contains an eigenfunction expansion of unknown complex coefficients. The expressions for these unknown coefficients are obtained as a system of infinite linear algebraic equations. Through a numerical procedure, this system can be solved approximately. This method was adopted to solve the E-polarized plane wave diffraction and radiation phenomenon in a waveguide by Büyükaksoy and Birbir [41]. Such methods were initially developed to tackle the problems governed by Helmholtz equation and waveguide boundaries described by Neumann (Rigid), Dirichlet (Soft) or Robin (Mixed) conditions. The solution of these problems contains the eigenfunction expansion. Ikiz et al. [56] used the name numerical-analytical method instead of hybrid method. The main objective of using this method is to modify the analytical methods which works well at high frequencies while numerical method works well at low frequencies.

Also the diffraction phenomenon was studied in a bifurcated waveguide using a dominant mode wave incident on a soft-hard half-plane amidst an infinite parallel-plate with hard boundary by Büyükaksoy and Polot [57]. Transmission and reflection coefficients are acquired in a bifurcated waveguide by Rawlin [58]. Pace and Mithra [59] studied the problem involving a trifurcated parallel-plate waveguide with an arbitrary spacing between the plates. Jones [60] considered

the waves scattering from the waveguide containing three semi-infinite parallel soft and equidistant plates. Asgher et al. [61] extended the Jones' problem [60] for point and line source scattering. Rawlin [62] also studied the radiation of a surface wave mode propagating in a semi-infinite cylindrical waveguide. Hassan and Rawlin [63] solved the problem of sound radiation from a waveguide (Semi-infinite duct) placed symmetrically within an infinite duct. Later on the radiation phenomenon was studied in a trifurcated parallel-plate waveguide by Rawlin and Hassan [64]. Morse and Feshbach [65] considered the problem of scattering in a perfectly conducting and an impedance loaded parallel-plate waveguide having the same impedances on lower and upper faces of the plates. Later on Johansen [66] considered the same geometry for different surface impedances using a coupled system of modified Wiener-Hopf equations. Büyükaksoy et al. [67] and Idemen [68] uncoupled the coupled system of modified Wiener-Hopf equations by using the week factorization method and obtained the exact solutions of the vector Wiener-Hopf equations. Abrahams [69] introduced a "pole removal technique" to uncouple the coupled system of modified Wiener-Hopf equations. This technique can be seen in some classical articles, to mention a few [70, 71, 72, 73].

1.3 AVANT GARDE

The main aspiration of this dissertation is to investigate that how a particular class of structural problems related to wave scattering may be solved while using different semi-analytic techniques. In particular when a cold plasma is immersed in the waveguide structure would be the topic of interest. Broadly speaking the present work can be seen as a continuation of ongoing studies, refer for instance to [1, 6, 10, 12]. The major part of this research is carried out in the following perspective:

(1) The derivation of governing Helmholtz equation in cold plasma from the well-known Maxwell equations.

(2) Inclusion of cold plasma permittivity values ϵ_1 and ϵ_2 in the given model.

(3) The use of Wiener-Hopf technique together with the Mode-Matching technique in order to yield a larger part of solutions to above model.

(4) The mathematical and numerical study related to the effect of cold plasma on scattering of E-polarized plane wave by step discontinuity.

(5) The discussion concerning the effect of cold plasma permittivity due to impedance loaded parallel-plate waveguide located in cold plasma.

(6) The consideration of radiation problem with an impedance loaded parallel-plate waveguide radiator.

(7) The study of problems involving the diffracted and transmitted fields.

(8) The graphical behavior of diffracted, transmitted and radiated field versus different physical parameters of our choice.

(9) In fact the major contribution towards the development of present study is to quantify the effects of ionosphere plasma on the communicating signals between earth station and an artificial satellite in the earth's atmosphere. In the process the standard Wiener-Hopf and somehow Mode-matching techniques are used to find appropriate solutions for such models. In fact the Wiener-Hopf technique with Mode Matching technique is used to show the effect of cold plasma permittivity in different waveguide structures. Briefly saying the Wiener-Hopf analysis and the effect of cold plasma permittivity in a waveguide are the major focus for this thesis.

1.4 DISSERTATION CATALOG

This thesis is summarized in the order below.

CHAPTER (2) begins with the review of generalized form of boundary-valued problems in cold plasma. As mentioned earlier this thesis is concerned mostly with the effect of cold plasma permittivity and scattering of waves in a waveguide structure. For this purpose, it contains some basic definitions and mathematical preliminaries which will be utilized in the succeeding chapters. A canonical problem is modeled in cold plasma and solved while using a modified Wiener-Hopf technique.

CHAPTER (3) consists of impedances loaded step problem in cold plasma. Here, a waveguide is designed in cold plasma containing by a two separated half-planes with different surface impedances and afterwards these half-planes were joined vertically by a hard step. Typically such kind of geometries can be used in constructing antennas. The contents of this chapter has already been submitted to the **Journal of Waves in Random and Complex Media** for possible publication.

In CHAPTER (4), the effect of cold plasma permittivity is analyzed on E-polarized plane wave diffraction by an impedance loaded parallel-plate waveguide in cold plasma. Also the effect of different parameters such as surface impedance and plate separation is observed. The model problem is solved by hybrid method i.e., Mode-Matching technique in conjunction with Fourier transform. These type of geometries in the ionosphere (plasma) are important in communication between the vehicles and the earth station. The contents of this chapter have been published in **Physica Scripta**, 89(8): Paper ID. e095207, (2014).

CHAPTER (5) deals with radiation phenomenon where an impedance loaded parallel-plate waveguide radiator in cold plasma is considered. This geometry is designed by a parallel plane and half-plane having all having different faces different surface impedances located in cold plasma. Here the effect of cold plasma permittivity is investigated on the radiation problem. The contents of

Chapter (5) are published in **Mathematical Methods in the Applied Sciences**, *DOI* : 10.1002/*mma*.3464.

CHAPTER (6) investigates the diffracted and transmitted fields from a waveguide located in cold plasma. The geometry of the problem is designed from the three half-planes where one half-plane is located between the other two in opposite direction. The surface material properties of the half-planes are characterized either by soft (Dirichlet type), hard (Neumann type) or impedances (Robin type). The solution to the underline problem is obtained with the help of hybrid method that reduces the boundary-valued problem to the modified Wiener-Hopf equation. This investigation has already been submitted to **New Journal of Physics** for possible publication.

CHAPTER 2

PRELIMINARIES

This chapter contains some of the mathematical preliminaries and compact reviews of the techniques which will be used in the subsequent chapters. These consist of Fourier transform [74], Wiener-Hopf technique [8, 57], Maliuzhinetz's function [75, 76, 77, 78, 79, 80] and Helmholtz equation in cold plasma [81]. Certainly these preliminaries will help to successful completion of thesis document.

2.1 ANALYTICAL PROPERTIES OF THE FOURIER TRANSFORM

The Fourier transform is a useful technique and plays an important role in solving a partial differential equation. This technique is applicable for the majority of the problem whether their domain is finite or infinite. Consider a function $h(x)$ defined for $x \in (-\infty, \infty)$. Then $h(x)$ can be written in the form as under

$$h(x) = h_+(x) + h_-(x), \tag{2.1}$$

where

$$h_+(x) = \begin{cases} h(x) & x > 0 \\ 0 & x < 0, \end{cases} \tag{2.2}$$

and

$$h_-(x) = \begin{cases} h(x) & x < 0 \\ 0 & x > 0. \end{cases} \tag{2.3}$$

$H(\alpha)$ represents the Fourier transform of $h(x)$ which is defined as under

$$H(\alpha) = \frac{1}{\sqrt{2\pi}} \int_{-\infty}^{\infty} h(x) e^{\iota \alpha x} dx, \tag{2.4}$$

where the integral in the above expression exists and h(x) is bounded for all x in the given domain. Use of equations (2.2) and (2.3) in equation (2.4) gives

$$H(\alpha) = \frac{1}{\sqrt{2\pi}} \int_{-\infty}^{\infty} [h_-(x) + h_+(x)] e^{\iota \alpha x} dx. \tag{2.5}$$

After simplification, equation (2.5) takes the form

$$H(\alpha) = \frac{1}{\sqrt{2\pi}} \int_{-\infty}^{0} h_-(x) e^{\iota \alpha x} dx + \frac{1}{\sqrt{2\pi}} \int_{0}^{\infty} h_+(x) e^{\iota \alpha x} dx, \tag{2.6}$$

that is

$$H(\alpha) = H_-(\alpha) + H_+(\alpha), \tag{2.7}$$

where

$$H_-(\alpha) = \frac{1}{\sqrt{2\pi}} \int_{-\infty}^{0} h_-(x) e^{\iota \alpha x} dx, \tag{2.8}$$

and

$$H_+(\alpha) = \frac{1}{\sqrt{2\pi}} \int_{0}^{\infty} h_+(x) e^{\iota \alpha x} dx. \tag{2.9}$$

The analytic properties of $H(\alpha)$ are the properties of $H_-(\alpha)$ and $H_+(\alpha)$. Initially, consider the properties of $H_+(\alpha)$ as follow:

If the function $h_+(x)$ is of exponential order, i.e.,

$$|h_+(x)| < M e^{\tau - x} \qquad \text{as} \quad x \to \infty, \tag{2.10}$$

then the function $H_+(\alpha)$ is a regular function of the complex variable $\alpha = \sigma + \imath\tau$ and $H_+(\alpha) \to 0$ as $|\alpha| \to \infty$ in the domain $\Im\mathrm{m}(\alpha) > \tau_-$. Perceiving that

$$Me^{\tau_- x} e^{\imath\alpha x} = Me^{(\tau_- - \tau)x} e^{\imath\sigma x} \tag{2.11}$$

is bounded if $\tau > \tau_-$. Now taking the inverse Fourier transform of $H_+(\alpha)$, one obtains

$$h_+(x) = \frac{1}{\sqrt{2\pi}} \int_0^\infty H_+(\alpha) e^{-\imath\alpha x} d\alpha, \tag{2.12}$$

where integration will be taken over any straight line in the region $\Im\mathrm{m}(\alpha) > \tau_-$ and parallel to $x-$axis in the complex $\alpha-$plane.

Now for the problem considered in this thesis, the strip of the analyticity can be calculated by considering the following cases.

(i) For $\tau_- < 0$ the function $h_+(x)$ decreases, the domain of the analyticity of $h_+(x)$ contains the real axis and equation (2.12) will be integrated along the positive real axis.

(ii) For $\tau_- > 0$ the function $h_+(x)$ increases but not faster than the exponential function with linear exponent, the domain of the analyticity of $h_+(x)$ lies above the real axis of the complex $\alpha-$plane and equation (2.12) will be integrated above the positive real axis.

Now consider the function $h_-(x)$ satisfies the exponential order condition, so one can write

$$|h_-(x)| < Me^{\tau_+ x} \qquad \text{as} \quad x \to \infty, \tag{2.13}$$

$$H_-(\alpha) = \int_0^\infty h_-(x) e^{\imath\alpha x} dx \tag{2.14}$$

is regular in the lower half plane $\Im\mathrm{m}(\alpha) < \tau_+$.

Now taking into account the inverse Fourier transform of $H_-(\alpha)$ gives

$$h_-(x) = \frac{1}{\sqrt{2\pi}} \int_0^\infty H_-(\alpha) e^{-\iota\alpha x} d\alpha, \tag{2.15}$$

for $\tau_+ > 0$ the domain of analyticity of $H_-(\alpha)$ contains the negative real axis and for $\tau_+ < 0$, is below the negative real axis. Hence equation (2.15) is analytic in region $\tau_- < \Im\mathfrak{m}(\alpha) < \tau_+$ as shown in Fig. (2.1)

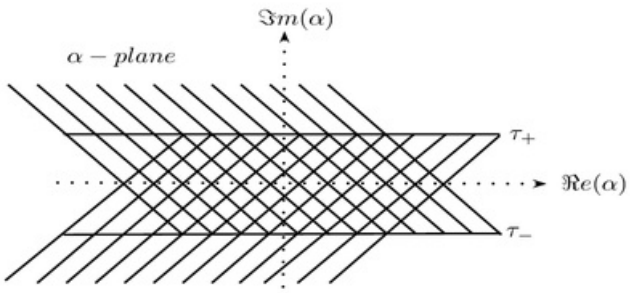

FIGURE 2.1. *Strip of analyticity*

2.2 WIENER-HOPF TECHNIQUE

Wiener-Hopf technique was introduced by N. Wiener and E. Hopf in 1931. Initially, this was used to solve singular integral equation of the form

$$f(x) = \phi(x) + \int_0^\infty K(x-y) f(y) dy, \qquad 0 < x < \infty, \tag{2.16}$$

where $\phi(x)$ and $K(x-y)$ are given known function while $f(y)$ is unknown function to be calculated. This equation had arisen in Hopf's work on Milne-Schwarzschild equation. This technique also reduces the problem of diffraction by a semi-infinite plate to the solution of singular integral equation. All physical phenomena are associated with ordinary or partial differential equations. These

partial differential equations may be solved by using certain method depending upon the geometry of the problem. The method of separation of variables is one of these methods that fails for certain geometries such as semi-infinite regions, waveguide structure with non planer boundaries etc. The detailed description of the technique is mentioned below.

2.2.1 GENERAL SCHEME OF WIENER-HOPF TECHNIQUE

In this technique it is required to determined the unknown function $F_-(\alpha)$ and $F_+(\alpha)$ of a complex variable α occurring in the below Wiener-Hopf equation. These functions are analytic in the half-planes $\Im\mathrm{m}(\alpha) < \tau_+$ and $\Im\mathrm{m}(\alpha) > \tau_-$, respectively, and approach to zero as $|\alpha| \to \infty$, satisfying the functional equation

$$\mathscr{A}(\alpha)F_+(\alpha) + \mathscr{B}(\alpha)F_-(\alpha) + \mathscr{C}(\alpha) = 0, \tag{2.17}$$

in the region $\tau_- < \Im\mathrm{m}(\alpha) < \tau_+$. Here $\mathscr{A}(\alpha)$, $\mathscr{B}(\alpha)$ and $\mathscr{C}(\alpha)$ are the known functions regular in the strip $\tau_- < \Im\mathrm{m}(\alpha) < \tau_+$ and $\mathscr{A}(\alpha)$ and $\mathscr{B}(\alpha)$ are non- zero in the strip. For the solution of the Wiener equation the main step is to replace

$$\frac{\mathscr{A}(\alpha)}{\mathscr{B}(\alpha)} = \frac{P_+(\alpha)}{P_-(\alpha)}, \tag{2.18}$$

where the functions $P_+(\alpha)$ and $P_-(\alpha)$ are non zero and regular, respectively, in the half-planes $\Im\mathrm{m}(\alpha) > \tau_-$ and $\Im\mathrm{m}(\alpha) < \tau_+$. On using equation (2.18) in equation (2.17), one can write

$$P_+(\alpha)F_+(\alpha) + P_-(\alpha)F_-(\alpha) + P_-(\alpha)\frac{\mathscr{C}(\alpha)}{\mathscr{B}(\alpha)} = 0. \tag{2.19}$$

The last term of the equation (2.19) can be decomposed as

$$P_-(\alpha)\frac{\mathscr{C}(\alpha)}{\mathscr{B}(\alpha)} = K_+(\alpha) + K_-(\alpha), \tag{2.20}$$

where the functions $K_+(\alpha)$ and $K_-(\alpha)$ are analytic in the half-planes $\Im\mathfrak{m}(\alpha) > \tau_-$ and $\Im\mathfrak{m}(\alpha) < \tau_-$, respectively. In the strip the following equation holds true

$$P_+(\alpha)F_+(\alpha) + K_+(\alpha) = -P_-(\alpha)F_-(\alpha) - K_-(\alpha) = S(\alpha). \tag{2.21}$$

The above equation is valid in the strip $\tau_- < \Im\mathfrak{m}(\alpha) < \tau_+$. The left-hand side of the equation (2.21) is regular in the half-plane $\Im\mathfrak{m}(\alpha) > \tau_-$ while the right-hand side of the equation (2.21) is regular in the half-plane $\Im\mathfrak{m}(\alpha) < \tau_+$. Hence by the analytic continuation principal one can define $S(\alpha)$ over the complex $\alpha - plane$. Let us suppose that

$$|P_+(\alpha)F_+(\alpha) + K_+(\alpha)| < |\alpha|^p \; as \quad \alpha \to \infty, \; \Im\mathfrak{m}(\alpha) > \tau_- \tag{2.22}$$

and

$$|P_-(\alpha)F_-(\alpha) + K_-(\alpha)| < |\alpha|^q \; as \quad \alpha \to \infty, \; \Im\mathfrak{m}(\alpha) < \tau_+. \tag{2.23}$$

Then on using the extended Liouvillle's theorem which states that "If $S(\alpha)$ is an integral function such that $|S(\alpha)| < M|\alpha|^p$ as $\alpha \to \infty$ where M and p are constant then $S(\alpha)$ is a polynomial of degree less than or equal to $[p]$ where $[p]$ is the integral part of p." Here, $S(\alpha)$ represents a polynomial $P(\alpha)$ whose degree is less than or equal to the integral part of (p, q) i.e.,

$$F_+(\alpha) = \frac{P(\alpha) - K_+(\alpha)}{P_+(\alpha)} \tag{2.24}$$

and

$$F_-(\alpha) = \frac{-P(\alpha) - K_-(\alpha)}{P_-(\alpha)}. \tag{2.25}$$

The above equations determine $F_+(\alpha)$ and $F_-(\alpha)$ in term of $P(\alpha)$. Thus, the representation of equations (2.24) and (2.25) form a base to use the Wiener-Hopf technique. It is important to annotate that factorization of function expressed

in equation (2.18) and decomposition of function expressed in equation (2.20) is possible under certain conditions. The possibility of these representations is guaranteed by the following theorems.

2.3 ADDITIVE DECOMPOSITION THEOREM

Statement:

Let $F(\alpha)$ be a regular function in the region $\tau_- < \Im\mathfrak{m}(\alpha) < \tau_+$ and $F(\alpha) \to 0$ uniformly in the given region as $|\alpha| \to \infty$, then $F(\alpha)$ can be decomposed in the given region as under

$$F(\alpha) = F_-(\alpha) + F_+(\alpha), \tag{2.26}$$

where $F_+(\alpha)$ and $F_-(\alpha)$ are regular functions in the region $\Im\mathfrak{m}(\alpha) > \tau_-$ and $\Im\mathfrak{m}(\alpha) < \tau_+$, respectively.

Proof:

Consider a rectangle $P_1P_2P_3P_4$ bounded by the lines $\Im\mathfrak{m}(\alpha) = \tau'_-$, $\Im\mathfrak{m}(\alpha) = \tau'_+$, $\Re\mathfrak{e}(\alpha) = T$ and $\Re\mathfrak{e}(\alpha) = -T$ containing an arbitrary complex number $\alpha = \sigma + \iota\tau$ and lying in the given strip such that $\tau_- < \tau'_- < \Im\mathfrak{m}(\alpha) < \tau'_- < \tau_-$ as shown in the Fig. (2.2).

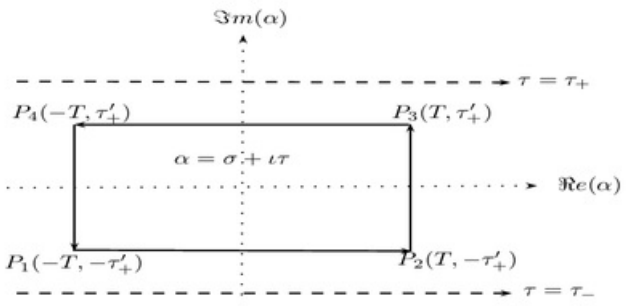

FIGURE 2.2. *Contour of integration*

According to Cauchy's integral formula, one can write

$$F(\alpha) = \frac{1}{2\pi\iota}\int_{-T+\iota\tau'_-}^{T+\iota\tau'_-}\frac{f(\zeta)}{\zeta-\alpha}d\zeta + \frac{1}{2\pi\iota}\int_{T+\iota\tau'_-}^{T+\iota\tau'_+}\frac{f(\zeta)}{\zeta-\alpha}d\zeta + \frac{1}{2\pi\iota}\int_{T+\iota\tau'_+}^{-T+\iota\tau'_+}\frac{f(\zeta)}{\zeta-\alpha}d\zeta + \frac{1}{2\pi\iota}\int_{-T+\iota\tau'_+}^{-T+\iota\tau'_-}\frac{f(\zeta)}{\zeta-\alpha}d\zeta. \tag{2.27}$$

On taking the limit $T \to \infty$, the second and fourth integrals on the right-hand side of equations (2.27) will tend to zero and hence equations (2.27) will take the form

$$F(\alpha) = F_-(\alpha) + F_+(\alpha), \tag{2.28}$$

where

$$F_-(\alpha) = -\frac{1}{2\pi\iota}\int_{-\infty+\iota\tau'_+}^{\infty+\iota\tau'_+}\frac{f(\zeta)}{\zeta-\alpha}d\zeta \tag{2.29}$$

and

$$F_+(\alpha) = \frac{1}{2\pi\iota}\int_{-\infty+\iota\tau'_-}^{\infty+\iota\tau'_-}\frac{f(\zeta)}{\zeta-\alpha}d\zeta. \tag{2.30}$$

$F_+(\alpha)$ and $F_-(\alpha)$ are regular functions in upper $\alpha-plane$ $\Im\mathfrak{m}(\alpha) > \tau_-$ and in lower $\alpha-plane$ $\Im\mathfrak{m}(\alpha) < \tau_+$, respectively. The arbitrary complex number $\alpha = \sigma + \iota\tau$ does not lie on the contour of integration.

2.4 MULTIPLICATIVE DECOMPOSITION THEOREM

Statement:

Let $\Psi(\alpha)$ be a non zero and regular function in the strip $\tau_- < \Im\mathfrak{m}(\alpha) < \tau_+$ and $\Psi(\alpha) \to 0$ uniformly as $|\alpha| \to \infty$ in the strip. Then $\Psi(\alpha)$ can be factorized in the given strip as

$$\Psi(\alpha) = \Psi_-(\alpha)\Psi_+(\alpha), \tag{2.31}$$

where the functions $\Psi_+(\alpha)$ and $\Psi_-(\alpha)$ are non-zero and regular in the half-planes $\Im\mathrm{m}(\alpha) > \tau_-$ and $\Im\mathrm{m}(\alpha) < \tau_+$, respectively.

Proof:

Let

$$F(\alpha) = \log \Psi(\alpha), \tag{2.32}$$

which satisfies all the condition of additive decomposition theorem. Thus, $F(\alpha)$ can be expressed as

$$F(\alpha) = F_-(\alpha) + F_+(\alpha), \tag{2.33}$$

where

$$F_+(\alpha) = \log \Psi_+(\alpha) \tag{2.34}$$

and

$$F_-(\alpha) = \log \Psi_-(\alpha). \tag{2.35}$$

Substituting the equations (2.32), (2.34) and (2.35) in equation (2.33) gives

$$\log \Psi(\alpha) = \log \Psi_+(\alpha) + \log \Psi_-(\alpha). \tag{2.36}$$

After simplification equation (2.36) takes the form

$$\Psi(\alpha) = \Psi_+(\alpha)\Psi_-(\alpha). \tag{2.37}$$

2.5 MALIUZHINETZ'S FUNCTION

Maliuzhinetz function plays a nobel role in the study of diffraction theory by an impedances half planes. The function denoted by $\mathscr{M}_\pi(z)$ and defined as

$$\mathscr{M}_\pi(z) = \exp\left[-\frac{1}{8\pi}\int_0^z \frac{\pi \sin t - 2\sqrt{2}\sin\frac{t}{2} + 2t}{\cos t}\, dt\right], \tag{2.38}$$

known as Maliuzhinetz's function introduced by Maliuzhinetz. Volakis and Senior [82] expressed the Maliuzhinetz's function for small and large complex arguments. For small arguments,

$$\mathscr{M}_\pi(z) = 1 - bz^2 + O(z^4), \tag{2.39}$$

where $b = \frac{1}{16}(1 + \frac{2}{\pi} - \sqrt{2})$. The small complex arguments approximation of Maliuzhinetz's function is, therefore,

$$\mathscr{M}_\pi(z) = 1 - 0.013900388z^2. \tag{2.40}$$

If $\Im\mathrm{m}(z) >> 0$, then

$$\mathscr{M}_\pi(z) = 1.05302\left[\cos\frac{1}{4}(z - \imath\ln 2)\right]^{\frac{1}{2}} \qquad \Im\mathrm{m}(z) > 8. \tag{2.41}$$

Equations (2.40) and (2.41) must be valid within the strip $0 < z < \frac{\pi}{2}$. For the remaining values of $\Re\mathrm{e}(z)$ the $\mathscr{M}_\pi(z)$ relates to its value at the corresponding point within the strip

$$\mathscr{M}_\pi(z) = \left[\mathscr{M}_\pi\left(\frac{\pi}{2}\right)\right]^2 \frac{\cos(\frac{z}{4} - \frac{\pi}{8})}{\mathscr{M}_\pi(z - \pi)}, \tag{2.42}$$

$$\mathscr{M}_\pi(z) = \mathscr{M}_\pi(-z) \tag{2.43}$$

and

$$\bar{\mathscr{M}}_\pi(z) = \mathscr{M}_\pi(\bar{z}), \tag{2.44}$$

where bar complex conjugate. Maliuzhinetz's function is an even regular function of a complex variable z.

2.6 HELMHOLTZ EQUATION IN COLD PLASMA

In order to have a mathematical model for the problems in the subsequent chapters, we first derive the Helmholtz equation in cold plasma. For the reasons Fel-

son and Marcuvits [81] defined the tensor of dielectric permittivity for the cold plasma and expressed the electric field component in term of the magnetic field $H_z(x, y)$ by using the Maxwell's equations along with tensor of dielectric permittivity for the cold plasma as under:

The tensor of dielectric permittivity for the cold plasma is defined as

$$\epsilon = \begin{bmatrix} \epsilon_1 & -\iota\epsilon_2 & 0 \\ \iota\epsilon_2 & \epsilon_1 & 0 \\ 0 & 0 & \epsilon_z \end{bmatrix}, \tag{2.45}$$

with

$$\epsilon_1 = 1 - \left(\frac{\omega_p}{\omega}\right)^2 \left[1 - \left(\frac{\omega_c}{\omega}\right)^2\right]^{-1}, \tag{2.46}$$

$$\epsilon_2 = \left(\frac{\omega_p}{\omega}\right)^2 \left[\frac{\omega}{\omega_c} - \frac{\omega_c}{\omega}\right]^{-1} \tag{2.47}$$

and

$$\epsilon_z = 1 - \left(\frac{\omega_c}{\omega}\right)^2, \tag{2.48}$$

where

$$\omega_p^2 = \frac{N_e e^2}{m\epsilon_0} \tag{2.49}$$

and

$$\omega_c = \frac{|e|\mu_0 H_{dc}}{m}. \tag{2.50}$$

Here, e, N_e, m, ω, ω_c, ω_p and H_{dc} represent the electric charge, electron density, electron mass, operating, cyclotron, plasma frequencies and magnitude of the dc magnetic field vector, respectively.

The electric field component in term of the magnetic field are as follow

$$E_x = \frac{\iota\epsilon_1}{\omega\epsilon_0(\epsilon_1^2 - \epsilon_2^2)} \frac{\partial B_z}{\partial y} + \frac{\epsilon_2}{\omega\epsilon_0(\epsilon_1^2 - \epsilon_2^2)} \frac{\partial B_z}{\partial x}, \tag{2.51}$$

$$E_y = \frac{\epsilon_2}{\omega\epsilon_0(\epsilon_1^2-\epsilon_2^2)}\frac{\partial B_z}{\partial y} + \frac{\iota\epsilon_1}{\omega\epsilon_0(\epsilon_1^2-\epsilon_2^2)}\frac{\partial B_z}{\partial x}. \tag{2.52}$$

It is known that Maxwell's equations are valid in plasma so, one can write

$$\nabla \times \vec{E} = \frac{1}{c^2}\frac{\partial^2}{\partial t^2}\vec{B}, \tag{2.53}$$

where

$$\vec{E} = E_x i + E_y j + E_z k \text{ and } \vec{B} = B_x i + B_y j + B_z k\,. \tag{2.54}$$

Thus, using equations (2.51) and (2.52) in equation (2.53), one obtains the required Helmholtz's equation in cold plasma as follow

$$\frac{\partial^2}{\partial x^2}H_z(x,y) + \frac{\partial^2}{\partial y^2}H_z(x,y) + k_{eff}^2 H_z(x,y) = 0, \tag{2.55}$$

with

$$k_{\text{cff}}^2 = k^2\left(\frac{\epsilon_1^2-\epsilon_2^2}{\epsilon_1}\right), \quad k = \omega\sqrt{\epsilon_0\mu_0} \text{ and } B_z = e^{-\iota\omega t}H_z(x,y). \tag{2.56}$$

where the time dependence is assumed to be $e^{-\iota\omega t}$ and k_{cff} depends on k, ϵ_1 and ϵ_2.

2.7 CANONICAL PROBLEM IN COLD PLASMA

In this section we consider a prototype problem arising in cold plasma that concerned with wave scattering in waveguide designed by three semi-infinite plates. The material properties of these plates are impedance, rigid and soft. The rigid plate is defined in term of Neumann boundary condition whereas the soft plat are defined in term of Dirichlet condition. The Winer-Hopf technique along with Mode-Matching technique is used to obtain the approximate solution.

2.7.1 MATHEMATICAL MODEL OF THE PROBLEM

Here, we consider the scattering of a plane wave which is incident with angle θ_0 in the waveguide region in cold plasma formed by two half-planes S_1 define by

$\{(x,y,z)|\ x\in(-\infty,0),\ y=b,\ z\in(-\infty,\infty)\}$ and S_2 defined by $\{(x,y,z)|\ x\in(0,\infty),\ y=0,\ z\in(-\infty,\infty)\}$. The characteristic properties of the upper face of half-plane S_1 is characterized by surface impedance Z and the upper face of the half-plane S_1 is rigid. These two planes are combined by a soft vertical step of hight b as shown in Fig. (2.3):

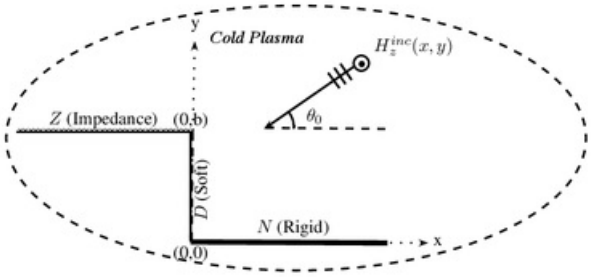

FIGURE 2.3. *The physical configuration of the waveguide structure in cold plasma*

The total field takes the form as under

$$H_z^T(x,y)=\begin{cases} H_z^1(x,y)+H_z^{inc}(x,y)+H_z^{ref}(x,y), & y\in(b,\infty) \\ H_z^2(x,y), & y\in(a,b) \end{cases} \tag{2.57}$$

where $H_z^{inc}(x,y)$ and $H_z^{ref}(x,y)$ stand for incident and reflected field, respectively, given by

$$H_z^{inc}(x,y)=e^{-\imath k_{\text{eff}}(x\cos\theta_0+y\sin\theta_0)} \tag{2.58}$$

and

$$H_z^{ref}(x,y)=-\frac{1-\eta\sin\theta_0}{1+\eta\sin\theta_0}e^{-\imath k_{\text{eff}}(x\cos\theta_0-(y-2b)\sin\theta_0)} \tag{2.59}$$

and $\{H_z^j \quad (j=1,2)\}$ satisfying the Helmholtz equation in cold plasma

$$\left[\frac{\partial^2}{\partial x^2}+\frac{\partial^2}{\partial y^2}+k_{\text{eff}}^2\right]\left[H_z^j(x,y)\right]=0, \tag{2.60}$$

with the following corresponding boundary conditions along with the continuity relations

$$\left(1+\frac{\eta}{\iota k_{\text{eff}}}\right)H_z^1(x,b)=0, \qquad x\in(-\infty,0), \tag{2.61}$$

$$\frac{\partial}{\partial y}H_z^2(x,0)=0, \qquad x\in(0,\infty), \tag{2.62}$$

$$H_z^2(0,y)=0, \qquad y\in(a,b), \tag{2.63}$$

$$H_z^1(x,b)+H_z^{inc}(x,b)+H_z^{ref}(x,b)=H_z^2(x,b), \qquad x\in(0,\infty), \tag{2.64}$$

$$\frac{\partial}{\partial y}H_z^1(x,b)+\frac{\partial}{\partial y}H_z^{inc}(x,b)+\frac{\partial}{\partial y}H_z^{ref}(x,b)=\frac{\partial}{\partial y}H_z^2(x,b). \qquad x\in(0,\infty). \tag{2.65}$$

The radiation and edge conditions for the uniqueness of the boundary-valued problem defined by the set of equations (2.60) - (2.65) are given by [83].

$$\sqrt{\rho}\left[\frac{\partial}{\partial\rho}H_z^1(x,y)-\iota k_{\text{eff}}H_z^1(x,y)\right]=0, \quad \rho=\sqrt{x^2+y^2}\to\infty \tag{2.66}$$

and

$$H_z^T(x,y)=\mathcal{O}(|x|^{\frac{1}{2}}), \quad \frac{\partial}{\partial y}H_z^T(x,y)=\mathcal{O}(|x|^{-\frac{1}{2}}), \quad |x|\to 0 \tag{2.67}$$

respectively.

2.7.2 FORMULATION OF WIENER-HOPF EQUATION

Since Helmholtz equation in cold plasma is satisfied by the field $H_z^1(x,y)$ in the region $x\in(-\infty,\infty)$ and $y\in(b,\infty)$ which gives

$$\frac{\partial^2}{\partial x^2}H_z^1(x,y)+\frac{\partial^2}{\partial y^2}H_z^1(x,y)+k_{\text{eff}}^2H_z^1(x,y)=0. \tag{2.68}$$

The Fourier transform of equation (2.68) with respect to x yields

$$\left[\frac{\partial^2}{\partial y^2}+(k_{\text{eff}}^2-\alpha^2)\right]F(\alpha,y)=0, \tag{2.69}$$

where

$$F(\alpha, y) = \int_{-\infty}^{\infty} H_z^1(x, y) e^{\iota \alpha x} dx. \tag{2.70}$$

Using additive decomposition theorem $F(\alpha, y)$ can be decomposed as

$$F(\alpha, y) = F_-(\alpha, y) + F_+(\alpha, y), \tag{2.71}$$

where

$$F_\pm(\alpha, y) = \pm \int_{0}^{\pm\infty} H_z^1(x, y) e^{\iota \alpha} dx. \tag{2.72}$$

It is assumed that $F_+(\alpha, y)$ and $F_-(\alpha, y)$ are regular functions of α in the half-plane $\Im\mathrm{m}(\alpha) > \Im\mathrm{m}(k_{\text{eff}} \cos\theta_0)$ and $\Im\mathrm{m}(\alpha) < \Im\mathrm{m}(k_{\text{eff}})$, respectively.

The general solution of equation (2.69) satisfying the radiation condition represented by equations (2.66) yields

$$F(\alpha, y) = A(\alpha) e^{\iota \mathfrak{L}(\alpha)(y-b)}, \tag{2.73}$$

where

$$\mathfrak{L}(\alpha) = \sqrt{k_{\text{eff}}^2 - \alpha^2}. \tag{2.74}$$

The square-root function $\mathfrak{L}(\alpha) = \sqrt{k_{\text{eff}}^2 - \alpha^2}$ is defined in the complex α-plane with branch cuts along $\alpha = k_{\text{eff}}$ to $\alpha = k_{\text{eff}} + \iota\infty$ and $\alpha = -k_{\text{eff}}$ to $\alpha = -k_{\text{eff}} - \iota\infty$ such that $\mathfrak{L}(0) = k_{\text{eff}}$ as shown in the Fig. (2.4).

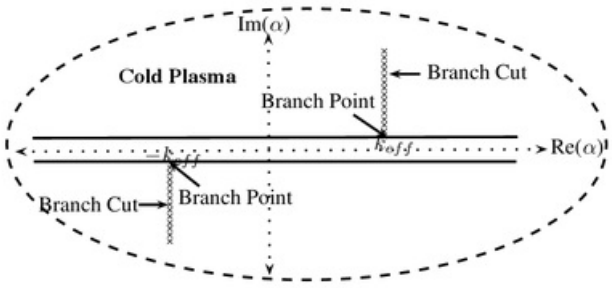

FIGURE 2.4. *The depiction of Branch cuts*

To find the unknown coefficient $A(\alpha)$, we can use the transformed form of boundary condition represented by equation (2.61) which gives

$$A(\alpha) = \frac{k_{\text{eff}}}{\mathfrak{L}(\alpha)} \mathscr{R}_+(\alpha)\chi(\eta,\alpha), \tag{2.75}$$

with

$$\mathscr{R}_+(\alpha) = F_+(\alpha,b) + \frac{\eta}{\iota k_{\text{eff}}} F'_+(\alpha,b) \tag{2.76}$$

and

$$\chi(\eta,\alpha) = \frac{\mathfrak{L}(\alpha)}{\eta\mathfrak{L}(\alpha) + k_{\text{eff}}}\ , \tag{2.77}$$

where the prime sign in equation (2.75) denotes the derivative with respect to y. Replacing equations (2.71) and (2.75) in equation (2.73), one gets

$$F_-(\alpha,y) + F_+(\alpha,y) = \frac{k_{\text{eff}}}{\mathfrak{L}(\alpha)} \mathscr{R}_+(\alpha)\chi(\eta,\alpha) e^{\iota\mathfrak{L}(\alpha)(y-b)}. \tag{2.78}$$

In the region $x \in (0,\infty)$ and $y \in (a,b)$, $H_z^2(x,y)$ satisfies the Helmholtz equation in cold plasma gives

$$\frac{\partial^2}{\partial x^2} H_z^2(x,y) + \frac{\partial^2}{\partial y^2} H_z^2(x,y) + k_{\text{eff}}^2 H_z^2(x,y) = 0. \tag{2.79}$$

On multiplying equation (2.79) by $e^{\iota\alpha x}$ and integrating with respect to x from 0 to ∞, one obtains

$$\left[\frac{\partial^2}{\partial y^2} + \mathfrak{L}^2(\alpha)\right] \mathscr{G}_+(\alpha,y) = \mathfrak{f}(y), \tag{2.80}$$

with

$$\mathfrak{f}(y) = \frac{\partial}{\partial x} H_z^2(0,y) \tag{2.81}$$

and $\mathscr{G}_+(\alpha,y)$ is defined by

$$\mathscr{G}_+(\alpha,y) = \int_0^\infty H_z^2(x,y) e^{\iota\alpha x} dx, \tag{2.82}$$

which is a regular function in the half-plane.

The general solution of the non homogenous differential equation (2.80) can be obtained by using the method of variation of parameter as follow

$$\mathscr{G}_+(\alpha,y) = B(\alpha)\cos\mathfrak{L}(\alpha)y + C(\alpha)\sin\mathfrak{L}(\alpha)y + \frac{1}{\mathfrak{L}(\alpha)}\int_0^y \mathfrak{f}(t)\sin\mathfrak{L}(\alpha)(y-t)dt, \tag{2.83}$$

where $B(\alpha)$ and $C(\alpha)$ are the unknown spectral coefficients and $\mathfrak{L}(\alpha)$ is defined in equation (2.74).

Combining the transformed form of the boundary condition represented by the equation (2.62) and equation (2.83) gives

$$\mathscr{G}_+(\alpha,y) = B(\alpha)\cos\mathfrak{L}(\alpha)y + \frac{1}{\mathfrak{L}(\alpha)}\int_0^y \mathfrak{f}(t)\sin\mathfrak{L}(\alpha)(y-t)dt. \tag{2.84}$$

In the above expression $B(\alpha)$ can be obtained by adding the transformed form of equations (2.64) and $\frac{\eta}{\imath k_{\mathfrak{eff}}}$ time of (2.65) as under

$$B(\alpha) = \frac{\mathscr{R}_+(\alpha)}{\mathscr{W}(\alpha)} + \frac{1}{\mathscr{W}(\alpha)}\int_0^b \mathfrak{f}(t)\left(\frac{\sin\mathfrak{L}(\alpha)(b-t)}{\mathfrak{L}(\alpha)} + \frac{\eta}{\imath k_{\mathfrak{eff}}}\cos\mathfrak{L}(\alpha)(b-t)\right)dt, \tag{2.85}$$

where

$$\mathscr{W}(\alpha) = \cos\mathfrak{L}(\alpha)b - \frac{\eta}{\imath k_{\mathfrak{eff}}}\mathfrak{L}(\alpha)\sin\mathfrak{L}(\alpha)b. \tag{2.86}$$

Using equation (2.85) in equation (2.84), one gets

$$\begin{aligned}\mathscr{G}_+(\alpha,y) = &\frac{\cos\mathfrak{L}(\alpha)y}{\mathscr{W}(\alpha)}\left[\mathscr{R}_+(\alpha) - \int_0^b \mathfrak{f}(t)\left(\frac{\sin\mathfrak{L}(\alpha)(b-t)}{\mathfrak{L}(\alpha)} + \frac{\eta}{\imath k_{\mathfrak{eff}}}\cos\mathfrak{L}(\alpha)(b-t)\right)dt\right] \\ &+ \frac{1}{\mathfrak{L}(\alpha)}\int_0^y \mathfrak{f}(t)\sin\mathfrak{L}(\alpha)(b-t)dt.\end{aligned} \tag{2.87}$$

The left-hand side (i.e., $\mathscr{G}_+(\alpha,y)$) of the equation (2.87) is analytic in the upper half-plane $\mathfrak{Im}(\alpha) > \mathfrak{Im}(k_{\mathfrak{eff}}\cos\theta_0)$. However, the analyticity of the right-hand side

is violated by the appearance of simple poles lying at the zeros of $\mathcal{W}(\alpha)$, i.e., $\alpha = \pm\alpha_m$ satisfying

$$\mathcal{W}(\pm\alpha_m) = 0, \qquad \Im\mathrm{m}(\alpha_m) > \Im\mathrm{m}(k_{eff}), \qquad m = 1,2,3.... \tag{2.88}$$

The poles in the equation (2.87) can be removed by using the condition that the residues of these poles are zero. Then from equation (2.87), it is found that

$$\mathcal{R}_+(\alpha_m) = \mathcal{D}_m\left(\frac{\sin\mathfrak{L}_m b}{\mathfrak{L}_m} + \frac{\eta}{\iota k_{\mathfrak{eff}}}\cos\mathfrak{L}_m b\right)\mathfrak{f}_m, \tag{2.89}$$

where $\mathfrak{f}_m$ is defined by

$$\mathfrak{f}(t) = \sum_{n=1}^{\infty}\mathfrak{f}_m\cos\mathfrak{L}_m t, \tag{2.90}$$

with

$$\mathfrak{L}_m = \sqrt{k_{\mathfrak{eff}}^2 - \alpha_m^2} \tag{2.91}$$

and

$$\mathcal{D}_m = \frac{\mathfrak{L}_m\sin\mathfrak{L}_m b}{2\alpha_m}\frac{\partial}{\partial\alpha}\mathcal{W}(\alpha_m). \tag{2.92}$$

Combining equations (2.87) and (2.78) with the help of the transformed domain of continuity relation given by equation (2.65), one can obtain

$$\begin{aligned}\iota k_{\mathfrak{eff}}\mathcal{R}_+(\alpha)\chi(\eta,\alpha) - \overset{\prime}{F}_-(\alpha,b) &= -\frac{2k_{\mathfrak{eff}}\sin\theta_0 e^{-\iota k_{\mathfrak{eff}} b\sin\theta_0}}{(\eta\sin\theta_0+1)(\alpha - k_{\mathfrak{eff}}\cos\theta_0)}\\ &+ \frac{\mathfrak{L}(\alpha)\sin\mathfrak{L}(\alpha)b}{\mathcal{W}(\alpha)}\left[\mathcal{R}_+(\alpha) - \int_0^b\mathfrak{f}(t)\left(\frac{\sin\mathfrak{L}(\alpha)(b-t)}{\mathfrak{L}(\alpha)} + \frac{\eta}{\iota k_{\mathfrak{eff}}}\cos\mathfrak{L}(\alpha)(b-t)\right)dt\right]\\ &+ \int_0^b\mathfrak{f}(t)\cos\mathfrak{L}(\alpha)(b-t)dt.\end{aligned} \tag{2.93}$$

After simplification the above expression can take the form

$$\frac{\iota k_{\text{eff}}\mathscr{R}_+(\alpha)\chi(\eta,\alpha)}{\mathscr{N}(\alpha)} - \overset{\prime}{F}_-(\alpha,b) = -\frac{2k_{\text{eff}}\sin\theta_0 e^{-\iota k_{\text{eff}} b\sin\theta_0}}{(\eta\sin\theta_0+1)(\alpha-k_{\text{eff}}\cos\theta_0)} + \frac{1}{\mathscr{W}(\alpha)}\int_0^b \mathfrak{f}(t)\cos\mathfrak{L}(\alpha)t\,dt, \tag{2.94}$$

where

$$\mathscr{N}(\alpha) = \mathscr{W}(\alpha)e^{\iota\mathfrak{L}(\alpha)b}. \tag{2.95}$$

Using equation (2.90) in equation (2.94), one obtains the required Wiener-Hopf equation valid in the strip $\Im\mathrm{m}(-k_{\text{eff}}) < \Im\mathrm{m}(\alpha) < \Im\mathrm{m}(k_{\text{eff}})$ as follows:

$$\frac{\iota k_{\text{eff}}\chi(\eta,\alpha)\mathscr{R}_+(\alpha)}{\mathscr{N}(\alpha)} - \overset{\prime}{F}_-(\alpha,b) = -\frac{2k_{\text{eff}}\sin\theta_0 e^{-\iota k_{\text{eff}} b\sin\theta_0}}{(\eta_2\sin\theta_0+1)(\alpha-k_{\text{eff}}\cos\theta_0)} + \sum_{m=1}^{\infty}\frac{\mathfrak{L}_m\sin\mathfrak{L}_m b\mathfrak{f}_m}{\alpha^2-\alpha_m^2}. \tag{2.96}$$

2.7.3 SOLUTION OF WIENER-HOPF EQUATION

To solve the Wiener-Hopf equation, the kernel functions $\mathscr{N}(\alpha)$ and $\chi(\eta,\alpha)$ in equation (2.96) can be factorized by using the known results as following [8]:

$$\mathscr{N}_+(\alpha) = \left[\cos k_{\text{eff}} b + \iota\eta\sin k_{\text{eff}} b\right]^{\frac{1}{2}} \times \exp\left[\frac{\mathfrak{L}(\alpha)b}{\pi}\ln\left(\frac{\alpha+\iota\mathfrak{L}(\alpha)}{k_{\text{eff}}}\right) + \frac{\iota\alpha b}{\pi}\left(1-C+\ln\left[\frac{2\pi}{k_{\text{eff}}b}\right]+\iota\frac{\pi}{2}\right)\right]\prod_{m=1}^{\infty}\left(1+\frac{\alpha}{\alpha_m}\right)e^{\frac{\iota\alpha b}{m\pi}}, \tag{2.97}$$

and

$$\mathscr{N}_-(\alpha) = \mathscr{N}_+(-\alpha). \tag{2.98}$$

In equation (2.97), C denotes the Euler-Mascheroni constant given by $C = 0.5772156649....$ Similarly the factor of $\chi(\eta,\alpha)$ can be expressed in the form of the Maliuzhinetz's function [82] as follows

$$\chi_-(\eta, k_{\text{eff}}\cos\theta) = \frac{4[\mathscr{M}_\pi(3\pi/2-\theta-\psi)\mathscr{M}_\pi(\pi/2-\theta+\psi)]^2\sin(\theta/2)}{\sqrt{\eta}[\mathscr{M}_\pi(\pi/2)]^4 \times \left(1+\sqrt{2}\cos[\frac{3\pi/2-\theta-\psi}{2}]\right)\left(1+\sqrt{2}\cos[\frac{\pi/2-\theta+\psi}{2}]\right)} \tag{2.99}$$

and

$$\chi_+(\eta, k_{\text{eff}}\cos\theta) = \chi_-(\eta, -k_{\text{eff}}\cos\theta), \tag{2.100}$$

with $\mathscr{M}_\pi(z)$ and ψ are defined by

$$\mathscr{M}_\pi(z) = \exp\left[-\frac{1}{8\pi}\int_0^z \frac{\pi\sin u - 2\sqrt{2}\pi\sin(u/2)+2u}{\cos u}du\right] \tag{2.101}$$

and

$$\eta = \sin^{-1}\left(\frac{1}{\psi}\right). \tag{2.102}$$

Now, multiplying the Wiener-Hopf equation (2.96) on both sides with $\frac{\mathscr{N}_-(\alpha)}{\chi_-(\eta,\alpha)}$, one obtains

$$\frac{\iota k_{\text{eff}}\chi_+(\eta,\alpha)\mathscr{R}_+(\alpha)}{\mathscr{N}_+(\alpha)} - \frac{\mathscr{N}_-(\alpha)}{\chi_-(\eta,\alpha)}F'_-(\alpha,b) = -\frac{2k_{\text{eff}}\sin\theta_0 e^{-\iota k_{\text{eff}}b\sin\theta_0}\mathscr{N}_-(\alpha)}{(\eta\sin\theta_0+1)(\alpha-k_{\text{eff}}\cos\theta_0)\chi_-(\eta,\alpha)} + \sum_{m=1}^{\infty}\frac{\mathfrak{L}_m\sin\mathfrak{L}_m b\mathfrak{f}_m\mathscr{N}_-(\alpha)}{(\alpha^2-\alpha_m^2)\chi_-(\eta,\alpha)}. \tag{2.103}$$

With the help of Cauchy's integral formula the terms at right-hand side of the equation (2.103) can be decomposed as

$$\begin{aligned}&\frac{2k_{\text{eff}}\sin\theta_0 e^{-\iota k_{\text{eff}}b\sin\theta_0}\mathscr{N}_-(\alpha)}{(\eta\sin\theta_0+1)(\alpha-k_{\text{eff}}\cos\theta_0)\chi_-(\eta_2,\alpha)}\\ &= \frac{2k_{\text{eff}}\sin\theta_0 e^{-\iota k_{\text{eff}}b\sin\theta_0}}{(\eta\sin\theta_0+1)(\alpha-k_{\text{eff}}\cos\theta_0)}\left[\frac{\mathscr{N}_-(\alpha)}{\chi_-(\eta,\alpha)} - \frac{\mathscr{N}_-(k_{\text{eff}}\cos\theta_0)}{\chi_-(\eta,k_{\text{eff}}\cos\theta_0)}\right]\\ &+ \frac{2k_{\text{eff}}\sin\theta_0 e^{-\iota k_{\text{eff}}b\sin\theta_0}\mathscr{N}_-(k_{\text{eff}}\cos\theta_0)}{(\eta\sin\theta_0+1)(\alpha-k_{\text{eff}}\cos\theta_0)\chi_-(\eta,k_{\text{eff}}\cos\theta_0)}\end{aligned} \tag{2.104}$$

and

$$\sum_{m=1}^{\infty}\frac{\mathfrak{L}_m\sin\mathfrak{L}_m b\mathscr{N}_-(\alpha)\mathfrak{f}_m}{(\alpha^2-\alpha_m^2)\chi_-(\eta,\alpha)}=\sum_{m=1}^{\infty}\frac{\mathfrak{L}_m\sin\mathfrak{L}_m b\mathfrak{f}_m}{(\alpha+\alpha_m)}$$
$$\times\left[\frac{\mathscr{N}_-(\alpha)}{(\alpha-\alpha_m)\chi_-(\eta,\alpha)}-\frac{\mathscr{N}_+(\alpha_m)}{2\alpha_m\chi_+(\eta,\alpha_m)}\right]+\sum_{m=1}^{\infty}\frac{\mathfrak{L}_m\sin\mathfrak{L}_m b\mathscr{N}_+(\alpha_m)\mathfrak{f}_m}{2\alpha_m(\alpha+\alpha_m)\chi_+(\eta,\alpha_m)}. \tag{2.105}$$

Now using equations (2.104) and (2.105) in equation (2.103), then placing the terms which are analytic in the upper half-plane ($\Im\mathfrak{m}(\alpha)>-k_{\mathfrak{eff}}$)and those which analytic in lower half-plane ($\Im\mathfrak{m}(\alpha)<k_{\mathfrak{eff}}$) at the right-hand side,which yields

$$\frac{\iota k_{\mathfrak{eff}}\chi_+(\eta,\alpha)\mathscr{R}_+(\alpha)}{\mathscr{N}_+(\alpha)}+\frac{2k_{\mathfrak{eff}}\sin\theta_0 e^{-\iota k_{\mathfrak{eff}}b\sin\theta_0}\mathscr{N}_-(k_{\mathfrak{eff}}\cos\theta_0)}{(\eta\sin\theta_0+1)(\alpha-k_{\mathfrak{eff}}\cos\theta_0)\chi_-(\eta,k_{\mathfrak{eff}}\cos\theta_0)}$$
$$-\sum_{m=1}^{\infty}\frac{\mathfrak{L}_m\sin\mathfrak{L}_m b\mathscr{N}_+(\alpha_m)\mathfrak{f}_m}{2\alpha_m(\alpha+\alpha_m)\chi_+(\eta,\alpha_m)}=\frac{\mathscr{N}_-(\alpha)}{\chi_-(\eta,\alpha)}F'_-(\alpha,b)$$
$$-\frac{2k_{\mathfrak{eff}}\sin\theta_0 e^{-\iota k_{\mathfrak{eff}}b\sin\theta_0}}{(\eta\sin\theta_0+1)(\alpha-k_{\mathfrak{eff}}\cos\theta_0)}\left[\frac{\mathscr{N}_-(\alpha)}{\chi_-(\eta,\alpha)}-\frac{\mathscr{N}_-(k_{\mathfrak{eff}}\cos\theta_0)}{\chi_-(\eta,k_{\mathfrak{eff}}\cos\theta_0)}\right]$$
$$+\sum_{m=1}^{\infty}\frac{\mathfrak{L}_m\sin\mathfrak{L}_m b\mathfrak{f}_m}{(\alpha+\alpha_m)}\left[\frac{\mathscr{N}_-(\alpha)}{(\alpha-\alpha_m)\chi_-(\eta,\alpha)}-\frac{\mathscr{N}_+(\alpha_m)}{2\alpha_m\chi_+(\eta,\alpha_m)}\right]. \tag{2.106}$$

The required solution of Wiener-Hopf equation can be obtained by using analytical continuation principle complying the extended Liouville's theorem as under

$$\frac{\chi_+(\eta,\alpha)\mathscr{R}_+(\alpha)}{\mathscr{N}_+(\alpha)}=\frac{2\iota\sin\theta_0 e^{-\iota k_{\mathfrak{eff}}b\sin\theta_0}\mathscr{N}_-(k_{\mathfrak{eff}}\cos\theta_0)}{(\eta\sin\theta_0+1)(\alpha-k_{\mathfrak{eff}}\cos\theta_0)\chi_-(\eta,k_{\mathfrak{eff}}\cos\theta_0)}$$
$$-\sum_{m=1}^{\infty}\frac{\iota\mathfrak{L}_m\sin\mathfrak{L}_m b\mathscr{N}_+(\alpha_m)\mathfrak{f}_m}{2k_{\mathfrak{eff}}\alpha_m(\alpha+\alpha_m)\chi_+(\eta,\alpha_m)}. \tag{2.107}$$

Placing equation (2.89) into equation (2.107), gives

$$\frac{\mathscr{D}_n\chi_+(\eta,\alpha_n)}{\mathscr{N}_+(\alpha_n)}\left(\frac{\sin\mathfrak{L}_n b}{\mathfrak{L}_n}+\frac{\eta}{\iota k_{\mathfrak{eff}}}\cos\mathfrak{L}_n b\right)\mathfrak{f}_n$$
$$=\frac{2\iota\sin\theta_0 e^{-\iota k_{\mathfrak{eff}}b\sin\theta_0}\mathscr{N}_-(k_{\mathfrak{eff}}\cos\theta_0)}{(\eta\sin\theta_0+1)(\alpha_n-k_{\mathfrak{eff}}\cos\theta_0)\chi_-(\eta,k_{\mathfrak{eff}}\cos\theta_0)}$$
$$-\sum_{m=1}^{\infty}\frac{\iota\mathfrak{L}_m\sin\mathfrak{L}_m b\mathscr{N}_+(\alpha_m)\mathfrak{f}_m}{2k_{\mathfrak{eff}}\alpha_m(\alpha_n+\alpha_m)\chi_+(\eta,\alpha_m)}. \tag{2.108}$$

The above expression is system of infinite number of equation and these system of equation can be solved numerically after truncating after N terms.

2.7.4 THE DIFFRACTED FIELD

The required diffracted field $H_z^1(x,y)$ can be acquired by using the inverse Fourier transform of $F(\alpha,y)$. Thus from equation (2.78), one can get

$$H_z^1(x,y)=\frac{1}{2\pi}\int_{\mathscr{L}}\frac{k_{\text{eff}}\chi(\eta,\alpha)\mathscr{R}_+(\alpha)}{\mathfrak{L}(\alpha)}e^{\iota\mathfrak{L}(\alpha)(y-b)}e^{-\iota\alpha x}d\alpha. \tag{2.109}$$

Using the replacement of the function $\chi(\eta,\alpha)$ and the variables $\alpha=-k_{\text{eff}}\cos t$, $x=\rho\cos\theta$ and $y=\rho\sin\theta$ in the equation (2.109), one obtains

$$H_z^1(\rho,\theta)=\frac{1}{2\pi}\int_{\mathscr{L}}\frac{\mathscr{R}_+(-k_{\text{eff}}\cos t)}{1+\eta\sin t}e^{-\iota k_{\text{eff}}b\sin t+\iota k_{\text{eff}}\rho\cos(t-\theta)}k_{\text{eff}}\sin t\,dt. \tag{2.110}$$

The asymptotic evaluation of the integral in the equation (2.110) can be obtained via saddle-point technique. Here, saddle-point rests at $t=\theta$ which gives

$$\begin{aligned}H_z^1(\rho,\theta)=&\frac{\sin\theta e^{-\iota k\sqrt{(\epsilon_1^2-\epsilon_2^2)/\epsilon_1}\rho+\frac{\iota3\pi}{4}-\iota k\sqrt{(\epsilon_1^2-\epsilon_2^2)/\epsilon_1}b\sin\theta}}{\sqrt{2\pi}\sqrt{k\rho\sqrt{(\epsilon_1^2-\epsilon_2^2)/\epsilon_1}(1+\eta\sin\theta)}}\\
&\times\left[\frac{2\iota\sin\theta_0 e^{-\iota k\sqrt{(\epsilon_1^2-\epsilon_2^2)/\epsilon_1}b\sin\theta_0}\mathscr{N}_-(k\sqrt{(\epsilon_1^2-\epsilon_2^2)/\epsilon_1}\cos\theta_0)\mathscr{N}_-(k\sqrt{(\epsilon_1^2-\epsilon_2^2)/\epsilon_1}\cos\theta)}{(\eta\sin\theta+1)(\cos\theta+\cos\theta_0)\chi_-(\eta,k\sqrt{(\epsilon_1^2-\epsilon_2^2)/\epsilon_1}\cos\theta_0)\chi_-(\eta,k\sqrt{(\epsilon_1^2-\epsilon_2^2)/\epsilon_1}\cos\theta)}\right.\\
&\left.-\sum_{m=1}^{\infty}\frac{\iota\mathfrak{L}_m\sin\mathfrak{L}_m b\mathscr{N}_+(\alpha_m)\mathscr{N}_-(k\sqrt{(\epsilon_1^2-\epsilon_2^2)/\epsilon_1}\cos\theta)\mathfrak{f}_m}{2k\sqrt{(\epsilon_1^2-\epsilon_2^2)/\epsilon_1}\alpha_m(\alpha_m-k\sqrt{(\epsilon_1^2-\epsilon_2^2)/\epsilon_1}\cos\theta)\chi_+(\eta,\alpha_m)\chi_-(\eta,k\sqrt{(\epsilon_1^2-\epsilon_2^2)/\epsilon_1}\cos\theta)}\right].\end{aligned} \tag{2.111}$$

2.7.5 COMPUTATIONAL RESULTS AND DISCUSSION

In this section, we have analyzed the numerical results for various physical parameters of interest by plotting graphs. Fig. (2.5) depicts the variation in the

diffracted field amplitude versus the truncation number "N". It is apparent that the effect of the truncation number is negligible for $N \geq 40$. Hence, the system containing infinite number of algebraic equations represented by the equation (2.108) can be managed to deal as finite. Where as the Fig. (2.6) has been plotted by varying the plate separations "b". The amplitude of the diffracted field decreases with increase in b. Fig. (2.7) depicts the variations of diffracted fields versus incident angle θ_0 ($0^o \leq \theta_0 \leq 90^o$). It is interesting to note that the value of diffracted field amplitude lies at 90^o when $\theta_0 = 90^o$. Where as this peak values moves to 120^o and 150^o for $\theta_0 = 60^o$ and $\theta_0 = 30^o$, respectively. As long as the angle of incident increases the center of diffracted field amplitude shifted towards 90^0. Fig. (2.8) shows the variation in the diffracted field amplitude versus the impedance "η". The variation in the diffracted field amplitude versus effect of cold plasma permittivity values for ϵ_1 and ϵ_2 have been analyzed in Figs. (2.9) and (2.10), respectively. Here it is noted that the amplitude of the diffracted field decreases by increasing the value of ϵ_1 where as slightly increases by increasing ϵ_2 but the effect of ϵ_2 is negligible as compare with ϵ_1.

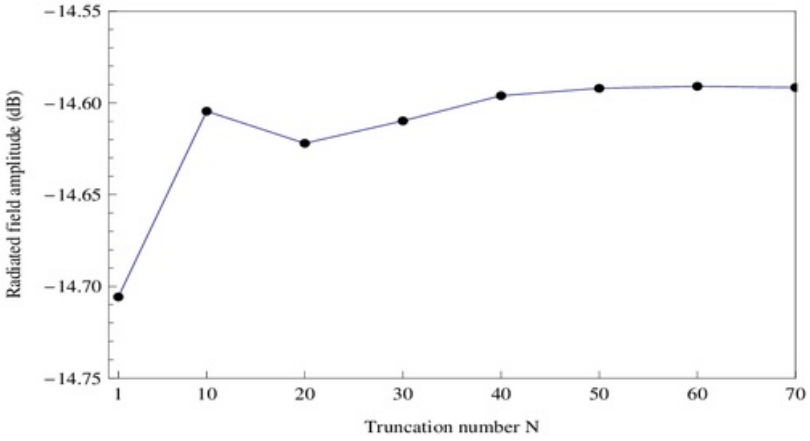

FIGURE 2.5. *Variation in the diffracted field amplitude versus "N" at $k = 5$, $\theta_0 = 90^o$, $\theta = 60^o$, $\eta = 0.3\iota$, $\epsilon_1 = 0.8$, $\epsilon_2 = 0.1$ and $b = 0.2\lambda$.*

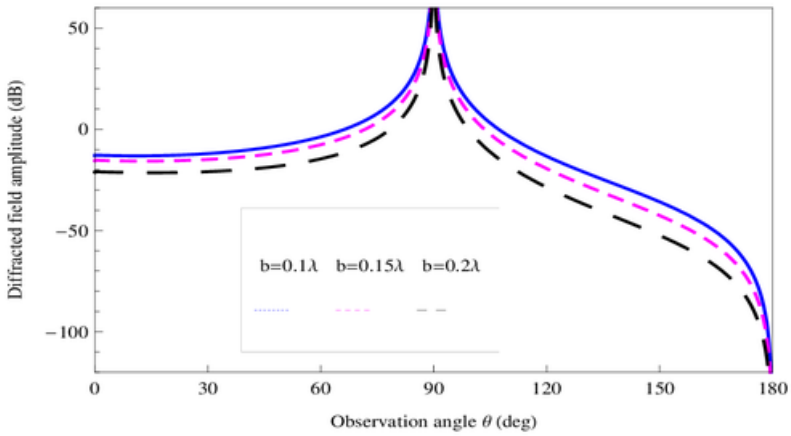

FIGURE 2.6. *Variation in the diffracted field amplitude versus "b" at* $k = 5$, $\theta_0 = 90^o$, $\eta = 0.7\iota$, $\epsilon_1 = 0.8$ *and* $\epsilon_2 = 0.1$.

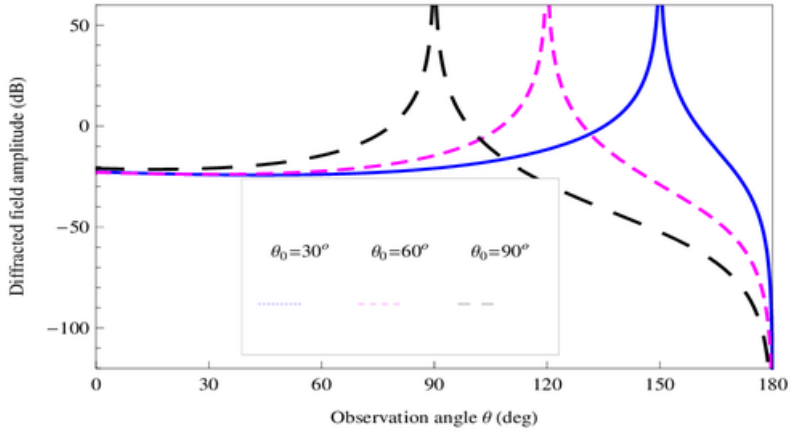

FIGURE 2.7. *Variation in the diffracted field amplitude versus "*θ_0*" at* $k = 5$, $\eta = 0.7\iota$, $\epsilon_1 = 0.8$, $\epsilon_2 = 0.1$ *and* $b = 0.2\lambda$.

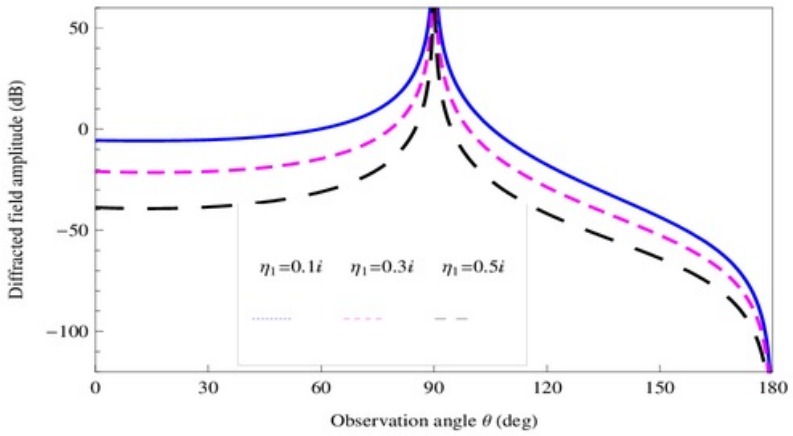

FIGURE 2.8. *Variation in the diffracted field amplitude versus "η" at $\theta_0 = 90^0$, $k = 5$, $\epsilon_1 = 0.8$, $\epsilon_2 = 0.1$ and $b = 0.2\lambda$.*

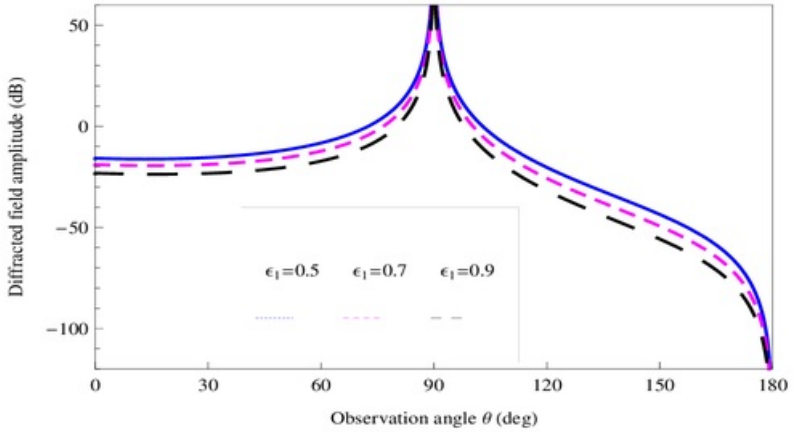

FIGURE 2.9. *Variation in the diffracted field amplitude versus "ϵ_1" at $k = 5$, $\theta_0 = 90^o$, $\eta = 0.7\iota$, $\epsilon_2 = 0.1$ and $b = 0.2\lambda$.*

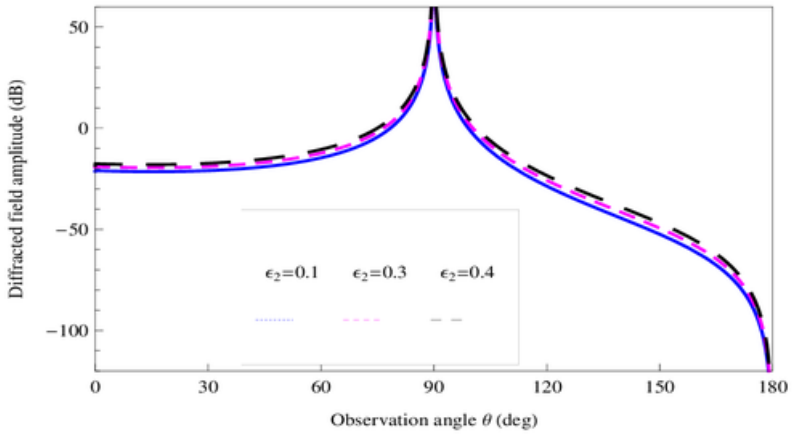

FIGURE 2.10. *Variation in the diffracted field amplitude versus "ϵ_2" at $k = 5$, $\theta_0 = 90^o$, $\eta = 0.7\imath$, $\epsilon_1 = 0.8$ and $b = 0.2\lambda$.*

CHAPTER 3

EFFECT OF COLD PLASMA PERMITTIVITY ON SCATTERING OF E-POLARIZED PLANE WAVE BY AN IMPEDANCE LOADED STEP

In this chapter, the scattering of E-polarized plane wave by two half-planes combined by a step of hight b is discussed. These types of geometries play a vital role in diffraction theory and many problems in science and engineering. Initially, Johansen [84] considered the problem of diffraction by two half-planes having same surfaces impedances combined by a step of hight h. After that Büyükaksoy and Birbir [85] studied the similar geometry for different impedances of the different surfaces. Yener and Serbest [11] considered the diffraction phenomenon in cold plasma considering by a single surface impedance half-plane. Here, in this chapter two half-planes of different surface impedances joined by rigid vertical step of hight b located in cold plasma is considered.

The contents of this chapter are organized in the following order. The boundary-valued problem is developed in Section (3.1) whereas Section (3.2) is dedicated to the formulation of Wiener-Hopf equation. The solution of Wiener-Hopf equation is obtained in Section (3.3). The diffracted field expression is shown in Section (3.4). Few numerical results for different parameters are plotted and discussed in the last Section (3.5).

3.1 MATHEMATICAL MODEL OF THE PROBLEM IN COLD PLASMA

Here, consider the scattering of a plane wave making an incident angle θ_0 in the region designed by two half-planes S_1 define by $\{(x,y,z)|\ x \in (-\infty,0),\ y=0,\ z \in (-\infty,\infty)\}$ and S_2 defined by $\{(x,y,z)|\ x \in (0,\infty),\ y=b,\ z \in (-\infty,\infty)\}$. The top faces of the half-planes S_1 and S_2 are characterized by the impedances Z_1 and Z_2, respectively. While vertical step surface is rigid as shown in Fig. (3.1):

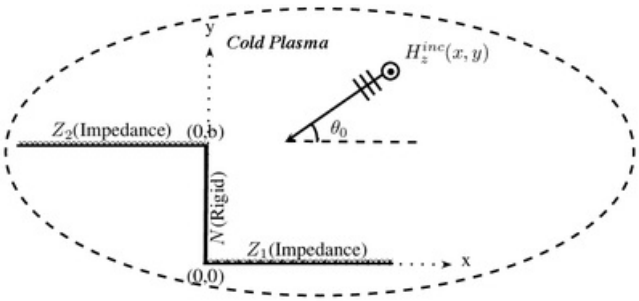

FIGURE 3.1. *Geometrical configuration of the waveguide structure in cold plasma*

The total field takes the form as under

$$H_z^T(x,y) = \begin{cases} H_z^1(x,y) + H_z^{inc}(x,y) + H_z^{ref}(x,y), & y \in (b,\infty) \\ H_z^2(x,y), & y \in (a,b) \end{cases} \tag{3.1}$$

where $H_z^{inc}(x,y)$ and $H_z^{ref}(x,y)$ stand for the incident and reflected fields, respectively, given by

$$H_z^{inc}(x,y) = e^{-\iota k_{\epsilon ff}(x\cos\theta_0 + y\sin\theta_0)} \tag{3.2}$$

and

$$H_z^{ref}(x,y) = -\frac{1-\eta_2\sin\theta_0}{1+\eta_2\sin\theta_0} e^{-\iota k_{\epsilon ff}(x\cos\theta_0 - (y-2b)\sin\theta_0)}, \tag{3.3}$$

with

$$k_{\epsilon ff} = k\sqrt{(\epsilon_1^2 - \epsilon_2^2)/\epsilon_1}. \tag{3.4}$$

$\{H_z^j \quad (j=1,2)\}$ satisfying the Helmholtz equation in cold plasma, i.e.,

$$\left[\frac{\partial^2}{\partial x^2}+\frac{\partial^2}{\partial y^2}+k_{\text{eff}}^2\right]\left[H_z^j(x,y)\right]=0, \tag{3.5}$$

with the following corresponding boundary conditions and continuity relations

$$\left(1+\frac{\eta_2}{\iota k_{\text{eff}}}\frac{\partial}{\partial y}\right)H_z^1(x,b)=0, \qquad x\in(-\infty,0) \tag{3.6}$$

$$\left(1+\frac{\eta_1}{\iota k_{\text{eff}}}\frac{\partial}{\partial y}\right)H_z^2(x,0)=0, \qquad x\in(0,\infty) \tag{3.7}$$

$$\frac{\partial}{\partial x}H_z^2(0,y)=0, \qquad y\in(0,b) \tag{3.8}$$

$$H_z^1(x,b)+H_z^{inc}(x,b)+H_z^{ref}(x,b)=H_z^2(x,b), \qquad x\in(0,\infty) \tag{3.9}$$

$$\frac{\partial}{\partial y}H_z^1(x,b)+\frac{\partial}{\partial y}H_z^{inc}(x,b)+\frac{\partial}{\partial y}H_z^{ref}(x,b)=\frac{\partial}{\partial y}H_z^2(x,b). \qquad x\in(0,\infty) \tag{3.10}$$

The radiation and edge conditions for the uniqueness of the boundary-valued problem defined by the set of equations (3.5) - (3.10) are given by

$$\sqrt{\rho}\left[\frac{\partial}{\partial\rho}H_z^1(x,y)-\iota k_{\text{eff}}H_z^1(x,y)\right]=0, \quad \rho=\sqrt{x^2+y^2}\to\infty \tag{3.11}$$

and

$$H_z^T(x,y)=\mathcal{O}(|x|^{\frac{1}{2}}), \quad \frac{\partial}{\partial y}H_z^T(x,y)=\mathcal{O}(|x|^{-\frac{1}{2}}), \quad |x|\to 0 \tag{3.12}$$

respectively.

3.2 FORMULATION OF WIENER-HOPF EQUATION

The Fourier transform of the Helmholtz equation in cold plasma which is satisfied by the field $H_z^1(x,y)$ in the domain $x\in(-\infty,\infty)$ and $y\in(b,\infty)$ leads to

$$\left[\frac{d^2}{dy^2}+(k_{\text{eff}}^2-\alpha^2)\right]F(\alpha,y)=0, \tag{3.13}$$

where $F(\alpha,y)$ is defined earlier.

Using the radiation condition represented by equation (3.11), the solution of equation (3.13) gives

$$F(\alpha, y) = A_1(\alpha) e^{\iota \mathfrak{L}(\alpha)(y-b)}, \tag{3.14}$$

where

$$\mathfrak{L}(\alpha) = \sqrt{k_{\text{eff}}^2 - \alpha^2} \tag{3.15}$$

and $A_1(\alpha)$ is the unknown spectral coefficient.

The square-root function $\mathfrak{L}(\alpha) = \sqrt{k_{\text{eff}}^2 - \alpha^2}$ represents the branch cuts along $\alpha = k_{\text{eff}}$ to $\alpha = k_{\text{eff}} + \iota\infty$ and $\alpha = -k_{\text{eff}}$ to $\alpha = -k_{\text{eff}} - \iota\infty$ such that $\mathfrak{L}(0) = k_{\text{eff}}$.

To find $A_1(\alpha)$, using the transformed form of the boundary condition represented by equation (3.6), one obtains

$$A_1(\alpha) = \frac{k_{\text{eff}} \mathscr{R}_+^1(\alpha)}{k_{\text{eff}} + \eta_2 \mathfrak{L}(\alpha)}, \tag{3.16}$$

with

$$\mathscr{R}_+^1(\alpha) = F_+(\alpha, b) + \frac{\eta_2}{\iota k_{\text{eff}}} F'_+(\alpha, b), \tag{3.17}$$

where the prime sign in equation (3.17) represents the derivative with respect to y. Using the additive decomposition theorem and placing equation (3.16) in equation (3.14), one gets

$$F_-(\alpha, y) + F_+(\alpha, y) = \frac{k_{\text{eff}} \mathscr{R}_+^1(\alpha)}{k_{\text{eff}} + \eta_2 \mathfrak{L}(\alpha)} e^{\iota \mathfrak{L}(\alpha)(y-b)}. \tag{3.18}$$

The derivative of equation (3.18) with respect to y at $y = b$ takes the form

$$F'_+(\alpha, b) = \frac{\iota k_{\text{eff}} \mathfrak{L}(\alpha) \mathscr{R}_+(\alpha)}{k_{\text{eff}} + \eta_2 \mathfrak{L}(\alpha)} - F'_-(\alpha, b). \tag{3.19}$$

As the Helmholtz equation in cold plasma is satisfied by field $H_z^2(x, y)$ in equation (3.5) in the domain $x \in (0, \infty)$ and $y \in (a, b)$, multiplying this equation by $e^{\iota \alpha x}$ and

integrating the resultant equation with respect to x from 0 to ∞ leads to

$$\left[\frac{d^2}{dy^2} - \mathfrak{L}^2(\alpha)\right] \mathcal{G}_+(\alpha, y) = -\iota\alpha \mathfrak{g}(y), \tag{3.20}$$

where

$$\mathfrak{g}(y) = H_z^2(0, y) \tag{3.21}$$

and $\mathcal{G}_+(\alpha, y)$ defined by

$$\mathcal{G}_+(\alpha, y) = \int_0^\infty H_z^2(x, y) e^{\iota\alpha x} dx, \tag{3.22}$$

is a regular function in the half-plane.

Owing the method of variation of parameter the solution of non homogenous differential equation (3.20) gives

$$\mathcal{G}_+(\alpha, y) = C_1(\alpha)\cos\mathfrak{L}(\alpha)y + C_2(\alpha)\sin\mathfrak{L}(\alpha)y - \frac{\iota\alpha}{\mathfrak{L}(\alpha)}\int_0^y \mathfrak{g}(t)\sin\mathfrak{L}(\alpha)(b-t)dt, \tag{3.23}$$

where $C_1(\alpha)$ and $C_2(\alpha)$ are the unknown spectral coefficients.

To find $C_1(\alpha)$ one can apply the transformed form of the boundary condition represented by the equation (3.7), to get

$$C_1(\alpha) = -\frac{\eta_1}{\iota k_{\text{eff}}}\mathfrak{L}(\alpha)C_2(\alpha). \tag{3.24}$$

Substituting equation (3.24) in equation (3.23) yields

$$\begin{aligned}\mathcal{G}_+(\alpha, y) = &\left[\sin\mathfrak{L}(\alpha)y - \frac{\eta_1}{\iota k_{\text{eff}}}\mathfrak{L}(\alpha)\cos\mathfrak{L}(\alpha)y\right] C_2(\alpha) \\ &- \frac{\iota\alpha}{\mathfrak{L}(\alpha)}\int_0^y \mathfrak{g}(t)\sin\mathfrak{L}(\alpha)(b-t)dt.\end{aligned} \tag{3.25}$$

$C_2(\alpha)$ can be obtained by adding the transformed form of equations (3.9) and $\frac{\eta_1}{\iota k_{\text{eff}}}$ time of (3.10)

$$C_2(\alpha) = \frac{\mathscr{R}_+^1(\alpha)}{\mathscr{W}_1(\alpha)} + \frac{1}{\mathscr{W}_1(\alpha)} \int_0^b \mathfrak{f}(t) \left(\frac{\sin \mathfrak{L}(\alpha)(b-t)}{\mathfrak{L}(\alpha)} + \frac{\eta_1}{\iota k_{\text{eff}}} \cos \mathfrak{L}(\alpha)(b-t) \right) dt, \tag{3.26}$$

where

$$\mathscr{W}_1(\alpha) = \left(\frac{\eta_2 - \eta_1}{\iota k_{\text{eff}}} \right) \cos \mathfrak{L}(\alpha) b + \left(1 - \frac{\eta_1 \eta_2}{k_{\text{eff}}^2} \mathfrak{L}^2(\alpha) \right) \frac{\sin \mathfrak{L}(\alpha) b}{\mathfrak{L}(\alpha)}. \tag{3.27}$$

Using equation (3.26) in equation (3.25), one gets

$$\begin{aligned} \mathscr{G}_+(\alpha, y) = & \frac{\sin \mathfrak{L}(\alpha) y - \frac{\eta_1}{\iota k_{\text{eff}}} \mathfrak{L}(\alpha) \cos \mathfrak{L}(\alpha) y}{\mathfrak{L}(\alpha) \mathscr{W}_1(\alpha)} \\ & \times \left[\mathscr{R}_+^1(\alpha) + \iota \alpha \int_0^b \mathfrak{g}(t) \left(\frac{\sin \mathfrak{L}(\alpha)(b-t)}{\mathfrak{L}(\alpha)} + \frac{\eta_2}{\iota k_{\text{eff}}} \cos \mathfrak{L}(\alpha)(b-t) \right) dt \right] \\ & - \frac{\iota \alpha}{\mathfrak{L}(\alpha)} \int_0^y \mathfrak{g}(t) \sin \mathfrak{L}(\alpha)(b-t) dt. \end{aligned} \tag{3.28}$$

The left-hand side (i.e., $\mathscr{G}_+(\alpha, y)$) of the equation (3.28) is analytic in the upper half-plane $\Im\mathfrak{m}(\alpha) > \Im\mathfrak{m}(k_{\text{eff}} \cos\theta_0)$. However, the analyticity of the right-hand side is desecrated by the appearance of simple poles lying at the zeros of $\mathscr{W}_1(\alpha)$, i.e., $\alpha = \pm\alpha_m$ satisfying

$$\mathscr{W}_1(\pm\alpha_m) = 0, \quad \Im\mathfrak{m}(\alpha_m) > \Im\mathfrak{m}(k_{\text{eff}}), \quad m = 1, 2, 3.... \tag{3.29}$$

The poles in the equation (3.28) can be removed by applying the condition that the residues of these poles are zero. Then from equation (3.28), it is found that

$$\mathscr{R}_+^1(\alpha_m) = \mathscr{D}_m^1 \left(\frac{\eta_2}{\iota k_{eff}} \mathfrak{L}_m \sin \mathfrak{L}_m b - \cos \mathfrak{L}_m b \right) \mathfrak{g}_m, \tag{3.30}$$

where $\mathfrak{g}_m$ is denoted by

$$\mathfrak{g}_m = \frac{1}{\mathscr{D}_m^1}\int_0^b \mathfrak{g}(t)\left(\frac{\sin \mathfrak{L}_m t}{\mathfrak{L}_m} - \frac{\eta_1}{\iota k_{\mathfrak{eff}}}\cos \mathfrak{L}_m t\right) dt, \tag{3.31}$$

with

$$\mathfrak{L}_m = \sqrt{k_{\mathfrak{eff}}^2 - \alpha_m^2} \tag{3.32}$$

and

$$\mathscr{D}_m^1 = \frac{\iota \mathfrak{L}_m}{2}\left(\frac{\cos \mathfrak{L}_m b}{\mathfrak{L}_m} + \frac{\eta_1}{\iota k_{\mathfrak{eff}}}\sin \mathfrak{L}_m b\right)\frac{d}{d\alpha}\mathscr{W}_1(\alpha_m). \tag{3.33}$$

Hence, considering equations (3.19) and (3.28) in the transformed domain of continuity relation given by equation (3.10) together, one can write

$$\begin{aligned}
&\iota k_{\mathfrak{eff}}\mathscr{R}_+^1(\alpha)\chi(\eta_2,\alpha) - \overset{\prime}{F}_-(\alpha,b) = -\frac{2k_{\mathfrak{eff}}\sin\theta_0 e^{-\iota k_{\mathfrak{eff}} b\sin\theta_0}}{(\eta_2\sin\theta_0+1)(\alpha - k_{\mathfrak{eff}}\cos\theta_0)} \\
&+\frac{\cos \mathfrak{L}b + \frac{\eta_1}{\iota k_{\mathfrak{eff}}}\mathfrak{L}\sin \mathfrak{L}b}{\mathscr{W}_1(\alpha)}\left[\mathscr{R}_+^1(\alpha) + \iota\alpha\int_0^b \mathfrak{g}(t)\left(\frac{\sin \mathfrak{L}(b-t)}{\mathfrak{L}(\alpha)} + \frac{\eta_2}{\iota k_{\mathfrak{eff}}}\cos \mathfrak{L}(b-t)\right)dt\right] \\
&-\iota\alpha\int_0^b \mathfrak{g}(t)\cos \mathfrak{L}(b-t)dt,
\end{aligned} \tag{3.34}$$

where

$$\chi(\eta_j,\alpha) = \frac{\mathfrak{L}(\alpha)}{\eta_j\mathfrak{L}(\alpha) + k_{\mathfrak{eff}}}. \tag{3.35}$$

After simplification, equation (3.34) takes the form

$$\begin{aligned}
&\frac{\chi(\eta_2,\alpha)\mathscr{R}_+^1(\alpha)}{\chi(\eta_1,\alpha)\mathscr{N}^1(\alpha)} + \overset{\prime}{F}_-(\alpha,b) = \frac{2k_{\mathfrak{eff}}\sin\theta_0 e^{-\iota k_{\mathfrak{eff}} b\sin\theta_0}}{(\eta_2\sin\theta_0+1)(\alpha - k_{\mathfrak{eff}}\cos\theta_0)} \\
&+\frac{\iota\alpha}{\mathscr{W}_1(\alpha)}\int_0^b \mathfrak{g}(t)\left(\frac{\sin \mathfrak{L}(\alpha)t}{\mathfrak{L}(\alpha)} - \frac{\eta_1}{\iota k_{\mathfrak{eff}}}\cos \mathfrak{L}(\alpha)t\right)dt,
\end{aligned} \tag{3.36}$$

where

$$\mathscr{N}^1(\alpha) = \mathscr{W}_1(\alpha)e^{\iota\mathfrak{L}(\alpha)b}. \tag{3.37}$$

Owing to equation (3.31), $\mathfrak{g}(t)$ can be expanded into a series of eigen-functions as under

$$\mathfrak{g}(t) = \sum_{m=1}^{\infty} \mathfrak{g}_m \left(\frac{\sin \mathfrak{L}_m t}{\mathfrak{L}_m} - \frac{\eta_1}{\iota k_{\mathfrak{eff}}} \cos \mathfrak{L}_m t \right). \tag{3.38}$$

Using equation (3.38) in equation (3.36), one obtains the required Wiener-Hopf equation valid in the strip $\mathfrak{Im}(-k_{\mathfrak{eff}}) < \mathfrak{Im}(\alpha) < \mathfrak{Im}(k_{\mathfrak{eff}})$ as follows:

$$\begin{aligned} &\frac{\chi(\eta_2,\alpha)\mathscr{R}^1_+(\alpha)}{\chi(\eta_1,\alpha)\mathscr{N}^1(\alpha)} + \overset{'}{F}_-(\alpha,b) = \frac{2k_{\mathfrak{eff}} \sin\theta_0 e^{-\iota k_{\mathfrak{eff}} b \sin\theta_0}}{(\eta_2 \sin\theta_0 + 1)(\alpha - k_{\mathfrak{eff}} \cos\theta_0)} \\ &- \sum_{m=1}^{\infty} \frac{\iota\alpha \mathfrak{L}_m \mathfrak{g}_m}{\alpha^2 - \alpha_m^2} \left(\frac{\cos \mathfrak{L}_m b}{\mathfrak{L}_m} + \frac{\eta_1}{\iota k_{eff}} \sin \mathfrak{L}_m b \right). \end{aligned} \tag{3.39}$$

3.3 SOLUTION OF WIENER-HOPF EQUATION

To solve the Wiener-Hopf equation the kernel functions $\mathscr{N}^1(\alpha)$ and $\chi(\eta_j,\alpha)$ in equation (3.39) can be factorized by applying the known results as following:

$$\begin{aligned} \mathscr{N}^1_+(\alpha) &= \left[\left(\frac{\eta_2 - \eta_1}{\iota k_{\mathfrak{eff}}} \right) \cos k_{\mathfrak{eff}} b + (1 - \eta_1\eta_2) \frac{\sin k_{\mathfrak{eff}} b}{k_{\mathfrak{eff}}} \right]^{\frac{1}{2}} \\ &\times \exp\left[\frac{\mathfrak{L}(\alpha) b}{\pi} \ln\left(\frac{\alpha + \iota\mathfrak{L}(\alpha)}{k_{\mathfrak{eff}}} \right) + \frac{\iota\alpha b}{\pi} \left(1 - C + \ln\left[\frac{2\pi}{k_{\mathfrak{eff}} b} \right] + \iota\frac{\pi}{2} \right) \right] \prod_{m=1}^{\infty} \left(1 + \frac{\alpha}{\alpha_m} \right) e^{\frac{\iota\alpha b}{m\pi}}, \end{aligned} \tag{3.40}$$

and

$$\mathscr{N}^1_-(\alpha) = \mathscr{N}^1_+(-\alpha). \tag{3.41}$$

Similarly the factor of $\chi(\eta_j,\alpha)$ can be expressed in form of the Maliuzhinetz's function as discussed in earlier.

Now, multiplying the Wiener-Hopf equation (3.39) on both sides by $\frac{\chi_-(\eta_1,\alpha)\mathscr{N}^1_-(\alpha)}{\chi_-(\eta_2,\alpha)}$, one obtains

$$\frac{\chi_+(\eta_2,\alpha)\mathscr{R}^1_+(\alpha)}{\mathscr{N}^1_+(\alpha)\chi_+(\eta_1,\alpha)}+\frac{\chi_-(\eta_1,\alpha)\mathscr{N}^1_-(\alpha)}{\chi_-(\eta_2,\alpha)}{}'F_-(\alpha,b)$$
$$=\frac{2k_{\text{eff}}\sin\theta_0 e^{-\iota k_{\text{eff}}b\sin\theta_0}\chi_-(\eta_1,\alpha)\mathscr{N}^1_-(\alpha)}{(\eta_2\sin\theta_0+1)(\alpha-k_{\text{eff}}\cos\theta_0)\chi_-(\eta_2,\alpha)}$$
$$-\sum_{m=1}^{\infty}\frac{\iota\alpha\mathfrak{g}_m\mathfrak{L}_m\chi_-(\eta_1,\alpha)\mathscr{N}^1_-(\alpha)}{(\alpha^2-\alpha_m^2)\chi_-(\eta_2,\alpha)}\left(\frac{\cos\mathfrak{L}_m b}{\mathfrak{L}_m}+\frac{\eta_1}{\iota k_{eff}}\sin\mathfrak{L}_m b\right). \tag{3.42}$$

With the aid of Cauchy's integral formula the terms on right-hand of the equation (3.42) can be decomposed as

$$\frac{2k_{\text{eff}}\sin\theta_0 e^{-\iota k_{\text{eff}}b\sin\theta_0}\chi_-(\eta_1,\alpha)\mathscr{N}^1_-(\alpha)}{(\eta_2\sin\theta_0+1)(\alpha-k_{\text{eff}}\cos\theta_0)\chi_-(\eta_2,\alpha)}=\frac{2k_{\text{eff}}\sin\theta_0 e^{-\iota k_{\text{eff}}b\sin\theta_0}}{(\eta_2\sin\theta_0+1)(\alpha-k_{\text{eff}}\cos\theta_0)}$$
$$\times\left[\frac{\chi_-(\eta_1,\alpha)\mathscr{N}^1_-(\alpha)}{\chi_-(\eta_2,\alpha)}-\frac{\chi_-(\eta_1,k_{\text{eff}}\cos\theta_0)\mathscr{N}^1_-(k_{\text{eff}}\cos\theta_0)}{\chi_-(\eta_2,k_{\text{eff}}\cos\theta_0)}\right]$$
$$+\frac{2k_{\text{eff}}\sin\theta_0 e^{-\iota k_{\text{eff}}b\sin\theta_0}\chi_-(\eta_4,k_{\text{eff}}\cos\theta_0)\mathscr{N}^1_-(k_{\text{eff}}\cos\theta_0)}{(\eta_1\sin\theta_0+1)(\alpha-k_{\text{eff}}\cos\theta_0)\chi_-(\eta_2,k_{\text{eff}}\cos\theta_0)} \tag{3.43}$$

and

$$\sum_{m=1}^{\infty}\frac{\iota\alpha\mathfrak{L}_m\mathfrak{g}_m\chi_-(\eta_1,\alpha)\mathscr{N}^1_-(\alpha)}{(\alpha^2-\alpha_m^2)\chi_-(\eta_2,\alpha)}\left(\frac{\cos\mathfrak{L}_m b}{\mathfrak{L}_m}+\frac{\eta_1}{\iota k_{eff}}\sin\mathfrak{L}_m b\right)$$
$$=\sum_{m=1}^{\infty}\frac{\iota\mathfrak{L}_m}{(\alpha+\alpha_m)}\left(\frac{\cos\mathfrak{L}_m b}{\mathfrak{L}_m}+\frac{\eta_2}{\iota k_{eff}}\sin\mathfrak{L}_m b\right)$$
$$\times\left[\frac{\alpha\mathfrak{g}_m\chi_-(\eta_1,\alpha)\mathscr{N}^1_-(\alpha)}{(\alpha-\alpha_m)\chi_-(\eta_2,\alpha)}-\frac{\alpha_m\mathfrak{g}_m\chi_+(\eta_1,\alpha_m)\mathscr{N}^1_+(\alpha_m)}{2\alpha_m\chi_+(\eta_2,\alpha_m)}\right]$$
$$+\sum_{m=1}^{\infty}\frac{\iota\mathfrak{L}_m\alpha_m\mathfrak{g}_m\chi_+(\eta_1,\alpha_m)\mathscr{N}^1_+(\alpha_m))}{2\alpha_m\chi_+(\eta_1,\alpha_m)(\alpha+\alpha_m)}\left(\frac{\cos\mathfrak{L}_m b}{\mathfrak{L}_m}+\frac{\eta_1}{\iota k_{eff}}\sin\mathfrak{L}_m b\right). \tag{3.44}$$

On using equations (3.43) and (3.44) in equation (3.42), and then separating the terms which are analytic in the upper half-plane ($\Im\mathfrak{m}(\alpha) > -k_{\text{eff}}$) at left-hand side and those which are analytic in lower half-plane ($\Im\mathfrak{m}(\alpha) < k_{\text{eff}}$) at the right-hand

side yields

$$\frac{\chi_+(\eta_2,\alpha)\mathscr{R}^1_+(\alpha)}{\mathscr{N}^1_+(\alpha)\chi_+(\eta_1,\alpha)} - \frac{2k_{\text{eff}}\sin\theta_0 e^{-\iota k_{\text{eff}} b\sin\theta_0}\chi_-(\eta_1,k_{\text{eff}}\cos\theta_0)\mathscr{N}^1_-(k_{\text{eff}}\cos\theta_0)}{(\eta_2\sin\theta_0+1)(\alpha-k_{\text{eff}}\cos\theta_0)\chi_-(\eta_2,k_{\text{eff}}\cos\theta_0)}$$
$$+\sum_{m=1}^{\infty}\frac{\iota\alpha_m\mathfrak{L}_m\mathfrak{g}_m\chi_+(\eta_1,\alpha_m)\mathscr{N}^1_+(\alpha_m))}{2\alpha_m\chi_+(\eta_2,\alpha_m)(\alpha+\alpha_m)}\left(\frac{\cos\mathfrak{L}_m b}{\mathfrak{L}_m}+\frac{\eta_1}{\iota k_{\text{eff}}\sin\mathfrak{L}_m b}\right)$$
$$=-\frac{\chi_-(\eta_1,\alpha)\mathscr{N}^1_-(\alpha)}{\chi_-(\eta_2,\alpha)}F'_-(\alpha,b)+\frac{2k_{\text{eff}}\sin\theta_0 e^{-\iota k_{\text{eff}} b\sin\theta_0}}{(\eta_2\sin\theta_0+1)(\alpha-k_{\text{eff}}\cos\theta_0)}$$
$$\times\left[\frac{\chi_-(\eta_1,\alpha)\mathscr{N}^1_-(\alpha)}{\chi_-(\eta_2,\alpha)}-\frac{\chi_-(\eta_1,k_{\text{eff}}\cos\theta_0)\mathscr{N}^1_-(k_{\text{eff}}\cos\theta_0)}{\chi_-(\eta_2,k_{\text{eff}}\cos\theta_0)}\right]$$
$$-\sum_{m=1}^{\infty}\frac{\iota\mathfrak{L}_m}{(\alpha+\alpha_m)}\left(\frac{\cos\mathfrak{L}_m b}{\mathfrak{L}_m}+\frac{\eta_1}{\iota k_{eff}}\sin\mathfrak{L}_m b\right)$$
$$\times\left[\frac{\alpha\mathfrak{g}_m\chi_-(\eta_1,\alpha)\mathscr{N}^1_-(\alpha)}{(\alpha-\alpha_m)\chi_-(\eta_2,\alpha)}-\frac{\alpha_m\mathfrak{g}_m\chi_+(\eta_1,\alpha_m)\mathscr{N}^1_+(\alpha_m)}{2\alpha_m\chi_+(\eta_2,\alpha_m)}\right]. \tag{3.45}$$

The required solution of Wiener-Hopf equation can be obtained by using analytical continuation principle complying the extended Liouville's theorem as under

$$\frac{\chi_+(\eta_2,\alpha)\mathscr{R}^1_+(\alpha)}{\chi_+(\eta_1,\alpha)\mathscr{N}^1_+(\alpha)}=\frac{2k_{\text{eff}}\sin\theta_0 e^{-\iota k_{\text{eff}} b\sin\theta_0}\chi_-(\eta_1,k_{\text{eff}}\cos\theta_0)\mathscr{N}^1_-(k_{\text{eff}}\cos\theta_0)}{(\eta_2\sin\theta_0+1)(\alpha-k_{\text{eff}}\cos\theta_0)\chi_-(\eta_2,k_{\text{eff}}\cos\theta_0)}$$
$$-\sum_{m=1}^{\infty}\frac{\iota\alpha_m\mathfrak{L}_m\mathfrak{g}_m\ \chi_+(\eta_1,\alpha_m)\mathscr{N}^1_+(\alpha_m)}{2\alpha_m(\alpha+\alpha_m)\chi_+(\eta_2,\alpha_m)}\left(\frac{\cos\mathfrak{L}_m b}{\mathfrak{L}_m}+\frac{\eta_1}{\iota k_{\text{eff}}}\sin\mathfrak{L}_m b\right). \tag{3.46}$$

While placing equation (3.30) in equation (3.46) at $\alpha=\alpha_m$, one can obtain

$$\frac{\chi_+(\eta_2,\alpha_n)\mathscr{D}^1_n}{\chi_+(\eta_1,\alpha_n)\mathscr{N}^1_+(\alpha_n)}\left(\frac{\eta_2}{\iota k_{eff}}\mathfrak{L}_n\sin\mathfrak{L}_n b-\cos\mathfrak{L}_n b\right)\mathfrak{g}_n$$
$$=\frac{2k_{\text{eff}}\sin\theta_0 e^{-\iota k_{\text{eff}} b\sin\theta_0}\chi_-(\eta_1,k_{\text{eff}}\cos\theta_0)\mathscr{N}^1_-(k_{\text{eff}}\cos\theta_0)}{(\eta_2\sin\theta_0+1)(\alpha_n-k_{\text{eff}}\cos\theta_0)\chi_-(\eta_2,k_{\text{eff}}\cos\theta_0)}$$
$$-\sum_{m=1}^{\infty}\frac{\iota\alpha_m\mathfrak{L}_m\mathfrak{g}_m\chi_+(\eta_1,\alpha_m)\mathscr{N}^1_+(\alpha_m)}{2\alpha_m(\alpha_n+\alpha_m)\chi_+(\eta_2,\alpha_m)}\left(\frac{\cos\mathfrak{L}_m b}{\mathfrak{L}_m}+\frac{\eta_1}{\iota k_{\text{eff}}}\sin\mathfrak{L}_m b\right). \tag{3.47}$$

The above expression is the system of infinite number of algebraic equations that can be solved numerically by truncating after N terms.

3.4 THE DIFFRACTED FIELD

The diffracted field $H_z^1(x,y)$ is acquired by taking the inverse Fourier transform of $F(\alpha,y)$. On using equation (3.18), one gets

$$H_z^1(x,y)=\frac{1}{2\pi}\int_{\mathscr{L}}\frac{k_{\epsilon\mathfrak{f}\mathfrak{f}}\mathscr{R}_+^1(\alpha)}{k_{\epsilon\mathfrak{f}\mathfrak{f}}+\eta_2\mathfrak{L}(\alpha)}e^{\iota\mathfrak{L}(\alpha)(y-b)}e^{-\iota\alpha x}d\alpha. \tag{3.48}$$

Now placing the variables $\alpha=-k_{\epsilon\mathfrak{f}\mathfrak{f}}\cos t$, $x=\rho\cos\theta$ and $y=\rho\sin\theta$ in the equation (3.48) gives

$$H_z^1(\rho,\theta)=\frac{1}{2\pi}\int_{\mathscr{L}}\frac{\mathscr{R}_+^1(-k_{\epsilon\mathfrak{f}\mathfrak{f}}\cos t)}{1+\eta_2\sin t}e^{-\iota k_{\epsilon\mathfrak{f}\mathfrak{f}}b\sin t+\iota k_{\epsilon\mathfrak{f}\mathfrak{f}}\rho\cos(t-\theta)}k_{\epsilon\mathfrak{f}\mathfrak{f}}\sin t\,dt. \tag{3.49}$$

The asymptotic evaluation of the integral in the equation (3.49) can be obtained via saddle-point technique. Here, saddle-point rests at $t=\theta$, which gives

$$H_z^1(\rho,\theta)=\frac{k_{\epsilon\mathfrak{f}\mathfrak{f}}\sin\theta\mathscr{R}_+^1(-k_{\epsilon\mathfrak{f}\mathfrak{f}}\cos\theta)}{\sqrt{2\pi k_{\epsilon\mathfrak{f}\mathfrak{f}}\rho}(1+\eta_2\sin\theta)}e^{\iota k_{\epsilon\mathfrak{f}\mathfrak{f}}\rho-\frac{\iota\pi}{4}-\iota k_{\epsilon\mathfrak{f}\mathfrak{f}}b\sin\theta}. \tag{3.50}$$

On taking into account equations (3.4) and (3.46), the diffracted field takes the form

$$\begin{aligned}H_z^1(\rho,\theta)=&-\frac{k\sqrt{(\epsilon_1^2-\epsilon_2^2)/\epsilon_1}\sin\theta e^{\iota k\sqrt{(\epsilon_1^2-\epsilon_2^2)/\epsilon_1}\rho-\frac{\iota\pi}{4}-\iota k\sqrt{(\epsilon_1^2-\epsilon_2^2)/\epsilon_1}b\sin\theta}}{\sqrt{2\pi k\rho\sqrt{(\epsilon_1^2-\epsilon_2^2)/\epsilon_1}}(1+\eta_1\sin\theta)}\\
&\times\left[\left(\frac{2k\sqrt{(\epsilon_1^2-\epsilon_2^2)/\epsilon_1}\sin\theta_0 e^{-\iota k\sqrt{(\epsilon_1^2-\epsilon_2^2)/\epsilon_1}b\sin\theta_0}\chi_-(\eta_1,k_{\epsilon\mathfrak{f}\mathfrak{f}}\cos\theta_0)}{(\eta_2\sin\theta_0+1)(k\sqrt{(\epsilon_1^2-\epsilon_2^2)/\epsilon_1}\cos\theta+k\sqrt{(\epsilon_1^2-\epsilon_2^2)/\epsilon_1}\cos\theta_0)}\right)\times\right.\\
&\left(\frac{\mathscr{N}_-^1(k\sqrt{(\epsilon_1^2-\epsilon_2^2)/\epsilon_1}\cos\theta_0)\chi_-(\eta_1,k\sqrt{(\epsilon_1^2-\epsilon_2^2)/\epsilon_1}\cos\theta)\mathscr{N}_-^1(k\sqrt{(\epsilon_1^2-\epsilon_2^2)/\epsilon_1}\cos\theta)}{\chi_-(\eta_2,k\sqrt{(\epsilon_1^2-\epsilon_2^2)/\epsilon_1}\cos\theta_0)\chi_-(\eta_2,k\sqrt{(\epsilon_1^2-\epsilon_2^2)/\epsilon_1}\cos\theta)}\right)\\
&-\sum_{m=1}^{\infty}\left(\frac{\iota\alpha_m\mathfrak{L}_m\mathfrak{g}_m\,\chi_+(\eta_1,\alpha_m)\mathscr{N}_+^1(\alpha_m)\chi_-(\eta_1,k\sqrt{(\epsilon_1^2-\epsilon_2^2)/\epsilon_1}\cos\theta)}{2\alpha_m(k\sqrt{(\epsilon_1^2-\epsilon_2^2)/\epsilon_1}\cos\theta-\alpha_m)\chi_+(\eta_2,\alpha_m))}\right)\\
&\left.\times\frac{\mathscr{N}_-^1(k\sqrt{(\epsilon_1^2-\epsilon_2^2)/\epsilon_1}\cos\theta)}{\chi_-(\eta_2,k\sqrt{(\epsilon_1^2-\epsilon_2^2)/\epsilon_1}\cos\theta}\left(\frac{\cos\mathfrak{L}_m b}{\mathfrak{L}_m}+\frac{\eta_1}{\iota k\sqrt{(\epsilon_1^2-\epsilon_2^2)/\epsilon_1}}\sin\mathfrak{L}_m b\right)\right].\end{aligned} \tag{3.51}$$

3.5 COMPUTATIONAL RESULTS AND DISCUSSION

This section is devoted to analyze the numerical results for various physical parameters of interest. Fig. (3.2) shows the variation in the diffracted field amplitude versus the truncation number "N". It is clear that the effect of the truncation number is negligible for $N \geq 15$. Hence, the infinite system of algebraic equations in equation (3.47) can be managed to deal as finite. Fig. (3.3) explores the effect of separation "b" between the parallel plates on the diffracted field amplitude which shows that the diffracted field amplitude also depend upon the plate separation. While Fig. (3.4) represents the variation in diffracted field amplitude versus the incident angle "θ_0" ($0^o \leq \theta_0 \leq 90^o$). It is interesting to note that the value of diffracted field amplitude lies at 90^o when $\theta_0 = 90^o$. Whereas this peak values moves to 120^o and 150^o for $\theta_0 = 60^o$ and $\theta_0 = 30^o$, respectively. The effect of wall impedance η_1 on the amplitude of the diffracted field is shown in Fig. (3.5). Fig. (3.6) shows the variation in the diffracted field amplitude with wall impedance η_2. The effect of cold plasma permittivity has been analyzed in Figs. (3.7) and (3.8). Here, we have found that the increase in cold plasma permittivity decreases the diffracted field amplitude. In other words the diffracted field amplitude decreases with increasing ion number density in cold plasma or by decreasing plasma frequency. Here, in this problem it is observed that the diffracted field is highly effected with ϵ_1 while slightly with ϵ_2. Also it is noted that the diffracted field amplitude decreases with increase in permittivity value ϵ_1 while in case of ϵ_2 diffracted field amplitude decreases with increasing ϵ_2.

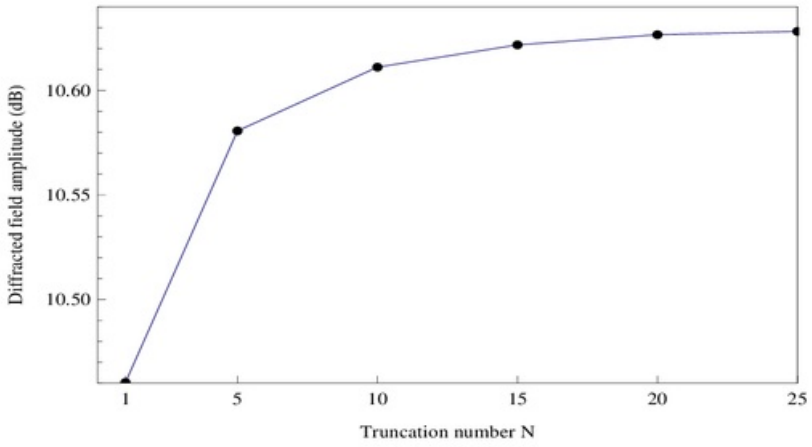

FIGURE 3.2. *Variation in the diffracted field amplitude versus "N" at* $k = 5$, $\theta_0 = 90^o$, $\theta = 60^o$, $\eta_1 = 0.3\iota$, $\eta_2 = 0.5\iota$, $\epsilon_1 = 0.8$, $\epsilon_2 = 0.1$ *and* $b = 0.2\lambda$.

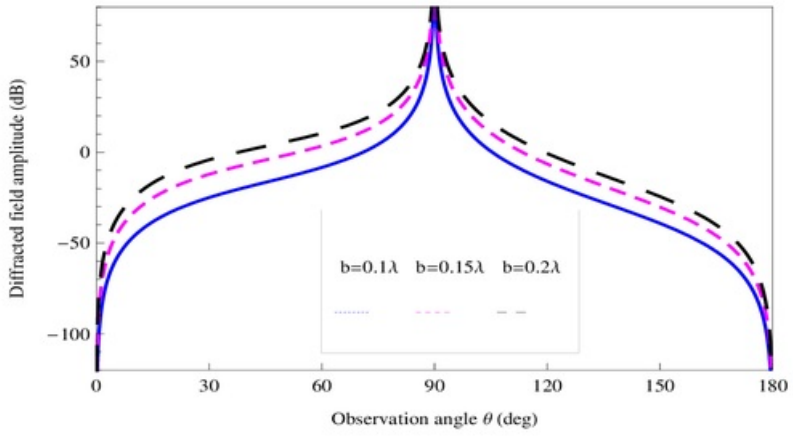

FIGURE 3.3. *Variation in the diffracted field amplitude versus "b" at* $k = 5$, $\theta_0 = 90^o$, $\eta_1 = 0.7\iota$, $\eta_2 = 0.5\iota$, $\epsilon_1 = 0.8$ *and* $\epsilon_2 = 0.1$.

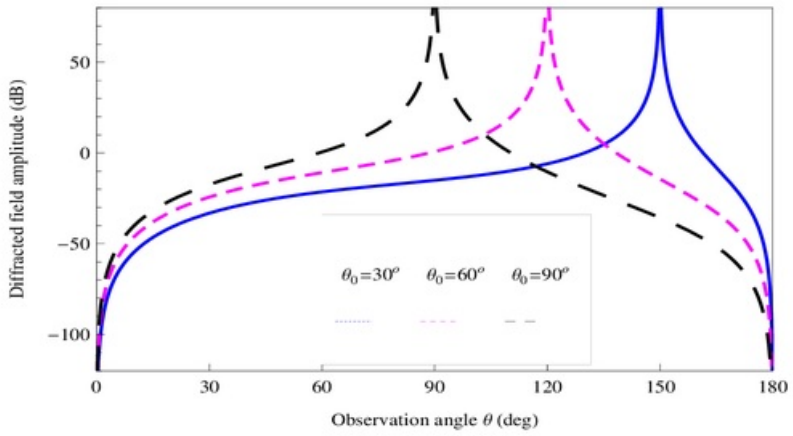

FIGURE 3.4. *Variation in the diffracted field amplitude versus "θ_0" at $k = 5$, $\eta_1 = 0.7\iota$, $\eta_2 = 0.5\iota$, $\epsilon_1 = 0.8$, $\epsilon_2 = 0.1$ and $b = 0.2\lambda$.*

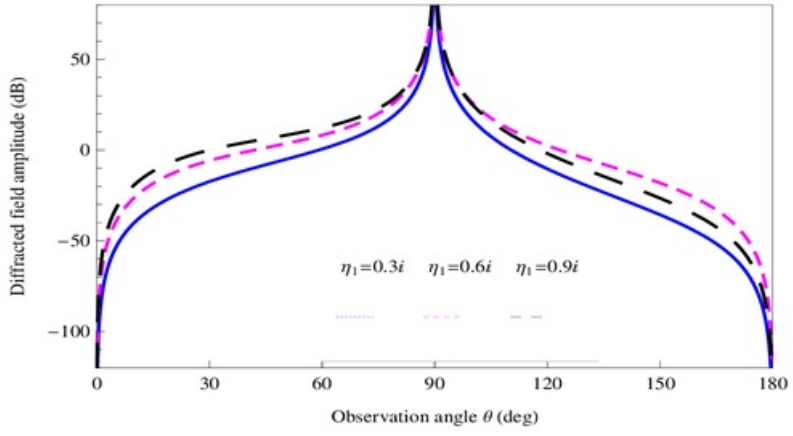

FIGURE 3.5. *Variation in the diffracted field amplitude versus "η_1" at $\theta_0 = 90^0$, $k = 5$, $\eta_2 = 0.5\iota$, $\epsilon_1 = 0.8$, $\epsilon_2 = 0.1$ and $b = 0.2\lambda$.*

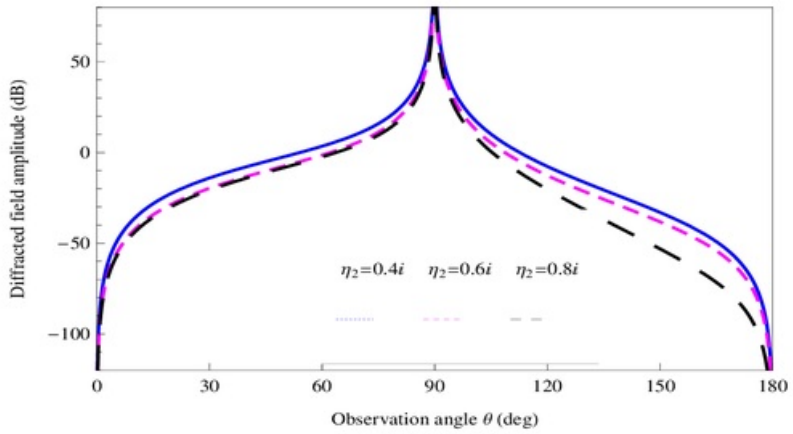

FIGURE 3.6. *Variation in the diffracted field amplitude versus "η_2" at $k = 5$, $\theta_0 = 90^0$, $\eta_1 = 0.3\iota$, $\epsilon_1 = 0.8$, $\epsilon_2 = 0.1$ and $b = 0.2\lambda$.*

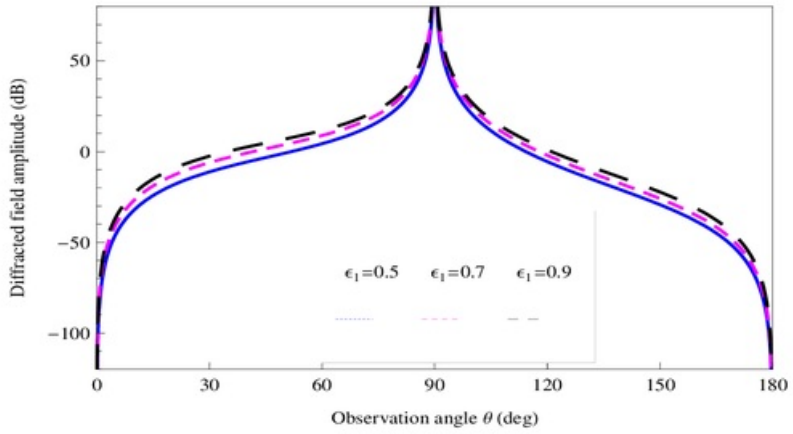

FIGURE 3.7. *Variation in the diffracted field amplitude versus "ϵ_1" at $k = 5$, $\theta_0 = 90^o$, $\eta_1 = 0.7\iota$, $\eta_2 = 0.5\iota$ $\epsilon_2 = 0.1$ and $b = 0.2\lambda$.*

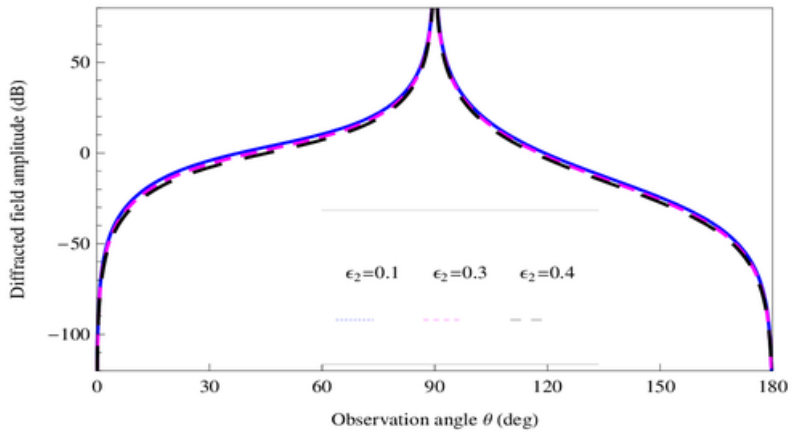

FIGURE 3.8. *Variation in the diffracted field amplitude versus "ϵ_2" at* $k = 5, \theta_0 = 90^o, \eta_1 = 0.7\iota,$ $\eta_2 = 0.5\iota\ \epsilon_1 = 0.8$ *and* $b = 0.2\lambda$.

CHAPTER 4

E-POLARIZED PLANE WAVE DIFFRACTION BY AN IMPEDANCE LOADED PARALLEL-PLATE WAVEGUIDE LOCATED IN COLD PLASMA

This chapter comprises the consideration of the diffraction of E-polarized plane wave by a waveguide designed by an infinite plane and a parallel half-plane having a different surface impedances in cold plasma. It plays an important role in diffraction theory and many problems in science and engineering. Initially, Büyükaksoy and Cinar [70] studied the problem of diffraction of a plane wave by a waveguide designed by an infinite plane and half-plane. The upper faces of the left and right part of the plane having different surface impedances. While the half-plane is parallel to the plane and perfectly conducting. This problem was solved with the help of matrix Wiener-Hopf equations. After that Cinar and Büyükaksoy [12] considered the same geometry but for different surface impedances of the half-plane instead of perfectly conducting half-plane. The solution of the problem was obtained by a hybrid method. Here, in this chapter the same geometry is considered in cold plasma.

This chapter is compiled with the subsequent order. Section (4.1) is dedicated to formulate boundary-valued problem governing the wave propagation in waveg-

uide located in cold plasma. Section (4.2) contains the formulation of Wiener-Hopf equation from the related model. The solution of the said Winer-Hopf equation is obtained in Section (4.3). Whereas Section (4.4) is devoted to the determination of infinite unknown coefficients. The diffracted field expression is presented in Section (4.5). Finally graphical results for different parameters are discussed in Section (4.6). The contents of this chapter have been published in **Physica Scripta**, 89(8): Paper ID. e095207, (2014).

4.1 MATHEMATICAL MODEL OF THE PROBLEM IN COLD PLASMA

Consider a waveguide constructed by a half-plane defined by $S_1 = \{(x, y, z) |\ x \in (-\infty, 0),\ y = b,\ z \in (-\infty, \infty)\}$ and an infinite plane defined by $S_2 = \{(x, y, z) |\ x \in (-\infty, \infty),\ y = 0,\ z \in (-\infty, \infty)\}$ designed in cold plasma. The surface impedances of the upper and lower faces of the half-plane S_1 are assumed to be $Z_1 = \eta_1 Z_0$ and $Z_2 = \eta_2 Z_0$, respectively. The surface impedances of the left and right upper faces of the plane S_2 are assumed to be $Z_3 = \eta_3 Z_0$ and $Z_4 = \eta_4 Z_0$, respectively, as shown in Fig. (4.1)

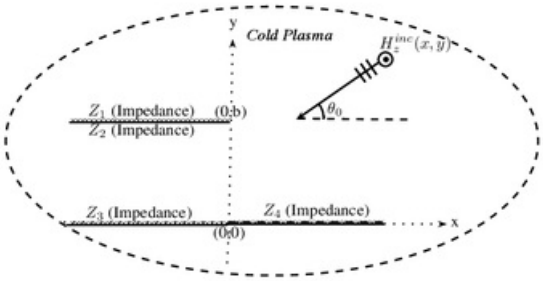

FIGURE 4.1. *Geometrical configuration of a waveguide structure in cold plasma*

For analysis purpose, it is convenient to express the total field as follows:

$$H_z^T(x,y) = \begin{cases} H_z^{inc}(x,y) + H_z^{ref}(x,y) + H_z^1(x,y), & y \in (b,\infty) \\ H_z^2(x,y)\mathscr{H}(-x) + H_z^3(x,y)\mathscr{H}(x), & y \in (0,b) \end{cases} \tag{4.1}$$

where $\mathscr{H}(x)$ represents the Heaviside unit step function. $H_z^{inc}(x,y)$ and $H_z^{ref}(x,y)$ denotes the incident and reflected fields, respectively, defined as below

$$H_z^{inc}(x,y) = e^{-\iota k_{\epsilon ff}(x\cos\theta_0 + y\sin\theta_0)} \tag{4.2}$$

and

$$H_z^{ref}(x,y) = \frac{\eta_1\sin\theta_0 - 1}{\eta_1\sin\theta_0 + 1} e^{-\iota k_{\epsilon ff}(x\cos\theta_0 - (y-2b)\sin\theta_0)}, \tag{4.3}$$

where

$$k_{\epsilon ff} = k\sqrt{\frac{\epsilon_1^2 - \epsilon_2^2}{\epsilon_1}} \quad \text{and} \quad k = \omega\sqrt{\epsilon_0\mu_0}. \tag{4.4}$$

Now, $H_z^j(x,y)$, $(j = 1,2,3)$ are scattered fields satisfying the Helmholtz equation in cold plasma as under

$$\left[\frac{\partial^2}{\partial x^2} + \frac{\partial^2}{\partial y^2} + k_{\epsilon ff}^2\right]\left[H_z^j(x,y)\right] = 0, \qquad j = 1,2,3 \tag{4.5}$$

with the following corresponding boundary conditions and continuity relations

$$\left(1 + \frac{\eta_1}{\iota k_{\epsilon ff}}\frac{\partial}{\partial y}\right) H_z^1(x,b) = 0, \qquad x \in (-\infty, 0) \tag{4.6}$$

$$\left(1 - \frac{\eta_2}{\iota k_{\epsilon ff}}\frac{\partial}{\partial y}\right) H_z^2(x,b) = 0, \qquad x \in (-\infty, 0) \tag{4.7}$$

$$\mathscr{H}(-x)\left(1 + \frac{\eta_3}{\iota k_{\epsilon ff}}\frac{\partial}{\partial y}\right) H_z^2(x,0) + \mathscr{H}(x)\left(1 + \frac{\eta_4}{\iota k_{\epsilon ff}}\frac{\partial}{\partial y}\right) H_z^3(x,0) = 0, \quad x \in (-\infty,\infty) \tag{4.8}$$

$$H_z^1(x,b) + H_z^{inc}(x,b) + H_z^{ref}(x,b) - H_z^3(x,b) = 0, \qquad x \in (0,\infty) \tag{4.9}$$

$$\frac{\partial}{\partial y}H_z^1(x,b) + \frac{\partial}{\partial y}H_z^{inc}(x,b) + \frac{\partial}{\partial y}H_z^{ref}(x,b) - \frac{\partial}{\partial y}H_z^3(x,b) = 0, \quad x \in (0,\infty) \tag{4.10}$$

$$H_z^2(0,y) - H_z^3(0,y) = 0, \qquad y \in (0,b) \tag{4.11}$$

$$\frac{\partial}{\partial x}H_z^2(0,y)-\frac{\partial}{\partial x}H_z^3(0,y)=0, \qquad y\in(0,b). \tag{4.12}$$

For the uniqueness of the boundary-value problem defined by the set of equations (4.6) - (4.12). One can take the radiation and edge conditions, respectively, as follow

$$\sqrt{\rho}\left[\frac{\partial}{\partial\rho}H_z^1(x,y)-\imath k_{\text{eff}}H_z^1(x,y)\right]=0, \quad \rho=\sqrt{x^2+y^2}\to\infty \tag{4.13}$$

and

$$H_z^T(x,y)=\mathcal{O}(|x|^{\frac{1}{2}}), \quad \frac{\partial}{\partial y}H_z^T(x,y)=\mathcal{O}(|x|^{-\frac{1}{2}}), \quad |x|\to 0. \tag{4.14}$$

4.2 FORMULATION OF WIENER-HOPF EQUATION

The Fourier transform of the Helmholtz equation in cold plasma is satisfied by the field $H_z^1(x,y)$ in the region $x\in(-\infty,\infty)$ and $y\in(b,\infty)$ gives

$$\left[\frac{d^2}{dy^2}+\mathfrak{L}^2(\alpha)\right]F(\alpha,y)=0, \tag{4.15}$$

where $F(\alpha,y)$ is defined as earlier.

The general solution of equation (4.15) satisfying the radiation condition represented by equations (4.13) yields

$$F(\alpha,y)=A_2(\alpha)e^{\imath\mathfrak{L}(\alpha)(y-b)}, \tag{4.16}$$

where

$$\mathfrak{L}(\alpha)=\sqrt{k_{\text{eff}}^2-\alpha^2}. \tag{4.17}$$

To find the unknown spectral coefficient $A_2(\alpha)$, using the boundary condition represented by the equation (4.6) in the transformed domain, one obtains

$$A_2(\alpha)=\frac{\mathscr{R}_+^2(\alpha)}{1+\frac{\eta_1}{k_{\text{eff}}}\mathfrak{L}(\alpha)}, \tag{4.18}$$

with

$$\mathscr{R}_+^2(\alpha) = F_+(\alpha, b) + \frac{\eta_1}{\iota k_{\text{eff}}} F_+'(\alpha, b). \tag{4.19}$$

Using the additive decomposition theorem and placing equation (4.48) in equation (4.16), one obtains

$$F_-(\alpha, y) + F_+(\alpha, y) = \frac{\mathscr{R}_+^2(\alpha)}{1 + \frac{\eta_1}{k_{\text{eff}}}\mathfrak{L}(\alpha)} e^{\iota\mathfrak{L}(\alpha)(y-b)}. \tag{4.20}$$

The derivative of equation (4.20) with respect to at $y = b$ takes the form

$$F_+'(\alpha, b) = \frac{\iota\mathfrak{L}(\alpha)\mathscr{R}_+^2(\alpha)}{1 + \frac{\eta_1}{k_{\text{eff}}}\mathfrak{L}(\alpha)} - F_-'(\alpha, b). \tag{4.21}$$

As the Helmholtz equation in cold plasma is satisfied by field $H_z^2(x, y)$ in the waveguide region $x \in (0, \infty)$ and $y \in (a, b)$, multiplying this equation by $e^{\iota\alpha x}$ and integrating the resultant equation with respect to x from 0 to ∞ gives

$$\left[\frac{d^2}{dy^2} - \mathfrak{L}^2(\alpha)\right] \mathscr{G}_+(\alpha, y) = \mathfrak{f}(t) - \iota\alpha\mathfrak{g}(t), \tag{4.22}$$

where

$$\mathfrak{f}(y) - \iota\alpha\mathfrak{g}(y) = \frac{\partial}{\partial x} H_z^3(0, y) - \iota\alpha H_z^3(0, y) \tag{4.23}$$

and $\mathscr{G}_+(\alpha, y)$ defined by

$$\mathscr{G}_+(\alpha, y) = \int_0^\infty H_z^3(x, y) e^{\iota\alpha x} dx, \tag{4.24}$$

is a regular function in the half-plane.

Owing the method of variation of parameter the solution of non-homogenous differential equation (3.20) yields

$$\mathscr{G}_+(\alpha,y)=C_5(\alpha)\cos\mathfrak{L}(\alpha)y+C_6(\alpha)\sin\mathfrak{L}(\alpha)y$$
$$+\frac{1}{\mathfrak{L}(\alpha)}\int_0^y(\mathfrak{f}(t)-\iota\alpha\mathfrak{g}(t))\sin\mathfrak{L}(\alpha)(b-t)dt. \tag{4.25}$$

Here $C_5(\alpha)$ and $C_6(\alpha)$ are the unknown spectral coefficients.

To find $C_5(\alpha)$, one uses the transformed form of the boundary condition represented by the equation (4.7) which gives

$$C_5(\alpha)=-\frac{\eta_4}{\iota k_{\mathfrak{eff}}}\mathfrak{L}(\alpha)C_6(\alpha). \tag{4.26}$$

Placing equation (4.26) in equation (4.25) yields

$$\mathscr{G}_+(\alpha,y)=\left[\sin\mathfrak{L}(\alpha)y-\frac{\eta_4}{\iota k_{\mathfrak{eff}}}\mathfrak{L}(\alpha)\cos\mathfrak{L}(\alpha)y\right]C_6(\alpha)$$
$$+\frac{1}{\mathfrak{L}(\alpha)}\int_0^y(\mathfrak{f}(t)-\iota\alpha\mathfrak{g}(t))\sin\mathfrak{L}(\alpha)(b-t)dt. \tag{4.27}$$

$C_6(\alpha)$ can be obtained by adding the transformed form of equations (4.9) and $\frac{\eta_1}{\iota k_{\mathfrak{eff}}}$ time of (4.10) as under

$$C_6(\alpha)=\frac{\mathscr{R}_+^2(\alpha)}{\mathfrak{L}(\alpha)\mathscr{W}_2(\alpha)}$$
$$-\frac{1}{\mathfrak{L}(\alpha)\mathscr{W}_2(\alpha)}\int_0^b(\mathfrak{f}(t)-\iota\alpha\mathfrak{g}(t))\left(\frac{\sin\mathfrak{L}(\alpha)(b-t)}{\mathfrak{L}(\alpha)}+\frac{\eta_1}{\iota k_{\mathfrak{eff}}}\cos\mathfrak{L}(\alpha)(b-t)\right)dt, \tag{4.28}$$

where

$$\mathscr{W}_2(\alpha)=\left(\frac{\eta_1-\eta_4}{\iota k_{\mathfrak{eff}}}\right)\cos\mathfrak{L}(\alpha)b+\left(1-\frac{\eta_1\eta_4}{k_{\mathfrak{eff}}^2}\mathfrak{L}^2(\alpha)\right)\frac{\sin\mathfrak{L}(\alpha)b}{\mathfrak{L}(\alpha)}. \tag{4.29}$$

Using equation (4.28) in equation (4.27), one gets

$$\mathscr{G}_+(\alpha,y)=\frac{\sin\mathfrak{L}(\alpha)y-\frac{\eta_4}{\iota k_{\mathfrak{eff}}}\mathfrak{L}(\alpha)\cos\mathfrak{L}(\alpha)y}{\mathfrak{L}(\alpha)\mathscr{W}_2(\alpha)}$$
$$\times\left[\mathscr{R}^2_+(\alpha)-\int_0^b(\mathfrak{f}(t)-\iota\alpha\mathfrak{g}(t))\left(\frac{\sin\mathfrak{L}(\alpha)(b-t)}{\mathfrak{L}(\alpha)}+\frac{\eta_1}{\iota k_{\mathfrak{eff}}}\cos\mathfrak{L}(\alpha)(b-t)\right)dt\right]$$
$$+\frac{1}{\mathfrak{L}(\alpha)}\int_0^y(\mathfrak{f}(t)-\iota\alpha\mathfrak{g}(t))\sin\mathfrak{L}(\alpha)(b-t)dt. \tag{4.30}$$

The left-hand side (i.e., $\mathscr{G}_+(\alpha,y)$) of the equation (4.30) is analytic in the upper half-plane $\mathfrak{Im}(\alpha)>\mathfrak{Im}(k_{\mathfrak{eff}}\cos\theta_0)$. However, the analyticity of the right-hand side is desecrated by the appearance of simple poles placing at the zeros of $\mathscr{W}_2(\alpha)$, i.e., $\alpha=\pm\alpha_m$ satisfying

$$\mathscr{W}_2(\pm\alpha_m)=0,\qquad \mathfrak{Im}(\alpha_m)>\mathfrak{Im}(k_{\mathfrak{eff}}),\qquad m=1,2,3.... \tag{4.31}$$

The poles in the equation (4.30) can be removed by applying the condition that the residues of these poles are zero. Then from equation (4.30), one gets

$$\mathscr{R}^2_+(\alpha_m)=\mathscr{D}^2_m\left(\frac{\eta_1}{\iota k_{eff}}\mathfrak{L}_m\sin\mathfrak{L}_m b-\cos\mathfrak{L}_m b\right)(\mathfrak{f}_m-\iota\alpha_m\mathfrak{g}_m), \tag{4.32}$$

where $\mathfrak{f}_m$ and $\mathfrak{g}_m$ are denoted by

$$\begin{bmatrix}\mathfrak{f}_m\\ \mathfrak{g}_m\end{bmatrix}=\frac{1}{\mathscr{D}^2_m}\int_0^b\begin{bmatrix}\mathfrak{f}(t)\\ \mathfrak{g}(t)\end{bmatrix}\left[\frac{\sin\mathfrak{L}_m t}{\mathfrak{L}_m}-\frac{\eta_4}{\iota k_{\mathfrak{eff}}}\cos\mathfrak{L}_m t\right]dt, \tag{4.33}$$

with

$$\mathfrak{L}_m=\sqrt{k^2_{\mathfrak{eff}}-\alpha^2_m} \tag{4.34}$$

and

$$\mathscr{D}^2_m=-\frac{\mathfrak{L}_m}{2\alpha_m}\left(\frac{\cos\mathfrak{L}_m b}{\mathfrak{L}_m}+\frac{\eta_4}{\iota k_{\mathfrak{eff}}}\sin\mathfrak{L}_m b\right)\frac{\partial}{\partial\alpha}\mathscr{W}_2(\alpha_m). \tag{4.35}$$

Hence, considering equation (4.21) and transformed domain of continuity relation given by equation (4.10), one can write

$$\begin{aligned}
&\iota\mathscr{R}_+^2(\alpha)\chi(\eta_1,\alpha) - \overset{\prime}{F}_-(\alpha,b) = -\frac{2k_{\mathfrak{eff}}\sin\theta_0 e^{-\iota k_{\mathfrak{eff}} b\sin\theta_0}}{(\eta_1\sin\theta_0+1)(\alpha-k_{\mathfrak{eff}}\cos\theta_0)} \\
&+\int_0^b (\mathfrak{f}(t)-\iota\alpha\mathfrak{g}(t))\cos\mathfrak{L}(b-t)\,dt + \frac{\cos\mathfrak{L}b+\frac{\eta_4}{\iota k_{\mathfrak{eff}}}\mathfrak{L}\sin\mathfrak{L}b}{\mathscr{W}_2(\alpha)} \\
&\times\left[\mathscr{R}_+^2(\alpha) - \int_0^b (\mathfrak{f}(t)-\iota\alpha\mathfrak{g}(t))\left(\frac{\sin\mathfrak{L}(b-t)}{\mathfrak{L}(\alpha)}+\frac{\eta_1}{\iota k_{\mathfrak{eff}}}\cos\mathfrak{L}(b-t)\right)dt\right],
\end{aligned} \tag{4.36}$$

where

$$\chi(\eta_j,\alpha) = \frac{\mathfrak{L}(\alpha)}{\eta_j\mathfrak{L}(\alpha)+k_{\mathfrak{eff}}}. \tag{4.37}$$

After simplification, equation (5.33) takes the form

$$\begin{aligned}
&\frac{\chi(\eta_1,\alpha)\mathscr{R}_+^2(\alpha)}{\chi(\eta_4,\alpha)\mathscr{N}^2(\alpha)} + \overset{\prime}{F}_-(\alpha,b) = \frac{2k_{\mathfrak{eff}}\sin\theta_0 e^{-\iota k_{\mathfrak{eff}} b\sin\theta_0}}{(\eta_1\sin\theta_0+1)(\alpha-k_{\mathfrak{eff}}\cos\theta_0)} \\
&-\frac{1}{\mathscr{W}_2(\alpha)}\int_0^b (\mathfrak{f}(t)-\iota\alpha\mathfrak{g}(t))\left(\frac{\sin\mathfrak{L}(\alpha)t}{\mathfrak{L}(\alpha)}-\frac{\eta_4}{\iota k_{\mathfrak{eff}}}\cos\mathfrak{L}(\alpha)t\right)dt,
\end{aligned} \tag{4.38}$$

where

$$\mathscr{N}^2(\alpha) = \mathscr{W}_2(\alpha)e^{\iota\mathfrak{L}(\alpha)b}. \tag{4.39}$$

Owing to equation (4.33), $\mathfrak{f}(t)$ and $\mathfrak{g}(t)$ can be expanded into a series of eigenfunctions as under

$$\begin{bmatrix}\mathfrak{f}(t)\\ \mathfrak{g}(t)\end{bmatrix} = \sum_{m=1}^{\infty}\begin{bmatrix}\mathfrak{f}_m\\ \mathfrak{g}_m\end{bmatrix}\left[\frac{\sin\mathfrak{L}_m t}{\mathfrak{L}_m}-\frac{\eta_4}{\iota k_{\mathfrak{eff}}}\cos\mathfrak{L}_m t\right]. \tag{4.40}$$

Using equation (4.40) in equation (4.38), one obtains the required Wiener-Hopf equation valid in the strip $\Im\mathfrak{m}(-k_{\mathfrak{eff}}) < \Im\mathfrak{m}(\alpha) < \Im\mathfrak{m}(k_{\mathfrak{eff}})$ as follows:

$$\frac{\chi(\eta_1,\alpha)\mathscr{R}_+^2(\alpha)}{\chi(\eta_4,\alpha)\mathscr{N}^2(\alpha)} + \overset{\prime}{F}_-(\alpha,b) = \frac{2k_{\mathfrak{eff}}\sin\theta_0 e^{-\iota k_{\mathfrak{eff}} b\sin\theta_0}}{(\eta_1\sin\theta_0+1)(\alpha-k_{\mathfrak{eff}}\cos\theta_0)} + \sum_{m=1}^{\infty}\frac{(\mathfrak{f}_m-\iota\alpha\mathfrak{g}_m)\mathfrak{L}_m}{\alpha^2-\alpha_m^2}\left(\frac{\cos\mathfrak{L}_m b}{\mathfrak{L}_m}+\frac{\eta_4}{\iota k_{\mathfrak{eff}}}\sin\mathfrak{L}_m b\right). \tag{4.41}$$

4.3 SOLUTION OF WIENER-HOPF EQUATION

To solve the Wiener-Hopf equation the kernel functions $\mathscr{N}^2(\alpha)$ and $\chi(\eta_j,\alpha))$ in equation (4.41) can be factorized by applying the known results as follows

$$\mathscr{N}_+^2(\alpha) = \left[\left(\frac{\eta_1-\eta_4}{\iota k_{\mathfrak{eff}}}\right)\cos k_{\mathfrak{eff}} b + (1-\eta_1\eta_4)\frac{\sin k_{\mathfrak{eff}} b}{k_{\mathfrak{eff}}}\right]^{\frac{1}{2}} \times \exp\left[\frac{\mathfrak{L}(\alpha)b}{\pi}\ln\left(\frac{\alpha+\iota\mathfrak{L}(\alpha)}{k_{\mathfrak{eff}}}\right)+\frac{\iota\alpha b}{\pi}\left(1-C+\ln\left[\frac{2\pi}{k_{\mathfrak{eff}}b}\right]+\iota\frac{\pi}{2}\right)\right]\prod_{m=1}^{\infty}\left(1+\frac{\alpha}{\alpha_m}\right)e^{\frac{\iota\alpha b}{m\pi}} \tag{4.42}$$

and

$$\mathscr{N}_-^2(\alpha) = \mathscr{N}_+^2(-\alpha). \tag{4.43}$$

Now, on multiplying the Wiener-Hopf equation (4.41) on both sides with $\frac{\chi_-(\eta_4,\alpha)\mathscr{N}_-^2(\alpha)}{\chi_-(\eta_1,\alpha)}$, one obtains

$$\frac{\chi_+(\eta_1,\alpha)\mathscr{R}_+^2(\alpha)}{\mathscr{N}_+^2(\alpha)\chi_+(\eta_4,\alpha)} + \frac{\overset{\prime}{F}_-(\alpha,b)\chi_-(\eta_4,\alpha)\mathscr{N}_-^2(\alpha)}{\chi_-(\eta_1,\alpha)} = \frac{2k_{\mathfrak{eff}}\sin\theta_0 e^{-\iota k_{\mathfrak{eff}} b\sin\theta_0}\chi_-(\eta_4,\alpha)\mathscr{N}_-^2(\alpha)}{(\eta_1\sin\theta_0+1)(\alpha-k_{\mathfrak{eff}}\cos\theta_0)\chi_-(\eta_1,\alpha)} + \sum_{m=1}^{\infty}\frac{(\mathfrak{f}_m-\iota\alpha\mathfrak{g}_m)\mathfrak{L}_m\chi_-(\eta_4,\alpha)\mathscr{N}_-^2(\alpha)}{(\alpha^2-\alpha_m^2)\chi_-(\eta_1,\alpha)}\left(\frac{\cos\mathfrak{L}_m b}{\mathfrak{L}_m}+\frac{\eta_4}{\iota k_{\mathfrak{eff}}}\sin\mathfrak{L}_m b\right). \tag{4.44}$$

With help of cauchy's integral formula the terms on the right-hand side of equation (4.44) can be decomposed as

$$\frac{2k_{\epsilon\mathfrak{f}\mathfrak{f}}\sin\theta_0 e^{-\iota k_{\epsilon\mathfrak{f}\mathfrak{f}} b\sin\theta_0}\chi_-(\eta_4,\alpha)\mathscr{N}_-^2(\alpha)}{(\eta_1\sin\theta_0+1)(\alpha-k_{\epsilon\mathfrak{f}\mathfrak{f}}\cos\theta_0)\chi_-(\eta_1,\alpha)} = \frac{2k_{\epsilon\mathfrak{f}\mathfrak{f}}\sin\theta_0 e^{-\iota k_{\epsilon\mathfrak{f}\mathfrak{f}} b\sin\theta_0}}{(\eta_1\sin\theta_0+1)(\alpha-k_{\epsilon\mathfrak{f}\mathfrak{f}}\cos\theta_0)}$$
$$\times\left[\frac{\chi_-(\eta_4,\alpha)\mathscr{N}_-^2(\alpha)}{\chi_-(\eta_1,\alpha)} - \frac{\chi_-(\eta_4,k_{\epsilon\mathfrak{f}\mathfrak{f}}\cos\theta_0)\mathscr{N}_-^2(k_{\epsilon\mathfrak{f}\mathfrak{f}}\cos\theta_0)}{\chi_-(\eta_1,k_{\epsilon\mathfrak{f}\mathfrak{f}}\cos\theta_0)}\right]$$
$$+\frac{2k_{\epsilon\mathfrak{f}\mathfrak{f}}\sin\theta_0 e^{-\iota k_{\epsilon\mathfrak{f}\mathfrak{f}} b\sin\theta_0}\chi_-(\eta_4,k_{\epsilon\mathfrak{f}\mathfrak{f}}\cos\theta_0)\mathscr{N}_-^2(k_{\epsilon\mathfrak{f}\mathfrak{f}}\cos\theta_0)}{(\eta_1\sin\theta_0+1)(\alpha-k_{\epsilon\mathfrak{f}\mathfrak{f}}\cos\theta_0)\chi_-(\eta_1,k_{\epsilon\mathfrak{f}\mathfrak{f}}\cos\theta_0)} \tag{4.45}$$

and

$$\sum_{m=1}^{\infty}\frac{\mathfrak{L}_m(\mathfrak{f}_m-\iota\alpha\mathfrak{g}_m)\chi_-(\eta_4,\alpha)\mathscr{N}_-^2(\alpha)}{(\alpha^2-\alpha_m^2)\chi_-(\eta_1,\alpha)}\left(\frac{\cos\mathfrak{L}_m b}{\mathfrak{L}_m}+\frac{\eta_4}{\iota k_{\epsilon\mathfrak{f}\mathfrak{f}}}\sin\mathfrak{L}_m b\right]$$
$$=\sum_{m=1}^{\infty}\frac{\mathfrak{L}_m}{(\alpha+\alpha_m)}\left(\frac{\cos\mathfrak{L}_m b}{\mathfrak{L}_m}+\frac{\eta_4}{\iota k_{\epsilon\mathfrak{f}\mathfrak{f}}}\sin\mathfrak{L}_m b\right)$$
$$\times\left[\frac{(\mathfrak{f}_m-\iota\alpha\mathfrak{g}_m)\chi_-(\eta_4,\alpha)\mathscr{N}_-^2(\alpha)}{(\alpha-\alpha_m)\chi_-(\eta_1,\alpha)}+\frac{(\mathfrak{f}_m+\iota\alpha_m\mathfrak{g}_m)\chi_+(\eta_4,\alpha_m)\mathscr{N}_+^2(\alpha_m)}{2\alpha_m\chi_+(\eta_1,\alpha_m)}\right]$$
$$-\sum_{m=1}^{\infty}\frac{\mathfrak{L}_m(\mathfrak{f}_m+\iota\alpha_m\mathfrak{g}_m)\chi_+(\eta_4,\alpha_m)\mathscr{N}_+^2(\alpha_m))}{2\alpha_m\chi_+(\eta_1,\alpha_m)(\alpha+\alpha_m)}\left(\frac{\cos\mathfrak{L}_m b}{\mathfrak{L}_m}+\frac{\eta_4}{\iota k_{\epsilon\mathfrak{f}\mathfrak{f}}}\sin\mathfrak{L}_m b\right). \tag{4.46}$$

Now using equations (4.45) and (4.46) in equation (4.44), then placing the terms which are analytic in the upper half-plane ($\mathfrak{Im}(\alpha) > -k_{\epsilon\mathfrak{f}\mathfrak{f}}$) at the left-hand side and those which analytic in lower half-plane ($\mathfrak{Im}(\alpha) < k_{\epsilon\mathfrak{f}\mathfrak{f}}$) at the right-hand side, gives

$$\frac{\chi_+(\eta_1,\alpha)\mathscr{R}_+^2(\alpha)}{\mathscr{N}_+^2(\alpha)\chi_+(\eta_4,\alpha)} - \frac{2k_{\epsilon\mathfrak{f}\mathfrak{f}}\sin\theta_0 e^{-\iota k_{\epsilon\mathfrak{f}\mathfrak{f}} b\sin\theta_0}\chi_-(\eta_4,k_{\epsilon\mathfrak{f}\mathfrak{f}}\cos\theta_0)\mathscr{N}_-^2(k_{\epsilon\mathfrak{f}\mathfrak{f}}\cos\theta_0)}{(\eta_1\sin\theta_0+1)(\alpha-k_{\epsilon\mathfrak{f}\mathfrak{f}}\cos\theta_0)\chi_-(\eta_1,k_{\epsilon\mathfrak{f}\mathfrak{f}}\cos\theta_0)}$$
$$+\sum_{m=1}^{\infty}\frac{\mathfrak{L}_m(\mathfrak{f}_m+\iota\alpha_m\mathfrak{g}_m)\chi_+(\eta_4,\alpha_m)\mathscr{N}_+^2(\alpha_m)}{2\alpha_m\chi_+(\eta_1,\alpha_m)(\alpha+\alpha_m)}\left(\frac{\cos\mathfrak{L}_m b}{\mathfrak{L}_m}+\frac{\eta_4}{\iota k_{eff}}\sin\mathfrak{L}_m b\right)$$
$$=-\frac{F_-'(\alpha,b)\chi_-(\eta_4,\alpha)\mathscr{N}_-^2(\alpha)}{\chi_-(\eta_1,\alpha)}+\sum_{m=1}^{\infty}\frac{\mathfrak{L}_m}{(\alpha+\alpha_m)}\left(\frac{\cos\mathfrak{L}_m b}{\mathfrak{L}_m}+\frac{\eta_4}{\iota k_{\epsilon\mathfrak{f}\mathfrak{f}}}\sin\mathfrak{L}_m b\right)$$
$$\times\left[\frac{(\mathfrak{f}_m-\iota\alpha\mathfrak{g}_m)\chi_-(\eta_4,\alpha)\mathscr{N}_-^2(\alpha)}{(\alpha-\alpha_m)\chi_-(\eta_1,\alpha)}+\frac{(\mathfrak{f}_m+\iota\alpha_m\mathfrak{g}_m)\chi_+(\eta_4,\alpha_m)\mathscr{N}_+^2(\alpha_m)}{2\alpha_m\chi_+(\eta_1,\alpha_m)}\right]$$
$$+\sum_{m=1}^{\infty}\frac{\mathfrak{L}_m}{(\alpha+\alpha_m)}\left(\frac{\cos\mathfrak{L}_m b}{\mathfrak{L}_m}+\frac{\eta_4}{\iota k_{\epsilon\mathfrak{f}\mathfrak{f}}}\sin\mathfrak{L}_m b\right)$$
$$\times\left[\frac{(\mathfrak{f}_m-\iota\alpha\mathfrak{g}_m)\chi_-(\eta_4,\alpha)\mathscr{N}_-^2(\alpha)}{(\alpha-\alpha_m)\chi_-(\eta_1,\alpha)}+\frac{(\mathfrak{f}_m+\iota\alpha_m\mathfrak{g}_m)\chi_+(\eta_4,\alpha_m)\mathscr{N}_+^2(\alpha_m)}{2\alpha_m\chi_+(\eta_1,\alpha_m)}\right]. \tag{4.47}$$

The required solution of Wiener-Hopf equation can be obtained by using analytical continuation principle following the extended Liouville's theorem gives

$$\frac{\chi_+(\eta_1,\alpha)\mathscr{R}^2_+(\alpha)}{\chi_+(\eta_4,\alpha)\mathscr{N}_+(\alpha)} = \frac{2k_{\text{eff}}\sin\theta_0 e^{-\iota k_{\text{eff}} b\sin\theta_0}\chi_-(\eta_4,k_{\text{eff}}\cos\theta_0)\mathscr{N}^2_-(k_{\text{eff}}\cos\theta_0)}{(\eta_1\sin\theta_0+1)(\alpha-k_{\text{eff}}\cos\theta_0)\chi_-(\eta_1,k_{\text{eff}}\cos\theta_0)}$$
$$-\sum_{m=1}^{\infty}\frac{(\mathfrak{f}_m+\iota\alpha_m\mathfrak{g}_m)\mathfrak{L}_m}{2\alpha_m(\alpha+\alpha_m)}\left(\frac{\cos\mathfrak{L}_m b}{\mathfrak{L}_m}+\frac{\eta_4}{\iota k_{\text{eff}}}\sin\mathfrak{L}_m b\right)\frac{\chi_+(\eta_4,\alpha_m)\mathscr{N}^2_+(\alpha_m)}{\chi_+(\eta_1,\alpha_m)}. \tag{4.48}$$

4.4 DETERMINATION OF THE UNKNOWN COEFFICIENTS

The equation (4.48) contains infinite number of unknown coefficients. To find out these unknown coefficients one uses method of Mode-Matching technique with the Fourier transform [70]. The Mode-Matching technique enables us to declare the field components defined in the waveguide region in terms of normal modes, as

$$H^2_z(x,y) = \sum_{m=1}^{\infty} a_n\left(\frac{\sin\zeta_n y}{\zeta_n}-\frac{\eta_3}{\iota k_{\text{eff}}}\cos\zeta_n y\right)e^{-\iota\beta_n x}, \tag{4.49}$$

where

$$\beta_n = \sqrt{k^2_{\text{eff}}-\zeta^2_n}, \quad \Im\mathfrak{m}(\beta_n) > \Im\mathfrak{m}(k_{\text{eff}}), \quad n=1,2,3,.... \tag{4.50}$$

To find β_n and ζ_n, placing equations (4.49) in equation (4.7) gives

$$\frac{(\eta_3+\eta_2)}{\iota k_{\text{eff}}}\cos\zeta_n b-(1+\frac{\eta_2\eta_3}{k^2_{\text{eff}}}\zeta^2_n)\frac{\sin\zeta_n y}{\zeta_n}=0, \qquad n=1,2,3,.... \tag{4.51}$$

Using equations (4.40) and (4.49) in equation (4.23), then multiplying the resulting equation by $(\frac{\sin\mathfrak{L}_j y}{\mathfrak{L}_j}-\frac{\eta_4}{\iota k_{\text{eff}}}\cos\mathfrak{L}_j y)$ and integrating with respect to y from $y=0$ to $y=b$, one obtains

$$\mathfrak{f}_m-\iota\alpha_m\mathfrak{g}_m = -\frac{\iota}{\mathscr{D}^2_m}\sum_{n=1}^{\infty}\mathfrak{a}_n(\alpha+\beta_n)\Delta_{nm}, \tag{4.52}$$

where Δ_{nm} is

$$\Delta_{nm} = \frac{(\eta_3 - \eta_4)}{\iota k_{\text{eff}}(\zeta_n^2 - \mathfrak{L}_m^2)} + \frac{(\eta_2 + \eta_1)\mathfrak{L}_m \zeta_n}{\iota k_{\text{eff}}(\zeta_n^2 - \mathfrak{L}_m^2)} \left(\frac{\cos \zeta_n b}{\zeta_n} + \frac{\eta_3}{\iota k_{\text{eff}}} \sin \zeta_n b \right) \times \left(\frac{\cos \mathfrak{L}_m b}{\mathfrak{L}_m} + \frac{\eta_4}{\iota k_{\text{eff}}} \sin \mathfrak{L}_m b \right). \tag{4.53}$$

Placing equation (4.52) in equation (4.32), then using the resulting equation in equation (4.48) to yield

$$\sum_{n=1}^{\infty} \mathscr{A}_n(\alpha_j)\mathfrak{a}_n = I(\alpha_j), \qquad j = 1,2,3,..., \tag{4.54}$$

where

$$\mathscr{A}_n(\alpha_j) = -\iota \left(\frac{\eta_1}{k_{\text{eff}}} \mathfrak{L}_j \sin \mathfrak{L}_j b - \cos \mathfrak{L}_m b \right)(\alpha_j + \beta_n)\Delta_{nj} - \frac{\iota \mathscr{N}_+^2(\alpha_j)\chi_+(\eta_4, \alpha_j)}{\chi_+(\eta_1, \alpha_j)} \sum_{m=1}^{\infty} \frac{\mathfrak{L}_m(\beta_n - \alpha_m)\Delta_{nm}}{2\alpha_m \mathscr{D}_m^2(\alpha_j + \alpha_m)} \left(\frac{\cos \mathfrak{L}_m b}{\mathfrak{L}_m} + \frac{\eta_4}{\iota k} \sin \mathfrak{L}_m b \right) \frac{\chi_+(\eta_4, \alpha_m)\mathscr{N}_+^2(\alpha_m)}{\chi_+(\eta_1, \alpha_m)}, \tag{4.55}$$

and

$$I(\alpha_j) = \frac{2k_{\text{eff}} \sin\theta_0 e^{-\iota k_{\text{eff}} b \sin\theta_0} \chi_-(\eta_4, k_{\text{eff}} \cos\theta_0)\mathscr{N}_-^2(k_{\text{eff}} \cos\theta_0)\mathscr{N}_+^2(\alpha_j)\chi_+(\eta_4, \alpha_j)}{(\eta_1 \sin\theta_0 + 1)(\alpha_j - k_{\text{eff}} \cos\theta_0)\chi_+(\eta_1, \alpha_j)\chi_-(\eta_1, k_{\text{eff}} \cos\theta_0)}. \tag{4.56}$$

The infinite system of algebraic equations represented by equation (4.54) is solved numerically. To solve this infinite system of algebraic equations we have truncated it after first N terms in order to obtain required diffracted field.

4.5 THE DIFFRACTED FIELD

The diffracted field $H_z^1(x, y)$ is acquired redby taking the inverse Fourier transform of $F(\alpha, y)$. By using equation (4.20), one obtains

$$H_z^1(x, y) = \frac{1}{2\pi} \int_{\mathscr{L}} \frac{\mathscr{R}_+^2(\alpha)}{1 + \frac{\eta_1}{k_{\text{eff}}} \mathfrak{L}(\alpha)} e^{\iota \mathfrak{L}(\alpha)(y-b)} e^{-\iota \alpha x} d\alpha. \tag{4.57}$$

Using the change of variables $\alpha = -k_{\text{eff}}\cos t$, $x = \rho\cos\theta$ and $y = \rho\sin\theta$ in the equation (4.57), one yields

$$H_z^1(\rho,\theta) = \frac{1}{2\pi}\int_{\mathscr{L}} \frac{\mathscr{R}_+^2(-k_{\text{eff}}\cos t)k_{\text{eff}}\sin t}{1+\eta_1\sin t} e^{-\iota k_{\text{eff}}\sin t + \iota k_{\text{eff}}\rho\cos(t-\theta)}\,dt. \tag{4.58}$$

The asymptotic evaluation of the integral in the equation (4.58) can be obtained via saddle-point technique. Here, saddle-point rests at $t=\theta$ whose contribution is

$$H_z^1(\rho,\theta) = P_1(P_2+P_2), \tag{4.59}$$

where

$$P_1 = \left(\frac{k\sqrt{(\epsilon_1^2-\epsilon_2^2)/\epsilon_1}\sin\theta e^{\iota k\rho\sqrt{(\epsilon_1^2-\epsilon_2^2)/\epsilon_1}-\iota\frac{\pi}{4}-\iota k\sqrt{(\epsilon_1^2-\epsilon_2^2)/\epsilon_1}b\sin\theta}}{\sqrt{2\pi k\rho}(1+\eta_1\sin t)}\right) \times\left(\frac{\chi_-(\eta_4,k\sqrt{(\epsilon_1^2-\epsilon_2^2)/\epsilon_1}\cos\theta_0)\mathscr{N}_-(k\sqrt{(\epsilon_1^2-\epsilon_2^2)/\epsilon_1}\cos\theta_0)}{\chi_-(\eta_1,k\sqrt{(\epsilon_1^2-\epsilon_2^2)/\epsilon_1}\cos\theta_0)}\right), \tag{4.60}$$

$$P_2 = \left(\frac{2k\sqrt{(\epsilon_1^2-\epsilon_2^2)}\sin\theta_0 e^{-\iota k\sqrt{(\epsilon_1^2-\epsilon_2^2)/\epsilon_1}b\sin\theta_0}\mathscr{N}_-(k\sqrt{(\epsilon_1^2-\epsilon_2^2)/\epsilon_1}\cos\theta_0)}{\sqrt{\epsilon_1}(\eta_1\sin\theta_0+1)(\cos\theta+\cos\theta_0)}\right) \times\left(\frac{\chi_-(\eta_4,k\sqrt{(\epsilon_1^2-\epsilon_2^2)/\epsilon_1}\cos\theta_0)}{\chi_-(\eta_1,k\sqrt{\times(\epsilon_1^2-\epsilon_2^2)/\epsilon_1}\cos\theta_0)}\right) \tag{4.61}$$

and

$$P_3 = \sum_{m=1}^{\infty}\left(\frac{(\mathfrak{f}_m+\iota\alpha_m\mathfrak{g}_m)\mathfrak{L}_m}{2\alpha_m(\alpha_m-(k\sqrt{(\epsilon_1^2-\epsilon_2^2)/\epsilon_1}\cos\theta))}\frac{\chi_+(\eta_4,\alpha_m)\mathscr{N}_+(\alpha_m)}{\chi_+(\eta_1,\alpha_m)}\right) \times\left(\frac{\cos\mathfrak{L}_m b}{\mathfrak{L}_m}+\frac{\eta_4}{\iota k\sqrt{(\epsilon_1^2-\epsilon_2^2)/\epsilon_1}}\sin\mathfrak{L}_m b\right). \tag{4.62}$$

4.6 COMPUTATIONAL RESULTS AND DISCUSSION

In this section, we have analyzed and potted the numerical results for various physical parameters of interest. Fig. (4.2) depicts the variation in the diffracted field amplitude versus the truncation number "N". It is apparent that the effect of the truncation number is negligible for $N \geq 80$. Hence, the infinite system of algebraic equations in equation (4.54) can be managed to deal as finite. Fig. (4.3) explores the effect of separation between the parallel plates on the diffracted field amplitude. The amplitude of the diffracted field decreases with the increase of wall impedance $|\eta_1|$ as shown in Fig. (4.4). Figs. (4.5) and (4.6) show that the diffracted field amplitude is not affected by impedances η_2 and η_3, which is similar to the result obtained by Cinar and Büyükaksoy [12]. Fig. (4.7) shows the variation in the diffracted field amplitude with wall impedance η_4. The effect of cold plasma permittivity values ϵ_1 and ϵ_2 has been analyzed in Fig. (4.8) and (4.9), respectively. Here, we have found that the increase in cold plasma permittivity value ϵ_1 highly decreases the diffracted field amplitude while the effect of ϵ_1 is negligibly small. In other words the diffracted field amplitude decreases with increasing ion number density in cold plasma or by decreasing plasma frequency. Here, in this problem it is observed that the diffracted field is highly effected with ϵ_1 while slightly with ϵ_2.

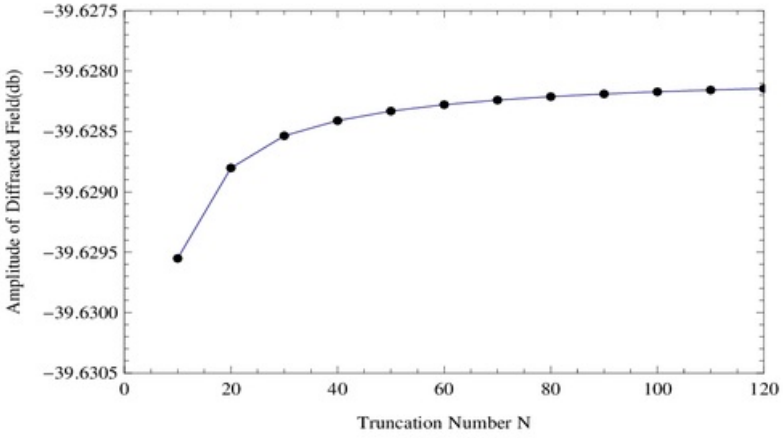

FIGURE 4.2. *Variation in the diffracted field amplitude versus truncation number "N" at* $\theta_0 = 90^o$, $\theta = 45^o$, $k = 5$, $\eta_1 = 0.3\iota$, $\eta_2 = 0.9\iota$, $\eta_3 = 0.6\iota$, $\eta_4 = 0.4\iota$, $\epsilon_1 = 0.8$, $\epsilon_2 = 0.0$ *and* $b = 0.2\lambda$.

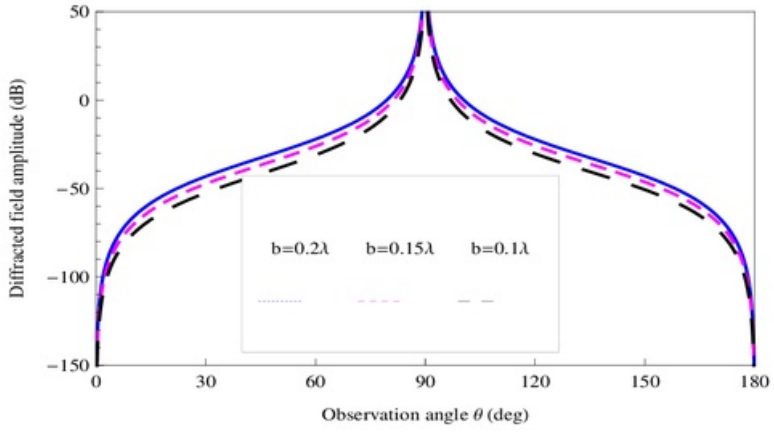

FIGURE 4.3. *Variation in the diffracted field amplitude versus "b" at* $\theta_0 = 90^o$, $k = 5$, $\eta_1 = 0.6\iota$, $\eta_2 = 0.4\iota$, $\eta_3 = 0.7\iota$, $\eta_4 = 0.5\iota$, $\epsilon_1 = 0.8$ *and* $\epsilon_2 = 0$.

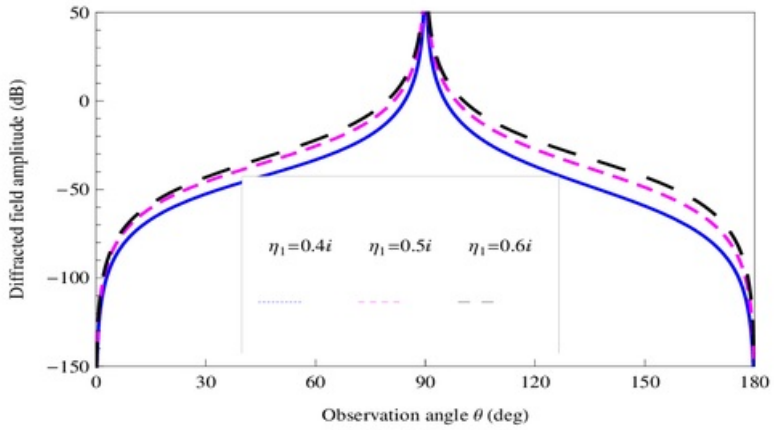

FIGURE 4.4. *Variation in the diffracted field amplitude versus "η_1" at $\phi_0 = 90^o$, $k = 5$, $\eta_2 = 0.4\iota$, $\eta_3 = 0.7\iota$, $\eta_4 = 0.5\iota$, $t\epsilon_1 = 0.8$, $\epsilon_2 = 0$ and $b = 0.2\lambda$.*

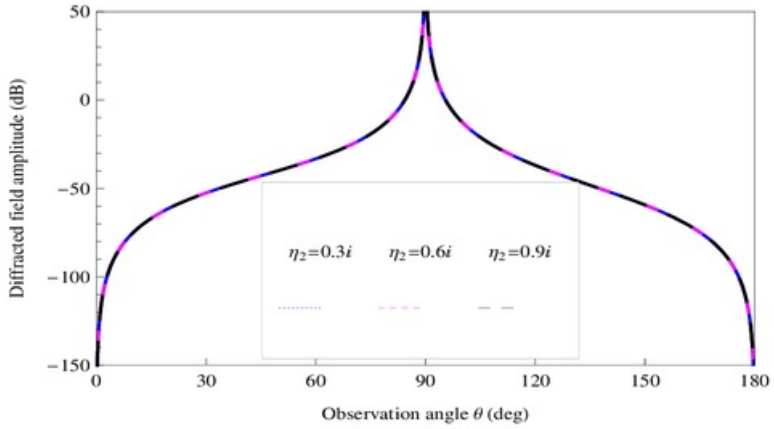

FIGURE 4.5. *Variation in the diffracted field amplitude versus "η_2" at $\theta_0 = 90^o$, $k = 5$, $\eta_1 = 0.4\iota$, $\eta_3 = 0.7\iota$, $\eta_4 = 0.5\iota$, $\epsilon_1 = 0.8$, $\epsilon_2 = 0$ and $b = 0.2\lambda$.*

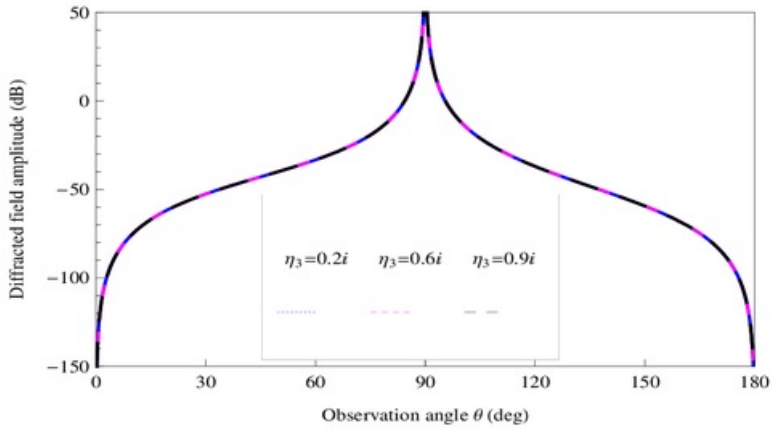

FIGURE 4.6. *Variation in the diffracted field amplitude versus "η_3" at $\theta_0 = 90^o$, $k = 5$, $\eta_1 = 0.4\iota$, $\eta_2 = 0.3\iota$, $\eta_4 = 0.5\iota$, $\epsilon_1 = 0.8$, $\epsilon_2 = 0$ and $b = 0.2\lambda$.*

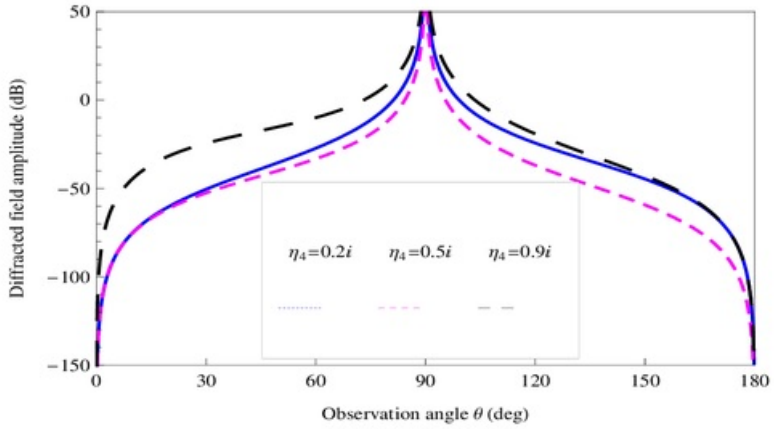

FIGURE 4.7. *Variation in the diffracted field amplitude versus "η_4" at $\theta_0 = 90^o$, $k = 5$, $\eta_1 = 0.4\iota$, $\eta_2 = 0.3\iota$, $\eta_3 = 0.5\iota$, $\epsilon_1 = 0.8$, $\epsilon_2 = 0$ and $b = 0.2\lambda$.*

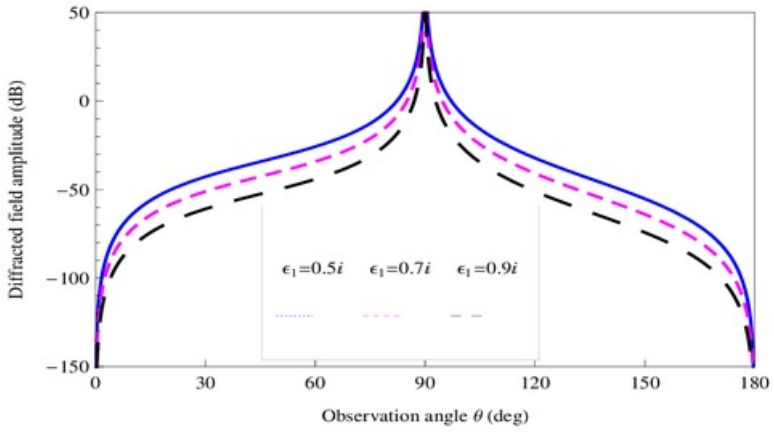

FIGURE 4.8. *Variation in the diffracted field amplitude versus "ϵ_1" at $\theta_0 = 90^o$, $k = 5$, $\eta_1 = 0.4\iota$, $\eta_2 = 0.3\iota$, $\eta_3 = 0.5\iota$, $\eta_4 = 0.7$, $\epsilon_2 = 0$ and $b = 0.2\lambda$.*

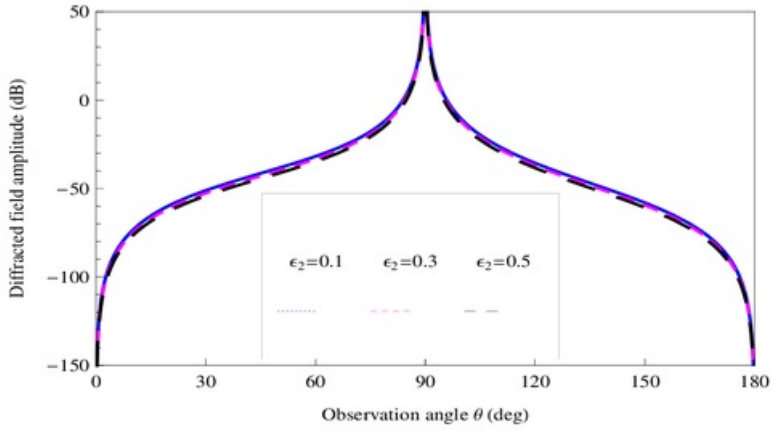

FIGURE 4.9. *Variation in the diffracted field amplitude versus "ϵ_2" at $\theta_0 = 90^o$, $k = 5$, $\eta_1 = 0.4\iota$, $\eta_2 = 0.3\iota$, $\eta_3 = 0.5\iota$, $\eta_4 = 0.7$, $\epsilon_1 = 0.9$ and $b = 0.2\lambda$.*

CHAPTER 5

EFFECT OF COLD PLASMA PERMITTIVITY ON THE RADIATION OF THE DOMINANT TEM-WAVE BY AN IMPEDANCE LOADED PARALLEL-PLATE WAVEGUIDE RADIATOR

In this chapter, the aim is to determine the effect of cold plasma permittivity and other parameters on the radiation phenomenon. For this purpose an impedance coated parallel-plate waveguide radiator located in cold plasma is considered. This radiation phenomenon was initially considered by Rulf and Hurd [86]. According to them, the presence of surface impedances $+Z_1$ on the upper and $-Z_1$ on the lower faces is the merely combination of impedances that converts the boundary-valued problem into a scalar Wiener-Hopf equation. After that Büyükaksoy and Birbir [41] generalized the problem for different upper and lower faces surface impedances and solved by the hybrid method consisting of Fourier transform with Mode Matching technique.

The section wise summery of this chapter is arranged as follow. Section (5.1) consists of boundary-valued problem for radiation phenomenon obtained from the geometry of the problem. Using this mathematical model, the Wiener-Hopf

equation is formulated in Section (5.2) while the solution of Wiener-Hopf equation is obtained in Section (5.3). In Section (5.4) the infinite number of unknown coefficients are determined. The mathematical expression for the radiated field is obtained in Section (5.5) whereas the numerical results are shown in Section (5.6). The contents of this chapter are published in **Mathematical Methods in the Applied Sciences**, *DOI* : 10.1002/*mma*.3464.

5.1 MATHEMATICAL MODEL OF THE PROBLEM

Here, we consider the radiation of the dominant transverse electromagnetic wave (TEM-wave) which is incident from the left in the parallel-plate waveguide region formed by two-part impedance plane S_1 define by $\{(x,y,z)|\ x\in(-\infty,\infty),\ y=0,\ z\in(-\infty,\infty)\}$ and a parallel impedance half-plane S_2 defined by $\{(x,y,z)|\ x\in(-\infty,0),\ y=b,\ z\in(-\infty,\infty)\}$. The left and right parts of the plane S_1 are coated by the impedances Z_1 and Z_2, respectively. The surface impedance of the lower and upper faces of the half-plane S_2 are assumed to be Z_3 and Z_4, respectively, as shown in Fig. (5.1).

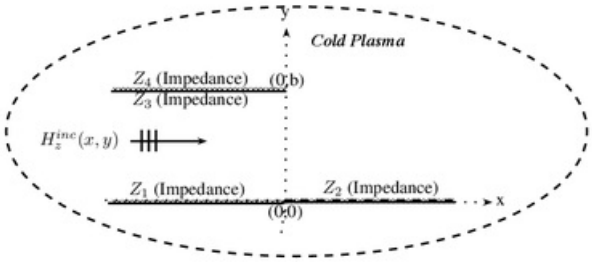

FIGURE 5.1. *Geometry of the impedance loaded parallel-plate waveguide radiator located in cold plasma*

The total field can be expressed as follows:

$$H_z^T(x,y)=\begin{cases} H_z^1(x,y), & y\in(b,\infty)\\ \left[H_z^{inc}(x,y)+H_z^2(x,y)\right]\mathscr{H}(-x)+H_z^3(x,y)\mathscr{H}(x), & y\in(0,b), \end{cases} \tag{5.1}$$

where $\mathscr{H}(x)$ denotes the Heaviside unit step function, $H_z^{inc}(x,y)$ is the incident field given by

$$H_z^{inc}(x,y) = e^{\iota k_{\text{eff}} x}, \tag{5.2}$$

with

$$k_{\text{eff}} = k\sqrt{\frac{\epsilon_1^2 - \epsilon_2^2}{\epsilon_1}} \quad \text{and} \quad k = \omega\sqrt{\epsilon_0\mu_0}. \tag{5.3}$$

$H_z^j \quad (j = 1,2,3)$ are the scattered fields satisfy the Helmholtz's equation in cold plasma

$$\left[\frac{\partial^2}{\partial x^2} + \frac{\partial^2}{\partial y^2} + k_{\text{eff}}^2\right]\left[H_z^j(x,y)\right] = 0, \tag{5.4}$$

with the following corresponding boundary conditions and continuity relations

$$\left(\eta_4 k_{\text{eff}} + \frac{\partial}{\partial y}\right) H_z^1(x,b) = 0, \qquad x \in (-\infty, 0), \tag{5.5}$$

$$\left(\eta_3 k_{\text{eff}} - \frac{\partial}{\partial y}\right) H_z^2(x,b) = 0, \qquad x \in (-\infty, 0), \tag{5.6}$$

$$\mathscr{H}(-x)\left(\eta_1 k_{\text{eff}} + \frac{\partial}{\partial y}\right) H_z^2(x,0) + \mathscr{H}(x)\left(\eta_2 k_{\text{eff}} + \frac{\partial}{\partial y}\right) H_z^3(x,0) = 0, \quad x \in (-\infty, \infty), \tag{5.7}$$

$$H_z^1(x,b) = H_z^3(x,b), \qquad x \in (0,\infty), \tag{5.8}$$

$$\frac{\partial}{\partial y} H_z^1(x,b) = \frac{\partial}{\partial y} H_z^3(x,b), \qquad x \in (0,\infty), \tag{5.9}$$

$$H_z^{inc}(0,y) + H_z^2(0,y) = H_z^3(0,y), \qquad y \in (0,b), \tag{5.10}$$

$$\frac{\partial}{\partial x} H_z^{inc}(0,y) + \frac{\partial}{\partial x} H_z^2(0,y) = \frac{\partial}{\partial x} H_z^3(0,y), \qquad y \in (0,b). \tag{5.11}$$

The radiation and edge conditions are discussed as earlier.

5.2 FORMULATION OF WIENER-HOPF EQUATION

Fourier transform of the Helmholtz equation in cold plasma is satisfied by the field $H_z^1(x,y)$ in the waveguide region $x \in (-\infty,\infty)$ and $y \in (b,\infty)$ gives

$$\left[\frac{d^2}{dy^2} + (k_{\text{eff}}^2 - \alpha^2)\right] F(\alpha, y) = 0, \tag{5.12}$$

With the help of radiation condition solution of equation (5.12) leads to

$$F(\alpha, y) = A_3(\alpha) e^{\iota \mathfrak{L}(\alpha)(y-b)}, \tag{5.13}$$

where

$$\mathfrak{L}(\alpha) = \sqrt{k_{\text{eff}}^2 - \alpha^2}. \tag{5.14}$$

To find the unknown coefficient $A_3(\alpha)$, using the transformed domain of the boundary condition represented by the equation (5.5), one obtains

$$A_3(\alpha) = \frac{\mathscr{R}_+^3(\alpha)}{\eta_4 k_{\text{eff}} + \iota \mathfrak{L}(\alpha)}, \tag{5.15}$$

with

$$\mathscr{R}_+^3(\alpha) = \eta_4 k_{\text{eff}} F_+(\alpha, b) + \overset{\prime}{F}_+(\alpha, b), \tag{5.16}$$

where the prime sign in equation (5.16) denotes the derivative with respect to y. On using the additive decomposition theorem and equation (5.15) in equation (5.13), one gets

$$F_+(\alpha, y) + F_-(\alpha, y) = \frac{\mathscr{R}_+^3(\alpha)}{\eta_4 k_{\text{eff}} + \iota \mathfrak{L}(\alpha)} e^{\iota \mathfrak{L}(\alpha)(y-b)}. \tag{5.17}$$

The derivative of equation (5.17) with respect to y at $y = b$ takes the form

$$\overset{\prime}{F}_+(\alpha, b) = \frac{\iota \mathfrak{L}(\alpha) \mathscr{R}_+^3(\alpha)}{\eta_4 k_{\text{eff}} + \iota \mathfrak{L}(\alpha)} - \overset{\prime}{F}_-(\alpha, b). \tag{5.18}$$

As in equation (5.4), the Helmholtz equation in cold plasma is satisfied by field $H_z^2(x, y)$ in the waveguide region $x \in (0, \infty)$ and $y \in (a, b)$, multiplying this equation by $e^{\iota \alpha x}$ and integrating the resultant equation with respect to x from 0 to ∞ yields

$$\left[\frac{d^2}{dy^2} - \mathfrak{L}^2(\alpha)\right] \mathscr{G}_+(\alpha, y) = \mathfrak{f}(t) - \iota \alpha \mathfrak{g}(t), \tag{5.19}$$

where

$$\mathfrak{f}(y) - \iota\alpha\mathfrak{g}(y) = \frac{\partial}{\partial x} H_z^3(0,y) - \iota\alpha H_z^3(0,y) \tag{5.20}$$

and $\mathscr{G}_+(\alpha, y)$ defined by

$$\mathscr{G}_+(\alpha, y) = \int_0^\infty H_z^3(x,y) e^{\iota\alpha x} dx, \tag{5.21}$$

is a regular function in the half-plane.

Owing the method of variation of parameter the solution of the non-homogenous differential equation (5.19) gives

$$\begin{aligned}\mathscr{G}_+(\alpha, y) &= C_7(\alpha)\cos\mathfrak{L}(\alpha)y + C_8(\alpha)\sin\mathfrak{L}(\alpha)y \\ &+ \frac{1}{\mathfrak{L}(\alpha)}\int_0^y (\mathfrak{f}(t) - \iota\alpha\mathfrak{g}(t))\sin\mathfrak{L}(\alpha)(b-t)dt,\end{aligned} \tag{5.22}$$

where $C_7(\alpha)$ and $C_8(\alpha)$ are the unknown spectral coefficients.

To find $C_8(\alpha)$ applying the transformed form of the boundary condition represented by the equation (5.7), one gets

$$C_8(\alpha) = -\frac{\eta_2 k_{\mathfrak{eff}}}{\mathfrak{L}(\alpha)} C_7(\alpha). \tag{5.23}$$

Placing equation (5.23) in equation (5.22) yields

$$\begin{aligned}\mathscr{G}_+(\alpha, y) &= \left[\cos\mathfrak{L}(\alpha)y - \eta_2 k_{\mathfrak{eff}}\frac{\sin\mathfrak{L}(\alpha)y}{\mathfrak{L}(\alpha)}\right] C_7(\alpha) \\ &+ \frac{1}{\mathfrak{L}(\alpha)}\int_0^y (\mathfrak{f}(t) - \iota\alpha\mathfrak{g}(t))\sin\mathfrak{L}(\alpha)(b-t)dt.\end{aligned} \tag{5.24}$$

$C_7(\alpha)$ can be obtained by adding the transformed form of equation (5.9) and $\eta_4 k_{eff}$ times of equation (5.8) gives

$$C_7(\alpha) = \frac{\mathscr{R}_+^2(\alpha)}{\mathscr{W}_3(\alpha)} - \frac{1}{\mathfrak{L}(\alpha)\mathscr{W}_3(\alpha)} \int_0^b ((\mathfrak{f}(t) - \iota\alpha\mathfrak{g}(t)) \left(\eta_4 k_{eff} \sin \mathfrak{L}(\alpha)(b-t) + \mathfrak{L}(\alpha) \cos \mathfrak{L}(\alpha)(b-t)\right) dt, \quad (5.25)$$

where $$\mathscr{W}_3(\alpha) = (\eta_4 - \eta_2) k_{eff} \cos \mathfrak{L}(\alpha) b - (1 + \eta_2 \eta_4 k_{eff}^2) \frac{\sin \mathfrak{L}(\alpha) b}{\mathfrak{L}(\alpha)}. \quad (5.26)$$

Substituting equation (5.25) in equation (5.24) gives

$$\mathscr{G}_+(\alpha, y) = \frac{\mathfrak{L}(\alpha) \cos \mathfrak{L}(\alpha) y - k_{eff} \eta_2 \sin \mathfrak{L}(\alpha) y}{\mathfrak{L}(\alpha)\mathscr{W}_3(\alpha)} \times \left\{ \mathscr{R}_+^3(\alpha) - \int_0^b (\mathfrak{f}(t) - \iota\alpha\mathfrak{g}(t)) \left(\cos \mathfrak{L}(\alpha)(b-t) + k_{eff}\eta_4 \frac{\sin \mathfrak{L}(\alpha)(b-t)}{\mathfrak{L}(\alpha)} \right) dt \right\} + \frac{1}{\mathfrak{L}(\alpha)} \int_0^y (\mathfrak{f}(t) - \iota\alpha\mathfrak{g}(t)) \sin \mathfrak{L}(\alpha)(y-t) dt. \quad (5.27)$$

The left-hand side (i.e., $\mathscr{G}_+(\alpha, y)$) of the equation (5.27) is analytic in the region $\mathfrak{Im}(\alpha) > \mathfrak{Im}(k_{eff} \cos\theta_0)$. However, the analyticity of the right-hand side is desecrated due to the appearance of simple poles lying at the zeros of $\mathscr{W}_3(\alpha)$, i.e., $\alpha = \pm\alpha_m$ satisfying

$$\mathscr{W}_3(\pm\alpha_m) = 0, \quad \mathfrak{Im}(\alpha_m) > \mathfrak{Im}(k_{eff}), \quad m = 1, 2, 3.... \quad (5.28)$$

The poles in the equation (5.27) can be removed by enforcing the condition that residues of these poles are zero. Then from equation (5.27), one obtains

$$\mathscr{R}_+^3(\alpha_m) = \mathscr{D}_m^3(\mathfrak{f}_m - \iota\alpha_m\mathfrak{g}_m) \left(\cos \mathfrak{L}_m b + k_{eff}\eta_4 \frac{\sin \mathfrak{L}_m b}{\mathfrak{L}_m} \right), \quad (5.29)$$

where $\mathfrak{f}_m$ and $\mathfrak{g}_m$ are denoted by

$$\begin{bmatrix} \mathfrak{f}_m \\ \mathfrak{g}_m \end{bmatrix} = \frac{1}{\mathscr{D}_m^3} \int_0^b \begin{bmatrix} \mathfrak{f}(t) \\ \mathfrak{g}(t) \end{bmatrix} \left[\cos \mathfrak{L}_m t - \eta_2 k_{\mathfrak{eff}} \frac{\sin \mathfrak{L}_m t}{\mathfrak{L}_m} \right] dt, \tag{5.30}$$

with

$$\mathfrak{L}_m = \sqrt{k_{\mathfrak{eff}}^2 - \alpha_m^2}\,, \tag{5.31}$$

and

$$\mathscr{D}_m^3 = \frac{1}{2\alpha_m} \left(\cos \mathfrak{L}_m b - \eta_2 k_{\mathfrak{eff}} \frac{\sin \mathfrak{L}_m b}{\mathfrak{L}_m} \right) \frac{\partial}{\partial \alpha} \mathscr{W}_3(\alpha_m). \tag{5.32}$$

Hence, considering equation (5.17) and the Fourier transform of the continuity relation given by equation (5.8), one can write

$$\begin{aligned} &\frac{\mathscr{R}_+^3(\alpha)}{\eta_4 k_{\mathfrak{eff}} + \imath \mathfrak{L}(\alpha)} - F_-(\alpha, b) = \frac{\mathfrak{L}(\alpha) \cos \mathfrak{L}(\alpha) b - k_{\mathfrak{eff}} \eta_2 \sin \mathfrak{L}(\alpha) b}{\mathfrak{L}(\alpha) \mathscr{W}_3(\alpha)} \\ &\times \left\{ \mathscr{R}_+^3(\alpha) - \int_0^b (\mathfrak{f}(t) - \imath \alpha \mathfrak{g}(t)) \left(\cos \mathfrak{L}(\alpha)(b-t) + k_{\mathfrak{eff}} \eta_4 \frac{\sin \mathfrak{L}(\alpha)(b-t)}{\mathfrak{L}(\alpha)} \right) dt \right\} \\ &+ \frac{1}{\mathfrak{L}(\alpha)} \int_0^b (\mathfrak{f}(t) - \imath \alpha \mathfrak{g}(t)) \sin \mathfrak{L}(\alpha)(b-t) dt. \end{aligned} \tag{5.33}$$

After simplification the above expression takes the form

$$\begin{aligned} &\frac{\eta_2 \chi(\frac{\imath}{\eta_4}, \alpha) \mathscr{R}_+^3(\alpha)}{\eta_4 \chi(\frac{\imath}{\eta_2}, \alpha) \mathscr{N}^3(\alpha)} + F_-(\alpha, b) \\ &= \frac{1}{\mathscr{W}_3(\alpha)} \int_0^b [\mathfrak{f}(t) - \imath \alpha \mathfrak{g}(t)] \left[\cos \mathfrak{L}(\alpha) t - k_{\mathfrak{eff}} \eta_2 \frac{\sin \mathfrak{L}(\alpha) t}{\mathfrak{L}(\alpha)} \right] dt, \end{aligned} \tag{5.34}$$

with

$$\chi(\eta_j, \alpha) = \frac{\mathfrak{L}(\alpha)}{\eta_j \mathfrak{L}(\alpha) + k_{\mathfrak{eff}}} \quad \text{and} \quad \mathscr{N}^3(\alpha) = \mathscr{W}_3(\alpha) e^{\imath \mathfrak{L}(\alpha) b}, \tag{5.35}$$

and $\mathfrak{f}(t)$ and $\mathfrak{g}(t)$ are expanded into a series of eigen-functions as

$$\begin{bmatrix} \mathfrak{f}(t) \\ \mathfrak{g}(t) \end{bmatrix} = \sum_{m=1}^{\infty} \begin{bmatrix} \mathfrak{f}_m \\ \mathfrak{g}_m \end{bmatrix} \left[\cos \mathfrak{L}_m t - \eta_2 k_{\mathfrak{eff}} \frac{\sin \mathfrak{L}_m t}{\mathfrak{L}_m} \right]. \tag{5.36}$$

Using equation (5.36) into equation (5.34), one gets the required Wiener-Hopf equation valid within the strip $\mathfrak{Im}(-k_{\mathfrak{eff}}) < \mathfrak{Im}(\alpha) < \mathfrak{Im}(k_{\mathfrak{eff}})$ as follow:

$$\frac{\eta_2 \chi(\frac{\iota}{\eta_4}, \alpha) \mathscr{R}_+^3(\alpha)}{\eta_4 \chi(\frac{\iota}{\eta_2}, \alpha) \mathscr{N}^3(\alpha)} + F_-(\alpha, b) = \sum_{m=1}^{\infty} \frac{\mathfrak{f}_m - \iota\alpha \mathfrak{g}_m}{\alpha^2 - \alpha_m^2} \left(\cos \mathfrak{L}_m b - k_{\mathfrak{eff}} \eta_2 \frac{\sin \mathfrak{L}_m b}{\mathfrak{L}_m} \right). \tag{5.37}$$

5.3 SOLUTION OF WIENER-HOPF EQUATION

To obtain the required solution of Wiener-Hopf equation the kernel functions $\mathscr{N}^3(\alpha)$ and $\chi(\eta_j, \alpha))$ in equation (5.37) can be factorized by applying the known results as follows

$$\begin{aligned} \mathscr{N}_+^3(\alpha) &= \left[k_{\mathfrak{eff}} (\eta_4 - \eta_2) \cos k_{\mathfrak{eff}} b - k_{\mathfrak{eff}} (1 + \eta_2 \eta_4) \sin k_{\mathfrak{eff}} b \right]^{\frac{1}{2}} \\ &\times \exp \left[\frac{\mathfrak{L}(\alpha) b}{\pi} \ln \left(\frac{\alpha + \iota \mathfrak{L}(\alpha)}{k_{\mathfrak{eff}}} \right) + \frac{\iota \alpha b}{\pi} \left(1 - C + \ln [\frac{2\pi}{k_{\mathfrak{eff}} b}] + \iota \frac{\pi}{2} \right) \right] \prod_{m=1}^{\infty} \left(1 + \frac{\alpha}{\alpha_m} \right) e^{\frac{\iota \alpha b}{m\pi}} \end{aligned} \tag{5.38}$$

and

$$\mathscr{N}_-^3(\alpha) = \mathscr{N}_+^3(-\alpha), \tag{5.39}$$

where the factors of $\chi(\eta_j, \alpha)$ and C are discussed in earlier chapters.
Now, multiplying the Wiener-Hopf equation (5.37) on both sides with $\frac{\chi_-(\frac{\iota}{\eta_2}, \alpha)\, \mathscr{N}_-^3(\alpha)}{\chi_-(\frac{\iota}{\eta_4}, \alpha)}$, one obtains

$$\begin{aligned} &\frac{\eta_2 \chi_+(\frac{\iota}{\eta_4}, \alpha) \mathscr{R}_+^3(\alpha)}{\eta_4 \chi_+(\frac{\iota}{\eta_2}, \alpha) \mathscr{N}_+^3(\alpha)} + \frac{\chi_-(\frac{\iota}{\eta_2}, \alpha) \mathscr{N}_-^3(\alpha)}{\chi_-(\frac{\iota}{\eta_4}, \alpha)} F_-(\alpha, b) \\ &= \frac{\chi_-(\frac{\iota}{\eta_2}, \alpha) \mathscr{N}_-^3(\alpha)}{\chi_-(\frac{\iota}{\eta_4}, \alpha)} \sum_{m=1}^{\infty} \frac{\mathfrak{f}_m - \iota\alpha \mathfrak{g}_m}{\alpha^2 - \alpha_m^2} \left(\cos \mathfrak{L}_m b + k_{\mathfrak{eff}} \eta_2 \frac{\sin \mathfrak{L}_m b}{\mathfrak{L}_m} \right) \end{aligned} \tag{5.40}$$

With help of cauchy integral formula the terms on right-hand of the equation (5.40) can be decomposed as

$$\begin{aligned}
&\frac{\chi_-(\frac{\iota}{\eta_2},\alpha)\mathcal{N}_-^3(\alpha)}{\chi_-(\frac{\iota}{\eta_4},\alpha)}\sum_{m=1}^{\infty}\frac{\mathfrak{f}_m-\iota\alpha\mathfrak{g}_m}{\alpha^2-\alpha_m^2}\left(\cos\mathfrak{L}_m b+k_{\mathfrak{eff}}\eta_2\frac{\sin\mathfrak{L}_m b}{\mathfrak{L}_m}\right)\\
&=\sum_{m=1}^{\infty}\frac{1}{\alpha+\alpha_m}\left(\cos\mathfrak{L}_m b+k_{\mathfrak{eff}}\eta_2\frac{\sin\mathfrak{L}_m b}{\mathfrak{L}_m}\right)\\
&\left[\frac{(\mathfrak{f}_m-\iota\alpha\mathfrak{g}_m)\chi_-(\frac{\iota}{\eta_2},\alpha)\mathcal{N}_-^3(\alpha)}{(\alpha-\alpha_m)\chi_-(\frac{\iota}{\eta_4},\alpha)}+\frac{(\mathfrak{f}_m+\iota\alpha\mathfrak{g}_m)\chi_+(\frac{\iota}{\eta_2},\alpha)\mathcal{N}_+^3(\alpha)}{2\alpha_m\chi_+(\frac{\iota}{\eta_4},\alpha)}\right]\\
&-\sum_{m=1}^{\infty}\left(\cos\mathfrak{L}_m b+k_{\mathfrak{eff}}\eta_2\frac{\sin\mathfrak{L}_m b}{\mathfrak{L}_m}\right)\frac{(\mathfrak{f}_m+\iota\alpha\mathfrak{g}_m)\chi_+(\frac{\iota}{\eta_2},\alpha)\mathcal{N}_+^3(\alpha)}{2\alpha_m(\alpha+\alpha_m)\chi_+(\frac{\iota}{\eta_4},\alpha)}.
\end{aligned}\tag{5.41}$$

Now using equation (5.41) in equation (5.40) and then placing all those terms on the left-hand side which are analytic in the region ($\Im\mathfrak{m}(\alpha)>-k_{\mathfrak{eff}}$) and the terms which are analytic in the region ($\Im\mathfrak{m}(\alpha)<k_{\mathfrak{eff}}$) on the right-hand side which yields

$$\begin{aligned}
&\frac{\eta_2\chi_+(\frac{\iota}{\eta_4},\alpha)\mathscr{R}_+(\alpha)}{\eta_4\chi_+(\frac{\iota}{\eta_2},\alpha)\mathcal{N}_+(\alpha)}+\sum_{m=1}^{\infty}\left(\cos\mathfrak{L}_m b+k_{\mathfrak{eff}}\eta_2\frac{\sin\mathfrak{L}_m b}{\mathfrak{L}_m}\right)\frac{(\mathfrak{f}_m+\iota\alpha\mathfrak{g}_m)\chi_+(\frac{\iota}{\eta_2},\alpha)\mathcal{N}_+(\alpha)}{2\alpha_m(\alpha+\alpha_m)\chi_+(\frac{\iota}{\eta_4},\alpha)}\\
&=-\frac{\chi_-(\frac{\iota}{\eta_2},\alpha)\mathcal{N}_-(\alpha)}{\chi_-(\frac{\iota}{\eta_4},\alpha)}F_-(\alpha,b)+\sum_{m=1}^{\infty}\frac{1}{\alpha+\alpha_m}\left(\cos\mathfrak{L}_m b+k_{\mathfrak{eff}}\eta_2\frac{\sin\mathfrak{L}_m b}{\mathfrak{L}_m}\right)\\
&\left[\frac{(\mathfrak{f}_m-\iota\alpha\mathfrak{g}_m)\chi_-(\frac{\iota}{\eta_2},\alpha)\mathcal{N}_-(\alpha)}{(\alpha-\alpha_m)\chi_-(\frac{\iota}{\eta_4},\alpha)}+\frac{(\mathfrak{f}_m+\iota\alpha\mathfrak{g}_m)\chi_+(\frac{\iota}{\eta_2},\alpha)\mathcal{N}_+(\alpha)}{2\alpha_m\chi_+(\frac{\iota}{\eta_4},\alpha)}\right].
\end{aligned}\tag{5.42}$$

The required solution of Wiener-Hopf equation can be obtained by using analytical continuation principle following Liouville's theorem gives

$$\begin{aligned}
&\frac{\eta_2\chi_+(\frac{\iota}{\eta_4},\alpha)\mathscr{R}_+^3(\alpha)}{\eta_4\chi_+(\frac{\iota}{\eta_2},\alpha)\mathcal{N}_+^3(\alpha)}=\\
&-\sum_{m=1}^{\infty}\frac{(\mathfrak{f}_m+\iota\alpha_m\mathfrak{g}_m)}{2\alpha_m(\alpha+\alpha_m)}\left(\cos\mathfrak{L}_m b-k_{\mathfrak{eff}}\eta_2\frac{\sin\mathfrak{L}_m b}{\mathfrak{L}_m}\right)\frac{\chi_+(\frac{\iota}{\eta_2},\alpha_m)\mathcal{N}_+^3(\alpha_m)}{\chi_+(\frac{\iota}{\eta_4},\alpha_m)}.
\end{aligned}\tag{5.43}$$

5.4 DETERMINATION OF THE UNKNOWN COEFFICIENTS

The equation(5.43) contains infinite number of unknown coefficients. In order to determine these unknown coefficients we employ the well-known Mode-Matching technique along with the Fourier transform. The Mode-Matching technique is a standard method to handle the waveguide structures. This technique has been used extensively [87, 88] to analyze the scattered field at the junction. In this investigation the Mode-Matching technique enables us to declare the field component defined in the waveguide region in terms of normal modes as

$$H_z^2(x,y) = \sum_{n=1}^{\infty} a_n \left(\cos\zeta_n y - k_{\text{eff}}\eta_1 \frac{\sin\zeta_n y}{\zeta_n}\right) e^{-\iota\beta_n x}, \tag{5.44}$$

where

$$\beta_n = \sqrt{k_{\text{eff}}^2 - \zeta_n^2}, \quad \Im\mathfrak{m}(\beta_n) > \Im\mathfrak{m}(k_{\text{eff}}), \quad n = 1,2,3,.... \tag{5.45}$$

β_n's and ζ_n's can be obtained by using equations (5.6) together with (5.44) as under

$$k_{\text{eff}}(\eta_1+\eta_3)\cos\zeta_n b + (\zeta_n^2 - k_{\text{eff}}^2\eta_1\eta_3)\frac{\sin\zeta_n y}{\zeta_n} = 0, \qquad n = 0,1,2,3,.... \tag{5.46}$$

Placing the continuity relations represented by the equations (5.10) and (5.11) in equation (5.20), one yields

$$\mathfrak{f}(y) - \iota\alpha\mathfrak{g}(y) = \iota(k_{\text{eff}} - \alpha) + \frac{\partial}{\partial x}H_z^2(0,y) - \iota\alpha H_z^2(0,y). \tag{5.47}$$

Substituting equations (5.44) and (5.30) in equation (5.47), then multiplying the resulting equation by $(\frac{\sin\mathfrak{L}_j y}{\mathfrak{L}_j} - \frac{\eta_4}{\iota k_{\text{eff}}}\cos\mathfrak{L}_j y)$ and integrating from $y = 0$ to $y = b$, one obtains

$$\mathfrak{f}_m - \iota\alpha_m\mathfrak{g}_m = \frac{\iota(k_{\text{eff}} - a)}{\mathscr{D}_m^3\mathfrak{L}_m^2}\left(k_{\text{eff}}\eta_2\cos\mathfrak{L}_m b + \mathfrak{L}_m\sin\mathfrak{L}_m b - k_{\text{eff}}\eta_2\right)$$
$$- \frac{\iota}{\mathscr{D}_m^3}\sum_{n=1}^{\infty}\mathfrak{a}_n(\alpha+\beta_n)\Delta_{nm}, \tag{5.48}$$

where Δ_{nm} is

$$\Delta_{nm} = \frac{k_{\text{eff}}(\eta_2-\eta_1)}{\zeta_n^2-\mathfrak{L}_m^2} - \frac{k_{\text{eff}}(\eta_3+\eta_4)}{\zeta_n^2-\mathfrak{L}_m^2}\left(\cos\zeta_n b - k_{\text{eff}}\eta_1\frac{\sin\zeta_n b}{\zeta_n}\right) \times\left(\cos\mathfrak{L}_m b - k_{\text{eff}}\eta_2\frac{\sin\mathfrak{L}_m b}{\mathfrak{L}_m}\right). \tag{5.49}$$

Substituting equation (5.48) into equation (5.29) and then using the resulting equation into equation (5.43) to yield

$$\sum_{n=1}^{\infty}\mathscr{A}_n(\alpha_j)\mathfrak{a}_n = I(\alpha_j), \qquad j=1,2,3,\ldots \tag{5.50}$$

where

$$\mathscr{A}_n(\alpha_j) = -\iota(\alpha_j+\beta_n)\Delta_{nj}\left(\cos\mathfrak{L}_j b + k_{\text{eff}}\eta_4\frac{\sin\mathfrak{L}_j b}{\mathfrak{L}_j}\right) + \frac{\iota\eta_4^2\mathscr{N}_+^3(\alpha_j)\chi_+(\frac{\iota}{\eta_2},\alpha_j)}{\eta_2^2\chi_+(\frac{\iota}{\eta_4},\alpha_j)}\sum_{m=1}^{\infty}\frac{(\beta_n-\alpha_m)\Delta_{nm}}{2\alpha_m\mathscr{D}_m^3(\alpha_j+\alpha_m)} \times\left(\cos\mathfrak{L}_m b + k_{\text{eff}}\eta_4\frac{\sin\mathfrak{L}_m b}{\mathfrak{L}_m}\right)\frac{\chi_+(\frac{\iota}{\eta_2},\alpha_m)\mathscr{N}_+^3(\alpha_m)}{\chi_+(\frac{\iota}{\eta_4},\alpha_m)} \tag{5.51}$$

and

$$I(\alpha_j) = \iota(k_{\text{eff}}-\alpha_j)\left(\cos\mathfrak{L}_j b + k_{\text{eff}}\eta_4\frac{\sin\mathfrak{L}_j b}{\mathfrak{L}_j}\right)\left(\frac{\sin\mathfrak{L}_j b}{\mathfrak{L}_j} + k_{\text{eff}}\eta_2\frac{\cos\mathfrak{L}_j b}{\mathfrak{L}_j} - \frac{k_{\text{eff}}\eta_2}{\mathfrak{L}_j^2}\right) + \frac{\eta_4^2\chi_+(\frac{\iota}{\eta_2},\alpha_j)\mathscr{N}_+^3(\alpha_j)}{\eta_2^2\chi_+(\frac{\iota}{\eta_4},\alpha_j)}\sum_{m=1}^{\infty}\frac{\iota(k_{\text{eff}}+\alpha_m)}{2\alpha_m\mathscr{D}_m^3(\alpha_j+\alpha_m)}\left(\frac{\sin\mathfrak{L}_m b}{\mathfrak{L}_m} + k_{\text{eff}}\eta_2\frac{\cos\mathfrak{L}_m b}{\mathfrak{L}_m} - \frac{\eta_2 k_{\text{eff}}}{\mathfrak{L}_m^2}\right) \times\left(\cos\mathfrak{L}_m b + k_{\text{eff}}\eta_2\frac{\sin\mathfrak{L}_m b}{\mathfrak{L}_m}\right)\frac{\chi_+(\frac{\iota}{\eta_2},\alpha_m)\mathscr{N}_+^3(\alpha_m)}{\chi_+(\frac{\iota}{\eta_4},\alpha_m)}. \tag{5.52}$$

The infinite system of algebraic equations represented by equation (5.50) is solved numerically. To solve this infinite system of algebraic equations we have truncated it after first N terms in order to obtain required radiated field.

5.5 RADIATED FIELD

The radiated field $H_z^1(x,y)$ is obtained by taking the inverse Fourier transform of $F(\alpha,y)$. By using equation (5.17), one obtains

$$H_z^1(x,y)=\frac{1}{2\pi}\int_{\mathscr{L}}\frac{\mathscr{R}_+^3(\alpha)}{\eta_4 k_{\text{eff}}+\iota\mathfrak{L}(\alpha)}e^{\iota\mathfrak{L}(\alpha)(\alpha)(y-b)}e^{-\iota\alpha x}d\alpha. \tag{5.53}$$

Using the change of variables $\alpha=-k_{\text{eff}}\cos t$, $x=\rho\cos\theta$ and $y=\rho\sin\theta$ in the equation (5.53), one obtains

$$H_z^1(\rho,\theta)=\frac{1}{2\pi}\int_{\mathscr{L}}\frac{\mathscr{R}_+^3(-k_{\text{eff}}\cos t)k_{\text{eff}}\sin t}{\eta_2+\iota\sin t}e^{-\iota k_{\text{eff}}\sin t+\iota k_{\text{eff}}\rho\cos(t-\theta)}dt. \tag{5.54}$$

The integral in equation (5.53) can be evaluated asymptotically through the saddle point technique. Here, saddle point occurs at $t=\theta$. On taking into account equations (5.3) and (5.43), the radiated field takes the form:

$$\begin{aligned}
&H_z^1(\rho,\theta)=\\
&-\frac{\eta_2^2 k\sqrt{(\epsilon_1^2-\epsilon_2^2)/\epsilon_1}\sin\theta e^{\iota k\rho\sqrt{(\epsilon_1^2-\epsilon_2^2)/\epsilon_1}-\iota\frac{\pi}{4}}\chi_-(\frac{\iota}{\eta_2},k\sqrt{(\epsilon_1^2-\epsilon_2^2)/\epsilon_1}\cos\theta)}{\sqrt{2\pi k\rho}(\eta_2+\sin t)\eta_4^2\chi_-(\frac{\iota}{\eta_4},k\sqrt{(\epsilon_1^2-\epsilon_2^2)/\epsilon_1}\cos\theta)}\\
&\times\left[\left(\sum_{m=1}^{\infty}\frac{(\mathfrak{f}_m+\iota\alpha_m\mathfrak{g}_m)\chi_+(\frac{\iota}{\eta_2},\alpha_m)\mathscr{N}_+^3(\alpha_m)\mathscr{N}_-^3(k\sqrt{(\epsilon_1^2-\epsilon_2^2)/\epsilon_1}\cos\theta)}{2\alpha_m(\alpha_m-(k\sqrt{(\epsilon_1^2-\epsilon_2^2)/\epsilon_1}\cos\theta))\chi_+(\frac{\iota}{\eta_4},\alpha_m)}\right)\right.\\
&\left.\times\left(\cos\mathfrak{L}_m b-\eta_2 k\sqrt{(\epsilon_1^2-\epsilon_2^2)/\epsilon_1}\frac{\sin\mathfrak{L}_m b}{\mathfrak{L}_m}\right)\right].
\end{aligned} \tag{5.55}$$

5.6 COMPUTATIONAL RESULTS AND DISCUSSION

In this section, we have presented some useful numerical results to show the effects of various physical parameters of interest on the radiated field amplitude. Actually the solution of Wiener-Hopf equation contains a set of infinitely many constants satisfying an infinite system of algebraic equations. To solve this

infinite system of algebraic equations we have truncated it after N terms in order to obtain the required radiated field. Fig. (5.2) illustrates the variation in the radiated field amplitude versus the truncation number "N". It is apparent that the effect of the truncation number is negligible for $N > 20$. Hence, the infinite system of algebraic equations in equation (5.50) can be managed to deal as finite. Fig. (5.3) shows the variation in the radiated field amplitude with increasing plate separation parameter b. Clearly, the radiated (diffracted) field amplitude enhances when we increase the ratio b/λ. Physically, such an increase in the diffracted field amplitude is due to the fact that plate separation parameter b becomes comparable to the wavelength λ of the incident wave. The amplitude will be maximum for $b/\lambda = 1$. Figs. (5.4) and (5.5) shows the variation in the radiated field amplitude with impedances η_1 and η_2 both for inductive and capacitative cases. Fig. (5.4) shows that in case of η_1 (for capacitative and inductive cases) the amplitude decreases with increasing impedance where as for η_2 (See Fig. (5.5)) for capacitative case the amplitude decreases and for inductive case it rises. Fig. (5.6) explores the effect of η_3 (both for capacitative and inductive cases) wherein the amplitude decreases with increasing impedance, however, the case is different for the variation of η_4 as shown in Fig. (5.7). These impedance dependent variations are actually related to the magnetic and electric susceptibilities of the waveguide surfaces. Actually, the surface impedances Z_j ($j = 1,2,3,4$) are normalized by Z_0 i.e., $Z_j = \eta_4 Z_0$. Here $Z_0 = \sqrt{\mu_0/\epsilon_0}$ is the characteristic impedance of surrounding medium and μ_0 and ϵ_0 are, respectively, the magnetic permeability and dielectric permittivity of the free space. Since the surface impedances of a conductive medium (plasma) are imaginary in magnitude, that is, $Z = \sqrt{i\omega\mu/(\sigma + i\omega\epsilon)}$, where σ is conductivity of cold plasma, so in the present model it would be taken as complex. Z in the normalized form is $\eta = \sqrt{i\omega\mu/(\sigma + i\omega\epsilon)}/Z_0$, which for free space becomes unity. Fig. (5.8) demonstrates the effect of cold plasma permittivity ϵ_1 on the radiation

phenomenon. The radiated field amplitude is effected drastically in the presence of an anisotropic plasma medium. The field amplitude enhances with increasing plasma permittivity ϵ_1, actually for fixed number densities of ions and electrons in cold plasma, the parameter increases with the increase in incident wave frequency ω, i.e., $\epsilon_1 \approx 1 - (\frac{\omega_p}{\omega})^2$ (for high frequency signal). The electric field of such a high frequency signal oscillates the electrons about the cold ionic centers and such oscillating electrons then radiate enormously thereby increasing the amplitude of the radiated field. Fig. (5.9) demonstrates the effect of parameter ϵ_2 on the radiated field amplitude. Clearly, the amplitude of the radiated field diminishes with the increase in parameter ϵ_2. Actually, the increase in the parameter ϵ_2 leads to the decrease in the signal frequency for which the electron oscillation under the low frequency of incident wave diminishes the radiated amplitude. The results obtained in this work can be a useful knot in order to improve the radiated signal quality transmitted by an artificial satellite in the ionosphere for communication means to an earth station.

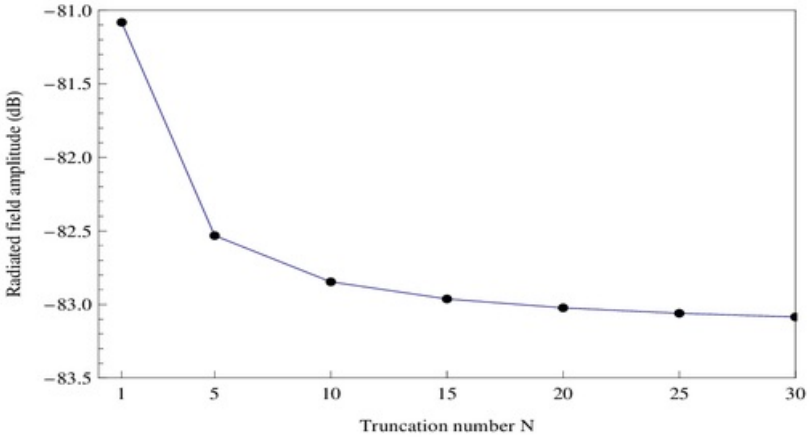

FIGURE 5.2. *Variation in the radiated field amplitude versus truncation number "N". The other parameters are* $\theta = 45^o$ $\eta_1 = 0.2$, $\eta_2 = 0.5$, $\eta_3 = 0.3$, $\eta_4 = 0.6$, $\epsilon_1 = 0.8$, $\epsilon_2 = 0$, $k = 5$ *and* $b = 0.2\lambda$.

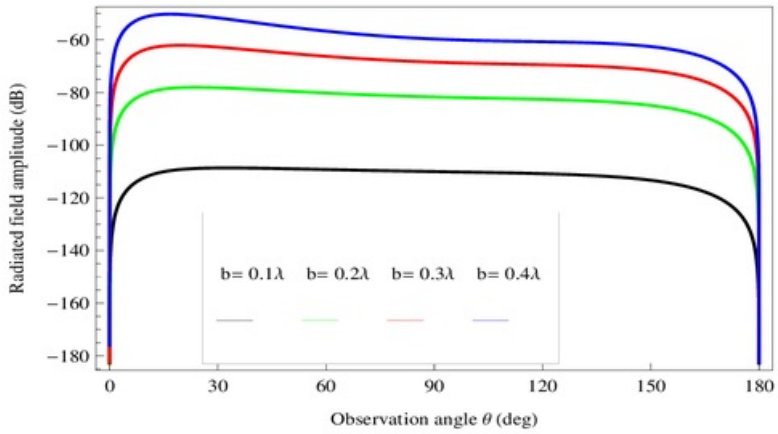

FIGURE 5.3. *Variation in the radiated field amplitude versus "b". The other parameters are* $k = 5$, $\eta_1 = 0.5$, $\eta_2 = 0.3$, $\eta_3 = 0.6$, $\eta_4 = 0.7$, $\epsilon_1 = 0.8$ *and* $\epsilon_2 = 0$.

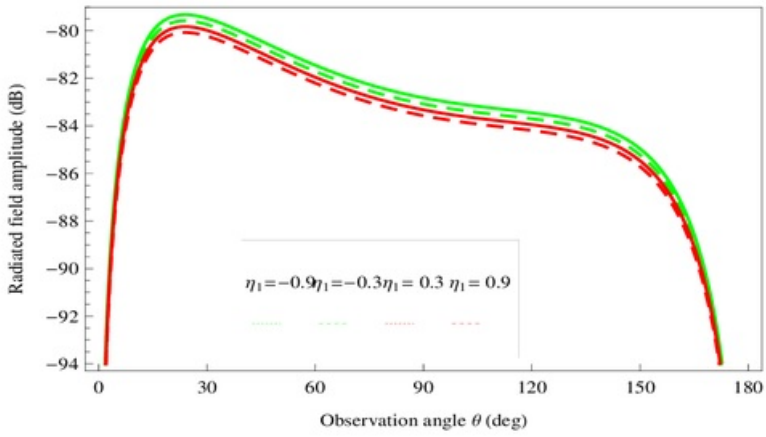

FIGURE 5.4. *Variation in the radiated field amplitude versus "*η_1*". The other parameters are* $k = 5$, $\eta_2 = 0.3$, $\eta_3 = 0.6$, $\eta_4 = 0.5$, $\epsilon_1 = 0.8$, $\epsilon_2 = 0$ *and* $b = 0.2\lambda$.

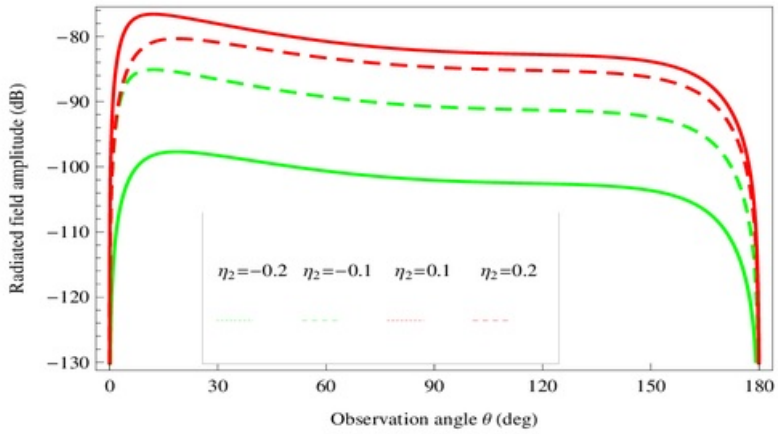

FIGURE 5.5. *Variation in the radiated field amplitude versus "η_2". The other parameters are $k = 5$, $\eta_1 = 0.7$, $\eta_3 = 0.6$, $\eta_4 = 0.4$, $\epsilon_1 = 0.8$, $\epsilon_2 = 0$ and $b = 0.2\lambda$.*

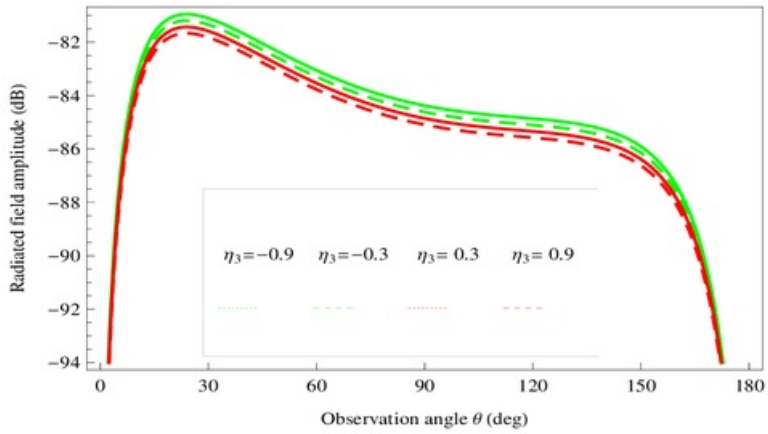

FIGURE 5.6. *Variation in the radiated field amplitude versus "η_3". The other parameters are $k = 5$ $\eta_1 = 0.5$, $\eta_2 = 0.3$, $\eta_4 = 0.4$, $\epsilon_1 = 0.8$, $\epsilon_2 = 0$ and $b = 0.2\lambda$.*

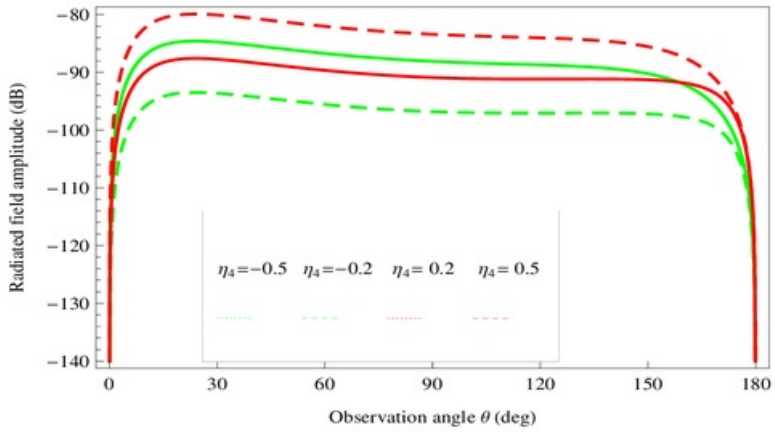

FIGURE 5.7. *Variation in the radiated field amplitude versus "η_4". The other parameters are* $k = 5$, $\eta_1 = 0.5$, $\eta_2 = 0.3$, $\eta_3 = 0.6$, $\epsilon_1 = 0.8$, $\epsilon_2 = 0$ *and* $b = 0.2\lambda$.

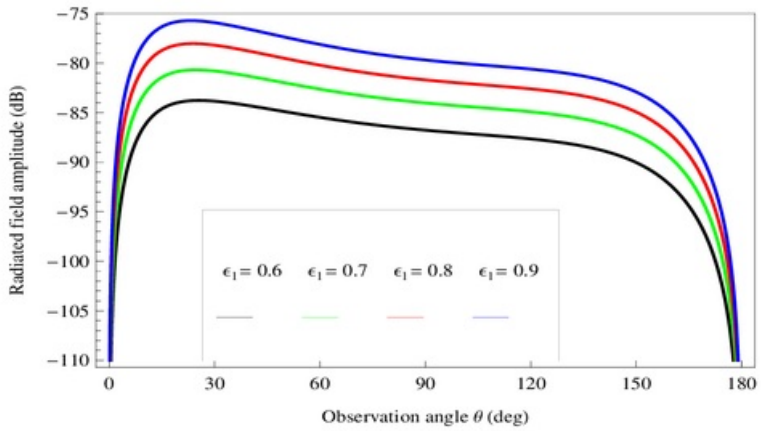

FIGURE 5.8. *Variation in the radiated field amplitude versus "ϵ_1". The other parameters are* $k = 5$, $\eta_1 = 0.5$, $\eta_2 = 0.3$, $\eta_3 = 0.6$, $\eta_4 = 0.7$, $\epsilon_2 = 0$ *and* $b = 0.2\lambda$.

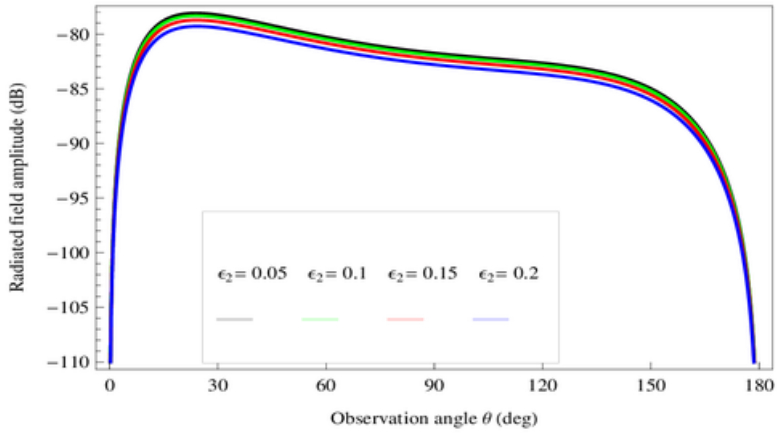

FIGURE 5.9. *Variation in the radiated field amplitude versus "ϵ_2". The other parameters are* $k = 5$, $\eta_1 = 0.5$, $\eta_2 = 0.3$, $\eta_3 = 0.6$, $\eta_4 = 0.7$, $\epsilon_1 = 0.8$ *and* $b = 0.2\lambda$.

CHAPTER 6

DIFFRACTED AND TRANSMITTED FIELDS BY AN IMPEDANCE LOADED WAVEGUIDE LOCATED IN COLD PLASMA

In this chapter, the problem of diffraction of plane wave by an impedance loaded waveguide designed in cold plasma is considered. The structure of waveguide is constructed from three parallel impedance loaded half-planes such that one amidst in the opposite direction. Such type of problem was initially considered by Weinstein [89, 90] and Boersma [91] for the case of two half-planes characteristic by either soft (Dirichlet) or rigid (Neumann) surface material properties of all faces of the half-planes. After that Cinar and Büyükaksoy [85] generalized the problem for surface impedance (Robin) and each face of the half-planes is loaded by different impedances. Here, the case is considered for soft, rigid and impedance surface material properties of the waveguide located in cold plasma as shown in Fig. (6.1).

The chapter is arranged as follows. In the next Section (6.1) mathematical model of the problem in cold plasma is stated. The Wiener-Hopf equation is formulated in Section (6.2) whereas the solution of Wiener-Hopf equation is developed in Section (6.3). The unknown coefficients are obtained with the help of Mode-Matching technique in Section (6.4). The diffracted and transmitted fields are

considered in Section (6.5). In the end the Section (6.6) is devoted to numerical results and discussions.

6.1 MATHEMATICAL MODEL OF THE PROBLEM IN COLD PLASMA

In this chapter consider an incident time harmonic wave propagating in cold plasma and making an incident angle θ_0. On striking the waveguide surface the incident field generates reflected and transmitted fields. Let ω denotes the angular frequency and k be the wave number. The geometry of the problem is formed by three parallel half-planes represented by $S_1=\{(x,y,z)|\ x\in(-\infty,0),\ y=b,\ z\in(-\infty,\infty)\}$, $S_2=\{(x,y,z)|\ x\in(-\infty,0),\ y=-b,\ z\in(-\infty,\infty)\}$ and $S_3=\{(x,y,z)|\ x\in(0,\infty),\ y=0,\ z\in(-\infty,\infty)\}$, respectively. The material property of waveguide surface impedance of the upper and lower faces of the half-planes S_1 and S_2 are assumed to be Z_1 and Z_2, respectively, as shown in the Fig. (6.1)

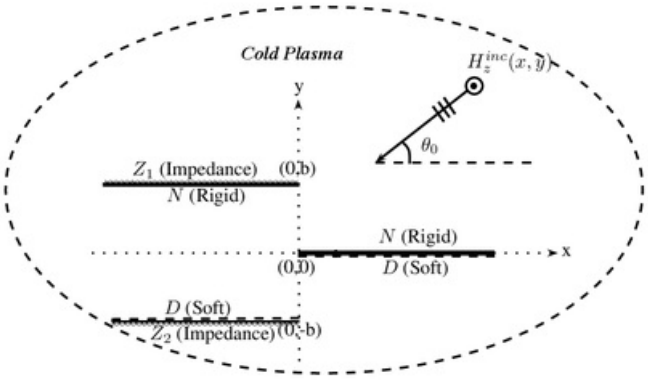

FIGURE 6.1. *The physical configuration of the waveguide located in cold plasma*

The total field can be expressed as follows:

$$H_z^T(x,y)=\begin{cases} H_z^1(x,y)+H_z^{inc}(x,y)+H_z^{ref}(x,y), & y\in(b,\infty)\\ H_z^3(x,y)\mathcal{H}(-x)+H_z^2(x,y)\mathcal{H}(x), & y\in(0,b)\\ H_z^3(x,y)\mathcal{H}(-x)+H_z^4(x,y)\mathcal{H}(x), & y\in(-b,0)\\ H_z^5(x,y), & y\in(-\infty,-b). \end{cases} \tag{6.1}$$

where $\mathscr{H}(x)$, $H_z^{inc}(x,y)$ and $H_z^{ref}(x,y)$ stand for Heaviside unit step function, incident and reflected fields, respectively, which are already defined in Chapter (4). $\{H_z^j \quad (j=1,2,3,4,5)\}$ are the scattered fields satisfy the Helmholtz equation in cold plasma as under

$$\left[\frac{\partial^2}{\partial x^2}+\frac{\partial^2}{\partial y^2}+k_{\text{eff}}^2\right]\left[H_z^j(x,y)\right]=0, \tag{6.2}$$

with the following corresponding boundary conditions and continuity relations

$$\left(1+\frac{\eta_1}{\imath k_{\text{eff}}}\frac{\partial}{\partial y}\right)H_z^1(x,b)=0, \qquad x\in(-\infty,0) \tag{6.3}$$

$$\frac{\partial}{\partial y}H_z^2(x,0)=0, \qquad x\in(0,\infty) \tag{6.4}$$

$$\frac{\partial}{\partial y}H_z^3(x,b)=0, \qquad x\in(-\infty,0) \tag{6.5}$$

$$H_z^2(x,-b)=0, \qquad x\in(-\infty,0) \tag{6.6}$$

$$H_z^4(x,0)=0, \qquad x\in(0,\infty) \tag{6.7}$$

$$\left(1-\frac{\eta_2}{\imath k_{\text{eff}}}\frac{\partial}{\partial y}\right)H_z^5(x,-b)=0, \qquad x\in(-\infty,0) \tag{6.8}$$

$$H_z^1(x,b)+H_z^{inc}(x,b)+H_z^{ref}(x,b)=H_z^2(x,b), \qquad x\in(0,\infty) \tag{6.9}$$

$$\frac{\partial}{\partial y}H_z^1(x,b)+\frac{\partial}{\partial y}H_z^{inc}(x,b)+\frac{\partial}{\partial y}H_z^{ref}(x,b)=\frac{\partial}{\partial y}H_z^2(x,b), \qquad x\in(0,\infty) \tag{6.10}$$

$$H_z^3(0,y)=H_z^2(0,y), \qquad x\in(0,b) \tag{6.11}$$

$$\frac{\partial}{\partial x}H_z^3(0,y)=\frac{\partial}{\partial x}H_z^2(0,y), \qquad x\in(0,b) \tag{6.12}$$

$$H_z^3(0,y)=H_z^4(0,y), \qquad x\in(-b,0) \tag{6.13}$$

$$\frac{\partial}{\partial x}H_z^3(0,y)=\frac{\partial}{\partial x}H_z^4(0,y), \qquad x\in(-b,0) \tag{6.14}$$

$$H_z^4(x,-b)=H_z^5(x,-b), \qquad x\in(0,\infty) \tag{6.15}$$

$$\frac{\partial}{\partial y}H_z^4(x,-b) = \frac{\partial}{\partial y}H_z^5(x,-b), \qquad x \in (0,\infty). \tag{6.16}$$

6.2 FORMULATION OF WIENER-HOPF EQUATION

Since Helmholtz equation in cold plasma is satisfied by the field $H_z^1(x,y)$ in the waveguide region $x \in (-\infty,\infty)$ and $y \in (b,\infty)$ whose Fourier transform gives

$$\left[\frac{d^2}{dy^2} + (k_{\text{eff}}^2 - \alpha^2)\right] F(\alpha,y) = 0. \tag{6.17}$$

Using the radiation condition the general solution of equation (6.17) is as under

$$F(\alpha,y) = A_4(\alpha)e^{\iota\mathfrak{L}(\alpha)(y-b)}. \tag{6.18}$$

To find the unknown spectral coefficient $A_4(\alpha)$, using the transformed domain of the boundary condition represented by equation (6.3) gives

$$A_4(\alpha) = \frac{k_{\text{eff}}}{\mathfrak{L}(\alpha)}\mathscr{R}_+^4(\alpha)\chi(\eta_1,\alpha), \tag{6.19}$$

where

$$\mathscr{R}_+^4(\alpha) = F_+(\alpha,b) + \frac{\eta_1}{\iota k_{\text{eff}}}F_+'(\alpha,b) \tag{6.20}$$

and $\chi(\eta_1,\alpha)$ are defined in previous chapter.

Using the additive decomposition theorem and substituting equation (6.19) in equation (6.18), one can write

$$F_-(\alpha,y) + F_+(\alpha,y) = \frac{k_{\text{eff}}}{\mathfrak{L}(\alpha)}\mathscr{R}_+^4(\alpha)\chi(\eta_1,\alpha)e^{\iota\mathfrak{L}(\alpha)(y-b)}. \tag{6.21}$$

The derivative of equation (6.21) with respect to y at $y = b$ takes the form

$$F_+'(\alpha,b) = \iota k_{\text{eff}}\mathscr{R}_+^4(\alpha)\chi(\eta_1,\alpha) - F_-'(\alpha,b). \tag{6.22}$$

As the Helmholtz equation in cold plasma is satisfied by field $H_z^2(x,y)$ in equation (6.2) in the waveguide region $x \in (0,\infty)$ and $y \in (0,b)$, on multiplying this equation by $e^{\iota\alpha x}$ and then integrating the resultant equation with respect to x from 0 to ∞, one gets

$$\left[\frac{d^2}{dy^2} + \mathfrak{L}^2(\alpha)\right] \mathcal{G}_+(\alpha, y) = \mathfrak{f}(y) - \iota\alpha\mathfrak{g}(y), \tag{6.23}$$

where $\mathcal{G}_+(\alpha,y)$, $\mathfrak{f}(y)$ and $\mathfrak{g}(y)$ are also defined as earlier.

The general solution of the non-homogenous differential equation (6.23) can be obtained by using the method of variation of parameter yields

$$\mathcal{G}_+(\alpha,y) = C_9(\alpha)\cos\mathfrak{L}(\alpha)y + C_{10}(\alpha)\sin\mathfrak{L}(\alpha)y + \frac{1}{\mathfrak{L}(\alpha)}\int_0^y \mathfrak{f}(t)\sin\mathfrak{L}(\alpha)(b-t)\,dt, \tag{6.24}$$

where $C_9(\alpha)$ and $C_{10}(\alpha)$ are the unknown spectral coefficients.

Using the transformed form of boundary condition given by the equation (6.4), one gets

$$\mathcal{G}_+(\alpha,y) = C_9(\alpha)\cos\mathfrak{L}(\alpha)y + \frac{1}{\mathfrak{L}(\alpha)}\int_0^y [\mathfrak{f}(t) - \iota\alpha\mathfrak{g}(t)]\sin\mathfrak{L}(\alpha)(y-t)\,dt. \tag{6.25}$$

The transformed form of the continuity relation represented by the equations (6.9) and (6.18), respectively, gives

$$F_+(\alpha,b) + \frac{2i\eta_1\sin\theta_0 e^{-\iota k_{\mathfrak{eff}} b\sin\theta_0}}{(1+\eta_1\sin\theta_0)(\alpha - k_{\mathfrak{eff}}\cos\theta_0)} = \mathcal{G}_+(\alpha,b) \tag{6.26}$$

and

$$F'_+(\alpha,b) + \frac{2k_{\mathfrak{eff}}\sin\theta_0 e^{-\iota k_{\mathfrak{eff}} b\sin\theta_0}}{(1+\eta_1\sin\theta_0)(\alpha - k_{\mathfrak{eff}}\cos\theta_0)} = \mathcal{G}'_+(\alpha,b). \tag{6.27}$$

Adding equation (6.26) and $\frac{\eta_1}{ik_{\mathfrak{eff}}}$ times of equation (6.27), one can obtain

$$\mathcal{G}_+(\alpha,b) + \frac{\eta_1}{ik_{\mathfrak{eff}}}\mathcal{G}'_+(\alpha,b) = \mathcal{R}_+^4(\alpha). \tag{6.28}$$

$C_9(\alpha)$ can be obtained by placing equation (6.25) in equation (6.28) which yields

$$C_9(\alpha) = \frac{\mathscr{R}_+^4(\alpha)}{\mathscr{W}_4(\alpha)} - \frac{1}{\mathscr{W}_4(\alpha)} \int_0^b (\mathfrak{f}(y) - \iota\alpha\mathfrak{g}(y)) \left(\frac{\sin \mathfrak{L}(\alpha)(b-t)}{\mathfrak{L}(\alpha)} + \frac{\eta_1}{\iota k_{\mathfrak{eff}}} \cos \mathfrak{L}(\alpha)(b-t) \right) dt, \tag{6.29}$$

with

$$\mathscr{W}_4(\alpha) = \cos \mathfrak{L}(\alpha) b - \frac{\eta_1}{\iota k_{\mathfrak{eff}}} \mathfrak{L}(\alpha) \sin \mathfrak{L}(\alpha) b. \tag{6.30}$$

Placing equation (6.29) in equation (6.25) gives

$$\mathscr{G}_+(\alpha, y) = \frac{1}{\mathfrak{L}(\alpha)} \int_0^y (\mathfrak{f}(y) - \iota\alpha\mathfrak{g}(y)) \sin \mathfrak{L}(\alpha)(y-t) dt +$$
$$\frac{\cos \mathfrak{L}(\alpha) y}{\mathscr{W}_4(\alpha)} \left\{ \mathscr{R}_+^4(\alpha) - \int_0^b (\mathfrak{f}(y) - \iota\alpha\mathfrak{g}(y)) \left(\frac{\sin \mathfrak{L}(\alpha)(b-t)}{\mathfrak{L}(\alpha)} + \frac{\eta_1}{\iota k_{\mathfrak{eff}}} \cos \mathfrak{L}(\alpha)(b-t) \right) dt \right\}. \tag{6.31}$$

The left-hand side (i.e., $\mathscr{G}_+(\alpha, y)$) of the equation (6.31) is analytic in the upper half-plane $\mathfrak{Im}(\alpha) > \mathfrak{Im}(k_{\mathfrak{eff}} \cos\theta_0)$. However, the analyticity of the right-hand side is desecrated by the appearance of simple poles placing at the zeros of $\mathscr{W}_4(\alpha)$, i.e., $\alpha = \pm\alpha_m$ satisfying

$$\mathscr{W}_4(\pm\alpha_m) = 0, \quad \mathfrak{Im}(\alpha_m) > \mathfrak{Im}(k_{\mathfrak{eff}}), \quad m = 1, 2, 3.... \tag{6.32}$$

The poles in the equation (6.31) can be removed by imposing the condition that residues of these poles are zero. Then from equation (6.31), one obtains

$$\mathscr{R}_+^4(\alpha_m) = \int_0^b (\mathfrak{f}(t) - \iota\alpha_m\mathfrak{g}(t)) \left(\frac{\sin \mathfrak{L}_m(b-t)}{\mathfrak{L}_m} + \frac{\eta_1}{\iota k_{\mathfrak{eff}}} \cos \mathfrak{L}_m(b-t) \right) dt. \tag{6.33}$$

After simplifying equation (6.34), one gets

$$\mathscr{R}_{+}^{4}(\alpha_m) = \left(\frac{\sin \mathfrak{L}_m b}{\mathfrak{L}_m} + \frac{\eta_1}{\iota k_{\text{eff}}} \cos \mathfrak{L}_m b\right) \int_0^b (\mathfrak{f}(t) - \iota \alpha_m \mathfrak{g}(t)) \cos \mathfrak{L}_m t \, dt. \tag{6.34}$$

$\mathfrak{f}(t)$ and $\mathfrak{g}(t)$ can be express in the form of eigen-functions as follows:

$$\mathfrak{f}(t) - \iota \alpha \mathfrak{g}(t) = \sum_{n=1}^{\infty} (\mathfrak{f}_n - \iota \alpha \mathfrak{g}_n) \cos \mathfrak{L}_n t. \tag{6.35}$$

Substituting equation (6.35) in equation (6.34) leads to

$$\mathscr{R}_{+}^{4}(\alpha_m) = \left(\frac{\sin \mathfrak{L}_m b}{\mathfrak{L}_m} + \frac{\eta_1}{\iota k_{\text{eff}}} \cos \mathfrak{L}_m b\right) \int_0^b \sum_{n=1}^{\infty} (\mathfrak{f}_n - \iota \alpha_m \mathfrak{g}_n) \cos \mathfrak{L}_n t \cos \mathfrak{L}_m t \, dt. \tag{6.36}$$

After simplifying the equation (6.36), one can write

$$\mathscr{R}_{+}^{4}(\alpha_m) = \mathfrak{D}_m^4 (\mathfrak{f}_m - \iota \alpha \mathfrak{g}_m) \left(\frac{\sin \mathfrak{L}_m b}{\mathfrak{L}_m} + \frac{\eta_1}{i k_{\text{eff}}} \cos \mathfrak{L}_m b\right), \tag{6.37}$$

with

$$\mathfrak{L}_m = \sqrt{k_{\text{eff}}^2 - \alpha_m^2} \tag{6.38}$$

and

$$\mathfrak{D}_m^4 = \frac{\mathfrak{L}_m \sin \mathfrak{L}_m b}{2\alpha_m} \frac{\partial}{\partial \alpha} \mathscr{W}_4(\alpha_m). \tag{6.39}$$

The Fourier transform of the continuity relation given by equation (6.18) gives

$$\overset{\prime}{F}_{+}(\alpha, b) + \frac{2k_{\text{eff}} \sin\theta_0 e^{-\iota k_{\text{eff}} b \sin\theta_0}}{(1+\eta_1 \sin\theta_0)(\alpha - k_{\text{eff}} \cos\theta_0)} = \overset{\prime}{\mathscr{G}}_{+}(\alpha, b). \tag{6.40}$$

While placing equations (6.22) and (6.31) in equation (6.40) yields

$$\iota k_{\text{eff}}\mathscr{R}_{+}^{4}(\alpha)\chi(\eta_1,\alpha)-\overset{'}{F}_{-}(\alpha,b)+\frac{2k_{\text{eff}}\sin\theta_0 e^{-\iota k_{\text{eff}}b\sin\theta_0}}{(1+\eta_1\sin\theta_0)(\alpha-k_{\text{eff}}\cos\theta_0)}$$
$$=\frac{-\mathfrak{L}(\alpha)(\alpha)\sin\mathfrak{L}(\alpha)b\mathscr{R}_{+}^{4}(\alpha)}{\mathscr{W}_4(\alpha)}+\frac{1}{\mathscr{W}_4(\alpha)}\int_0^b[\mathfrak{f}(t)-\iota\alpha\mathfrak{g}(t)]\cos\mathfrak{L}(\alpha)t\,dt. \tag{6.41}$$

Rearranging equations (6.41), one gets

$$\frac{\iota\eta_1\chi(\eta_1,\alpha)\mathscr{R}_{+}^{4}(\alpha)}{\mathscr{N}^4(\alpha)}+\overset{'}{F}_{-}(\alpha,b)=\frac{2k_{\text{eff}}\sin\theta_0 e^{-\iota k_{\text{eff}}b\sin\theta_0}}{(1+\eta_1\sin\theta_0)(\alpha-k_{\text{eff}}\cos\theta_0)}$$
$$-\frac{1}{\mathscr{W}_4(\alpha)}\int_0^b(\mathfrak{f}(t)-\iota\alpha\mathfrak{g}(t))\cos\mathfrak{L}(\alpha)t\,dt, \tag{6.42}$$

where

$$\mathscr{N}^4(\alpha)=\mathscr{W}_4(\alpha)e^{\iota\mathfrak{L}(\alpha)b}. \tag{6.43}$$

Using equation (6.35) into equation (6.42), one obtains

$$\frac{\iota\eta_1\chi(\eta_1,\alpha)\mathscr{R}_{+}^{4}(\alpha)}{\mathscr{N}^4(\alpha)}+\overset{'}{F}_{-}(\alpha,b)=\frac{2k_{\text{eff}}\sin\theta_0 e^{-\iota k_{\text{eff}}b\sin\theta_0}}{(1+\eta_1\sin\theta_0)(\alpha-k_{\text{eff}}\cos\theta_0)}$$
$$-\frac{1}{\mathscr{W}_4(\alpha)}\int_0^b\sum_{m=1}^{\infty}(\mathfrak{f}_m+\iota\alpha\mathfrak{g}_m)\cos\mathfrak{L}_m t\cos\mathfrak{L}(\alpha)t\,dt. \tag{6.44}$$

After simplifying the equation (6.44), one can obtain the required Wiener-Hopf equation valid within the strip $\Im\mathfrak{m}(k_{\text{eff}}\cos\theta_0)<\Im\mathfrak{m}(\alpha)<\Im\mathfrak{m}(k_{\text{eff}})$ as follows:

$$\frac{\iota\eta_1\chi(\eta_1,\alpha)\mathscr{R}_{+}^{4}(\alpha)}{\mathscr{N}(\alpha)}+\overset{'}{F}_{-}(\alpha,b)=\frac{2k_{\text{eff}}\sin\theta_0 e^{-\iota k_{\text{eff}}b\sin\theta_0}}{(1+\eta_1\sin\theta_0)(\alpha-k_{\text{eff}}\cos\theta_0)}$$
$$-\sum_{m=1}^{\infty}\frac{\mathfrak{f}_m-\iota\alpha\mathfrak{g}_m}{\alpha^2-\alpha_m^2}(\mathfrak{L}_m\sin\mathfrak{L}_m b). \tag{6.45}$$

In order to calculate the transmitted field, the Fourier transform of the Helmholtz equation in cold plasma in the waveguide region $x\in(-\infty,\infty)$ and $y\in(-\infty,-b)$

results into

$$\left[\frac{d^2}{dy^2}+(k_{\text{eff}}^2-\alpha^2)\right]\Psi(\alpha,y)=0, \tag{6.46}$$

where

$$\Psi(\alpha,y)=\int_{-\infty}^{\infty}H_z^5(x,y)e^{\iota\alpha x}dx. \tag{6.47}$$

Using the radiation condition the general solution of equation (6.46) is as under

$$\Psi(\alpha,y)=A_5(\alpha)e^{-\iota\mathfrak{L}(\alpha)(y+b)}. \tag{6.48}$$

To find the unknown coefficient $A_5(\alpha)$, using the boundary condition represented by equation (6.8) in the transformed domain, one obtains

$$A_5(\alpha)=\frac{k_{\text{eff}}\mathscr{R}_+^5(\alpha)\chi(\eta_2,\alpha)}{\mathfrak{L}(\alpha)}, \tag{6.49}$$

where

$$\mathscr{R}_+^5(\alpha)=\Psi_+(\alpha,-b)-\frac{\eta_2}{\iota k_{\text{eff}}}\Psi_+'(\alpha,-b). \tag{6.50}$$

Using the additive decomposition theorem and equation (6.49) in equation (6.48), it is found that

$$\Psi_+(\alpha,y)+\Psi_-(\alpha,y)=\frac{k_{\text{eff}}\mathscr{R}_+^4(\alpha)\chi(\eta_2,\alpha)}{\mathfrak{L}(\alpha)}e^{-\iota\mathfrak{L}(\alpha)(y+b)}, \tag{6.51}$$

whereas the derivative of equation (6.51) with respect to y at $y=b$ takes the form

$$\Psi_+'(\alpha,-b)=-\iota k_{\text{eff}}\mathscr{R}_+^4(\alpha)\chi(\eta_2,\alpha)-\Psi_-'(\alpha,-b). \tag{6.52}$$

From equation (6.2), we observe that $H_z^4(x,y)$ satisfies the Helmholtz equation in cold plasma in the waveguide region $x\in(0,\infty)$ and $y\in(-b,0)$. After multiplying

by $e^{\iota\alpha x}$ and integrating with respect to x from 0 to ∞, takes the form as under

$$\left[\frac{d^2}{dy^2}+\mathfrak{L}^2(\alpha)\right]G_+(\alpha,y)=\mathfrak{p}(y)+\iota\mathfrak{q}(y), \tag{6.53}$$

with

$$\mathfrak{p}(y)=\frac{\partial}{\partial x}H_z^4(0,y),\quad \mathfrak{q}(y)=H_z^4(0,y) \tag{6.54}$$

and $G_+(\alpha,y)$ defined by

$$G_+(\alpha,y)=\int_0^\infty H_z^4(x,y)e^{\iota\alpha x}dx, \tag{6.55}$$

is a regular function in the half-plane.

The general solution of the non-homogenous differential equation (6.53) can be obtained by using the method of variation of parameter yields

$$G_+(\alpha,y)=C_{11}(\alpha)\cos\mathfrak{L}(\alpha)y+C_{12}(\alpha)\sin\mathfrak{L}(\alpha)y+\frac{1}{\mathfrak{L}(\alpha)}\int_{-b}^{y}(\mathfrak{p}(t)+\iota\mathfrak{q}(t))\sin\mathfrak{L}(\alpha)(y-t)dt. \tag{6.56}$$

To find $C_{11}(\alpha)$ using the transform form of the boundary condition represented by equation (6.7) gives

$$C_{11}(\alpha)=\frac{1}{\mathfrak{L}(\alpha)}\int_{-b}^{0}(\mathfrak{p}(t)-\iota\alpha\mathfrak{q}(t))\sin\mathfrak{L}(\alpha)tdt. \tag{6.57}$$

Substituting equations (6.57) in equations (6.56), one obtains

$$G_+(\alpha,y)=C_{12}(\alpha)\sin\mathfrak{L}(\alpha)y+\frac{\cos\mathfrak{L}(\alpha)y}{\mathfrak{L}(\alpha)}\int_{-b}^{0}(\mathfrak{p}(t)-\iota\alpha\mathfrak{q}(t))\sin\mathfrak{L}tdt$$
$$+\frac{1}{\mathfrak{L}(\alpha)}\int_{-b}^{y}(\mathfrak{p}(t)-\iota\alpha\mathfrak{g}(y))\sin\mathfrak{L}(\alpha)(y-t)dt. \tag{6.58}$$

The transformed form of the continuity relations represented by the equations (6.15) and (6.16), respectively, are as below

$$\Psi_+(\alpha,-b) = G_+(\alpha,-b) \tag{6.59}$$

and

$$\overset{\prime}{\Psi}_+(\alpha,-b) = \overset{\prime}{G}_+(\alpha,-b). \tag{6.60}$$

Subtracting equation (6.59) and $\frac{\eta_2}{\iota k_{\mathfrak{eff}}}$ times of equation (6.60) yields

$$G_+(\alpha,-b) - \frac{\eta_2}{\iota k_{\mathfrak{eff}}}\overset{\prime}{G}_+(\alpha,-b) = \mathscr{R}^5_+(\alpha). \tag{6.61}$$

To find $C_{12}(\alpha)$ placing equation (6.58) in equation (6.61), one obtains

$$C_{12}(\alpha) = \frac{-\mathscr{R}^5_+(\alpha)}{\mathscr{W}_5(\alpha)} + \frac{\cos\mathfrak{L}(\alpha)y - \frac{\eta_2}{\iota k_{\mathfrak{eff}}}\mathfrak{L}(\alpha)\sin\mathfrak{L}(\alpha)b}{\mathfrak{L}(\alpha)\mathscr{W}_5(\alpha)}\int_{-b}^{0}(\mathfrak{p}(t)-\iota\alpha\mathfrak{q}(t))\sin\mathfrak{L}(\alpha)t\,dt, \tag{6.62}$$

where

$$\mathscr{W}_5(\alpha) = \sin\mathfrak{L}(\alpha)b + \frac{\eta_2}{\iota k_{\mathfrak{eff}}}\mathfrak{L}(\alpha)\cos\mathfrak{L}(\alpha)b. \tag{6.63}$$

Using equation (6.62) in (6.58) yields

$$\begin{aligned} G_+(\alpha,y) &= \frac{-\mathscr{R}^5_+(\alpha)}{\mathscr{W}_5(\alpha)}\sin\mathfrak{L}(\alpha)y \\ &+ \frac{\cos\mathfrak{L}(\alpha)b - \frac{\eta_2}{\iota k_{\mathfrak{eff}}}\mathfrak{L}\sin\mathfrak{L}(\alpha)b}{\mathfrak{L}(\alpha)\mathscr{W}_5(\alpha)}\sin\mathfrak{L}(\alpha)y\int_{-b}^{0}(\mathfrak{p}(t)-\iota\alpha\mathfrak{q}(t))\sin\mathfrak{L}(\alpha)t\,dt \\ &+ \frac{\cos\mathfrak{L}y}{\mathfrak{L}(\alpha)}\int_{-b}^{0}(\mathfrak{p}(t)-\iota\alpha\mathfrak{q}(t))\sin\mathfrak{L}t\,dt + \frac{1}{\mathfrak{L}(\alpha)}\int_{-b}^{y}(\mathfrak{f}(t)-\iota\alpha\mathfrak{g}(t))\sin\mathfrak{L}(y-t)dt. \end{aligned} \tag{6.64}$$

Rearranging equation (6.64) takes the form

$$G_+(\alpha,y)=\frac{-\mathscr{R}_+^5(\alpha)}{\mathscr{W}_5(\alpha)}\sin\mathfrak{L}(\alpha)y+\frac{1}{\mathfrak{L}(\alpha)}\int_{-b}^{y}(\mathfrak{p}(t)-\iota\alpha\mathfrak{q}(t))\sin\mathfrak{L}(\alpha)(y-t)\,dt$$
$$+\frac{\sin\mathfrak{L}(\alpha)(y+b)+\frac{\eta_2}{\iota k_{\mathrm{eff}}}\mathfrak{L}(\alpha)\cos\mathfrak{L}(\alpha)(y+b)}{\mathfrak{L}(\alpha)\mathscr{W}_5(\alpha)}\int_{-b}^{0}(\mathfrak{p}(t)-\iota\alpha\mathfrak{q}(t))\sin\mathfrak{L}(\alpha)t\,dt. \tag{6.65}$$

The left-hand side (i.e., $G_+(\alpha,y)$) of the equation (6.65) is analytic in the upper half-plane $\Im\mathfrak{m}(\alpha)>\Im\mathfrak{m}(k_{\mathrm{eff}}\cos\theta_0)$. However, the analyticity of the right-hand side is violated by the appearance of simple poles placing at the zeros of $\mathscr{W}_5(\alpha)$, i.e., $\alpha=\pm\alpha_m$ satisfying

$$\mathscr{W}_5(\pm\nu_m)=0,\qquad \Im\mathfrak{m}(\nu_m)>\Im\mathfrak{m}(k_{\mathrm{eff}}),\qquad m=1,2,3.... \tag{6.66}$$

The poles in the equation (6.65) can be removed by imposing the condition that residues of these poles are zero. Then from equation (6.65), one obtains

$$\mathscr{R}_+^5(\nu_m)=-\left(\frac{\cos L_m b}{L_m}+\frac{\eta_2}{\iota k_{\mathrm{eff}}}\sin L_m b\right)\int_{-b}^{0}(\mathfrak{p}(t)-\iota\alpha\mathfrak{q}(t))\sin L_m t\,dt, \tag{6.67}$$

where

$$L_m=\sqrt{k_{\mathrm{eff}}^2-\nu_m^2}, \tag{6.68}$$

$\mathfrak{p}(t)$ and $\mathfrak{q}(t)$ can be expanded into a series of eigen-functions as follows:

$$\mathfrak{p}(t)-\iota\alpha\mathfrak{q}(t)=\sum_{n=1}^{\infty}(\mathfrak{p}_n-\iota\alpha\mathfrak{q}_n)\sin L_n t. \tag{6.69}$$

Using equation (6.69) in equation (6.67) yields

$$\mathscr{R}_{+}^{5}(\alpha_m) = -\left(\frac{\cos L_m b}{L_m} + \frac{\eta_2}{\iota k_{\mathfrak{eff}}} \sin L_m b\right) \int_{-b}^{0} \sum_{n=1}^{\infty} (\mathfrak{p}_n - \iota \alpha_m \mathfrak{q}_n) \sin L_n t \sin L_m t \, dt. \quad (6.70)$$

After simplification, equation (6.70) gives

$$\mathscr{R}_{+}^{4}(\alpha_m) = \mathfrak{D}_m^5 (\mathfrak{p}_m + \iota \mathfrak{q}_m) \left(\frac{\cos L_m b}{L_m} + \frac{\eta_2}{\iota k_{\mathfrak{eff}}} \sin L_m b\right), \quad (6.71)$$

$$\mathfrak{D}_m^5 = \frac{L_m \cos L_m b}{2\nu_m} \frac{\partial}{\partial \alpha} \mathscr{W}_5(\nu_m). \quad (6.72)$$

Using equations (6.52) and (6.65) in equation (6.60) yields

$$-\iota k_{\mathfrak{eff}} \mathscr{R}_{+}^{5}(\alpha) \chi(\eta_2, \alpha) - \overset{\prime}{\Psi}_{-}(\alpha, -b) = -\frac{\mathfrak{L}(\alpha) \mathscr{R}_{+}^{5}(\alpha)}{\mathscr{W}_5(\alpha)} \cos \mathfrak{L}(\alpha) b$$
$$-\frac{1}{\mathscr{W}_5(\alpha)} \int_{-b}^{0} (\mathfrak{p}(t) - \iota \alpha \mathfrak{q}(t)) \sin \mathfrak{L}(\alpha) t \, dt. \quad (6.73)$$

After simplifying equations (6.73), one can obtain

$$\frac{k_{\mathfrak{eff}} \chi(\eta_2, \alpha) \mathscr{R}_{+}^{5}(\alpha)}{\mathscr{N}^5(\alpha)} - \overset{\prime}{\Psi}_{-}(\alpha, -b) = -\frac{1}{\mathscr{W}_5(\alpha)} \int_{-b}^{0} (\mathfrak{p}(t) - \iota \alpha \mathfrak{q}(t)) \sin \mathfrak{L}(\alpha) t \, dt, \quad (6.74)$$

where

$$\mathscr{N}^5(\alpha) = \mathscr{W}_5(\alpha) e^{\iota \mathfrak{L}(\alpha) b}. \quad (6.75)$$

Using equation (6.69) into equation (6.74), one obtains the required Wiener-Hopf equation valid in the strip $\mathfrak{Im}(-k_{\mathfrak{eff}}) < \mathfrak{Im}(\alpha) < \mathfrak{Im}(k_{\mathfrak{eff}})$ as follows:

$$\frac{k_{\mathfrak{eff}} \chi(\eta_2, \alpha) \mathscr{R}_{+}^{5}(\alpha)}{\mathscr{N}^5(\alpha)} - \overset{\prime}{\Psi}_{-}(\alpha, -b) = -\frac{1}{\mathscr{W}_5(\alpha)} \int_{0}^{b} \sum_{m=1}^{\infty} (\mathfrak{p}_m - \iota \alpha \mathfrak{q}_m) \sin L_m t \sin \mathfrak{L}(\alpha) t \, dt. \quad (6.76)$$

From the above expression, one can write

$$\frac{k_{\text{eff}}\chi(\eta_2,\alpha)\mathscr{R}^5_+(\alpha)}{\mathscr{N}^5(\alpha)} - \overset{\prime}{\Psi}_-(\alpha,-b) = \sum_{m=1}^{\infty} \frac{\mathfrak{p}_m - \iota\alpha\mathfrak{q}_m}{\alpha^2-\nu_m^2}(L_m\cos L_m b). \tag{6.77}$$

6.3 SOLUTION OF WIENER-HOPF EQUATION

To solve the Wiener-Hopf equations the kernel functions $\mathscr{N}^4(\alpha)$, $\mathscr{N}^5(\alpha)$ and $\chi(\eta_j,\alpha))$ in equations (6.45) and (6.77) can be factorized by applying the known results as following:

$$\mathscr{N}^4(\alpha) = \mathscr{N}^4_+(\alpha)\mathscr{N}^4_-(\alpha), \tag{6.78}$$

$$\mathscr{N}^5(\alpha) = \mathscr{N}^5_+(\alpha)\mathscr{N}^5_-(\alpha), \tag{6.79}$$

where

$$\begin{aligned}\mathscr{N}^4_+(\alpha) &= \left[\cos k_{\text{eff}}b + \iota\eta_1\sin k_{\text{eff}}b\right]^{\frac{1}{2}} \\ &\times \exp\left[\frac{\mathfrak{L}(\alpha)b}{\pi}\ln\left(\frac{\alpha+\iota\mathfrak{L}(\alpha)}{k_{\text{eff}}}\right) + \frac{\iota\alpha b}{\pi}\left(1-C+\ln\left[\frac{2\pi}{k_{\text{eff}}b}\right]+\iota\frac{\pi}{2}\right)\right]\prod_{m=1}^{\infty}\left(1+\frac{\alpha}{\alpha_m}\right)e^{\frac{\iota\alpha b}{m\pi}}\end{aligned} \tag{6.80}$$

and

$$\begin{aligned}\mathscr{N}^5_+(\alpha) &= \left[\sin k_{\text{eff}}b - \iota\eta_2\cos k_{\text{eff}}b\right]^{\frac{1}{2}} \\ &\times \exp\left[\frac{\mathfrak{L}(\alpha)b}{\pi}\ln\left(\frac{\alpha+\iota\mathfrak{L}(\alpha)}{k_{\text{eff}}}\right) + \frac{\iota\alpha b}{\pi}\left(1-C+\ln\left[\frac{2\pi}{k_{\text{eff}}b}\right]+\iota\frac{\pi}{2}\right)\right]\prod_{m=1}^{\infty}\left(1+\frac{\alpha}{\alpha_m}\right)e^{\frac{\iota\alpha b}{m\pi}},\end{aligned} \tag{6.81}$$

such that

$$\mathscr{N}^4_-(\alpha) = \mathscr{N}^4_+(-\alpha), \tag{6.82}$$

$$\mathscr{N}^5_-(\alpha) = \mathscr{N}^5_+(-\alpha). \tag{6.83}$$

As mention before, the factor of $\chi(\eta_j,\alpha)$ can be written in terms of the Maliuzhinetz's function.

Now, multiplying the Wiener-Hopf equation (6.45) on both sides with $\frac{\mathscr{N}^4_-(\alpha)}{\chi_-(\eta_1,\alpha)}$, one obtains

$$\frac{\iota\eta_1\chi_+(\eta_1,\alpha)\mathscr{R}_+(\alpha)}{\mathcal{N}_+^4(\alpha)}+\frac{\mathcal{N}_-^4(\alpha)\acute{F}_-(\alpha,b)}{\chi_-(\eta_1,\alpha)}=\frac{2k_{\mathfrak{eff}}\sin\theta_0 e^{-\iota k_{\mathfrak{eff}}b\sin\theta_0}\mathcal{N}_-^4(\alpha)}{(1+\eta_1\sin\theta_0)(\alpha-k_{\mathfrak{eff}}\cos\theta_0)\chi_-(\eta_1,\alpha)}$$
$$-\sum_{m=1}^{\infty}\frac{\mathfrak{L}_m\sin\mathfrak{L}_m b(\mathfrak{f}_m-\iota\alpha\mathfrak{g}_m)\mathcal{N}_-^4(\alpha)}{(\alpha^2-\alpha_m^2)\chi_-(\eta_1,\alpha)}. \tag{6.84}$$

With the help of cauchy's integral formula the terms on right-hand of the equation (6.84) can be decomposed as

$$\frac{2k_{\mathfrak{eff}}\sin\theta_0 e^{-\iota k_{\mathfrak{eff}}\sin\theta_0}\mathcal{N}_-^4(\alpha)}{(1+\eta_1\sin\theta_0)(\alpha-k_{\mathfrak{eff}}\cos\theta_0)\chi_-(\eta_1,\alpha)}$$
$$=\frac{2k_{\mathfrak{eff}}\sin\theta_0 e^{-\iota k_{\mathfrak{eff}}b\sin\theta_0}}{(1+\eta_1\sin\theta_0)(\alpha-k_{\mathfrak{eff}}\cos\theta_0)}\left[\frac{\mathcal{N}_-^4(\alpha)}{\chi_-(\eta,\alpha)}-\frac{\mathcal{N}_-^4(k_{\mathfrak{eff}}\cos\theta_0)}{\chi_-(\eta_1,k_{\mathfrak{eff}}\cos\theta_0)}\right]$$
$$+\frac{2k_{\mathfrak{eff}}\sin\theta_0 e^{-\iota k_{\mathfrak{eff}}b\sin\theta_0}}{(1+\eta_1\sin\theta_0)(\alpha-k_{\mathfrak{eff}}\cos\theta_0)}\frac{\mathcal{N}_-^4(k_{\mathfrak{eff}}\cos\theta_0)}{\chi_-(\eta_1,k_{\mathfrak{eff}}\cos\theta_0)} \tag{6.85}$$

and

$$\sum_{m=1}^{\infty}\frac{\mathfrak{L}_m\sin\mathfrak{L}_m b(\mathfrak{f}_m-\iota\alpha\mathfrak{g}_m)\mathcal{N}_-^4(\alpha)}{(\alpha^2-\alpha_m^2)\chi_-(\eta_1,\alpha)}=-\sum_{m=1}^{\infty}\frac{\mathfrak{L}_m\sin\mathfrak{L}_m b(\mathfrak{f}_m+\iota\alpha_m\mathfrak{g}_m)\mathcal{N}_+^4(\alpha_m)}{2\alpha_m(\alpha+\alpha_m)\chi_+(\eta_1,\alpha_m)}$$
$$+\sum_{m=1}^{\infty}\frac{\mathfrak{L}_m\sin\mathfrak{L}_m b}{\alpha+\alpha_m}\left[\frac{(\mathfrak{f}_m-\iota\alpha\mathfrak{g}_m)\,\mathcal{N}_-^4(\alpha)}{(\alpha-\alpha_m)\chi_-(\eta,\alpha)}+\frac{(\mathfrak{f}_m+\iota\alpha_m\mathfrak{g}_m)\,\mathcal{N}_+^4(\alpha_m)}{2\alpha_m\chi_+(\eta_1,\alpha_m)}\right]. \tag{6.86}$$

Now using equations (6.85) and (6.86) in equation (6.84), then placing the terms which are analytic in the upper half-plane ($\mathfrak{Im}(\alpha)>-k_{\mathfrak{eff}}$) at the left-hand side and those which analytic in lower half-plane ($\mathfrak{Im}(\alpha)<k_{\mathfrak{eff}}$) at the right-hand side which gives

$$\frac{\iota\eta_1\chi_+(\eta_1,\alpha)\mathscr{R}_+^4(\alpha)}{\mathcal{N}_+^4(\alpha)}-\frac{2k_{\mathfrak{eff}}\sin\theta_0 e^{-\iota k_{\mathfrak{eff}}b\sin\theta_0}\mathcal{N}_-^4(k_{\mathfrak{eff}}\cos\theta_0)}{(1+\eta_1\sin\theta_0)(\alpha-k_{\mathfrak{eff}}\cos\theta_0)\chi_-(\eta_1,k_{\mathfrak{eff}}\cos\theta_0)}$$
$$+\sum_{m=1}^{\infty}\frac{(\mathfrak{f}_m+\iota\alpha_m\mathfrak{g}_m)\mathfrak{L}_m\sin\mathfrak{L}_m b\mathcal{N}_+^4(\alpha_m)}{2\alpha_m(\alpha+\alpha_m)\chi_+(\eta_1,\alpha_m)}=-\frac{F_-(\alpha,b)\mathcal{N}_-^4(\alpha)}{\chi_-(\eta_1,\alpha)}$$
$$+\frac{2k_{\mathfrak{eff}}\sin\theta_0 e^{-\iota k_{\mathfrak{eff}}b\sin\theta_0}}{(1+\eta_1\sin\theta_0)(\alpha-k_{\mathfrak{eff}}\cos\theta_0)}\left[\frac{\mathcal{N}_-^4(\alpha)}{\chi_-(\eta_1,\alpha)}-\frac{\mathcal{N}_-^4(k_{\mathfrak{eff}}\cos\theta_0)}{\chi_-(\eta_1,k_{\mathfrak{eff}}\cos\theta_0)}\right]$$
$$+\sum_{m=1}^{\infty}\frac{\mathfrak{L}_m\sin\mathfrak{L}_m b}{\alpha+\alpha_m}\left[\frac{(\mathfrak{f}_m-\iota\alpha\mathfrak{g}_m)\mathcal{N}_-^4(\alpha)}{(\alpha-\alpha_m)\chi_-(\eta_1,\alpha)}+\frac{(\mathfrak{f}_m+\iota\alpha_m\mathfrak{g}_m)\,\mathcal{N}_+^4(\alpha_m)}{2\alpha_m\chi_+(\eta_1,\alpha_m)}\right]. \tag{6.87}$$

The required solution of Wiener-Hopf equation for the diffracted can be obtained by using analytical continuation principle following extended Liouville's theorem yields

$$\frac{\iota\eta_1\chi_+(\eta_1,\alpha)\mathscr{R}_+(\alpha)}{\mathscr{N}_+^4(\alpha)} = \frac{2k_{\mathfrak{eff}}\sin\theta_0 e_-^{-\iota k_{\mathfrak{eff}} b\sin\theta_0}\mathscr{N}_-^4(k_{\mathfrak{eff}}\cos\theta_0)}{(1+\eta_1\sin\theta_0)(\alpha-k_{\mathfrak{eff}}\cos\theta_0)\chi_-(\eta_1,k_{\mathfrak{eff}}\cos\theta_0)} - \sum_{m=1}^{\infty}\frac{(\mathfrak{f}_m+\iota\alpha_m\mathfrak{g}_m)\mathfrak{L}_m\sin\mathfrak{L}_m b\mathscr{N}_+^4(\alpha_m)}{2\alpha_m(\alpha+\alpha_m)\chi_+(\eta_1,\alpha_m)}. \tag{6.88}$$

Now, multiplying the Wiener-Hopf equation (6.77) on both sides with $\frac{\mathscr{N}_-^5(\alpha)}{\chi_-(\eta_2,\alpha)}$, one obtains

$$\frac{k_{\mathfrak{eff}}\chi_+(\eta_2,\alpha)\mathscr{R}_+^4(\alpha)}{\mathscr{N}_+^5(\alpha)} - \frac{\mathscr{N}_-^5(\alpha)\Psi_-'(\alpha,b)}{\chi_-(\eta_2,\alpha)} = \sum_{m=1}^{\infty}\frac{L_m\sin L_m b(\mathfrak{p}_m-\iota\alpha\mathfrak{q}_m)\mathscr{N}_-^5(\alpha)}{(\alpha^2-\nu_m^2)\chi_-(\eta_2,\alpha)}. \tag{6.89}$$

With the aid of cauchy's integral formula the terms at the right-hand of the equation (6.89) can be decomposed as

$$\sum_{m=1}^{\infty}\frac{L_m\cos L_m b(\mathfrak{p}_m-\iota\alpha\mathfrak{q}_m)\mathscr{N}_-^5(\alpha)}{(\alpha^2-\nu_m^2)\chi_-(\eta_2,\alpha)} = -\sum_{m=1}^{\infty}\frac{(\mathfrak{p}_m+\iota\nu_m\mathfrak{q}_m)L_m\cos L_m b\mathscr{N}_+^5(\upsilon_m)}{2\upsilon_m(\alpha+\upsilon_m)\chi_+(\eta_2,\nu_m)} + \sum_{m=1}^{\infty}\frac{L_m\cos L_m b}{\alpha+\nu_m}\left[\frac{(\mathfrak{p}_m-\iota\alpha\mathfrak{q}_m)\ \mathscr{N}_-^5(\alpha)}{(\alpha-\upsilon_m)\chi_-(\eta_2,\alpha)} + \frac{(\mathfrak{p}_m+\iota\nu_m\mathfrak{q}_m)\ \mathscr{N}_+^5(\nu_m)}{2\nu_m\chi_+(\eta_2,\nu_m)}\right]. \tag{6.90}$$

Now substituting equation (6.90) in equation (6.89), then placing the terms which are analytic in the upper half-plane ($\Im\mathfrak{m}(\alpha) > -k_{\mathfrak{eff}}$) at the left-hand side and those which analytic in lower half-plane ($\Im\mathfrak{m}(\alpha) < k_{\mathfrak{eff}}$) at the right-hand side which gives

$$\frac{k\chi_+(\eta_2,\alpha)\mathscr{R}_+^5(\alpha)}{\mathscr{N}_+^4(\alpha)} + \sum_{m=1}^{\infty}\frac{(\mathfrak{p}_m+\iota\upsilon_m\mathfrak{q}_m)L_m\cos L_m b\mathscr{N}_+^5(\upsilon_m)}{2\upsilon_m(\alpha+\upsilon_m)\chi_+(\eta_2,\upsilon_m)} = \frac{F_-(\alpha,b)Q_-(\alpha)}{\chi_-(\eta_2,\alpha)} + \sum_{m=1}^{\infty}\frac{L_m\cos L_m b}{\alpha+\upsilon_m}\left[\frac{(\mathfrak{p}_m-\iota\alpha\mathfrak{q}_m)\ \mathscr{N}_-^5(\alpha)}{(\alpha-\upsilon_m)\chi_-(\eta_2,\alpha)} + \frac{(\mathfrak{p}_m+\iota\upsilon_m\mathfrak{q}_m)\ \mathscr{N}_+^5(\upsilon_m)}{2\upsilon_m\chi_+(\eta_2,\upsilon_m)}\right]. \tag{6.91}$$

The required solution of Wiener-Hopf equation for the transmitted can be obtained by using analytical continuation principle following extended Liouville's

theorem, the above expression gives

$$\frac{k\chi_+(\eta_1,\alpha)\mathscr{R}_+^5(\alpha)}{\mathscr{N}_+^5(\alpha)} = -\sum_{m=1}^{\infty}\frac{(\mathfrak{p}_m+\iota\upsilon_m\mathfrak{q}_m)L_m\cos L_m b\mathscr{N}_+^5(\upsilon_m)}{2\upsilon_m(\alpha+\upsilon_m)\chi_+(\eta_2,\upsilon_m)}. \tag{6.92}$$

6.4 DETERMINATION OF THE UNKNOWN COEFFICIENTS

The significant distinction of this sort of formulation from the one used by Cigar and Büyükaksoy [12], was the simultaneous use of Mode-Matching technique with the Fourier transform. The Mode-Matching technique enables us to express the field components defined in the waveguide region in terms of normal modes as

$$H_z^2(x,y) = \sum_{m=1}^{\infty} a_n \sin\zeta_n(y+b)e^{-\iota\beta_n x}. \tag{6.93}$$

With the help of boundary conditions represented by equations (6.5) and (6.6) β_n 's and ζ_n's are obtained from

$$\zeta_n\cos\zeta_n b = 0, \quad n = 1,2,3,..., \tag{6.94}$$

which gives

$$\zeta_n = (2n+1)\frac{\pi}{4b}, \quad \beta_n = \sqrt{k_{\text{eff}}^2-\zeta_n^2}, \quad \Im\mathrm{m}(\beta_n) > \Im\mathrm{m}(k_{\text{eff}}), \quad n = 1,2,.... \tag{6.95}$$

From continuity relations represented by equations (6.11) and (6.12) gives

$$\mathfrak{f}(y) - \iota\alpha\mathfrak{g}(y) = -\iota\sum_{n=1}^{\infty} a_n(\alpha+\beta_n)\sin\zeta_n(y+b). \tag{6.96}$$

Using equation (6.35) into equation (6.96) gives

$$\sum_{m=1}^{\infty}(\mathfrak{f}_m - \iota\alpha\mathfrak{g}_m)\cos\mathfrak{L}_m t = -\iota\sum_{n=1}^{\infty} a_n(\alpha+\beta_n)\sin\zeta_n(y+b). \tag{6.97}$$

Multiplying equation (6.97) by $\cos \mathfrak{L}_s t$ and integrating with respect y from $y = 0$ to $y = b$, one obtains

$$\mathfrak{f}_s - \iota\alpha\mathfrak{g}_s = -\frac{\iota}{\mathscr{D}_s^4}\sum_{n=1}^{\infty}\frac{\zeta_n \cos \mathfrak{L}_s b}{\zeta_n^2 - \mathfrak{L}_s^2}\mathfrak{a}_n(\alpha + \beta_n), \tag{6.98}$$

Using equation (6.98) in equation (6.37) gives

$$\mathscr{R}_+^4(\alpha_m) = -\iota\left(\frac{\sin \mathfrak{L}_m b}{\mathfrak{L}_m} + \frac{\eta_1}{i k_{\mathfrak{eff}}}\cos \mathfrak{L}_m b\right)\sum_{n=1}^{\infty}\frac{\zeta_n \cos \mathfrak{L}_m b}{\zeta_n^2 - \mathfrak{L}_m^2}\mathfrak{a}_n(\alpha_m + \beta_n) \tag{6.99}$$

Substituting equations (6.99) and (6.98) in equation (6.45) at $\alpha = \alpha_s$ leads to

$$\begin{aligned}
&\frac{\eta_1\chi_+(\eta_1,\alpha_s)}{\mathscr{N}_+^4(\alpha_s)}\left(\frac{\sin \mathfrak{L}_s b}{\mathfrak{L}_s} + \frac{\eta_1}{i k_{\mathfrak{eff}}}\cos \mathfrak{L}_s b\right)\sum_{n=1}^{\infty}\frac{\zeta_n \sin \mathfrak{L}_s b}{\zeta_n^2 - \mathfrak{L}_s^2}\mathfrak{a}_n(\alpha_s + \beta_n)\\
&= \frac{2k\sin\theta_0 e^{-ik_{eff}b\sin\theta_0}\mathscr{N}_-(k_{\mathfrak{eff}}\cos\theta_0)}{(1+\eta_1\sin\theta_0)(\alpha_s - k_{\mathfrak{eff}}\cos\theta_0)\chi_-(\eta_1, k_{\mathfrak{eff}}\cos\theta_0)}\\
&+ \sum_{m=1}^{\infty}\frac{\iota\mathfrak{L}_m \sin \mathfrak{L}_m b\mathscr{N}_+^4(\alpha_m)}{\mathscr{N}_m^4(\alpha_s+\alpha_m)2\alpha_m\chi_+(\eta_1,\alpha_m)}\sum_{n=1}^{\infty}\frac{\zeta_n \sin \mathfrak{L}_m b}{\zeta_n^2 - \mathfrak{L}_m^2}\mathfrak{a}_n(\beta_n - \alpha_m).
\end{aligned} \tag{6.100}$$

The above expression can be written as under

$$\sum_{n=1}^{\infty}\mathscr{A}_n(\alpha_s)\mathfrak{a}_n = I(\alpha_s), \qquad s = 1,2,3,\ldots \tag{6.101}$$

where

$$\begin{aligned}
\mathscr{A}_n(\alpha_s) &= \frac{\eta_1\chi_+(\eta_1,\alpha_s)}{\mathscr{N}_+(\alpha_s)}\left(\frac{\sin \mathfrak{L}_s b}{\mathfrak{L}_s} + \frac{\eta_1}{i k_{\mathfrak{eff}}}\cos \mathfrak{L}_j b\right)\frac{\zeta_n \sin \mathfrak{L}_s b}{\zeta_n^2 - \mathfrak{L}_s^2}(\alpha_s + \beta_n)\\
&+ \sum_{m=1}^{\infty}\frac{\iota\mathfrak{L}_m \sin \mathfrak{L}_m b\mathscr{N}_+^4(\alpha_m)\zeta_n \sin \mathfrak{L}_m b(\beta_n - \alpha_m)}{2\mathscr{N}_m^4\alpha_m(\alpha_j+\alpha_m)\chi_+(\eta_1,\alpha_m)(\zeta_n^2 - \mathfrak{L}_m^2)}
\end{aligned} \tag{6.102}$$

and

$$I(\alpha_s) = \frac{2k_{eff}\sin\theta_0 e^{-\iota k_{\mathfrak{eff}}b\sin\theta_0}\mathscr{N}_-(k_{\mathfrak{eff}}\cos\theta_0)}{(1+\eta_1\sin\theta_0)(\alpha_s - k_{\mathfrak{eff}}\cos\theta_0)\chi_-(\eta_1, k_{\mathfrak{eff}}\cos\theta_0)}\,. \tag{6.103}$$

The infinite system of algebraic equation in equation (6.101) will be solved numerically. To solve this system we truncate the infinite system of algebraic equations after the first N terms.

Now for transmitted field one can consider continuity relations represented by equations (6.13) and (6.14) as under

$$\mathfrak{p}(y) - \iota\alpha\mathfrak{q}(y) = -\iota\sum_{n=1}^{\infty}\mathfrak{a}_n(\alpha+\beta_n)\sin\zeta_n(y+b). \tag{6.104}$$

Using equation (6.69) into equation (6.104), gives

$$\sum_{m=1}^{\infty}(\mathfrak{p}_m - \iota\alpha\mathfrak{q}_m)\sin L_m t \;= -\iota\sum_{n=1}^{\infty}\mathfrak{a}_n(\alpha+\beta_n)\sin\zeta_n(y+b). \tag{6.105}$$

Multiplying equation (6.105) by $\sin L_s y$ and integrating from $y=-b$ to $y=0$, one obtains

$$\mathfrak{p}_s - \iota\alpha\mathfrak{q}_s = \frac{-\iota}{\mathscr{D}_s^5}\int_{-b}^{0}\sum_{n=1}^{\infty}\mathfrak{a}_n(\alpha+\beta_n)\sin\zeta_n(y+b)\sin L_s y\,dy, \tag{6.106}$$

simplification of which gives

$$\mathfrak{p}_s - \iota\alpha_s\mathfrak{q}_j = -\frac{\iota}{\mathscr{D}_m^5}\sum_{n=1}^{\infty}\mathfrak{a}_n(\alpha+\beta_n)\Delta_{ns}, \tag{6.107}$$

where Δ_{ns} is given by

$$\Delta_{ns} = \frac{1}{\zeta_n^2 - L_s^2}\left(L_s\sin\zeta_n b - \zeta_n\sin L_s b\right). \tag{6.108}$$

6.5 THE DIFFRACTED AND TRANSMITTED FIELDS

The diffracted field $H_z^1(x,y)$ is acquired by taking the inverse Fourier transform of $F(\alpha,y)$. While using equation (6.21), one gets

$$H_z^1(x,y) = \frac{1}{2\pi}\int_{\mathscr{L}}\frac{k_{\text{eff}}}{\mathfrak{L}(\alpha)}\mathscr{R}_+^4(\alpha)\chi(\eta_1,\alpha)e^{\iota\mathfrak{L}(\alpha)(y-b)}e^{-\iota\alpha x}\,d\alpha. \tag{6.109}$$

Using the replacement of function $\chi(\eta_1,\alpha)$ and variables $\alpha=-k_{\text{eff}}\cos t$, $x=\rho\cos\theta$ and $y=\rho\sin\theta$, equation (6.109) takes the form

$$H_z^1(\rho,\theta)=\frac{1}{2\pi}\int_{\mathscr{L}}\frac{\mathscr{R}_+^4(-k_{\text{eff}}\cos t)k_{\text{eff}}\sin t}{1+\eta_1\sin t}e^{-\iota k_{\text{eff}}\sin t+\iota k_{\text{eff}}\rho\cos(t-\theta)}dt. \tag{6.110}$$

The integral in equation (6.110) can be evaluated asymptotically through the saddle point technique. Here, saddle point occurs at $t=\theta$.

On taking into account equation (6.88), the diffracted field takes following form

$$\begin{aligned}H_z^1(\rho,\theta)=&\frac{k\sqrt{(\epsilon_1^2-\epsilon_2^2)/\epsilon_1}\,e^{\iota k\rho\sqrt{(\epsilon_1^2-\epsilon_2^2)/\epsilon_1}-\iota\frac{\pi}{4}-\iota k\sqrt{(\epsilon_1^2-\epsilon_2^2)/\epsilon_1}\,b\sin\theta}\sin\theta}{\sqrt{2\pi k\rho}(1+\eta_1\sin\theta)}\\&\times\left[\frac{2\iota\sin\theta_0 e^{-ik\sqrt{(\epsilon_1^2-\epsilon_2^2)/\epsilon_1}\,b\sin\theta_0}\mathscr{N}_-^4(k\sqrt{(\epsilon_1^2-\epsilon_2^2)/\epsilon_1}\cos\theta_0)}{\eta_1(1+\sin\theta_0)(\cos\theta+\cos\theta_0)\chi_-(\eta_1,k_{\text{eff}}\cos\theta_0)}+\right.\\&\left.\sum_{m=1}^{\infty}\frac{\iota\mathfrak{L}_m\sin\mathfrak{L}_m b\mathscr{N}_+^4(\alpha_m)(\mathfrak{f}_m+\iota\alpha_m\mathfrak{g}_m)}{2\eta_1\alpha_m(\alpha_m-k\sqrt{(\epsilon_1^2-\epsilon_2^2)/\epsilon_1}\cos\theta)\chi_+(\eta_1,\alpha_m)}\right]\frac{\mathscr{N}_-^4(k\sqrt{(\epsilon_1^2-\epsilon_2^2)/\epsilon_1}\cos\theta)}{\chi_-(\eta_1,k\sqrt{(\epsilon_1^2-\epsilon_2^2)/\epsilon_1}\cos\theta)}.\end{aligned} \tag{6.111}$$

The transmitted field $H_z^5(x,y)$ is obtained by taking the inverse Fourier transform of $\psi(\alpha,y)$. While using equation (6.51), one gets

$$H_z^5(x,y)=\frac{1}{2\pi}\int_{\mathscr{L}}\frac{k_{\text{eff}}\mathscr{R}_+^5(\alpha)\chi(\eta_2,\alpha)}{\mathfrak{L}(\alpha)}e^{-\iota\mathfrak{L}(y+b)}e^{-\iota\alpha x}d\alpha. \tag{6.112}$$

Using the replacement of function $\chi(\eta_2,\alpha)$ and change of variables $\alpha=-k_{\text{eff}}\cos t$, $x=\rho\cos\theta$ and $y=\rho\sin\theta$, equation (6.112) takes the form

$$H_z^5(\rho,\theta)=\frac{1}{2\pi}\int_{\mathscr{L}}\frac{\mathscr{R}_+^5(-k_{\text{eff}}\cos t)k_{\text{eff}}\sin t}{1+\eta_2\sin t}e^{-\iota k_{\text{eff}}\sin t+\iota k_{\text{eff}}\rho\cos(t+\theta)}dt. \tag{6.113}$$

The integral in equation (6.113) can be evaluated asymptotically through the saddle point technique. Here, saddle point occurs at $t=2\pi-\theta$. Taking into account

equation (6.92), the transmitted field takes the form:

$$H_z^5(\rho,\theta) = -\frac{\sqrt{(\epsilon_1^2-\epsilon_2^2)/\epsilon_1}\sin\theta e^{\iota k\rho\sqrt{(\epsilon_1^2-\epsilon_2^2)/\epsilon_1}-\frac{\iota\pi}{4}-\iota kb\sqrt{(\epsilon_1^2-\epsilon_2^2)/\epsilon_1}\sin\theta}}{\sqrt{2\pi k\rho}(1-\eta_2\sin\theta)}$$
$$\times\frac{\mathcal{N}_-^5(k\sqrt{(\epsilon_1^2-\epsilon_2^2)/\epsilon_1}\cos\theta)}{\chi_-(\eta_1,k\sqrt{(\epsilon_1^2-\epsilon_2^2)/\epsilon_1}\cos\theta)}\sum_{m=1}^{\infty}\frac{L_m\cos L_m b\mathcal{N}_+^5(\upsilon_m)(\mathfrak{p}_m+\iota\mathfrak{q}_m)}{2\upsilon_m(\upsilon_m-k_{\text{eff}}\cos\theta)\chi_+(\eta_2,\upsilon_m)}. \quad (6.114)$$

6.6 COMPUTATIONAL RESULTS AND DISCUSSION

In this section, we evaluate the numerical results for various physical parameters of interest. It is obvious to see that the diffracted and transmitted fields represented by the equations (6.111) and (6.114) contain infinite series. Fig. (6.2) shows the variation of the modulus of the diffracted field versus the truncation number "N". It is observed that the effect of the truncation number is negligible for $N \geq 100$. Hence, the infinite system of algebraic equations in equation (6.101) can be managed to deal as finite. Fig. (6.3) deals with variation of modulus of the transmitted field with respect to truncation number N and the result is obtained that the effect of the truncation number is negligible for $N \geq 80$. Fig. (6.4) depicts the variation in the diffracted field versus impedance η_1. It is apparent that the diffracted field decreases with increasing of surface impedance η_1. Whereas Figs. (6.5) and (6.6) show variation in the diffracted field versus the cold plasma permittivity values ϵ_1 and ϵ_2, respectively. It is interesting to note that the diffracted field highly decreases by increasing ϵ_1 but slightly increases with increasing ϵ_2. Also Fig. (6.7) explores the effect of surface impedance over the transmitted field. It is observed that the transmitted field also decreases with increasing η_2. The effect of cold plasma permittivity values ϵ_1 and ϵ_2 over the transmitted are shown in Figs. (6.8) and (6.9), respectively. It is observed here that the transmitted field highly decreases while increasing ϵ_1 whereas it increases slightly by increasing ϵ_2. In other words the diffracted and transmitted fields amplitude decreases with

increasing ion number density in cold plasma or by decreasing plasma frequency.

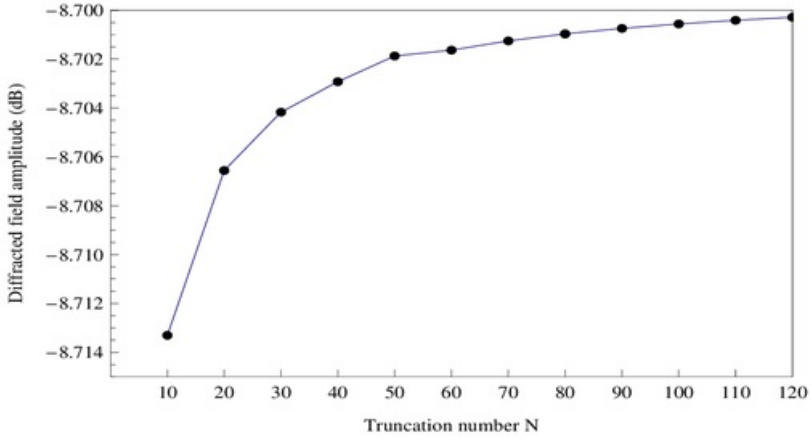

FIGURE 6.2. *Variation in the diffracted field amplitude versus "N" at* $k = 5$, $\theta_0 = 45^o$, $\theta = 90^0$, $\eta_1 = 0.2\iota$, $\epsilon_1 = 0.8$, $\epsilon_2 = 0.1$, $b = 0.2\lambda$.

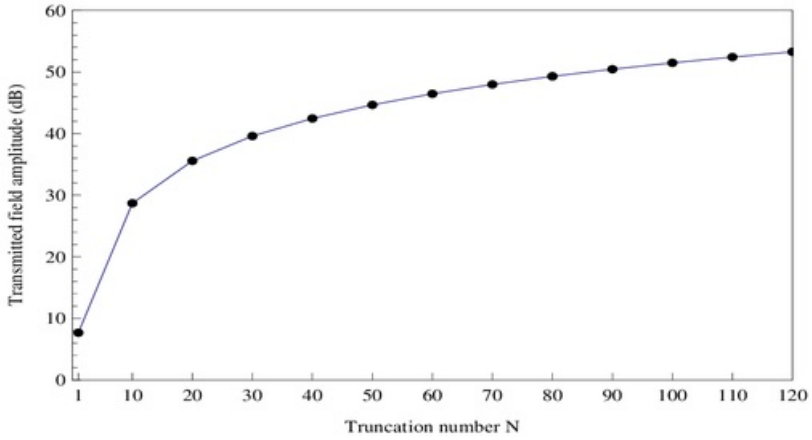

FIGURE 6.3. *Variation in the transmitted field amplitude versus "N" at* $k = 5$, $\theta_0 = 45^o$, $\theta = 90^0$, $\eta_5 = 0.4\iota$, $\epsilon_1 = 0.5$, $\epsilon_2 = 0.1$, $b = 0.2\lambda$.

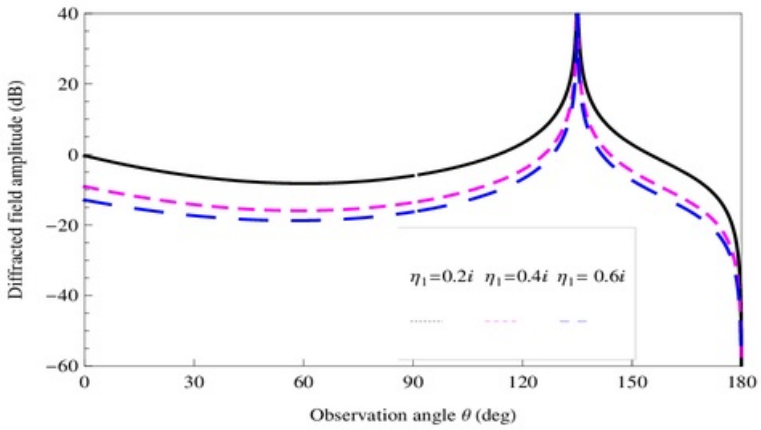

FIGURE 6.4. *Variation in the diffracted field amplitude versus "θ_1" at $\theta_0 = 45^0$, $k = 5$, $\epsilon_1 = 0.8$, $\epsilon_2 = 0.1$ and $b = 0.2\lambda$.*

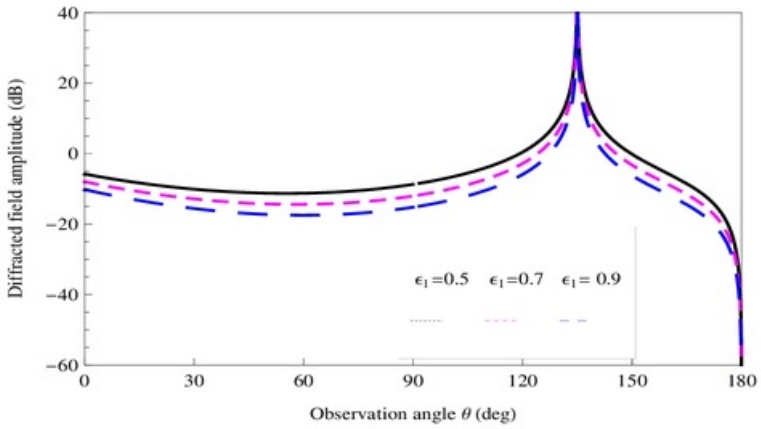

FIGURE 6.5. *Variation in the diffracted field amplitude versus "ϵ_1" at $k = 5$, $\theta_0 = 45^0$, $\eta_1 = 0.2\iota$, $\epsilon_2 = 0.1$ and $b = 0.2\lambda$.*

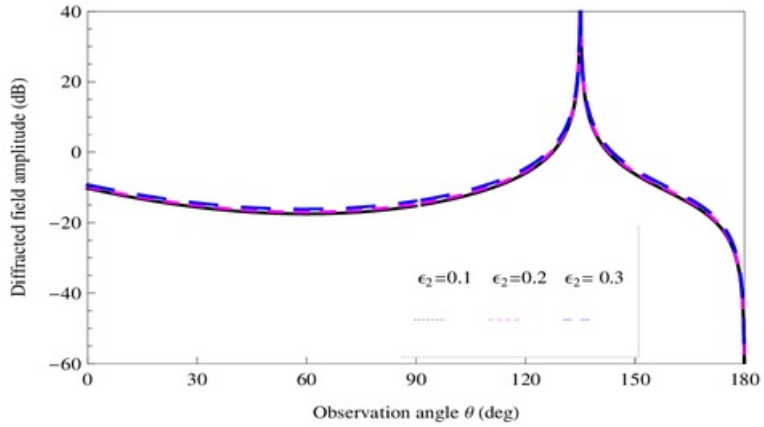

FIGURE 6.6. *Variation in the diffracted field amplitude versus "ϵ_2" at $k = 5$, $\theta_0 = 45^0$, $\eta_1 = 0.2\iota$, $\epsilon_1 = 0.8$ and $b = 0.2\lambda$.*

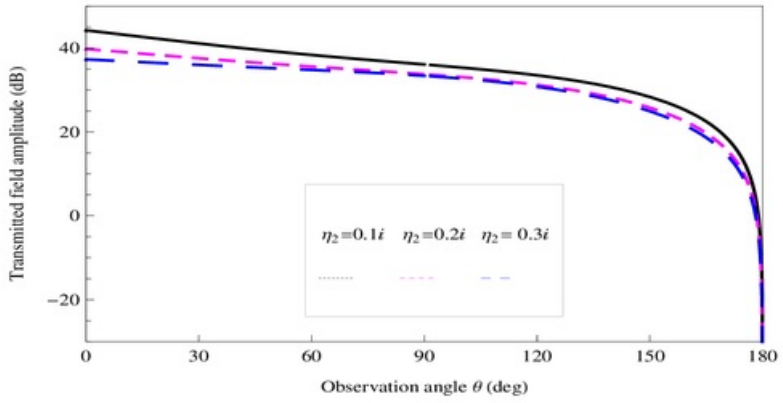

FIGURE 6.7. *Variation in the transmitted field amplitude versus "η_2" at $k = 5$, $\theta_0 = 45^o$, $\epsilon_1 = 0.8$, $\epsilon_2 = 0.1$ and $b = 0.2\lambda$.*

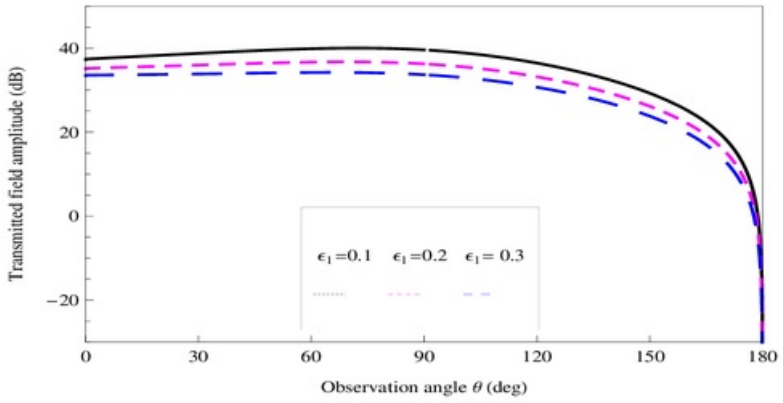

FIGURE 6.8. *Variation in the transmitted field amplitude versus "ϵ_1" at $k = 5$, $\eta_2 = 0.2\iota$, $\epsilon_2 = 0.1$ and $b = 0.2\lambda$.*

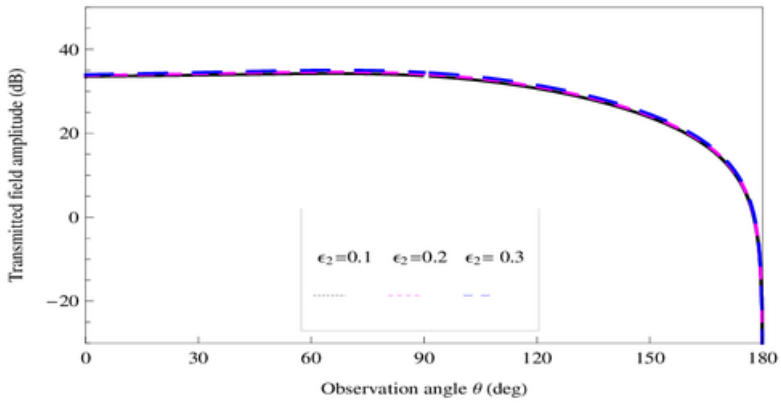

FIGURE 6.9. *Variation in the transmitted field amplitude versus "ϵ_2" at $k = 5$, $\eta_2 = 0.2\iota$, $\epsilon_1 = 0.8$ and $b = 0.2\lambda$.*

CHAPTER 7

CONCLUSION AND PERSPECTIVES

The study of plasma in wave scattering problems have been of significant interest in recent years due to a variety of associated applications in diverse domains. The particular application includes, the construction of antennas, communication between the vehicles and earth station, radio communication etc. We have investigated theoretically the effectiveness of ionosphere plasma, earth's magnetic field, structure and nature of the body material used as an artificial satellite. For analysis purpose the whole system was supposed to be immersed in a cold plasma. The underlying model problems present that how a particular class of boundary-valued problems related to wave scattering in cold plasma may be solved by using different semi-analytic techniques. The solutions to the problems have been focused using Wiener-Hopf technique together with the Mode-Matching technique.

In a first attempt, the model problem describing the effect of cold plasma on scattering of E-polarized plane wave by step discontinuity has been considered. For this purpose the Helmholtz equation in cold plasma has been retrieved from Maxwell's equations in the canonical problem. Then with the help of Fourier transform followed by the Wiener-Hopf technique the diffracted field expression was obtained successfully. It is concluded that the effect of the truncation number is negligible after 15 truncation term. Moreover the diffracted field amplitude

increases with the length of vertical plate. The analysis has also been performed for other parameters of interest such as incident angle and surface impedances. It is depicted that the amplitude of diffracted field increases while increasing the permittivity value ϵ_1. In other words amplitude increases by either decreasing electron number density (plasma frequency) or by increasing ion number density. Whereas in contrast to ϵ_1 the amplitude of diffracted field decreases with increase of the permittivity value ϵ_2. It has been noted that the diffracted field is greatly effected due to permittivity value ϵ_1 as compared with that of permittivity value ϵ_2. Moreover the results in the absence of cold plasma can be computed while taking $\epsilon_1 = 1$ and $\epsilon_2 = 0$ With this we may conclude that the existing model with out cold plasma's effects can be reduced from this model. This analysis has been carried out in Chapter (3).

Further, we have studied the effect of cold plasma permittivity by an impedance loaded parallel-plate waveguide. From the computed results it has been observed that diffracted field is mostly affected by varying the plate separations, whereas the variation of impedances η_2 and η_3 have negligibly small effects on the obtained diffracted field. These results are much consistent with that of already existing results in literature, for example [12]. Moreover the diffracted field amplitude decreases with increasing the permittivity values ϵ_1 and ϵ_2. Again the diffracted field is generally affected due to permittivity value ϵ_1 than that of ϵ_2. In this case the truncated parameter takes higher value in order to get appropriate results. These observations are related to Chapter (4) of this dissertation.

The effect of cold plasma permittivity on the radiation of the dominant TEM-wave by an impedance loaded parallel plate has been examined in Chapter (5). For the reason, the waveguide radiator with impedance loaded parallel-plate is considered. The Wiener-Hopf technique enables to obtain the radiated field while computing the unknown complex coefficients with the help of Mode-Matching technique. It has been concluded that the radiated field amplitude had impres-

sive variation against all physical parameters such as plate separation b, surface impedances η_1, η_2, η_3 and η_4 and permittivity values ϵ_1 and ϵ_2 for both reactive and capacitive cases. Moreover the radiated field amplitude for both cases (Reactive and Capacitive) decreases with the increasing of permittivity values ϵ_1 and ϵ_2. Likewise diffracted field, the radiated field has largely been affected due to permittivity value ϵ_1 instead of ϵ_2. Further the amplitude of radiated field is effected drastically in the presence of an ionosphere plasma medium. This observation can be depicted while ignoring the effect of cold plasma in the expression obtained for radiated field. It has also been observed throughout that the radiated field showed impedance dependant variations. These variations are actually related to the magnetic and electric susceptibilities of the waveguide surfaces. We conclude that these results can be used to improve the radiated signal quality transmitted by an artificial satellite in the ionosphere.

Finally, we have examined diffracted and transmitted fields due to an impedance loaded waveguide located in cold plasma. The ultimate objective was to study the effect of cold plasma permittivity on the diffracted and transmitted fields. Again hybrid methods such as Wiener-Hopf technique and Mode-Matching technique were opted to get the desired expressions of diffracted and transmitted fields. It is worthwhile to comment that up to 100 number of truncation terms are needed to achieve the better accuracy of the obtained solution. By this we can say that whilst computing diffracted and transmitted field one requires higher number of truncated terms as compared to problem of diffraction and radiation. The diffracted and transmitted fields have similar behavior (inverse proportionality) for both impedance parameters η_1 and η_2. A similar proportionality is observed when diffracted and transmitted fields were observed with respect to both permittivity values ϵ_1 and ϵ_2.

In addition, while solving field problems, there are mainly three types of techniques: experimental, analytical, and numerical. Experiments are expensive,

time consuming, and usually do not allow much flexibility in parameter variation. However analytical and numerical methods are much flexible. Numerical methods have become popular with the development of the computing capabilities, and although they give approximate solutions, have sufficient accuracy for engineering purposes. But as a particular choice in this thesis we have preferred analytical methods over numerical methods. As an argument we seek that the implication of numerical techniques restrict such models up to low frequency regime whereas the analytical/hybrid methods used here in do not have limitations for a specific range of frequency problems. So we have a preference to use hybrid methods which operate well for both low frequency problems as well as high frequency problems.

7.1 FUTURE DIRECTIONS AND OPEN QUESTIONS

The analysis to the proposed problems related to the effect of cold plasma and wave scattering requires further attention for more realistic models, for example, by taking into account non-linear higher order boundaries, modeling different physical edge conditions and computing related power expressions. Moreover, in view of their application for acoustic scattering, underwater acoustics, structural acoustics, electromagnetic wave scattering, the low-frequency approximations need due attention. The problems of coupled wave scattering with cold plasma effects finds many applications in a broad area of physics and engineering. For the problems involving planar boundaries such as soft, rigid or impedance, their solution can be obtained via standard Wiener-Hopf technique In such cases the obtained eigenfunctions in terms of either reflected, transmitted or radiated fields satisfy the usual orthogonal properties and required no more complications. Also these eigenfunctions are linearly independent. It would be of interest to consider more complicated boundary conditions on the faces of waveguide. Therefore for non-planar boundaries (flexible), the eigenfunctions

will no more be orthogonal as well as linearly independent. All such problems will lead to in some form of infinite sum. Obviously calculating an infinite sum is impractical (but still possible) but mathematical solutions will require higher order of accuracy. The demonstration of such an application of plasma physics and wave scattering will determine that how a particular class of model problems may be solved. The Wiener-Hopf technique will no longer exist to yield solution of these problems. Of course, for such type of problems, one have to develop appropriate orthogonality relations instead of usual ones. After that the matched eigenfunctions expansion may lead to the solution of problem. The eigenfunctions expansion with dependant sums will require the use of some extra conditions. Therefore some extra conditions in terms of edge conditions will be necessary to use. Otherwise the uniqueness and the convergence of the modeled problems will be questionable. The overall process will be the blend of analytic as well as numerical approaches. Further, while obtaining expressions for the power transferred through the boundaries as well as fluid would be an interesting and realistic choice. The present model could be extended to aforementioned studies with the help of some related investigations, refer for instance to [92, 93, 94, 95, 96].

BIBLIOGRAPHY

[1] S. L. Dvorak, R. W. Ziolkowski and D. G. Dudley, "Ultra-wide-band electromagnetic pulse propagation in a homogeneous cold plasma", *Radio Science*. 32: pp. 239–250 (1997). [cited at p. 1, 7]

[2] A. D. Avdeev, "On the special function of the problem of diffraction by a wedge in an anisotropic plasma", *Radio Tekhnika 1 Elektronika*. 39: pp. 885–892 (1994). [cited at p. 1]

[3] M. K. Tippet and R. W. Ziolkowski, "A bidirectional wave transformation of the cold plasma equations", *Journal of Mathematical Physics*. 32: pp. 488–492 (1991). [cited at p. 1]

[4] H. Rishbeth and M. Mendillo, "Patterns of f2-layer variability", *J. Math. Phys*. 32: pp. 488–492 (1991). [cited at p. 1]

[5] A. Nina, V. Cadez, V. Streckovic and D. Sulic, *Sect. b, beam interact. mater. Atoms. Nucl. Instrum. Methods Phys.* 279: pp. 110–113 (2012). [cited at p. 2]

[6] M. Grabner and V. Kvicera, "Refractive index measurements in the lowest troposphere in the czech republic", *J. Atoms. Solar-Terr. Phys.* 68: pp. 1334–1339 (2006). [cited at p. 2, 7]

[7] H. Rishbeth, "the ionospheric e layer and f layer dynamos", *J. Atoms. Solar-Terr. Phys.* 59: pp. 1873–1880 (1997). [cited at p. 2]

[8] B. Noble, *Methods based on the Wiener–Hopf technique*, Pergamon Press, London (1958). [cited at p. 3, 11, 29]

[9] R. Mittra and S. W. Lee, *Analytical Techniques in the theory of guided waves*, The macmillan Co, Newyork (1971). [cited at p. 3]

[10] I. Sahin, A. H. Serbest and M. A. Lyalinov, "Diffraction of plane waves by an impedance half-plane in cold plasma", *IEEE.* 38: pp. 569–572 (1998). [cited at p. 3, 7]

[11] H. Yener and A. H. Serbest, "Diffraction of plane waves by an impedance half-plane in cold plasma", *J. of Electromagn. Waves and Appl.* 16: pp.995–1005 (2002). [cited at p. 3, 37]

[12] G. Cinar and A. Büyükaksoy, "A hybrid method for the solution of plane wave diffraction by an impedance loaded parallel-plate waveguide", *PIER.* 60: pp. 293–310 (2006). [cited at p. 3, 7, 53, 66, 105, 116]

[13] Y. Y. Lau and R. J. Briggs, "Effects of cold plama on the negative mass instability of a relativistic electron layer", *Physics of Fluids.* 14(5) pp. 967–976 (1971). [cited at p. 4]

[14] S. J. Buchsbaum, L. Mower and S. C. Brown, "Interaction between cold plasmas and guidede electromagnetic waves", *Physics of Fluids.* 3(5): pp. 806–819 (1960). [cited at p. 4]

[15] L. Bardos and H. Barankova, "Radio frequency hollow cathode source for large area cold atmospheric plama applications", *Surface and Coatings Technology.* 133-134: pp. 523–527 (2000). [cited at p. 4]

[16] J. Galejs, "Impedance of a finite insulated cylindrical antenna in a cold plasma with a longitudinal magnetic field", *IEEE Traksactions on Antenna and Propagation.* ap-14(6): pp. 727–736 (1966). [cited at p. 4]

[17] A. V. Tyukhtin, "Diffraction of electromagnetic waves by a half-plane located in a moving cold plasma", *Radiophysics and Quantum Electronics*. 41(4): pp.314–328 (1998) [cited at p. 4]

[18] T. Ikiz and F. Karaomerlioglu, "Diffraction of plane waves by a two-impedance wedge in cold plasma", *J. Electromagn Waves and appl.* 18: pp. 1361–1372 (2004) [cited at p. 4]

[19] H. Ammari and H. Kang, F. Santosa, "Scattering of electromagnatic waves by thin dielectric struc- tures", *SAIM Journal on Mathematical Analysis*. 38: pp. 1329-1342 (2006). [cited at p. 4]

[20] H. Ammari and A. Khelifi, "Electromagnetic scattering by small dielectric inhomogeneties", *J. Math. Pures Appl.* 82: pp. 749–842 (2003). [cited at p. 4]

[21] H. Ammari and C. Latiri-Grous, "Electromagnetic scattering on an absorbing plane", *Integr. Equ. Oper. Theory*. 39: pp. 159-181 (2001). [cited at p. 4]

[22] H. Poincare, "Sur la polarization per diffraction", *Acta Math.* 16: pp. 297-339 (1892). [cited at p. 4]

[23] A. Sommerfeld, "Mathematische theorie der diffraction", *Math. Ann*. 47: pp.317–374 (1896). [cited at p. 4, 5]

[24] H. S. Carslaw, "Diffraction of waves by a wedge of any angle", *Proc. Lond. Math. Soc*.18:(2),291 (1919). [cited at p. 4]

[25] H. Levine and Schwinger, "On the theory of diffraction by an aperture in an infinite plane screen.I." *J. Phys. Rev.*, 74: 958 (1948). [cited at p. 4]

[26] H. Levine and Schwinger, "On the theory of diffraction by an aperture in an infinite plane screen.II." *J. Phys. Rev.*, 75: 1423 (1949). [cited at p. 4]

[27] E. T. Copson, "Diffraction by a plane screen", *Quart. J.Math.* 17: pp. 277-289 (1946). [cited at p. 5]

[28] A. D. Rawlins and W. E. Williams *Q. J. Mech. Appl. Math.* 34(1)(1981). [cited at p. 5]

[29] W. E. Williams, Proc. Camb. Phil.Soc. 55,195 (1959). [cited at p. 5]

[30] V. G. Daniele, "On the solution of two coupled wierner hopf equation", *SIAM J. Appl. Math.* 44: (1984). [cited at p. 5]

[31] A. D. Rawlins, "A note on Wiener-Hopf matrix factorization" *Q. J. Mech. Appl Math.* 38,433 (1985). [cited at p. 5]

[32] C. P. Bates and R. Mittra, "A factorization procedure for Wiener-Hopf kernels", *IEEE Trans on Antennas Propagat.* 26: pp. 614–616 (1978). [cited at p. 5]

[33] R. Nawaz, M. Afzal and M. Ayub, "Acoustic propagation in two-dimensional waveguide for membrane bounded ducts", *Communication in Non-Linear Science and Numerical Simulation.* 20(2): pp. 421-433 (2015). [cited at p. 5]

[34] M. Ayub, R. Nawaz and A. Naeem, "Line source diffraction by a slit in a moving fluid", *Canadian Journal of Physics.* 87(11): pp. 1139–1149 (2009). [cited at p. 5]

[35] M. Ayub, R. Nawaz and A. Naeem, "Diffraction of an impulsive line source with wake", *Physica Scripta*. 82: 045402(10PP) (2010). [cited at p. 5]

[36] P. R. Brazier-Smith, "The acoustic properties of two co-planar half-plane plates", *Proc. R. Soc. A.* 409: pp. 115–139 (1987). [cited at p. 5]

[37] A. N. Norris and G. R. Wickham, "Acoustic diffraction from the junction of two flat plates", *Proc. R. Soc. A.* 451: pp. 631–655 (1995). [cited at p. 5]

[38] P. A. Cannell, "Edge scattering of aerodynamic sound by a lightly loaded elastic half-plane", *Proc. R. Soc. Lond.* A-347: pp. 213–238 (1975). [cited at p. 5]

[39] D. P. Warren, J. B, Lawrie and I. M. Mohamed, "Acoustic scattering in waveguides with discontinuities in height and material property", *Wave Motion.* 36: pp. 119–142 (2002). [cited at p. 5]

[40] A. Büyükaksoy and F. Birbir, "Plane wave diffraction by a reactive step", *Int. J. Engng Sci.*, 35: pp. 311–319 (1997). [cited at p. 5]

[41] A. Büyükaksoy anf F. Birbir, "Analysis of an impedance loaded parallel-plate waveguide radiator", *Journal of Electromagnetic Waves and Applications*. 12: pp. 1509–1526 (1998). [cited at p. 5, 6, 71]

[42] E. Topsakal, A. Büyükaksoy and M. Idemen, "Scattering of electromagnatic waves by a rectangular impedance cylinder", *Wave Motion*. 31: pp. 273–296 (2000). [cited at p. 5]

[43] G. Cinar and A. Büyükaksoy, "Diffraction by a thick impedance half plane with a different end faces impedance", *Electromagetics*. 22: pp. 565–580 (2002). [cited at p. 5]

[44] P. Mclver and A. D. Rawlins, "Diffraction by a rigid barrier with a soft or perfectly absorbent end face", *Wave Motion*. 22: pp. 387–402 (1995). [cited at p. 5]

[45] S. W. Rienstra, "Acoustic radiation from semi-infinite annular in a uniform subsonis mean flow", *Journal of Sound and Vibration*. 92(2): pp. 267–288 (1984). [cited at p. 5]

[46] M. Hassan and A. D. Rawlins, "Sound radiation in a planar trifurcated lined duct", *Wave Motion*. 29: pp. 157–74 (1999). [cited at p. 5]

[47] M. Ayub, A. Naeem and R. Nawaz, "Sound due to an impulsive line source", *Computer and Mathematics with Applications*. 60(12): pp. 3123–3129 (2010). [cited at p. 6]

[48] M. Ayub, M. Ramzan and A. B. Mann, "Line source and point source diffraction by a reactive step", *Journal of Modern Optics.*, 56(7): pp. 893-902 (2009). [cited at p. 6]

[49] M. Ayub, M. H. Tiwana and A. B. Mann, "Wiener-Hopf analysis of an acoustic plane wave in a trifurcated waveguide", *Archive of Applied Mechanics*. 81: pp. 701–713 (2011). [cited at p. 6]

[50] M. Ayub, M. Ramzan and A. B. Mann, "Magnetic line source diffraction by an impedance step", *IEEE trans. on Antennas Propagat*. 57(4): pp. 1289–1293 (2009). [cited at p. 6]

[51] R. Nawaz, A. Wahab and A. Rasheed, "An intermediate range solution to a diffraction problem with impedance conditions", Journal of Modern Optics 61 (16), pp. 1324–1332 (2014). [cited at p. 6]

[52] R. Nawaz, "A note on acoustic diffraction by an absorbing finite strip". *Indian J. of Pure and Appl. Math.* 43(6): pp. 571-589 (2012). [cited at p. 6]

[53] R. Nawaz, A. Naeem, M. Ayub and A. Javaid, "Point source diffraction by a slit in a moving fluid", *Waves in Random and Complex Media*. 24(4): pp. 357-375 (2014). [cited at p. 6]

[54] R. Nawaz and M. Ayub, "An exact and asymptotic analysis of a diffraction problem", *Meccanica*. 48: pp. 653-662 (2012). [cited at p. 6]

[55] J. B. Lawrie and I. D. Abrahams, "A brief historical perspective of the Wiener-Hopf technique", *J*. Eng. Math. 59: pp. 351–358 (2007). [cited at p. 6]

[56] T. Ikiz, S. Koshikawa, K. Kobashi, E. I. Veliev and A. H. Serbest, "Solution of plane wave diffraction by an impedance strip using a Numerical-analytical Method: E-Polarized Case", *J*. Electromagn. Waves and Appl. 15(3): pp.315–340 (2001). [cited at p. 6]

[57] A. Büyükaksoy and B. Polot, "A bifurcated waveguide problem", *ARI*. 51: pp.196–102 (1999). [cited at p. 6, 11]

[58] A. Rawlins, "A bifurcated circular waveguide problem", *IMA J.Appl. Math*. 54: pp.59–81 (1995). [cited at p. 6]

[59] J. R. Pace and R. Mittra, "The trifurcated waveguide", *R*adio Science. 1: pp.117–122 (1965). [cited at p. 6]

[60] D. S. Jones, "Diffraction by three semi-infinite planes", *P*roc. R. Soc. London. 404: pp.299–321 (1986). [cited at p. 6, 7]

[61] S. Asghar, M. Ayub and B. Ahmad, "Point source diffraction by three half planes in a moving fluid", *W*ave Motion. 15: pp.201–220 (1992). [cited at p. 7]

[62] A. D. Rawlin, "Two waveguide trifurcation problem", *Math. Proc. Camb. Phil. Soc.* 121: pp.555–573 (1997). [cited at p. 7]

[63] M. Hassan and A. D. Rawlin, "Two problem of waveguide carrying mean fluid flow", *J. Sound and Vib.* 216(4): pp. 713–738 (1998). [cited at p. 7]

[64] A. D. Rawlin and M. Hassan, "Wave propagation in a waveguide", *ZAMM Z. Angrew. Math. Mech.*, 83(5): pp. 333–343 (2003). [cited at p. 7]

[65] P. M. Morse and H. Feshbach, *Methods of theoretical physics* Mc Graw-Hill, New York, 1953. [cited at p. 7]

[66] E. L. Johansen, "Scattering coefficient for wall impedances change in waveguides", *IRE Transaction on Microwave Theory and Techniques.* pp.26–29 (1967). [cited at p. 7]

[67] A. Büyükaksoy, E. Topsakal and M. Idemen, "Plane wave diffractionby a pair of parallel soft and hord overlapping half-planes", *W*ave Motion. 20(3): pp.273–282 (1994). [cited at p. 7]

[68] M. Idemen, "A new method to obtain exact solutions of vector Wiener-Hopf equations", *Z*AMM Z. Angew. Math. Mech. 59: pp.656–658 (1979). [cited at p. 7]

[69] I. D. Abrahams, "Scattering of sound wavesby two pallalel semi-infinite screens", *W*ave Motion. 9: pp.289–300 (1987). [cited at p. 7]

[70] A. Büyükaksoy and G. Cinar, "Solution of matrix Wiener-Hopf equation conected with a plane wave diffraction by an impedance loaded parallel-plate waveguide", *M*ath. Mech. Appl. Sci. 28(14): pp.1633–1645 (2005). [cited at p. 7, 53, 63]

[71] A. Büyükaksoy and A. Demer, "Radiation of sound from a semi-infinite duct inserted axially into a larger tube with wall impedance discontinuity", *ZAMM M. Angew. Math. Mech.* 86(7): pp.563–571 (2006). [cited at p. 7]

[72] A. Büyükaksoy, I. H. Tayyar ang G. Uzgoren, "Influance of ajunction of perfectly conducting and impedance parallel plate semi-infinite waveguides to the domi-

nent mode propagation", *First european conference on antennas and propagation, Eu CAP Nice France (2006).* [cited at p. 7]

[73] I. H. Tayyar, A. Büyükaksoy and A. Isikyer, "Wiener-Hopf analysis of the parallel-plate waveguide with opposing rectangular dielectric-filled grooves", Can. J. Physics. 869: pp.733–745 (2008). [cited at p. 7]

[74] E. C. Titchmarch, *Theory of Fourier Integral*, Oxford University Press, 1937. [cited at p. 11]

[75] G. D. Maliuzhinets, "Excitation, reflection and emission of surface waves from a wedge with given face impedances", *Sov. Phy. Dokl.* 3: pp.752–755 (1958). [cited at p. 11]

[76] O. M. Bucci, "On a function occuring in the theory of scattering from an impedance half plane", *Report, Institute, Universitario Navale, Napoli, Italy*,(1974). [cited at p. 11]

[77] G. D. Maliuzhinets, "Das sommerfelds integral and die losung von beugungsaufgaben in winkelgebieten", *Ann. Phy.* 6: pp.107–112 (1960). [cited at p. 11]

[78] G. D. Maliuzhinets, "Inversion formula for the summerfeld integral", *Sov. Phy. Dokl.* 3: pp.52–56 (1958). [cited at p. 11]

[79] J. Lin Hu, S. Lin and W. Wang, "Calculation of Maliuzhinetz function in complex region", *IEEE trans. on Antennas Propagat.* 44(8): pp.1195–1196 (1996). [cited at p. 11]

[80] A. Osipov and V. Stein, "The theory and numerical computation of maliuzhinetz'special function", *DLR Institute of Radio Frequency Technology 1999*. [cited at p. 11]

[81] L. B. Felson and N. Marcuvitz, *Radiation and Scattering of Waves*, Prentice Hall, Englewood Cliffs, 1973. [cited at p. 11, 21]

[82] J. L. Volakis and T. B. A. Senior, "Simple expressions for a function occuring in diffraction theory", *IEEE trans. on Antennas Propagat.* 33: pp. 678–680 (1985). [cited at p. 20, 29]

[83] A. D. Rawlins "The solution of a mixed boundary problem in the theory of diffraction by a semi-infinite plane" *R Soc Lond A*: pp. 469–484 (1975). [cited at p. 24]

[84] E. L. Johansen, "Surface wave scattering by a step", *IEEE Transactions on Antennas and Propagation.* AP-15: pp. 442–448 (1967). [cited at p. 37]

[85] A. Büyükaksoy and G. Cinar, "Plane wave diffraction by a reactive step", *Int. J. Engg Sci.* 35(4): pp. 311–319 (1997). [cited at p. 37, 89]

[86] B. Rulf and R. A. Hurd, "Radiation from an open waveguide with reactive walls", *IEEE Trans. Antennas and Propagat.* AP-26(5): (1978). [cited at p. 71]

[87] R. Nawaz and J. B. Lawree, "Scattering of a fluid-structure coupled wave at a flanged junction between two flexible waveguides", *Journal of Acoustic Society of America* 134(3): pp. 1939–1949 (2013). [cited at p. 80]

[88] M. Afzal, R. Nawaz, M.Ayub and A. Wahab, "Acoustic scattering in a flexiable wave guide involving in step discontinity", *PLoS ONE* 9(8):e103807 (2014). [cited at p. 80]

[89] L. A. Weinsrein, "Rigorous solution of the problem of an open-ended parallel-plate waveguide", *Izv. Akad. Nauk., Ser. Fiz.* 12: pp. 144–165 (1948). [cited at p. 89]

[90] L. A. Weinsrein, "On the theory of diffraction by two parallel half-planes", *Izv. Akad. Nauk., Ser. Fiz.* 12: pp. 166–180 (1948). [cited at p. 89]

[91] J. Boersma, "Diffraction by two parallel half-planes", *Q. J. Mech. Math.* 28: pp. 405-425 (1975). [cited at p. 89]

[92] J. B. Lawrie and Idil M. M. Guled, "On tuning a reactive silencer by varying the position of an internal membrane", *J. Acoust. Soc. Am*, 120(2): (2006). [cited at p. 119]

[93] J. B. Lawrie and R. Kirby, "Mode matching without root finding: Application to a dissipative silencer", *J. Acoust. Soc. Am*, 119: pp. 2050–2061 (2006). [cited at p. 119]

[94] Y. D. Kaplunov, I. V. Kirillova and Y. A. Postnova, "Dispersion of waves in a plane acoustic layer with fexible elastic walls", *Acoustical Physics*, 50: pp. 694–698 (2004). [cited at p. 119]

[95] J. B. Lawrie, "On eigenfunction expansions associated with wave propagation along ducts with wave-bearing boundaries", *IMA Jl Appl Math*, 72: pp. 376–394 (2002). [cited at p. 119]

[96] R. Alonso, L. Borcea and J. Garnier, "Wave propagation in waveguides with rough boundaries", *Communications in Mathematical Sciences*. 11: pp. 233–267 (2012). [cited at p. 119]

PhD

ORIGINALITY REPORT

18%	13%	12%	6%
SIMILARITY INDEX	INTERNET SOURCES	PUBLICATIONS	STUDENT PAPERS

MATCH ALL SOURCES (ONLY SELECTED SOURCE PRINTED)

6%

★ ceta.mit.edu

Internet Source

EXCLUDE QUOTES	ON	EXCLUDE MATCHES	< 3 WORDS
EXCLUDE BIBLIOGRAPHY	ON		